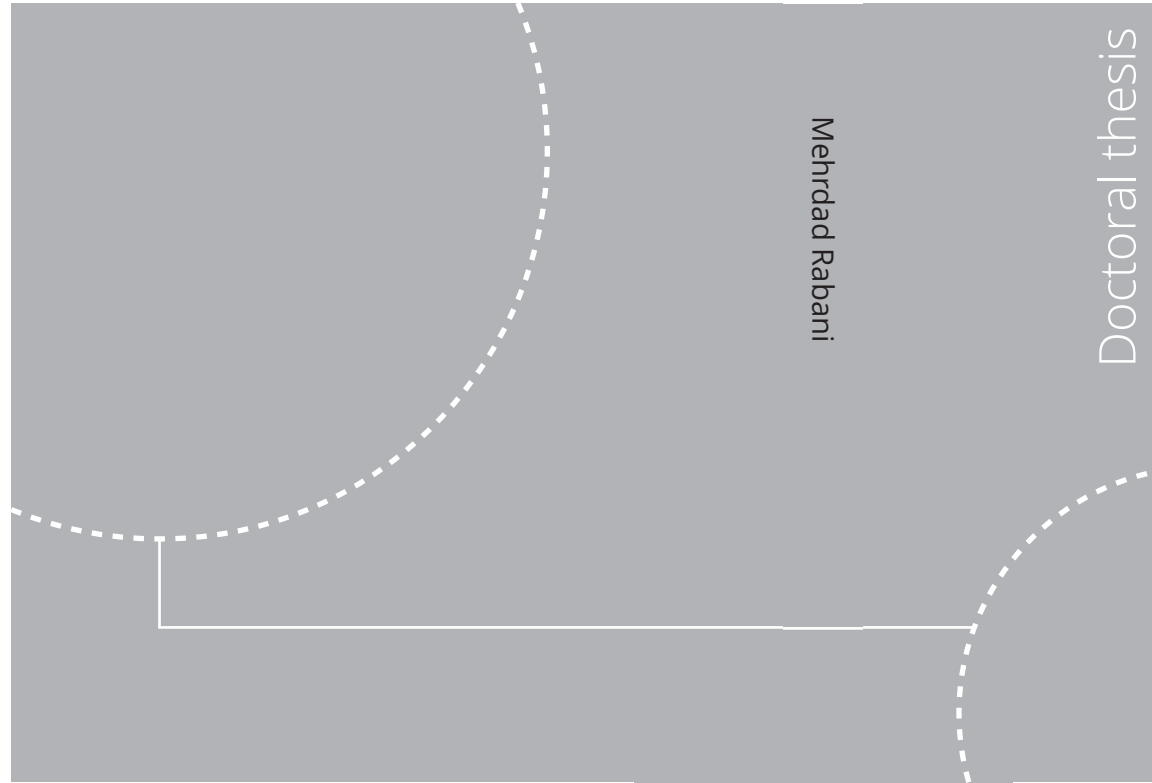


ISBN 978-82-326-5191-7 (printed ver.)
ISBN 978-82-326-5202-0
(electronic ver.)
ISSN 1503-8181 (printed ver.)



Doctoral theses at NTNU, 2021:403

Mehrdad Rabani

Retrofitting of Norwegian Office Buildings towards Nearly Zero Energy-Technical, Environmental, and Economic Aspects

Doctoral theses at NTNU, 2021:403

NTNU
Norwegian University of
Science and Technology
Thesis for the degree of
Philosophiae Doctor
Faculty of Engineering
Department of Energy and Process Engineering

 **NTNU**
Norwegian University of
Science and Technology

 NTNU

 **NTNU**
Norwegian University of
Science and Technology

Mehrdad Rabani

Retrofitting of Norwegian Office Buildings towards Nearly Zero Energy-Technical, Environmental, and Economic Aspects

Thesis for the degree of Philosophiae Doctor

Trondheim, December 2021

Norwegian University of Science and Technology
Faculty of Engineering
Department of Energy and Process Engineering



Norwegian University of
Science and Technology

NTNU

Norwegian University of Science and Technology

Thesis for the degree of Philosophiae Doctor

Faculty of Engineering
Department of Energy and Process Engineering

© Mehrdad Rabani

ISBN 978-82-326-5191-7 (printed ver.)

ISBN 978-82-326-5202-0 (electronic ver.)

ISSN 1503-8181 (printed ver.)

ISSN 2703-8084 (electronic ver.)

Doctoral theses at NTNU, 2021:403



Printed by Skipnes Kommunikasjon AS

Preface

This doctoral thesis was carried out in cooperation with the Norwegian University of Science and Technology (NTNU) and the Oslo Metropolitan University (OsloMet). The doctoral work was conducted under the supervision of Professor Natasa Nord in the Department of Energy and Process Engineering at NTNU and co-supervision of Associate Professor Habtamu Bayera Madessa in the Department of Civil Engineering and Energy Technology at OsloMet.

Abstract

The increasing proportion of energy use for buildings in urban environments has necessitated energy efficiency and advancement of the sustainable transformation of building stock towards the zero energy/emission level. In cold climate countries, such as Norway, the building energy efficiency is even more challenging due to cold climate conditions and high heating needs, which accounts for 40-60% of the total energy use. Apart from the energy use, the importance of indoor air quality (IAQ) in well-being and productivity of occupants in non-residential buildings, e.g. offices, cannot be ignored since the occupants spend a lot of their time in the indoor environment. Developing efficient approaches of building retrofitting by taking advantage of sustainable retrofitting technologies plays a key role in achieving such transformation. However, critical assessments of sustainable retrofitting interventions and their effectiveness are still restrained by the deficiency in systematic integration of modelling tools. These were addressed in this thesis with respect to retrofitting the Norwegian office buildings.

The thesis aims at facilitating the development of modelling methods to assist the sustainable retrofitting in the Norwegian office buildings towards the nearly zero energy building (nZEB) level.

In the first step towards nZEB level, various retrofitting scenarios were modelled and analyzed for a typical Norwegian office building of 3000 m² area through two different optimization approaches. In the first approach, the existing building characteristics were selected based on the Norwegian building code TEK 10 (2010 onwards), and small retrofitting measures (small cost-effective retrofit measures recommended in literature studies) were applied. In the second approach, the TEK 87 (1980s) building requirements were considered for the reference case and larger number of renovation measures were included. In this regard, the retrofit alternatives studied include the renovation of building envelope, fenestration, HVAC system and set points, window opening and shading control methods, and shading materials. Combined impacts and interdependencies among retrofits were also investigated. The optimization framework was developed through a Graphical Script module that implements the

connection among input, constraints, and outputs through a visualization interface. In addition, a post-processing detailed computational fluid dynamics (CFD) and daylight analysis was conducted for the optimal solution. The results in the first optimization approach showed that, compared to the reference case building, the energy saving potential of the retrofit measures was 43-56% in various cases in the small retrofitting strategy. Furthermore, the results showed that the high-quality window and external wall were always used in the optimized solutions, but the ground floor and the roof retrofitting were the costliest options and were recommended to be used only when the reduction of operational cost due to energy use was higher than the increase of the investment cost. According to the optimization results in the second retrofitting approach, the building energy use could be significantly reduced up to 77%, compared to the reference building case, while satisfying the thermal and visual comfort conditions. The results of second optimization approach also revealed that both optimized cases equipped with the radiator space heating (RSH) and all-air (AA) systems could satisfy the thermal comfort requirements, based on the comfort category II, for longer period of the year compared to the reference case. Additionally, the AA optimized case showed a better performance in terms of both thermal comfort and visual comfort conditions compared to the RSH optimized case. Various ventilation control strategies in AA cases allowed a better selection of optimization design variables, especially window to floor ratio and shading device control methods affecting the daylight conditions significantly.

Lastly, life cycle assessment (LCA) of CO₂-eq emissions was performed for the reference case TEK87 and the optimal solutions in the first optimization approach. The results showed that, compared to the reference building, the greenhouse gas (GHG) emissions associated with the operational energy use could be reduced up to 73% for the retrofitting strategies equipped with AA system. In this regard, the reduction of emissions associated with the operational energy use outweighed the produced embodied emissions of extra materials in the optimal solutions.

It is worth mentioning that the optimization approaches proposed in this thesis can be used at any stage of building design process and can help to improve the robustness of the building design to achieve a nZEB in Norway.

Acknowledgements

Foremost, I would like to thank my supervisors Natasa Nord and Habtamu Bayera Madessa for guiding me through my PhD. I am also very grateful for their support and understanding during the challenges I encountered in my PhD as well as their patience and time for countless discussions, which made the doctoral journey a truly enjoyable, productive, and enlightening one.

In addition to my official supervisors, I am indebted to Peter Schild for the guidance and suggestions he has so kindly provided while I was working on this thesis. I have also benefited from fruitful discussions with him. I am grateful to Omid Mohseni, Malin Ljungström, Lene Aamodt, Sandra Løvvold for the valuable discussions and collaboration by helping in conducting simulations.

I would like to thank my friends and colleagues, Alex, Amir, German, Petros, Simen, and Magda at OsloMet as well as Tymofii, Maria, Dmytro, Amar, and Haoran at NTNU for providing a decent environment in the office for scientific discussions and friendly talks.

Last but not least, I am forever grateful to my mother and father instilling in me many values that were very useful during my PhD, and to my elder brother Mehran and my twin brother Ramin for their loves and support.

List of publication

- Paper 1** M. Rabani, H. Bayera Madessa, O. Mohseni, N. Nord, Minimizing delivered energy and life cycle cost using Graphical script: An office building retrofitting case, *Applied Energy*, 268 (2020).
- Paper 2** M. Rabani, H. Bayera Madessa, N. Nord, Achieving zero-energy building performance with thermal and visual comfort enhancement through optimization of fenestration, envelope, shading device, and energy supply system, *Sustainable Energy Technologies and Assessments*, 44 (2021) 101020.
- Paper 3** M. Rabani, H. Bayera Madessa, N. Nord, Building retrofitting through coupling of building energy simulation-optimization tool with CFD and Daylight programs, *Energies* 14(8) (2021) 2180.
- Paper 4** M. Rabani, H. Bayera Madessa, M. Ljungström, L. Aamodt, S. Løvvold, N. Nord, Life cycle analysis of GHG emissions from retrofitting of building: The case of a Norwegian office building, *Building and Environment*, 204 (2021) 108159.

Other publications not included in the thesis:

- Paper 5** M. Rabani, V. Kalantar, M. Rabani, Heat transfer analysis of a Trombe wall with a projecting channel design, *Energy*, 134 (2017) 943-950.
- Paper 6** M. Rabani, H. Bayera Madessa, N. Nord, CFD study on the effect of Archimedes number and heating rate on the thermal stratification of a ventilated office, in: *Proceedings of The 59th Conference on Simulation and Modelling (SIMS 59)*, Linköping University Electronic Press, Oslo Metropolitan University, Norway, 2018.
- Paper 7** M. Rabani, H. Bayera Madessa, N. Nord, Active supply diffuser application in all-air heating systems, *REHVA*, Federation of European Heating, Ventilation and Air Conditioning Associations, 04 (2019) 13-17.
- Paper 8** A. Gonzalez-Caceres, M. Rabani, P.A. Wegertseder Martínez, A systematic review of retrofitting tools for residential buildings, in: *IOP Conference Series: Earth and Environmental Science*, SBE_Tokyo, 2019.
- Paper 9** M. Rabani, H.B. Madessa, N. Nord, P. Schild. Performance analysis of an active diffuser in mixing ventilation for cell office by using numerical approach. *E3S Web of Conferences, Bucharest, Romania* 111(8):04033, 2019
- Paper 10** M. Rabani, M. Rabani, Heating performance enhancement of a new design trombe wall using rectangular thermal fin arrays: An experimental approach, *Journal of Energy Storage*, 24 (2019) 100796.
- Paper 11** M. Rabani, H.B. Madessa, N. Nord, P. Schild, M. Mysen, Performance assessment of all-air heating in an office cubicle equipped with an active supply diffuser in a cold climate, *Building and Environment*, 156 (2019) 123-136.
- Paper 12** M. Rabani, H. Bayera Madessa, J. Torgersen, N. Nord, Parametric analysis of ground source heat pump system for heating of office buildings in Nordic climate, in: *International Conference Organised by IBPSA-Nordic, SINTEF proceedings*, Oslo, Norway, 2020.

Contents

1. Introduction.....	1
1.1. Background	1
1.2. Quantifying the existing Norwegian office buildings.....	2
1.3. Zero energy/emission definitions and ambitions levels.....	4
1.4. Building energy retrofitting methods and tools.....	7
1.4.1. Simulation-based optimization of building energy performance and indoor climate.....	8
1.4.2. Building indoor environmental climate modelling.....	15
1.4.2.1. Thermal indoor climate and indoor air quality.....	15
1.4.2.2. Visual comfort and daylight modelling.....	18
1.4.3. Life cycle assessment of greenhouse gas emissions in building retrofitting process.....	19
1.5. All-air heating/cooling system application in building retrofitting practice	26
1.6. Evolution of PhD.....	28
1.7. Research objectives	32
1.8. Thesis content.....	33
1.9. Contribution to publications	34
2. Method.....	36
2.1. Building energy performance	37
2.2. Thermal comfort of occupants	39
2.3. Visual comfort and daylight quality	41
2.4. Cost effectiveness of the retrofit measures.....	42
2.5. Environmental impact of the retrofit measures	43
2.6. Zero energy balance	47
3. Case study.....	49
4. Achieving zero energy building performance of an existing office building through optimization and small retrofitting measures.....	54
4.1. Reference building models	54
4.2. Minimizing delivered energy and LCC through small retrofitting.....	56

4.2.1. Input parameters, constraints, and objective functions.....	56
4.2.2. Optimization results of the first retrofitting approach.....	57
4.3. Improving thermal and visual comfort through optimization of fenestration, envelope, shading device, and energy supply system.....	62
4.3.1. Input parameters, constraints, and objective functions.....	62
4.3.2. Optimization framework and simulation tool.....	64
4.3.3. Optimization results of the second retrofitting approach.....	65
4.3.3.1. Optimization results.....	65
4.3.3.2. Results of ZEB balance.....	67
4.4. CFD and daylight programs for building retrofitting	70
4.4.1. Simulation setups.....	70
4.4.2. CFD and daylight simulation results for the energy optimized solution	74
4.4.2.1. BES-OPT analysis.....	74
4.4.2.2. CFD and daylight assessment.....	76
4.5. Life cycle analysis of GHG emissions from building retrofitting.....	80
4.5.1. LCA framework and material emissions.....	80
4.5.2. LCA results of various retrofitting strategies.....	82
5. Conclusions.....	88
5.1. Summary of thesis	88
5.2. Future work.....	90
References.....	92

List of Figures

Fig. 1. Age distribution of the existing Norwegian office buildings3

Fig. 2. Floor area of the existing Norwegian office buildings4

Fig. 3. Graphical illustration of three different ZEB balance methods [21].....5

Fig. 4. Illustration of three of the five ambition levels for Zero Emission Building (ZEB) [22]6

Fig. 5. Classification of indoor climate modelling methods 15

Fig. 6. Classification of visual comfort and daylight modelling methods..... 19

Fig. 7. Three different ambition levels of LCA for building retrofitting 21

Fig. 8. Display of tailored information for different stages of the building assessment based on EN 15987 [76]..... 23

Fig. 9. Different types of the all-air systems 26

Fig. 10. Definition of the sustainable building retrofitting 37




Fig. 11. Entire building life cycle stages according to NS 3720 [131] In color: those taken into account in the boundaries of LCA in this thesis. : Stages assessed through LCA tool database. : Those evaluated using information provided by BES tool. : Those not considered in this thesis 45

Fig. 12. (a) FN office building located in Arendal, which was built in 1965 and renovated in 2006 with gross area 2 590 m² [138], (b) Bassengbakken 1 office building located in Trondheim constructed in 2001 and rehabilitated in 2004 with gross area 8 425 m² [138], (c) An office building located in Bergen, which was completed in 2015 for the Norwegian Defence Estates Agency (NDEA) as a nearly zero energy building (nZEB) with gross internal area 2 035 m² [104], (d) Considered office building configuration modelled in the energy simulation software (IDA-ICE)..... 50

Fig. 13. Generic ground floor plan, the first floor plan (top), and the second and the third floor plans at level 3.4 m and 6.8 m (bottom) with thermal zones 51

Fig. 14. Annual (a) specific energy use and (b) variation of operative temperature for the TEK 87 and TEK 10 reference building models 55

Fig. 15. Model framework and optimization process through the GS module 58

Fig. 16. Optimization results through GS module for the building case with the RSH system for Oslo climate (Minimizing LCC)	59
Fig. 17. Optimization results through GS module for the building case with AA system for Oslo climate (Minimizing LCC)	59
Fig. 18. Effect of constraint function on the optimization solutions for (a) RSH system and (b) AA system for Oslo climate (Minimizing delivered energy).....	60
Fig. 19. Trade-off of optimal solutions considering both specific delivered energy and specific LCC for two strategies	61
Fig. 20. Proposed framework for the optimization process in the second retrofitting method.....	65
Fig. 21. Scatter plot of optimization results	67
Fig. 22. ZEB analysis process in terms of exported and imported primary energy use .	68
Fig. 23. Monthly variation of electricity portion in ZEB analysis in terms of (a) export/production and (b) import/consumption for the global optimal solution	69
Fig. 24. (a) monthly and (b) hourly production and consumption electricity with areas for ZEB balance	70
Fig. 25. Coupling framework of building energy optimization, daylight, and CFD	72
Fig. 26. Modelled configuration of the office cubicle in IDA-ICE.....	73
Fig. 27. Optimization results for (a) RSH system and (b) AA system in the second retrofitting approach	74
Fig. 28. Delivered energy to the building for two optimization cases	75
Fig. 29. Annual variation of average PPD for the cell office C.O.16 for the (a) reference case, (b) optimized RSH case (c) optimized AA case	77
Fig. 30. Box plot of vertical air temperature difference between the ankle and head levels for the cell office C.O.16 for different cases	78
Fig. 31. Spatial distribution of three visual daylight indexes for the cell office C.O.16 for (a) reference case (b) optimized RSH, and (c) optimized AA.....	79
Fig. 32. Total CO ₂ -eq emissions related to various stages of the building life cycle for the reference building (TEK 87) and retrofitting strategies	83

Fig. 33. Embodied CO₂-eq emissions from materials for the reference building and the retrofit strategies 84

Fig. 34. Time plot of CO₂-eq for the reference case and different retrofit strategies 85

Fig. 35. (a) CO₂-eq emissions for two types of PV panels to reach nZEB level and (b) total CO₂-eq emissions for the RSH_PH and two nZEB cases 86

Fig. 36. Time plot of CO₂-eq for the RSH_PH and two nZEB cases 87

List of Tables

Table 1. Summary of literature about the optimization of building energy performance tools	10
Table 2. Connection between research questions and publications.....	34
Table 3. Categories of thermal environment.....	40
Table 4. Assumptions and sources used for the LCA method.....	44
Table 5. Properties of the building envelope for the reference case.....	52
Table 6. Characteristics of the HVAC system in the reference building.....	53
Table 7. Details of constraint functions for two strategies	56
Table 8. Energy and LCC values of various optimal solutions for both strategies.....	62
Table 9. Various types of control methods for DCV system	71
Table 10. Extra materials' quantity and CO ₂ -eq emissions for different retrofitting strategies.....	81

1. Introduction

1.1. Background

The global average surface temperature has risen about 1°C since the industrial age, a change driven substantially by the increased carbon dioxide and other emissions related to human activities [1]. The European Union (EU) has set up an ambitious framework, in which the climate strategies should be aimed to reduce greenhouse gas (GHG) emissions by 40% and 80% by 2030 and 2050, respectively, compared to the levels in 1990 [2]. The key issue is improving the energy efficiency in all low-carbon scenarios, and hence upgrade of the energy efficiency in building sector is one of the main concerns in this regard. It is estimated that building stock accounts for approximately 28%, on a global scale, and 40%, in the EU, of the total energy use [3, 4]. Furthermore, growing critical challenges in energy need for improving building indoor environmental quality (IEQ) and comfort levels has led the building energy use to increase around 13% in EU, in the past 20 years [5]. The EU energy roadmap 2050 emphasized that improving energy efficiency in existing/new buildings is essential to transform the energy system and increase the share of renewable energy used in EU. It necessitates EU countries to establish prolonged national building renovation schemes proposed by the International Energy Agency [4].

Concerning the above EU strategic goals and challenges in building retrofiting, Norway has proactively involved in this energy efficiency roadmap. Residential and non-residential sectors account for 40% of the Norwegian total energy use, of which around 41% is used in non-residential buildings, for space heating, domestic hot water, lighting and operating electrical equipment, and around 59% is used in the residential buildings. However, the trend of energy use in Norway from 1990 to 2015 shows that the energy use in the non-residential sector has risen around 31%, while it has been approximately 9% in residential buildings [6]. In this regard, the Norwegian Building Regulations (TEK) has continuously set stricter requirements for energy efficiency in the Norwegian

buildings so that the energy use for all building categories should be reduced. Particularly, comparing the latest version of the Norwegian Building Regulations (TEK 17) with the previous version (TEK 10) shows that the reduction of the building energy use should happen to a large extent in the non-residential building sector, with the maximum energy reduction 23% for office buildings and hotels [7, 8].

Retrofitting has been known as one of the most effective methods to achieve a sustainable building performance for existing buildings. From an engineering point of view, building retrofitting is defined as actions that allow an upgrade of the building's energy, indoor climate, and environmental performance to a higher standard than was originally planned. An overview of potential retrofit strategies and retrofit actions which may improve performance figures can be categorized into three main strategies: (1) actions regarding building envelope and design aspects including insulation upgrades, air leakage reduction, improvement of doors and windows, control and exploitation of solar gain and daylight, etc.; (2) actions for building systems and installations including installation of high-effective heating, ventilation and air conditioning (HVAC) systems, improvement of electrical lighting systems, improvement of domestic appliances, installation of renewable energy, etc.; (3) actions associated with building services and management tools including monitoring and control of building during operation, utilization of metering services, clock controls, sensors, etc. [9]. The overall consequence of these retrofit strategies would be an energy efficient building with low greenhouse gas emission that is both comfortable for occupant and cost effective. However, achieving all these goals would be challenging when a passive house (PH) building level or a zero energy/emission level is the target. The passive house refers to an airtight and highly insulated building that may require little or no energy for space heating and cooling [10].

1.2. Quantifying the existing Norwegian office buildings

By 2020, the number of existing Norwegian office buildings was approximately 39 000 [11]. Most of office buildings were initially constructed in major regions in the Oslo and Vestland (Previously called Hordaland and Sogn og Fjordane) areas. The

development of Norwegian office buildings has traditionally been connected to particular time period. Fig. 1 shows the age distribution of the existing office buildings. The majority of the office buildings, around 85% of the total office buildings were constructed in the period 1960-2000, as highlighted with the purple dashed line in Fig. 1 [12, 13]. However, a very few new office buildings have been constructed in Norway since 2015 [11]. This implies that achieving both zero energy building (ZEB) and environmental performance targets in the Norwegian office buildings is primarily dependent on how efficiently the existing office buildings would be retrofitted.

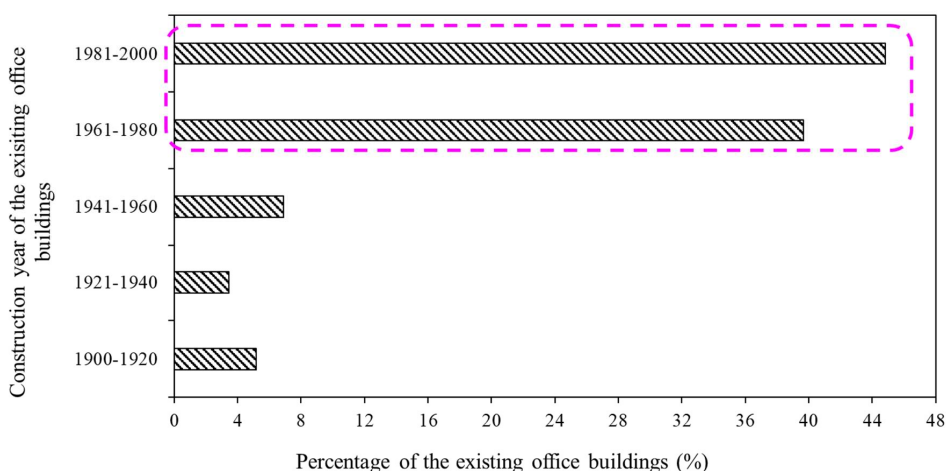


Fig. 1. Age distribution of the existing Norwegian office buildings

Fig. 2 shows the total floor area of the existing Norwegian office buildings. As it can be seen, most of the existing office buildings in Norway, around 64% (marked with purple dashed line), have a total building area of less than 10 000 m². However, there is still a great variation in the size of office buildings, and large gaps in the available data sources with regard to average size [13].

Since the largest data set for the office building area is from the Energy Label Scheme (Energimerkeordningen), this should be the most representative data source. The data from the Energy Labeling Scheme shows a significantly smaller average usable area than the other data sources, including Enova [14] and Norway’s statistics (SSB), for Norway. If we remove all buildings under 200 m² from the data set, as has been done in

SSB sample, the average building area in the data from the Energy Labeling Scheme is still below than others, with the average floor area around 3 000 m² [13]. This implies that this average floor area is not fully representative of the existing Norwegian office buildings.

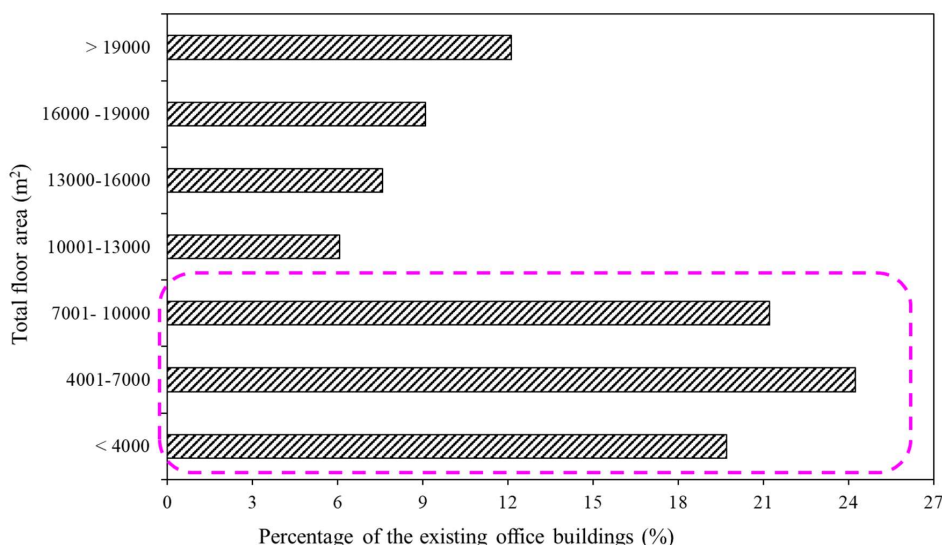


Fig. 2. Floor area of the existing Norwegian office buildings

In Norway, electricity has been the most common energy carrier in the commercial building stock especially for office buildings [15]. In a twenty-year period, from 1990 to 2010, the share of electricity varied from 78%-85%. However, the trend is decreasing due to increased use of district heating, around 19% per year from 2000 to 2010 [16]. Particularly, the use of district heating has been even more pronounced from 2011 to 2019 i.e., the share of district heating in commercial buildings has increased approximately 39% [17].

1.3. Zero energy/emission definitions and ambitions levels

Generally, a zero energy building (ZEB) is a residential or commercial building with zero net energy use, meaning that the total amount of energy used by the building on an annual basis can be compensated by onsite production of energy via renewable

energy technologies [18]. In the most general definition, the primary energy is used for energy balance. However, more than one metric can be adopted to express ZEB balance (e.g. primary energy, end-use energy, and carbon emissions) and different conversion factors can be applied to various energy carriers [19, 20]. In this respect, a zero emission building produces enough renewable energy to compensate for the building's greenhouse gas emissions over its life span.

Each ZEB definition includes a certain methodology to calculate the building energy/emission balance. In this respect, the balance boundaries can be often determined based on the three different methods identifying which energy boundaries are considered as shown in Fig. 3 [21]. The first method is called load/generation balance and it focuses on the balance between weighted onsite production and the calculated energy use. The second approach is the balance between the weighted need and the weighted supply and it is commonly referred to the import/export balance and it takes the grid interaction into consideration as well. The difference between the second and the first approaches is the self-used fraction of the onsite generated energy, defined as the share of onsite production that is used in the building.

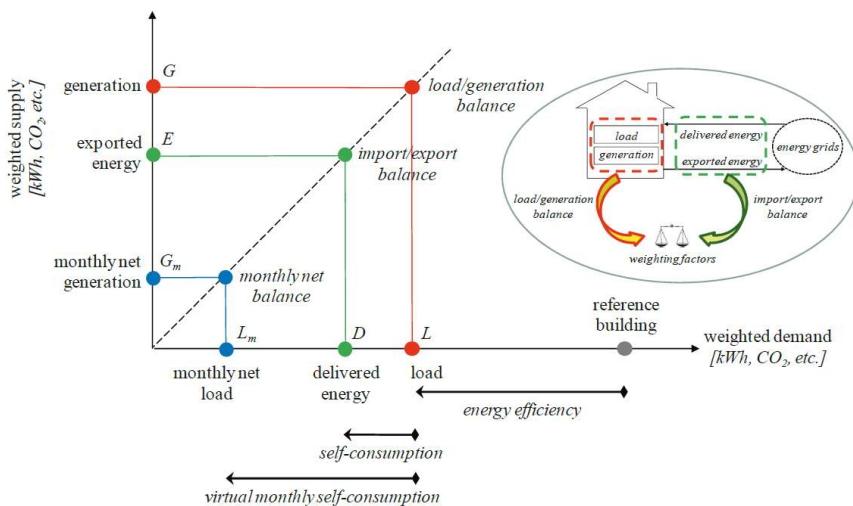


Fig. 3. Graphical illustration of three different ZEB balance methods [21]

The third method is called monthly net balance (the blue line in Fig. 3) representing only the monthly generation excess or remaining load added up to annual

totals. Nevertheless, the monthly net balance is relevant for investigation of the seasonal performance, whereas high-resolution simulations are required for balance of daily and hourly fluctuations [20].

In the Norwegian building context, there have been defined five different ambition levels for the ZEB balance over the building's lifetime, in terms of greenhouse gas equivalents (CO₂-eq), described in rising ambition, as shown in Fig. 4. Depending on the ambition level, the emissions from the various stages of the material life cycle, which is called embodied emissions, can be also included in ZEB balance [22]. These five ambition levels in Fig. 4 are explained as the following:

- ZEB-O÷EQ: Net emissions related to all operational energy use (excluding energy use for equipment) should be compensated by building's renewable energy production.
- ZEB-O: Same as ZEB-O÷EQ but including energy use for equipment.
- ZEB-OM: Emissions related to all operational energy use plus embodied emission from materials and installations should be compensated by renewable energy production.
- ZEB-COM: Same as ZEB-OM but including emissions related to the construction process of the building.
- ZEB-COMPLETE: Emissions related to a complete lifecycle emission analysis must be compensated for. The reuse, recovery and recycling can also be included.

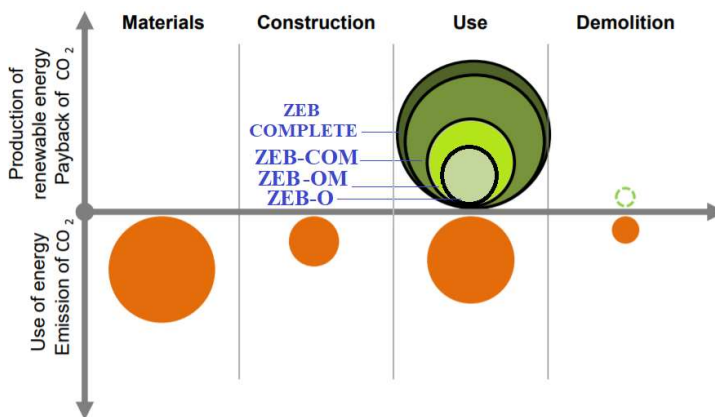


Fig. 4. Illustration of three of the five ambition levels for Zero Emission Building (ZEB) [22]

The aforementioned targets should be considered for more effective and sustainable retrofitting process. However, achieving a high level of ZEB is challenging for existing Norwegian office buildings and requires an efficient decision-making process because a large number of retrofit measures need to be involved. In addition, there is a strong motivation for transition of existing Norwegian office buildings to smart ones with automatic control of shading devices, window opening, building's HVAC system etc. Therefore, a more systematic and inclusive framework is essential to find sustainable retrofit solutions, which were not well studied in the literature.

1.4. Building energy retrofitting methods and tools

From a technical point of view, the aim of building retrofitting is upgrading existing building performance to decrease the building energy use, reduce the GHG emissions, and provide a comfortable indoor environment for occupants.

Different building retrofitting methods have already been developed to investigate the efficiency of building retrofit. The suitability of these methods depends on which building area is involved in retrofitting project. Data-driven method is one of the approaches that can cover a set of retrofitting interventions. This method generally takes advantage of statistical analysis to find the relationships between the building input and output variables without detailed knowledge of building physical behavior [23, 24]. Depending on the level of physical importance of the parameters used, these models are usually referred to as grey-box or black-box models such as the following [25]:

- Statistical learning: It is based on constructing a statistical model by implying relationships among different variables in the analyzed dataset and then is applied to make predictions on other similar datasets [26, 27].
- Machine learning technique: It finds algorithms that use statistical methods to learn from data without any particularly programmed guidance. The algorithms determine patterns in the dataset iteratively and consequently these patterns can be utilized to make predictions [28, 29].

The other class of methods that are based on the differential equations of the energy transfer flows in the building rooms or spaces are called deterministic methods, commonly referred to as white-box models. Deterministic methods are mostly based on the application of building energy simulation (BES) to investigate the energy performance of buildings in various retrofitting scenarios [25]. This method can be used in two different ways: (1) combining it with collected data from energy bills and questionnaires to compare the simulations with real use for prediction of energy savings related to specific retrofitting measures [30], (2) using the BES tools to evaluate various retrofit scenarios for finding cost-effective solutions to achieve low energy and ZEB levels [31, 32].

The third method is a hybrid model that makes use of both above-mentioned techniques i.e., adopting data-driven techniques to optimize the results obtained by deterministic methods. The data-driven algorithms can be used either to expand the obtained results to a larger group buildings [33] or to perform a multi-criteria optimization in order to find an optimal set of building retrofitting interventions [34, 35], which was the method used in this thesis.

1.4.1. Simulation-based optimization of building energy performance and indoor climate

Optimization approaches adopt machine learning techniques and algorithms such as genetic algorithm, particle swarm optimization, and sequential search to find the optimal set of building retrofit measures through an iterative process [35, 36].

One of the most prevalent methods in exploring optimal solutions for retrofitting projects is based on integrating the building performance simulation tools such as EnergyPlus, DOE-2, IDA-ICE, and TRNSYS, etc., with optimization engines including custom programming and general optimization tools such as MOBO, GenOpt, jEPlus, BeOpt, and MultiOpt, etc. [37]. Approaches, automating the search process in finding optimal solutions with less effort, have largely been studied. Table 1 summarizes these studies and their features including modelling approach, type of tools, objective functions and design parameters used in the building optimization procedure. From Table 1 it can

be found that the following features are included in most of the retrofitting projects for single/multi-objective optimization of the building performance:

- **Input parameters:** Insulation thickness of the building envelope elements, surface area and type of glazing, overhang tilt angle, overhang depth, and type of shading are mainly considered as the optimization input parameters for the building envelope. In addition, size of photovoltaic (PV) panel, solar thermal collector area, type of energy source, and heating and cooling temperature set points are selected as the major optimization input parameters for the building HVAC system.

- **Objective functions and constraints:** Building energy use, life cycle cost (LCC), life cycle GHG, and thermal comfort of occupants are the most selected targets as the optimization objective functions. The number of discomfort hours and daylight are also chosen as the thermal and visual constraint functions in the optimization process. In some researches [38, 39], no constraint function was used, but a post processing analysis of thermal comfort was instead performed to visualize the comfortable conditions for the optimized cases.

- **Optimization and building energy performance simulation tools:** GenOpt, MOBO, and jEPlus+EA tools as well as Genetic algorithm (GA) and NSGA-II algorithm developed in MATLAB are often chosen as the optimization tool. TRNSYS and EnergyPlus are used as the energy simulation tool for single/multi-objective optimization process. Furthermore, several researchers integrated optimization tools such as MOBO with IDA-ICE energy simulation software [39-42].

Table 1. Summary of literature about the optimization of building energy performance tools

Ref.	Model	Optimization and energy simulation tool	Objective function(s) and constraints	Input parameters
[43]	Multi-objective optimization	<ul style="list-style-type: none"> Artificial Neural Network (ANN) with multi-objective Genetic Algorithm (NSGA-II) TRNSYS 	<ul style="list-style-type: none"> Max thermal comfort Min building energy use Number of discomfort hours (constraint) 	<ul style="list-style-type: none"> Set points for cooling, heating, and relative humidity Supply airflow rate Window surface area Wall insulation thickness
[44]	Multi-objective optimization	<ul style="list-style-type: none"> GenOpt and a Tchebycheff optimization method developed in MATLAB TRNSYS 	<ul style="list-style-type: none"> Min retrofit cost Min energy saving Min number of discomfort hours 	<ul style="list-style-type: none"> Roof insulation materials Window type Wall insulation thickness and material type Solar collector type
[45]	Single-objective optimization	<ul style="list-style-type: none"> GenOpt TRNSYS 	<ul style="list-style-type: none"> Min primary energy use Indoor operative temperature (constraint) Daylight factor (constraint) 	<ul style="list-style-type: none"> Wall construction topology Roof construction topology Glass type and size Insulation thickness of external wall Absorption coefficient of wall's outer face Shading depth
[46]	Single and multi-objective optimization	<ul style="list-style-type: none"> NSGA-II algorithm developed in MATLAB TRNSYS 	<ul style="list-style-type: none"> Min energy use Min cost Min life cycle GHG Min thermal discomfort 	<ul style="list-style-type: none"> External and internal partition wall type Roof type Floor type Window type
[47]	Single-objective and multi-objective optimization	<ul style="list-style-type: none"> GA NSGA-II algorithm developed in MATLAB TRNSYS 	<ul style="list-style-type: none"> Min total cost Min carbon dioxide emission Min grid inter-action index of reference building Low energy building (LEB) (constraint) Zero energy building (ZEB) (constraint) 	<ul style="list-style-type: none"> PV size Wind turbine size Bio-diesel generator
[38]	Multi-objective optimization	<ul style="list-style-type: none"> NSGA-II in Multi-Objective Building Optimization tool (MOBO) TRNSYS 	<ul style="list-style-type: none"> Min energy use for cooling Min energy use for heating well Min life cycle cost 	<ul style="list-style-type: none"> External walls thermal transmittance Roof thermal transmittance Ground thermal transmittance Window to wall ratio at each façade Glazing type at each façade
[48]	Single-objective optimization	<ul style="list-style-type: none"> GenOpt EnergyPlus 	<ul style="list-style-type: none"> Min LCC 	<ul style="list-style-type: none"> External wall thermal insulation Roof thermal insulation Glass type

[49]	Multi-objective optimization	<ul style="list-style-type: none"> • jEPlus + EA tool • EnergyPlus 	<ul style="list-style-type: none"> • Min embodied CO₂/operational CO₂ • Min LCC/ LCCF (Life cycle carbon footprint) • Min annual energy consumption/annual energy spending 	<ul style="list-style-type: none"> • Exterior insulation thickness • Panel insulation thickness • Bricks thickness • Thermal bridges insulation • Window to wall
[50]	Multi-objective optimization	<ul style="list-style-type: none"> • jEPlus tool • MATLAB • EnergyPlus 	<ul style="list-style-type: none"> • Min annual cooling electricity • Min annual heating electricity • Min annual lighting electricity 	<ul style="list-style-type: none"> • Building orientation • Window size • Glazing properties • Wall thermal properties • Overhang depth and tilt angle
[51]	Single-objective and multi-objective optimization	<ul style="list-style-type: none"> • Multi-objective artificial bee colony (MOABC) developed in MATLAB • jEPlus tool • EnergyPlus 	<ul style="list-style-type: none"> • Min total annual building electricity consumption • Min Predicted Percentage of Dissatisfied (PPD) 	<ul style="list-style-type: none"> • Heating set point temperature • Cooling set point temperature • Wall thermal properties • Glazing properties • Building rotation
[52]	Single-objective optimization	<ul style="list-style-type: none"> • Ant Colony Optimization (ACOR) developed in MATLAB • GenOpt • EnergyPlus 	<ul style="list-style-type: none"> • Min annual building energy use 	<ul style="list-style-type: none"> • Roof thermal properties • Wall insulation thickness • Window size • Overhang depth • Heating set point • Cooling set point • Building orientation
[53]	Single-objective optimization	<ul style="list-style-type: none"> • GenOpt • EnergyPlus 	<ul style="list-style-type: none"> • Min total cost • PPD (constraint) 	<ul style="list-style-type: none"> • Building envelope insulation thickness • Supply-water temperature set points • Heat exchange area of the radiators
[54]	Multi-objective optimization	<ul style="list-style-type: none"> • NSGA-II algorithm developed in MATLAB • EnergyPlus 	<ul style="list-style-type: none"> • Min LCC • Max thermal comfort 	<ul style="list-style-type: none"> • Glazing type • Windows Area • Roof insulation thickness • Ground floor insulation thickness • Building orientation • Temperatures difference in infiltration controller • Air change value rate in infiltration controller
[55]	Multi-objective optimization	<ul style="list-style-type: none"> • Integrated multi-objective optimization (iMOO) tool • NSGA-II algorithm developed in MATLAB • EnergyPlus 	<ul style="list-style-type: none"> • Min Predicted Mean Vote (PMV) • Min initial investment Cost • Min thermal Energy Consumption • Min Net Present Value (NPV) • Global warming potential 	<ul style="list-style-type: none"> • Heating and cooling set point • Window type • Ventilation/window opening type

[56]	Multi-objective optimization	<ul style="list-style-type: none"> ● MATLAB ● multi-objective mixed-integer non-linear problem (MINLP) 	<ul style="list-style-type: none"> ● Min total annual primary energy consumption ● Min total investment cost 	<ul style="list-style-type: none"> ● Window type ● Door type ● Wall insulation type and thickness ● Floor structure ● Ceiling structure ● Electricity equipment power
[57]	Multi-objective optimization	<ul style="list-style-type: none"> ● Multi-objective optimization (MOO) tool ● Grasshopper ● EnergyPlus 	<ul style="list-style-type: none"> ● Min total annual net energy electricity use ● Max energy converted into electricity by the PV cells ● Max daylighting level in the zone measured as the continuous daylight autonomy 	<ul style="list-style-type: none"> ● Angle of louvre blades ● Z coordinate of the center point of each individual blade
[58]	Multi-objective and simultaneous optimization	<ul style="list-style-type: none"> ● Epsilon-constrained mixed integer linear program (MILP) using the CPLEX ● EnergyPlus 	<ul style="list-style-type: none"> ● Min Annualized costs ● Min life cycle GHG emissions 	<ul style="list-style-type: none"> ● Operating strategies for energy conversion and storage technologies including heat pumps, solar panels, biomass, oil boilers and thermal storage
[59]	Modified multi-objective optimization	<ul style="list-style-type: none"> ● Genetic algorithm PR_GA_RF developed in MATLAB ● IDA-ICE 	<ul style="list-style-type: none"> ● Min carbon dioxide equivalent (CO₂-eq) emissions ● Min investment cost ● Summer overheating degree-hour (constraint) 	<ul style="list-style-type: none"> ● Insulation thickness of wall, roof, and floor ● Window type ● Heat recovery type in air handling unit ● Shading type ● Heating/cooling system types
[40]	Multi-objective optimization	<ul style="list-style-type: none"> ● Pareto Archive NSGA-II algorithm in MOBO ● IDA-ICE 	<ul style="list-style-type: none"> ● Min additional investment cost ● Min annual space heating energy ● Additional investment cost (constraint) 	<ul style="list-style-type: none"> ● Insulation thickness of wall, roof, and floor ● Heat recovery efficiency ● Window type
[41]	Multi-objective optimization	<ul style="list-style-type: none"> ● NSGA-II algorithm and parallel computation in MOBO ● IDA-ICE 	<ul style="list-style-type: none"> ● Min LCC ● Min annual CO₂ emission 	<ul style="list-style-type: none"> ● Window U-value ● Wall and door U-value ● Floor U-value ● Solar thermal area and PV capacity ● Type of building energy source
[42]	Multi-objective optimization	<ul style="list-style-type: none"> ● Pareto Archive NSGA-II algorithm and in MOBO ● IDA-ICE 	<ul style="list-style-type: none"> ● Min LCC ● Min annual district heating energy use 	<ul style="list-style-type: none"> ● Solar collector area ● Storage Tank volume ● Tilt angle of solar collector
[39]	Multi-objective optimization	<ul style="list-style-type: none"> ● Pareto Archive NSGA-II algorithm and in MOBO ● IDA-ICE 	<ul style="list-style-type: none"> ● Min CO₂ emission of delivered energy to the building ● Min NPV of the 15-year LCC ● Min total occupant hours dissatisfaction (PDH) ● Maximum ventilation airflow rate (constraint) 	<ul style="list-style-type: none"> ● PV-panels area ● Insulation thickness of wall and roof ● Window type ● Type of lighting system ● Type of cooling and ventilation systems ● Dimensioning output power of ground source heat pump

Furthermore, as it can be seen in Table 1, window is the design variable that plays substantial role in optimizing the building energy use and visual and thermal comfort conditions. The type of glazing, window size, window to wall ratio, and the type of shading devices are the common design variables considered in the optimization of windows. However, some recent studies showed a high potential of optimizing the functional and physical properties of shading devices on the energy use, and visual and thermal comfort objectives simultaneously or separately. Naderi et al. [86] investigated the optimization of different design variables including shading control strategies, optical and thermal properties of blinds, and their distance to glazing. The objectives were minimizing the aforementioned objective functions in a simple room in Iran. Shading control strategies were mainly based on temperature and solar irradiance set points. Their results showed that the building energy use, thermal discomfort, and visual discomfort could reduce up to 48%, 56%, and 70%, respectively [86]. The authors in [87] investigated an optimization scheme on the impact of different depth of shading slats, distance between them, their angle rotation, window to wall ratio, and the type of glazing on the three aforementioned objectives. The optimization process was performed for a classroom in hot and dry climate. The results highlighted the role of optimizing the shading systems in achieving a tailored building envelope for good performance of buildings. Katsifaraki et al. [88] proposed three shading control strategies including slats' cut-off angle control with solar irradiance, radiation control, and optimization-based control in an office space in Germany. The shading control strategies were based on direct solar radiation on the façade, seasonal usage, and occupancy with the objective of maximizing visual comfort. The results demonstrated that the optimization-based control resulted in the maximum visual comfort and the minimum building energy use, by reducing cooling and lighting energy, among three control methods. Yun et al. [89] investigated the effect of different control strategies on the energy use and thermal comfort in an office cell in Korea. 10 control strategies for lighting and shading were considered. The shading control parameters were slats' angle, illuminance level, and user preference. They concluded that depending on the objective, the control strategy can differ by priority or by season. The research work in [90] focused on the shading control

parameters including indoor temperature set-points, illuminance level, occupancy, and solar irradiance. The results showed that shading control methods based on combined effect of temperature set points and illuminance level are the most effective to avoid glare and overheating in office building in the cold climate of Estonia.

Apart from the shading device control methods, window opening control strategies play also an important role on the thermal comfort conditions. Stazi et al. [91] developed automatic system for windows opening in an Italian school building. The control methods were based on adaptive thermal comfort theory including Humphrey's algorithm [92] and modified/integrated of this algorithm. The Humphrey's algorithm parameters were driven by temperature inputs such as the outdoor air temperature, the running mean outdoor temperature, the indoor air and operative temperature, and the comfort temperature. The modified method took the CO₂ level into consideration as well. The results showed that the second control method can ensure both users satisfaction and low CO₂ level. Alonso et al. [93] investigated the application of window opening control methods in a kindergarten in Norway. The control parameters were the indoor air temperature, occupancy, and the CO₂ level. Their objective was to reduce the building energy use for space heating (SH). Their results emphasized that the control algorithm for window opening in winter should be carefully tuned to avoid high SH demands. Psomas et al. [94] investigated discomfort risk during summer period by analyzing the ventilative cooling through window opening for a renovated single-family house in Denmark. The window was controlled by the operative temperature and the indoor natural ventilation cooling set point (dynamic and static), and step opening (3 or 5). Analysis of the results highlighted that the performance of the developed strategy was not affected by the number of opening steps for indoor ventilation cooling set points 22–24°C in these climatic conditions. The results also showed that the static trigger set points performed better than the dynamic ones.

The analysis of literature review on the shading device and window opening control method shows that the type of parameters adopted in various control methods can differ depending on the climate conditions. However, none of these studies investigated the combined effect of adopting both window opening and shading device control

strategies. It can be challenging to find an optimal control method where both control functions are in action. In addition, considering the optimization design variables shown in Table 1, there is no optimization study investigating the combined effect of considering window opening control methods, shading device strategies, and other common parameters of building envelope with HVAC system control set points. This becomes specifically important when studying the retrofitting of buildings towards nZEB level as the aim of such ambition level is to achieve the highest possible building energy performance with improved indoor thermal and visual comfort conditions.

1.4.2. Building indoor environmental climate modelling

Naturally, retrofitting of a building and its services strongly affect the physical indoor climate. It should also be underlined that the desires of users regarding the quality of the indoor climate establish provisions for the work of those involved in the building retrofitting process. The accomplishment of the retrofitting process depends on a comprehensive knowledge of four physical indoor environment parameters: thermal climate, indoor air quality, sound, and light [60].

1.4.2.1. Thermal indoor climate and indoor air quality

Regarding the thermal climate and indoor air quality, several models have already been developed to study the indoor climate at different stages of retrofitting process, as shown in Fig. 5.

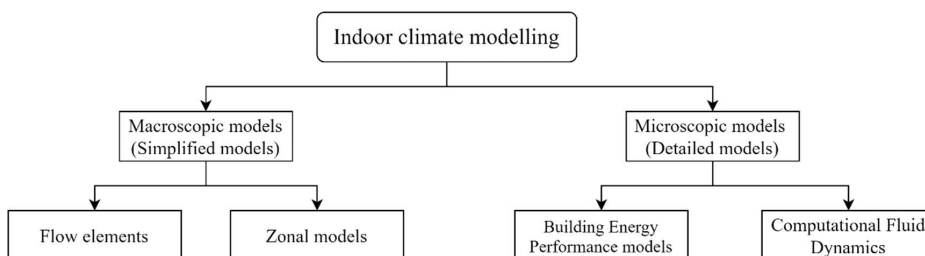


Fig. 5. Classification of indoor climate modelling methods

Simplified models such as flow elements are straightforward to use, especially at an early stage of design process. They are often steady-state and form the basis for the

zonal models. The flow elements models can also be grouped based on different air room movements including isothermal flow, non-isothermal flow, buoyant flow, and stratified flow, which can be addressed independently of flow and dimensions [61].

The key principle of zonal models is to divide the indoor space air into several control volumes with proposed uniform concentration and (usually uniform) temperature, and to solve the mass balance, the concentration balance, and the energy balance for each zone. The aim of such models is to determine the values of temperature, concentration, and the flow fields in the whole considered space. The uniform volumes in the zonal models can be generated by the two main processes. In the first process, where the room air is assumed to be fully mixed with the contaminants (mixing ventilation), the physical barriers and volumes with different flow elements play important roles in creating uniform spaces. However, the vertical temperature difference and buoyancy effect are the key factors in the generation of homogeneous volumes when the low velocity supplied air is dragged upwards by the plume above a heat source. This method, which divides the zone into a lower sub-zone with cold and outdoor air and an upper sub-zone with heated and contaminated air, is called displacement ventilation [60]. SimSPARK [62] and POMA [63] are the two software examples that are used to visualize indoor airflows through zonal modelling.

Building energy performance model, which is called also multizone technique or nodal method, is probably the simplest method for indoor climate modelling. It is dynamic and simulate the energy flow over a period. Its principle is based on the following assumptions: each building zone is a uniform volume characterized by uniform state variables. Therefore, one zone is approximated to a node that is described by a specific temperature, pressure, concentration, etc. The thermal transfer equations are solved for each node of the system. In this term, the nodal method can be considered as a one-dimensional approach. EnergyPlus and IDA-ICE are among the popular software applying the nodal approach for building simulations [64].

The most complete approach in the thermal building simulation which can predict air movement, temperature, contaminant distribution, as well as many other parameters of the room air distribution is Computational Fluid Dynamics (CFD). Unlike the multi-

zone modelling approach, CFD method has shown great potential in predicting the indoor air flow behavior [96]. In this method, the building zone is divided to a large number of control volumes and the Navier-Stokes equations are solved in these control volumes to precisely predict the air flow characteristics in the space [97]. Therefore, coupling BES software with CFD method can improve the quality of results and provide detailed information about the thermal load, building energy use, spatial air temperature and thermal comfort distributions. There are two methods of coupling BES and CFD, namely one-step and two-step coupling, which the first method only provides CFD with the boundary conditions obtained by BES while the latter also returns the simulated boundary conditions from CFD to BES. In this regard, several researchers investigated the coupling of BES and CFD.

Novoselac [98] developed a new tool for accurate analysis of building energy use and thermal comfort. Different coupling methods for exchanging data between BES and CFD were evaluated through two-step method. It was found that delivering heat flux to CFD as boundary conditions and giving surface temperature back to BES can provide more accurate calculation of surface heat flux than log-law wall functions in CFD. Tian et al. [99] made a comprehensive review on the methods and applications of integrating CFD to BES. They compared different one-step and two-step methods in terms of limitations, accuracy, stability, convergence, and speed for the co-simulation. The results showed that static coupling scheme can be used to transfer data fast between BES and CFD, because it performs data exchange only once. However, dynamic coupling schemes that allow multiple times of data exchange is preferred for transient simulation. Rodríguez-Vázquez et al. [100] reviewed the research studies in which the BES–CFD coupling was used to investigate building systems, building components, and building urban configurations. Their findings show that the integration of BES and CFD method provides an improvement that ranges between 10% and 50% for predicting the building energy requirements. Furthermore, the analysis showed that the computation time for implementing the CFD method could be reduced by importing the information from the BES. Shan et al. [101] coupled EnergyPlus for BES with FLUENT software for CFD simulation of the air temperature and PMV prediction. Furthermore, the air flow rates

across the virtual partition walls between two adjacent subzones obtained from CFD were given to EnergyPlus for using as inter-zone air flow. The aim was to find the optimal temperature set points for the subzones to achieve a uniform occupant thermal comfort and avoid overcooling in a large open office. Pandey et al. [102] also coupled the EnergyPlus and Ansys Fluent tools for BES-CFD simulations of phase change material (PCM) built environment and compared the results with those obtained from EnergyPlus. Their findings highlighted that the coupled simulation has better prediction accuracy than the BES tool for active use of PCM and passive use of PCM under forced convection. However, BES tool was recommended for modeling the passive use of PCM during natural convection.

As it can be noted, the literature studies suggest that coupling the BES and the CFD tools can provide more accurate information about the indoor air climate conditions than using the CFD tools entirely. Therefore, it is important to adopt the coupling method to better evaluate the quality of building retrofit measures in terms of indoor air thermal comfort conditions.

1.4.2.2. Visual comfort and daylight modelling

Light is a significant indoor environmental factor because it substantially affects the human perception of an environment. It can be divided to daylight and illumination by artificial light fittings, both needed for a desirable visual comfort. To analyze indoor daylight comfort, there are a large group of indexes detailing daylight conditions and availability, as shown in Fig. 6. Daylight availability shows the available daylight transmitted through facades into the room [65]. These indexes could be divided to static ones, such as the daylight factor (DF) and time dependent illuminances, and dynamic/climate-based indexes, such as daylight autonomy (DA), useful daylight illuminance (UDI), and annual sunlight exposure (ASE) [66-68]. In this regard, DF is defined as the percentage ratio of the inside illuminance at a fixed point to the outside horizontal illuminance under an overcast or uniform sky. This static metric depends only on the geometry, the architectural quality of buildings, and visible properties of glazing, because the location and orientation are insignificant with respect to an ideal cloudy sky.

Hence, the DF is a representative of the illuminance at a given point for the worst case condition under overcast sky conditions [69].

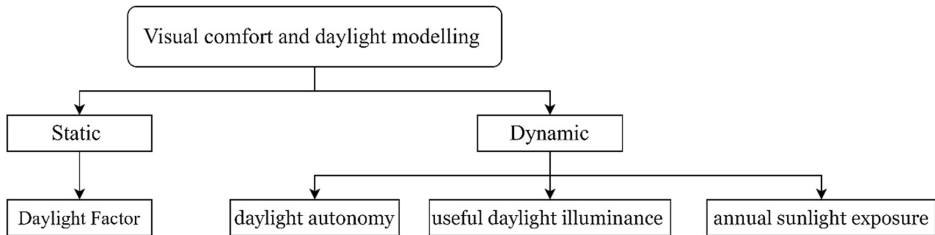


Fig. 6. Classification of visual comfort and daylight modelling methods

DA and UDI are defined as the percentage of the year when a minimum illuminance threshold and a specific illuminance limit are met by daylight alone, respectively. Therefore, these parameters, unlike DF, depend on the weather conditions, space location, occupancy hours, and shading control by occupants [66]. It is worth mentioning that in addition to daylight accessibility, visual comfort is also affected by glare problems. The indexes that evaluate risk of glare include the daylight glare index (DGI), daylight glare probability (DGP), and visual comfort availability (VCA). These indices calculate the vertical illuminance at the eye level and the luminance of different sources in the visual field that influences the space brightness [65, 70].

1.4.3. Life cycle assessment of greenhouse gas emissions in building retrofitting process

Reaching the greatest level of zero emission building in the retrofitting process, through reducing CO₂ emissions, requires a life cycle approach. A life cycle assessment (LCA) determines the potential environmental impact of a product or a service and is described in the ISO 14040:2006 [71] and ISO 14044:2006 [72] standards. A full LCA method can generally be divided to four phases:

- Determining the purpose and scope: It defines the objectives and scope of the analysis and includes system boundaries and level of detail. The scope of the analysis can vary greatly depending on the purpose and context in which the analysis is to be used.

- The Life Cycle Inventory (LCI): It involves collecting necessary environmental data about the system according to goals and scope and structuring the data in such a way that one can calculate the total environmental impact from the entire life cycle. The method used for the LCI is one of the main limitations in reliability of LCA studies.
- The Life Cycle Impact Assessment (LCIA): In this stage, the list of environmental emissions during the life cycle, collected from the inventory analysis, are translated to aggregated environmental impact categories so that the environmental significance of the results can be better understood.
- The interpretation phase: It includes interpretation and analysis of the results by finding the most important contributors in the system to be able to form a basis for conclusions, recommendations, and decisions according to purpose and scope.

Additionally, to evaluate different products against each other, the environmental performance deceleration (EPD) of the products should be studied. An EPD is an independently established document that transmits transparent and comparable information about the life cycle environmental impact of products and is based on ISO 14020 [73]. In Norway, there are more than 350 EPDs from over 100 companies published and freely available.

In the buildings' context, the LCA studies usually focus on the connection between the CO₂ or GHG emissions associated with extraction, construction, transport, installation, maintenance, and disposal of building construction materials (embodied emission/carbon) and those related to the energy used to operate the building while satisfying comfort conditions (operational emission/carbon). It should be underlined that although embodied energy and embodied carbon are two terms that are directly connected, the effect of any material on resource depletion and GHG may be different. It depends on the primary fuel used and the process of electricity production. In other words, the use of renewable energy can be considered to have zero emissions provided it is assumed that there is no embodied energy associated with collectors and generators [74, 75].

Technically, three different LCA methodologies for building retrofitting are used, as shown in Fig. 7. Three different ambition levels of LCA for building retrofitting The Full LCA method includes all the LCA stages as the following: Product stage (A1-3), Construction process stage (A4-5), Use stage (B1-7), and End of life stage (C1-4) as defined in EN 15978 standard [76]. The simplified method addresses only the assessment of the product (A1-3), replacement (B4) and operation energy use phase (B6). The operational stage assessment includes only the assessment impacts during the operational stage of the building [77].

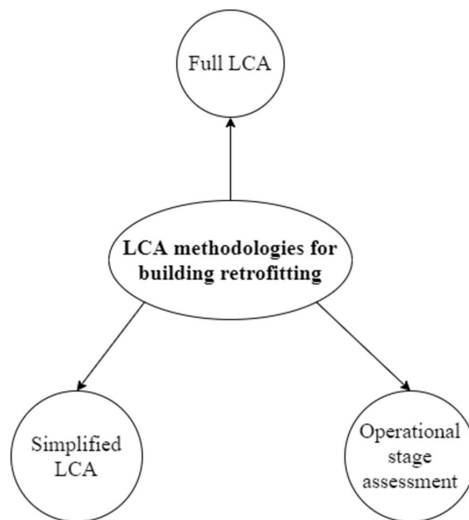


Fig. 7. Three different ambition levels of LCA for building retrofitting

Fig. 8 shows the stages related to LCA of buildings according to the EN 15987 [76]. As it can be seen, building retrofitting in LCA is described as its own module (B5), which includes several system boundaries as follows:

- New components' production of the building
- New components' transport
- Construction as part of the retrofitting process
- Waste management of the retrofitting process
- End of life of the replaced building components

Nevertheless, several interpretations have already been made considering different system boundaries in literature. It has been revealed that the main difference among the studies is due to the interpretation of the system boundaries, which makes it difficult to compare the results from different studies [74].

Various LCA tools are accessible to predict the life cycle impact of building retrofit interventions. To obtain reliable results, the selection of LCA software and tools becomes a crucial step in the LCA process. The accessibility of the impact category in a LCA tool depends on the impact evaluation method, which is available in the tool. Some software such as SimaPro [78] and GaBi [79] deliver a wide range of methods from energy evaluation and water traces to different impact category assessments. The methods can be prioritized according to the LCA scope. Some building-specific LCA tools such as Tally [80] and OneClick LCA [81] may provide the possibility to import data from building design and energy performance tools. These software has a plug-in to Revit, a 3D building information modelling tool. Furthermore, OneClick LCA, which is a web-based software, has a user-friendly platform that makes the LCA process straightforward for designers, especially when comparing different retrofitting measures [82].

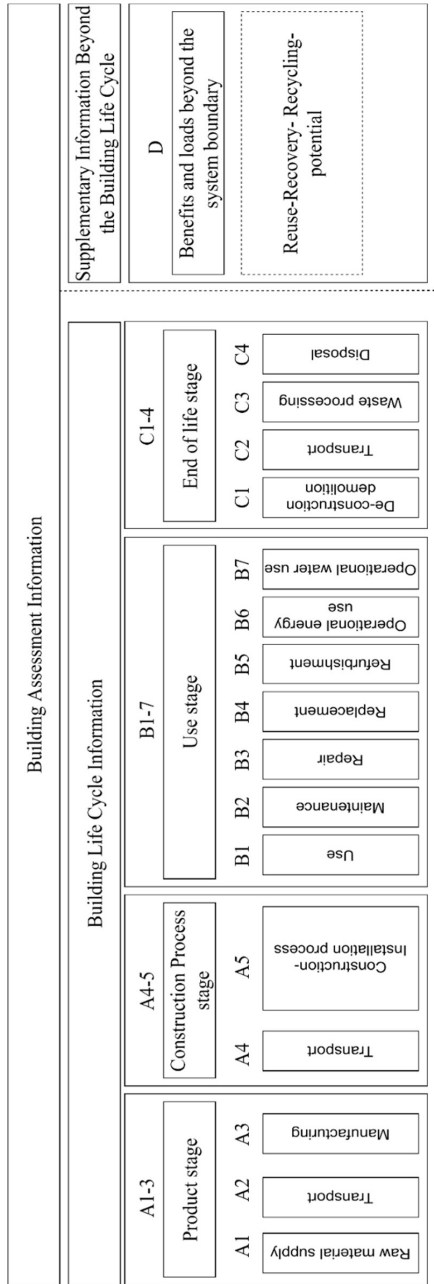


Fig. 8. Display of tailored information for different stages of the building assessment based on EN 15987 [76]

Many studies have investigated the environmental impacts associated with different stages of building retrofitting through LCA.

Asdrubali et al. [103] evaluated the energy use and carbon payback time of different retrofit scenarios for a school building through the LCA method for lifetime of 50 years in Northern Italy. Their findings show that a cost optimal case, in which the building energy use was around 70 kWh/m².year, had a carbon payback time around 3.2 years. Moschetti et al. [104] investigated alternative design solutions for a zero energy office building, located in Norway, in order to achieve a zero emission one. The building model was run using SimaPro tool, and the results revealed that it is difficult to totally balance the life cycle GHG emissions from materials by renewable energy, even with widespread use of PV panels. Piccardo et al. [105] conducted the LCA of a retrofitted Swedish building to passive house level. They considered various scenarios including use of different building materials and different electricity production scenarios. They pointed out that a careful choice of building materials can result in maximum 68% reduction of the net CO₂-eq in the retrofitted building than in the reference case, notably when selecting the wood material for building frames. Chen et al. [106] presented a multi-criteria evaluation approach for retrofitting of a residential building located in Norway. The aim was to reduce the primary energy, global costs, payback period and the CO₂ emission. Regarding the environmental impact, an CO₂-eq factor, corresponding to the emissions from different GHGs generated only during building operation, was considered on a time frame of 100 years. The results showed the CO₂-eq can drop up to 10.4 kg CO₂-eq/m². Pal et al. [107] proposed a LCA optimization approach to find the carbon-cost optimal solutions in terms of both operational and embodied CO₂ emissions for a house in Finland. The results showed that when the carbon optimal solution was the matter of concern, the contribution of carbon embodied emissions in the LCA process was 39%, while in the cost optimal solution, its share was reduced to 28%. Kristjansdottir et al. [108] studied the feasibility of achieving a zero emission building level, in terms of the life cycle energy and the material emission balance, through redesigning a single family pilot building located in Norway. The findings revealed that the embodied emissions can be compensated up to 60% using the new model. However, they pointed out that an

optimization of building design is necessary to reach the balance of the life cycle energy and material emissions. Wrålsen et al. [109] studied the LCA of retrofitting a residential building block from 1960s to nearly Norwegian passive house standard level over a 30 years period. The results of upgrading showed that all environmental impact categories reduced around 56-96% compared to the reference case, and the carbon payback period was 1.09 year. Llantoy et al. [110] developed a comparative LCA by focusing on different building insulation materials including polyurethane, extruded polystyrene, and mineral wool in several experimental cubicles located in Spain. The results showed that although all insulation materials demonstrated a net positive benefit over the lifetime 55 years, the highest environmental impact was corresponding to the polystyrene insulation material and the lowest one was for the mineral wool. Luo and Cheng [111] established a LCA of residential building materials in different regions in China. The results showed that the amount of CO₂ emissions in extreme cold area and hot summer/warm winter area was the largest and the smallest, respectively.

As the previous conducted LCA studies show, the environmental impacts associated with the building retrofitting are more pronounced in cold climate than in warm climate. In this regard, analysis of the LCA studies on Norwegian building stock show the potential of retrofitting in reducing the total environmental impacts of building life cycle with a short payback period. However, these studies did not investigate the environmental impacts associated with the optimal retrofit measures obtained based on different space heating and ventilation systems in Norwegian office buildings. Therefore, such analysis would provide worthwhile insights into the choice of a sustainable set of retrofit measures in the Norwegian office buildings towards nZEB.

1.5. All-air heating/cooling system application in building retrofitting practice

All-air (AA) systems have been conventionally used in North America and in several other parts of the world influenced by the USA, e.g., parts of Asia and the United Kingdom. AA generally means the supply of warm/cold air at acceptably hygienic airflow rates, usually via a ventilation system. Space cooling, heating, and dehumidification of the supply air delivered to the building rooms is the main function of this system.

Heating application of the AA systems is a challenging issue where SH needs are not negligible, due to almost constantly running of the fan to provide space heating in the zones. This implies that conventional AA systems are less suitable for Northern European climate, which is one the reasons why air-water system (space cooling (SC) by the ventilation system and space heating by hydronic radiator) is the major means for space heating and cooling in Northern Europe [60].

There are several types of AA systems which are mainly divided to single-duct, dual-duct, and multi-zone systems, as shown in Fig. 9 [60].

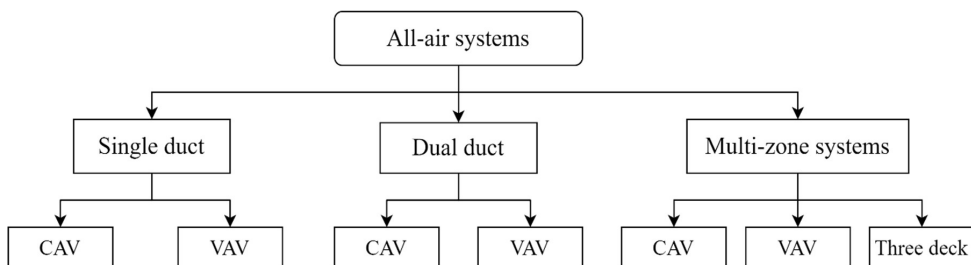


Fig. 9. Different types of the all-air systems

In the first type of AA system, the single duct, a low supply air temperature is provided by the air handling unit (AHU). If there is heating need for zones, the air temperature can be increased either centrally or in each zone, typically using a reheat coil before the supply air terminal. In dual-duct systems, one duct has a high temperature and the other one has a low temperature. In the zones, the supply air from the two ducts is mixed to the required supply air temperature in a dual duct box. In the multi-zone system,

each zone is supplied with a separate duct from AHU. The three deck system is a special type of multi-zone system and it is designed to handle the climates in Texas. Furthermore, in the constant air volume (CAV) system, the airflow rate is kept constant while the supply air temperature is varied if space heating/cooling is needed in zones. On the contrary, in the variable air volume (VAV) system, the supply air temperature is kept constant, whereas the airflow rate is changed depending on the heat load in zones. It should be noted that if the airflow rate in the VAV system is controlled by other factors than temperature, such as CO₂, pressure, and humidity, it is called demand control ventilation (DCV) [60].

From an economic and environmental point of view, AA could be an interesting solution for HVAC purposes because it can avoid the need for local space heating installations, such as radiators, and the costs and environmental impacts associated with the material use for their distribution system. However, the heating performance of the AA system, especially mixing ventilation method, might be questioned depending on the supply air temperature, outdoor conditions, and airflow rate. Early studies carried out on a simple form of room heating using overheated supply air temperature at ceiling level in 1970s showed a significant vertical temperature gradient (temperature stratification) and poor indoor air quality (IAQ) in the occupied zone. The reason was the poor quality of the building envelope and high space heating needs [83]. Several studies also reported the short-circuiting of the ventilation air between the supply air diffuser and the return terminals, especially when the exhaust terminal is located at ceiling levels [84, 85]. This implies that adopting only an efficient AA system unit may not be sufficient for achieving an energy efficient retrofitting. In other words, the efficiency of the AA system in retrofitting practice should be considered along with the combined effect of other factors such as decrease in space heating needs.

1.6. Evolution of PhD

Building retrofitting to the low-energy or the PH level can be considered as the ambitious level on a transitional way towards nearly zero energy building (nZEB). So far, numerous studies have investigated the building retrofitting towards the aforementioned ambition levels through the optimization of building energy performance. As it was described in Section 1.4.1, the common retrofit measures include improvement of building envelope, windows area, type of glazing, solar shading types, and set point controls of HVAC system in previous conducted studies. While such studies coupled various BES and optimization tools to evaluate the efficiency of retrofit measures, there are few-to-no studies used optimization process for the assessment of retrofit measures in Norwegian office buildings in detail. In addition, in literature studies, the coupling between BES and optimization tools was mostly based on developing and implementing optimization algorithms using programming languages [[47](#), [51](#), [52](#), [54](#)].

In the first stage of this PhD work, the above-mentioned retrofit measures were evaluated through a different optimization approach for a typical Norwegian office building. The design of the renovation was targeting the achievement of nZEB level. This study was the basis for several subsequent research questions that have been late answered during this PhD work.

In the following sections, how the research questions and objectives of this study were determined, what challenges were faced during this period, and how these challenges have been addressed are briefly described.

As mentioned, the first step of the study started by evaluating retrofitting of a Norwegian office building through optimization method. The main goal was to achieve nZEB with better indoor thermal comfort compared to the reference building designed according to the Norwegian building regulation TEK 10. The goal was achieved through two different strategies; in the first strategy, the possibility of minimizing the LCC of the energy retrofitting measures was assessed, while the energy use for SH and SC was

constrained to the Norwegian PH standard level. In the second strategy, minimizing the annual delivered energy to the building was evaluated while the LCC of the energy retrofitting measures was limited. In both strategies, two types of HVAC systems including radiator space heating (RSH) and AA were considered. For this task, the GenOpt optimization tool was coupled with IDA-ICE building performance simulation software. Instead of using programming language, the most prevalent method in previous studies, the integration was developed through a Graphical Script (GS) interface that implements an algorithm through an illustrative framework. The study was published in a journal paper as follows:

- **Paper I:** Rabani, H. Bayera Madessa, O. Mohseni, N. Nord, **Minimizing delivered energy and life cycle cost using Graphical script: An office building retrofitting case**, *Applied Energy*, 268 (2020).

The results of this optimization study showed that:

- Ground floor and the roof retrofitting are the costliest measures and should not be prioritized to window and external wall renovation in office building retrofitting in Norway.
- Existing Norwegian office buildings can achieve up to 55% better energy performance than the low energy buildings through retrofitting.

This PhD study raised the following research questions which became the basis for the next stages of the PhD work:

- In the study, the optimized solutions could reduce the building energy use considerably with higher thermal comfort than the reference TEK 10 building, similar to low energy building level. The question arose here was: To what extent the energy use could be reduced if the reference building is relatively old, and other criteria such as visual comfort is also considered in the optimization study?

- How much the energy savings with improved thermal and visual comfort conditions would be if the retrofitting includes a larger set of design variables in the energy optimization of Norwegian office buildings?

To answer these questions, firstly, an analysis on the construction year of Norwegian office buildings revealed that the majority of existing office buildings were built in the 1980s corresponding to Norwegian building regulation TEK 87. Therefore, the characteristics of the reference building was considered based on TEK 87. Furthermore, to have a more realistic pattern of internal heat load due to occupants and lighting, a measurement-based data of several cell offices in an office building in Norway was used [112]. To proceed with this study, the next step was to determine a large group of potential retrofit measures. Based on the results obtained in the first paper, the roof and floor retrofitting were omitted from the set of optimization design variables. In this process, it was important to carry out a review of the previous conducted studies to identify the new design variables influencing energy performance and thermal and visual comfort conditions simultaneously. Analyzing the previous studies highlighted the lack of including the combined effect of window opening and shading device control strategies with other common design variables. These parameters were accordingly introduced to this stage of optimization study. The results were critically analyzed in the paper:

- **Paper II:** M. Rabani, H. Bayera Madessa, N. Nord, **Achieving zero-energy building performance with thermal and visual comfort enhancement through optimization of fenestration, envelope, shading device, and energy supply system**, *Sustainable Energy Technologies and Assessments*, 44 (2021) 101020.

In the optimization process in this study, a daylight factor constraint function, based on the TEK 17 requirements, was considered as the new proposed design variables would substantially affect the visual comfort as well. The results underlined the critical role of physical and functional properties of windows when optimizing the building energy performance towards ZEB. However, this study was only focused on the conventional space heating and ventilation system in the Norwegian office buildings.

This posed another question: What the optimal set of the retrofit measures would be when an AA system is used in the Norwegian office buildings? How the energy performance and thermal and visual comfort conditions would be for the optimal solution in AA compared to that in the conventional HVAC system? These questions were answered in the following paper:

- **Paper III:** M. Rabani, H. Bayera Madessa, N. Nord, **Building retrofitting through coupling of building energy simulation-optimization tool with CFD and Daylight programs**, *Energies* 14(8) (2021) 2180.

During this PhD work, it was realized that there is a lack of detailed evaluation of thermal and visual comfort conditions. This was due to the fact that the volume/surface average values of thermal and visual comfort metrics were used in the optimization studies. In this regard, the literature studies suggest that coupling the BES tool with the CFD tools could provide detailed information about the indoor air climate conditions. However, there was no study adopting the integration of the BES, optimization, CFD, and daylight simulation tools for evaluating the quality of building retrofit measures for the Norwegian office buildings. The results of this PhD work compared the quality of optimal set of retrofit interventions for the two aforementioned HVAC systems and the reference TEK 87 building.

The final step to evaluate the environmental performance of the optimal retrofit measures, obtained in the previous steps, towards nZEB level, was analyzing the environmental impacts associated with these retrofit measures. For this purpose, a LCA analysis of the emissions corresponding to the optimal set of retrofit measures was conducted for both the conventional space heating system and the AA system. The details of the LCA method and the corresponding results were presented in the following paper:

- **Paper IV:** M. Rabani, H. Bayera Madessa, M. Ljungström, L. Aamodt, S. Løvvold, N. Nord, **Life cycle analysis of GHG emissions from retrofitting of building: The case of a Norwegian office building**, *Building and Environment*, 204 (2021) 108159.

1.7. Research objectives

The aim of this work was to identify an optimal set of retrofitting interventions for the existing office buildings in Norway towards nZEB level by considering energy, cost, occupant comfort, and environmental impacts. The main objectives of this work were focused on:

1. Determining an optimal set of retrofit interventions in terms of their cost-effectiveness, energy performance, and thermal comfort satisfaction considering both the AA system and the conventional space heating system. The aim was to provide technical insights for engineers and building professionals for sustainable transition of existing Norwegian office towards nZEB level.
2. Identifying an optimal set of retrofit measures that substantially improves the energy performance of the Norwegian office buildings and satisfies both the visual and thermal comfort of occupant.
3. LCA of the environmental impacts associated with the optimal retrofit solutions to provide further insights into how to achieve a net zero emission building.

The research objectives have been developed into the following research questions:

- Question 1: What retrofitting measures are more cost-effective and energy efficient in renovating the Norwegian office buildings considering both the AA system and the conventional space heating system?
- Question 2: To what extent the energy performance and thermal and visual comfort conditions of Norwegian office buildings can be improved through optimizing a large group of retrofit measures?
- Question 3: What are the environmental impacts of building retrofitting towards the nZEB level?

1.8. Thesis content

According to the tasks of this research, the thesis is divided into the six main chapters as the following:

- Chapter 2 provides a sustainable definition of the building retrofit measures and presents the requirements to achieve the ZEB level. In this regard, various aspects of the sustainable retrofitting including building energy performance, indoor climate conditions, and cost effectiveness of the retrofit measures along with their corresponding environmental impacts are discussed in the Norwegian building context. This chapter also presents a zero energy balance based on the annual balance between the weighted demand and the weighted supply.
- Chapter 3 presents the characteristics of Norwegian office buildings for assessment of the considered retrofit measures.
- Chapter 4 focuses on the details of building energy performance optimization and small retrofitting process. Various optimization frameworks are illustrated in terms of input parameters, constraints, objective functions, and the type of simulation tools adopted in the optimization process. In addition, the CFD and daylight analysis of indoor climate conditions for the optimal retrofit solutions and the LCA of their corresponding environmental impacts are considered as post-processing. Afterwards, the results are presented and discussed.
- Chapter 5 demonstrates the main conclusion of the PhD study along with the limitations of the research. Finally, the recommendations for the future work are presented.

The main results of the PhD research were introduced in the papers attached at the end of the thesis. The list of these papers is given below in Section 1.10.

1.9. Contribution to publications

The PhD thesis is comprised of four papers published in high-quality journals. The publications are associated with the research questions posed in the PhD study, and their connection to the research questions is given in Table 2.

Table 2. Connection between research questions and publications

Research questions	Pub. 1	Pub. 2	Pub. 3	Pub. 4
Question 1: What retrofitting measures are more cost-effective and energy efficient in renovating the Norwegian office buildings considering both the AA system and the conventional space heating system.				
Question 2: To what extent the energy performance and thermal and visual comfort conditions of Norwegian office buildings can be improved through optimizing a large group of retrofit measures?				
Question 3: What are the environmental impacts of building retrofitting towards the nZEB level?				

The author contribution to the papers is given as follows:

- **Paper 1:** M. Rabani, H. Bayera Madessa, O. Mohseni, N. Nord, Minimizing delivered energy and life cycle cost using Graphical script: An office building retrofitting case, *Applied Energy*, 268 (2020).

Author contribution: I initiated the paper by developing the methodology and the optimization framework. Omid Mohseni contributed to the implementation of optimization process and running the simulations. Habtamu Bayera Madessa carried out the supervision and reviewing the LCC and optimization process. Natasa Nord held supervision, revision and editing the paper.

- **Paper 2:** M. Rabani, H. Bayera Madessa, N. Nord, Achieving zero-energy building performance with thermal and visual comfort enhancement through optimization of fenestration, envelope, shading device, and energy supply system, *Sustainable Energy Technologies and Assessments*, 44 (2021) 101020.

Author contribution: I conceptualized the paper. I, as the main author, developed the optimization framework including building automation control system with envelope

retrofitting. The co-authors Natasa Nord and Habtamu Bayera Madessa formulated the research objectives, conducted supervision, and revision of the paper.

- **Paper 3:** M. Rabani, H. Bayera Madessa, N. Nord, Building retrofitting through coupling of building energy simulation-optimization tool with CFD and Daylight programs, *Energies* 14(8) (2021) 2180.

Author contribution: The paper was initiated by me. I developed the methodology and carried out the optimization and energy and daylight simulations. I also wrote the original draft of the paper. Natasa Nord and Habtamu Bayera Madessa performed formal analysis for the research methodology along with supervision, revision, and editing the paper.

- **Paper 4:** M. Rabani, H. Bayera Madessa, M. Ljungström, L. Aamodt, S. Løvvold, N. Nord, Life cycle analysis of GHG emissions from retrofitting of building: The case of a Norwegian office building, submitted to *Building and Environment*.

Author contribution: The concept of the paper was developed by the joint efforts of all the co-authors. I prepared the literature review, contributed to the LCA computations and analysis the results. I also wrote the original draft. Malin Ljungström, Lene Aamodt, and Sandra Løvvold provided the LCA inventory and performed the LCA computations. Habtamu Bayera Madessa made a formal analysis of the research method and conducted supervision, and revision of the paper. Natasa Nord undertook supervision, reviewing of the results, and thorough revision and editing of the paper.

2. Method

This section presents the definition of the sustainable building retrofitting and explains its criteria contributing to achieve ZEB level. These criteria include energy reduction with the increase share of renewable energy sources, thermal and visual comfort of occupant according to the Norwegian building regulations, and cost-effectiveness along with environmental impact mitigation of the retrofit measures.

Sustainable building retrofitting may be defined as measures improving the energy performance of the buildings. It is generally achieved by decreasing the energy need of building, improving the efficiency of the systems dealing with non-renewable energy sources, and increasing the use of renewable energy sources in building energy supply system towards ZEB level.

Nevertheless, improving building energy performance cannot solely be considered as the sustainable building renovation. According to TEK17 and ASHRAE standards concerning the satisfaction of occupants, the effectiveness of retrofitting should be assessed based on the occupants' perception in terms of combination of the indoor air temperature, humidity, IAQ, as well as daylight conditions [8, 113]. Furthermore, it has been required by energy policies [114] and Energy Performance Building Directives (EPBD) [2] that economic analysis of the measures dealing with the sustained financial profits, such as LCC of retrofit interventions, should be applied. It is also important that the retrofit measures assist in reducing the environmental impacts associated with different stages of building life cycle to achieve the EU target regarding climate change mitigation [115]. Therefore, selecting the most effective retrofitting scenario in Norwegian office buildings should be in accordance with in-depth understanding about predominant local climate conditions, present building energy use levels, and the characteristics of the Norwegian office buildings. In this respect, sustainable building retrofitting was defined in this thesis as shown in Fig. 10. The five criteria of the sustainable building retrofitting include energy reduction with increased share of renewable energy sources, prolonged cost effectiveness, environmental impact mitigation, and thermal and visual comfort of occupant.

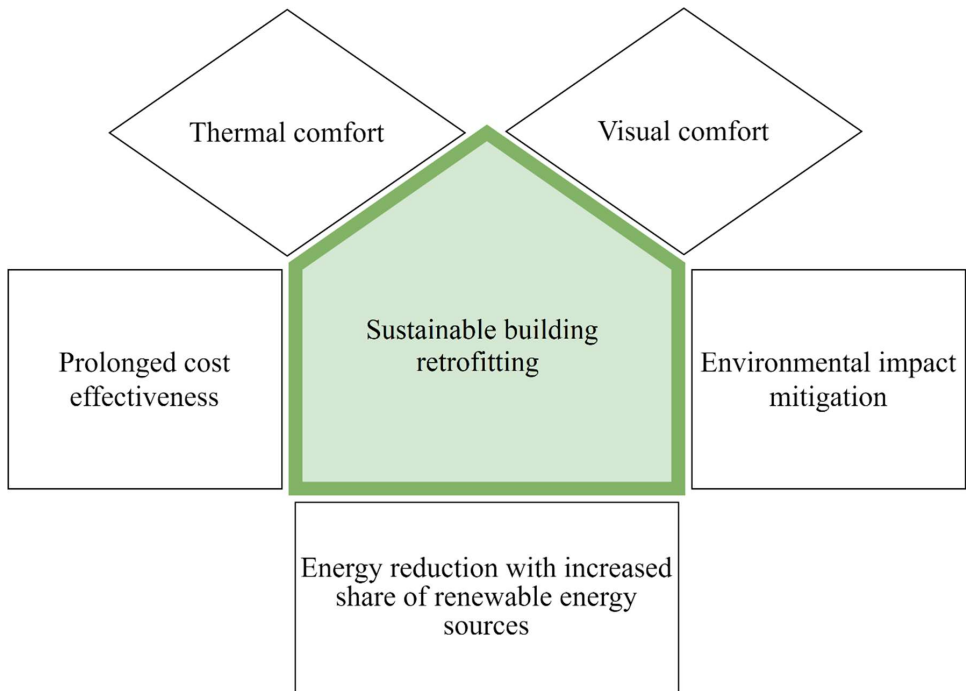


Fig. 10. Definition of the sustainable building retrofitting

2.1. Building energy performance

In this thesis the building energy performance was assessed in terms of delivered energy and primary energy, which the latter was used for ZEB analysis. The delivered energy is defined the sum of energy, expressed per energy commodity, delivered over the building's system boundaries to cover the building's overall energy need including system losses that are not (cannot be) recovered [116]. The primary energy means estimation of energy resources use in its original form which has not been transformed or converted into other energy forms. The primary energy was modelled by multiplying delivered energy by the associated primary energy factors for the considered energy carrier in Norway [117].

The energy calculations were performed using Indoor Climate and dynamic Energy Performance Simulation Program, IDA-ICE. It has broadly used and validated by ASHRAE 140–2004 CEN 13791, CEN 15255, CEN 15256 (2007), Technical

Memorandum 33 (TM33), and International Energy Agency SHC Task 34 [118]. Furthermore, the software includes several platforms and user interfaces for developing control macros for different components of building envelope and HVAC systems. The simulations were performed on hourly basis with maximum dynamic time step 1.5h and tolerance 0.02.

To evaluate the energy saving of retrofit interventions, IDA-ICE software was coupled with the generic optimization program, GenOpt [119]. The software has a well-proven background in building optimization projects along with a newly developed user interface in IDA-ICE software. This interface facilitates optimizing different types of design variables, HVAC system parameters, and their control strategies.

Regarding the coupling of optimization and BES tools, instead of using programming languages that were frequently adopted in literature studies, the process was implemented through the Graphical Script (GS) module. This module is an available interface in IDA-ICE software in which various sets of optimization input parameters, objectives, and constraints can be considered through an illustrative way by inserting and connecting components. The GS module is executed by IDA modeler without starting the IDA solver and it makes the manipulation of constraint functions, input parameters, and objective functions more understandable and convenient than the previous methods. Its principle can also be implemented in various energy simulation tools. The Particle Swarm Optimization (PSO) algorithm was selected as the main algorithm in the optimization process. Although NSGA II algorithm was reported as the most adopted algorithm in the previous conducted optimization studies [120], the PSO algorithm was preferred in this study due to its fast and simple computation properties. This was especially important as a large group of optimization input parameters were considered in the optimization tasks during the PhD work.

Additionally, in the optimization process, where the specific building energy need for space heating and cooling was required to be calculated for PH level, the following equations, defined based on Norwegian PH standard NS 3701 for commercial buildings [10], were used. It should be mentioned that the equations give the maximum allowed energy use for building space heating and cooling according to NS 3701.

$$E = EP_{H,0} + K_1(6.3 - \theta_{ym}) \quad (1)$$

$$Q_c = \beta(DUT_s - 20) \quad (2)$$

where E (kWh/(m².year)) and Q_c (kWh/(m².year)) were the specific space heating and space cooling needs respectively, $EP_{H,0}$ (kWh/(m².year)) was the basis for space heating calculation, K_1 was the climate coefficient for space heating calculation, θ_{ym} (°C) was annual average outdoor temperature. In addition, β was the space cooling coefficient and DUT_s (°C) was the outdoor temperature over 20°C in summer condition that did not exceed 50 hours in a normal year. The values of $EP_{H,0}$, K_1 and β were 20 kWh/(m².year), 3.6 and 1.4 kWh/(m².year.°C) for Norwegian office buildings. It should be noted that the Eq. (1) was used provided the building area was larger than 1000 m² and the annual average outdoor temperature was greater than 6.3°C [10].

2.2. Thermal comfort of occupants

The thermal comfort was evaluated in terms of predicted mean vote (PMV), predicted percentage dissatisfied (PPD), operative temperature, and air temperature stratification. The PMV and PPD metrics were calculated using the following equations:

$$PMV = (0.303 \cdot \exp(-0.036 \cdot M) + 0.028) \cdot L \quad (3)$$

where M is the metabolic rate and L is the thermal load on the body expressed as Eq. (4) [121].

$$\begin{aligned} L = M - \frac{3.05}{1000} \cdot (5733 - 6.99 \cdot (M - W) - Pa) - 0.42 \\ \cdot (M - W - 58.15) - \frac{1.7}{1000} \cdot (5867 - Pa) - 0.0014 \cdot M \\ \cdot (34 - Ta) - 3.96 \cdot 10^{-8} \cdot Fcl \\ \cdot ((Tcl + 273)^4 - (Tr + 273)^4) - Fcl \cdot hc \cdot (Tcl - Ta) \end{aligned} \quad (4)$$

where W is the active work, Fcl is the clothing area factor, hc (W/(m².K)) is the convective heat transfer coefficient, and Pa and Ta are the air pressure and temperature, respectively. The clothing surface temperature (Tcl (°C)) is calculated as follows:

$$\begin{aligned}
T_{cl} = & 35.7 - 0.028 \cdot (M - W) - 0.155 \cdot I_{cl} \\
& \cdot (3.96 \cdot 10^{-8} \cdot F_{cl} \cdot ((T_{cl} + 273)^4 - (T_r + 273)^4) + F_{cl} \cdot hc \\
& \cdot (T_{cl} - T_a)) \quad (5)
\end{aligned}$$

PPD was then given as Eq. (6)

$$PPD = 100 - 95 \cdot \exp(-0.03353 \cdot PMV^4 - 0.2179 \cdot PMV^2) \quad (6)$$

The criteria for these metrics and air temperature stratification were selected based on the comfort categories described in EN 15251 [122] and ISO 7730 [121] standards, as presented in Table 3. Category II is often regarded as the criterion for the office buildings.

Table 3. Categories of thermal environment

Category	PMV	PPD (%)	Temperature stratification * (K)
I	-0.2<PMV<0.2	< 6	< 2
II	-0.5<PMV<0.5	< 10	< 3
III	-0.7<PMV<0.7	< 15	< 4
IV	Above/under 0.7/-0.7	Above 15	Above 4

* between 0.1 and 1.1 m above the floor

Regarding the operative temperature, the requirements set by TEK 17 and the Norwegian Labor Inspection Authority 444 were considered in this thesis, stating a desirable operative temperature range between 19-26°C for easy work [123]. TEK17 also allows for a certain exceedance of the highest operative temperature limit at high outdoor temperature. The limit can be exceeded when the outdoor air temperature is higher than the limit value (outdoor air temperature) which in a normal year is exceeded by 50 hours.

The comfort metrics were implemented using both multizone technique and detailed CFD. The former technique was applied in IDA-ICE software using yearly dynamic simulation, which gave an annual average variation of the results. The detailed CFD analysis was implemented using OpenFOAM software that latter is already integrated in IDA-ICE. For this purpose, the spatial air temperature and velocity were first derived in the software through steady state and turbulent flow simulations.

Afterwards, the obtained results were exported to MATLAB for post-processing and calculation of PPD and PMV.

2.3. Visual comfort and daylight quality

In this thesis, both static and dynamic daylight indexes were investigated. The DF was considered as the static metric and UDI and DA (two types) were adopted as the dynamic metrics for daylight analysis. The daylight simulations were performed in the Radiance tool [124], which was already integrated with IDA-ICE software through the Daylight-tab in the software. In this regard, IDA-ICE employed the Radiance's genBSDF program to assess the solar bidirectional properties of the complex fenestration system with controllable shading. In addition, in the analysis of DF index, simulations were performed by considering super high precision, CIE Overcast sky type, and daylight measurement at desktop level. The reflection factors for the internal surfaces were selected based on the standard values stated in [125]. Accordingly, reflection factors 0.2, 0.5, and 0.7 were chosen for the internal floor, internal wall, and ceiling, respectively.

To analyze the dynamic daylight indexes, three metrics including UDI, continuous DA (cDA), and spatial DA (sDA) were calculated using Eqs. (7)-(9). cDA represents the percentage of the workhours when the illuminance is over or under a predefined threshold and sDA shows the percentage of the occupied hours when the illuminance is equal or greater than a specified limit [126, 127].

$$UDI(Pt_i) = \frac{1}{n} \sum_{j=1}^n H(L(Pt_i, j)) \times 100 \quad H(x) = \begin{cases} 1 & \text{Min} < x \leq \text{Max} \\ 0 & \text{out of range} \end{cases} \quad (7)$$

$$cDA(Pt_i) = \frac{1}{m} \sum_{j=1}^m H(L(Pt_i, j)) \times 100 \quad H(x) = \begin{cases} 1 & x \geq L_{Limit} \\ \frac{x}{L_{Limit}} & x < L_{Limit} \end{cases} \quad (8)$$

$$sDA(Pt_i) = \frac{1}{n} \sum_{j=1}^n H(L(Pt_i, j)) \times 100 \quad H(x) = \begin{cases} 1 & x \geq L_{Limit} \\ 0 & x < L_{Limit} \end{cases} \quad (9)$$

where n and m refer to total occupancy and daytime hours, respectively. In addition, $L(Pt_i, j)$ represents the daylight simulation results at point i (Pt_i) and time step j , $H(x)$ was

a function representing the illuminance value, and L_{Limit} was the illuminance limit determined by different standards. Therefore, a whole year illuminance daylight simulation with climate-based sky type (Perez), high precision, and controllable shading according to control signal were performed for evaluating the dynamic abovementioned metrics. It is worth pointing out that the Eqs. (7-9) were implemented in IDA-ICE using a MATLAB script.

Regarding the Norwegian Building Regulation for the daylight factor, TEK17 states that the average DF should be equal or greater than 2.0% for the most critical room regarding adequate daylight. However, the requirements concerning the dynamic daylight metrics are not still standardized in Norway.

2.4. Cost effectiveness of the retrofit measures

In this thesis, the cost effectiveness of the retrofit interventions was considered in the optimization process through LCC approach. The LCC (NOK), given in Eq. (10), included the following parts: (1) the total building cost, which represented the annual building operational cost (LCC_e), (2) the investment cost of building renovation measures such as building envelope refurbishments and improvement of HVAC system (IC_m), and (3) replacement cost of various components (RC), as follows:

$$LCC = LCC_e + IC_m + RC \quad (10)$$

where RC was the cost associated with replacing the old windows and replacement of necessary HVAC components due to maintenance. The profitability of the retrofitting measures was calculated using Eq. (11) as suggested in [128].

$$dLCC_i = LCC_i - LCC_r \quad (11)$$

where $dLCC_i$ (NOK) was the difference between the LCC after (LCC_i) and before (LCC_r) retrofitting. Moreover, LCC_e in this thesis was calculated using the net present value NPV of the operational costs during the building lifetime as shown in Eqs. (12) and (13).

$$LCC_e = ae_p E \quad (12)$$

$$a = \frac{1 - (a + r_e)^{-n}}{r_e} \quad , \quad r_e = \left(\frac{i - f}{1 + f} \right) - \frac{e}{1 + e} \quad (13)$$

where E (kWh/(m².year)) was the annual delivered energy, n was the lifetime, f was the inflation, e was the escalation rate, e_p was the energy price [129], and i was the nominal interest rate. It should be noted that the investment costs were based on the typical data from the Norwegian Price Book year, retrieved in 2019 [130].

2.5. Environmental impact of the retrofit measures

A LCA method was used for evaluating the environmental impacts associated with retrofitting of the building during its entire life cycle, which was described in terms of CO₂-eq. The analysis was implemented through a “cradle-to-grave” approach and using OneClick LCA software to address all the upstream and downstream stages before, including, and after the building operational energy use phase. The software was used for the LCA in accordance with the method described in national Norwegian standard NS 3720 [131]. OneClick LCA includes twelve third-party certifications and complies with more than 30 certifications and standards for life cycle assessment, including NS 3720. Data points used in the life cycle analysis were mainly Norwegian EPDs for Norway or other Nordic countries. In cases where none of the aforementioned databases were accessible, data from other countries are used.

The assumptions and the sources used for the greenhouse gas calculations at different life cycle stages in the OneClick LCA are shown in Table 4. In the LCA of the retrofit measures, the reuse, recovery, and recycling potential of materials/components (phase D in Fig. 8) were not taken into account due to considering a cut-off system modelling approach. This implies that the avoided burdens of the recyclable materials were not modelled throughout the way to where they are recycled to new production. Regarding the environmental impacts related to the building operational energy use (stage B6), the LCA tool performs the calculations based on electricity mix for 2050 from NS 3720 standard and latest 3-year average electricity mix (2016-2018) from IEA. It assumes that, during 60-year average, impacts will decline linearly until 2050 and remain at that

level until end of period. Full LCA inventory was calculated based on the data from eco-invent 3.3 with allocation by cut-off and CML-IA v 4.1, 2012 methodology. Electricity production efficiencies are based on Energy Efficiency indicators for Public Electricity Production from fossil fuels, IEA 2008 and Efficiency in electricity generation, Eurelectric 2003. Transmission losses of 6 % for 2050 scenario are assumed based on 3-year average (2016-2018) [132].

Table 4. Assumptions and sources used for the LCA method

LCA stage	Source/assumption
Material quantities in production stage (A1-A3)	Quantities and material types were entered manually in the LCA tool based on the requirements for the reference building case and retrofit cases.
Transport of material to the production site (A4)	Automatic regional transport scenarios were used representing typical transport distances. If there was no data for the materials, the LCA's Norwegian default distance was used. The vehicles' type used for transportation was modeled using the available database, so that the maximum capacity of the vehicles nearly matches the transported mass.
Construction and installation work (A5)	Emission from waste materials associated with the construction and installation work was calculated based on the available standard values for each individual product.
Replacement and retrofitting (B4-B5)	Estimated lifetime was based on typical values for each material. Maintenance and repairs were omitted from the assessment as the materials were assumed to be replaced at the end of their technical life.
Operational energy use (B6)	Emissions from energy use were calculated based on the findings from building energy simulations and optimization in BES tool
End of life service (C1-C4)	Emissions in connection with the end-of-life service were calculated according to the default scenarios in the tool representing the typical procedures for different types of material in accordance with the requirements in the Norwegian standard NS 3720.

Fig. 11 illustrates all the life cycle stages for building constructions. In this thesis, the focus was on the building CO₂ emissions, from four main stages, i.e. production of materials, construction phase, operation stage, and end of life (filled green and red boxes).

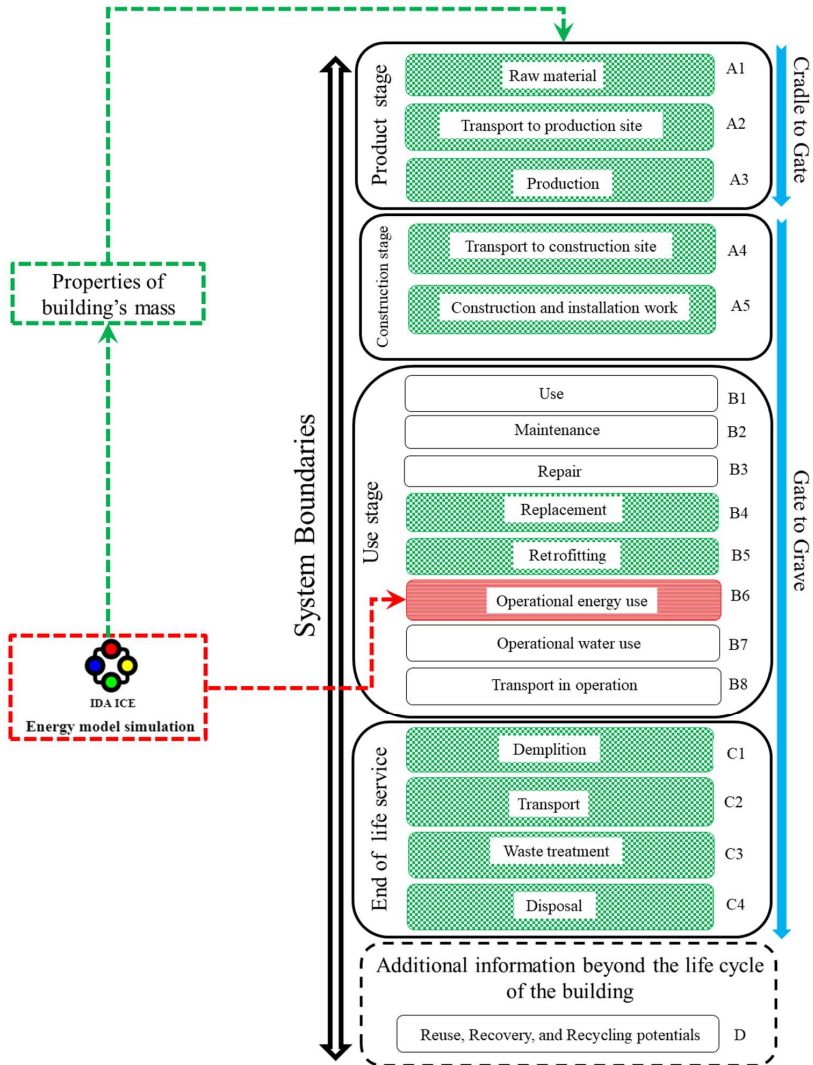


Fig. 11. Entire building life cycle stages according to NS 3720 [131] In color: those taken into account in the boundaries of LCA in this thesis. : Stages assessed through LCA tool database. : Those evaluated using information provided by BES tool. : Those not considered in this thesis

The first stage included extraction of raw materials, transport of them to the production site, and production (A1-A3). The second stage encompassed transportation of materials/components to the construction site, construction, and installation work (A4-A5). The embodied emissions related to the operation of the building included renovation and replacement of building materials and components during life service of the building (B2-B5). The embodied emissions in the last phase covered the demolition, transportation, waste processing, and disposal (C1-C4). The life service period for the retrofitted building and the reference case study was assumed to be 60 years. The input for calculation of CO₂ emissions associated with the operational energy use (B6) in the LCA tool, was based on the energy simulations performed in IDA-ICE version 4.8 SP2 by considering the details of retrofitting approaches described in previous sections [133]. In the product stage (A1-A3), the quantity of materials and technical information of the building structural foundation, which mostly concerned the reference building, and their corresponding CO₂ emission were obtained from the archive for the Norwegian Building Research Series for the office buildings constructed in the 1980s (TEK 87) [134].

For the retrofit solutions, only the quantity and CO₂ emissions associated with the extra building materials and components were taken into account. In the cases, where the re-insulation of building envelope and façade was essential, a new construction component was replaced. This was performed in order to have a correct calculation of life cycle assessment in OneClick LCA so that the replacement of component was taken into consideration. For instance, the floor was replaced and the outer layer of asphalt in the roof was replaced in order to re-insulate these building components with additional insulation. All the building envelope components including floor, roof, and exterior walls were re-insulated with Glava Extrem 32 in the LCA tool.

2.6. Zero energy balance

As mentioned earlier in Section 1.3, a common approach for all ZEB definitions is the annual balance between the weighted demand and the weighted supply [20, 21] and it is generally done by integrating PV cells to the building façade and roof. The weighted demand and supply can be calculated in different ways; the export/import balance, load/generation balance, and monthly net balance, which is the combination of two other methods. In this thesis, the export/import balance method was selected and calculated as follows:

$$ZEB = |E_{P,exp}| - |E_{P,imp}| \approx 0 \quad (14)$$

$$E_{P,imp} = \sum_i E_{imp}(i) \times w(i) \quad (15)$$

$$E_{P,exp} = \sum_i E_{exp}(i) \times w(i) \quad (16)$$

where w is the weighting factors/metrics used in this paper as the primary energy factor and i refers to different type of energy carrier. It should be mentioned that the export/import balance in this thesis took into consideration the self-consumption of generated electricity, and afterwards created a balance between the need for exported and imported energy as follows:

$$\begin{cases} E_{exp} = \left| \sum_{m=1}^{12} (E_{el,use} + E_{el,prod.}) \right| & \text{if } \sum_{m=1}^{12} (E_{el,use} + E_{el,prod.}) < 0 \\ E_{exp} = 0 & \text{if } \sum_{m=1}^{12} (E_{el,use} + E_{el,prod.}) \geq 0 \end{cases} \quad (17)$$

$$\begin{cases} E_{self,use} = \left| \sum_{m=1}^{12} E_{el,prod.} \right| & \text{if } \sum_{m=1}^{12} (E_{el,use} + E_{el,prod.}) > 0 \\ E_{self,use} = \sum_{m=1}^{12} E_{el,use} & \text{if } \sum_{m=1}^{12} (E_{el,use} + E_{el,prod.}) \leq 0 \end{cases} \quad (18)$$

$$E_{imp} = \sum_{m=1}^{12} E_{el,use} - E_{self,use} \quad (19)$$

where m is the number of months or hours for monthly or hourly calculations, respectively.

Finally, the mismatch factor or so called supply cover factor (γ), was calculated as follows [135]:

$$\gamma = \frac{\text{Self – consumption of generated electricity}}{\text{On – site electricity generation}} = \frac{E_{\text{self,use}}}{\sum_{m=1}^{12} E_{\text{el,prod.}}} \quad (20)$$

In the above-mentioned equations, $E_{\text{el,prod.}}$ (kWh) was the produced electricity by PV cells, $E_{\text{el,use}}$ (kWh) was the building energy use, $E_{\text{imp.}}$ (kWh) was the imported energy (kWh), and $E_{\text{exp.}}$ (kWh) was the delivered energy to the grid. $E_{\text{p,imp.}}$ (kWh) and $E_{\text{p,exp.}}$ (kWh) represented the primary imported and exported energy, respectively. In addition, the absolute sign was used, because the produced energy was given a negative sign and the used energy was given a positive sign. For hourly calculations, the number of samples was changed to 8760 for the entire year. The PV module had an average efficiency of 18% for monocrystalline PV cells [136]. Furthermore, a tilt angle of 35°, the optimal PV tilt angle in Oslo climate [137], module quality loss of 1.2%, and inverter operation loss of 8% were considered for the PV system, which gives a yearly average PR of 67% [137]. The weighting factor 2.3 was also considered for imported and exported primary energy for ZEB balance calculations [117].

3. Case study

To evaluate the efficiency of various set of retrofit measures in the Norwegian office buildings, the main challenge was to select a building case study representing a typical existing office building located in Norway. Analysis of the current office building configurations in Norway show that a large group of offices constructed in the period of 1965 to 2015 (Fig. 12 (a)-(c)) had almost a similar configuration. Fig. 12 shows three examples of the existing office buildings constructed in Norway in different years. Their common features were comparable rectangular shape with a combination of cell and landscape offices. Taking also into account that the average floor area of the existing Norwegian office buildings, as pointed out in Section 1.2 (see Fig. 2), was around 3 000 m² [13]. In addition, it was found, based on the statistics of office building stock in Norway (see Fig. 1 and Fig. 2), that most of existing office buildings were built in the 1980s with a total heated floor area less than 10 000. Therefore, an average building model was chosen and designed in IDA-ICE software as a typical office building in Norway in this thesis (Fig. 12 (d)). Accordingly, the building envelope characteristics, lighting system, and HVAC system were selected for a typical office building constructed in 1980s satisfying the Norwegian building code TEK 87 [134]. The building had a compact square design with a total internal volume of 9 062 m³ and a total floor area of 2 940 m². The total external wall area was 1 326 m² with doors covering a total of 21 m². Furthermore, the number of floors was set to three to avoid extensive computational cost for evaluation of retrofit interventions during optimization.

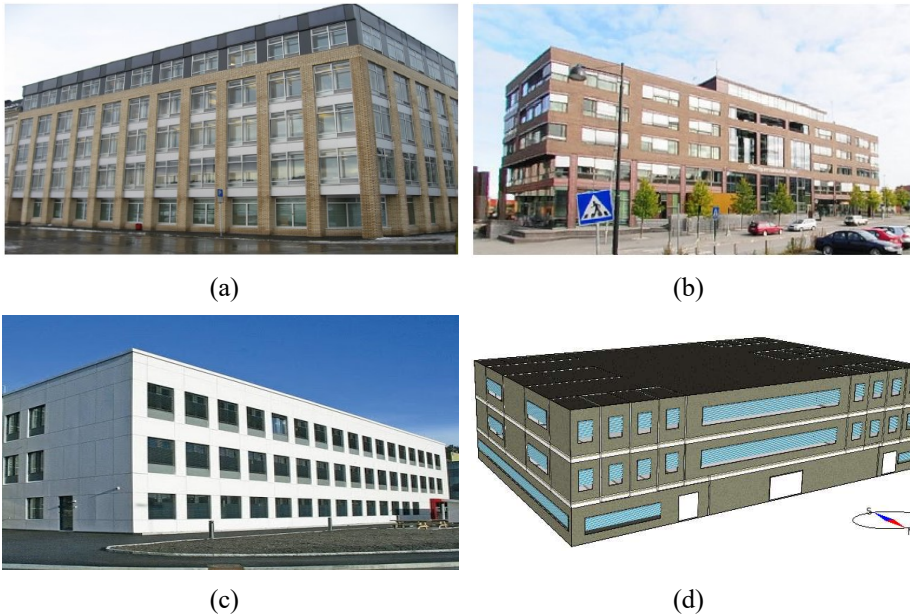


Fig. 12. (a) FN office building located in Arendal, which was built in 1965 and renovated in 2006 with gross area $2\,590\text{ m}^2$ [138], (b) Bassengbakken 1 office building located in Trondheim constructed in 2001 and rehabilitated in 2004 with gross area $8\,425\text{ m}^2$ [138], (c) An office building located in Bergen, which was completed in 2015 for the Norwegian Defence Estates Agency (NDEA) as a nearly zero energy building (nZEB) with gross internal area $2\,035\text{ m}^2$ [104], (d) Considered office building configuration modelled in the energy simulation software (IDA-ICE)

Fig. 13 shows the thermal zones and floor plans in the simulation model. Zoning of each floor was done with respect to a realistic scenario of possible solutions in office buildings. Zones were designed to comply with the area requirement in the Norwegian standard NS 3031 [116] which states that the area for the primary zones (with occupancy) should be at least 65% and the maximum of 35% for the secondary zones (without occupancy and equipment). The total area of primary zones was around $2\,230\text{ m}^2$. The first floor included a reception with a separate entrance and access to elevator and stairs, parking garage, and a designated section for business premises. The second and the third floors comprised of 16 cell offices, open plan office area, and meeting and conference rooms. The office building also had elevators, technical spaces, and toilets. In addition, the IDA-ICE zone multiplier function was used to simplify the duplicate cell offices in

the second and the third floors to reduce the computational time of simulations. Furthermore, the type of shading device for the windows was an exterior venetian blind, and the total window area was selected based on TEK 87, so that the window to floor area ratio did not exceed 15%, corresponding to total window area 286 m².

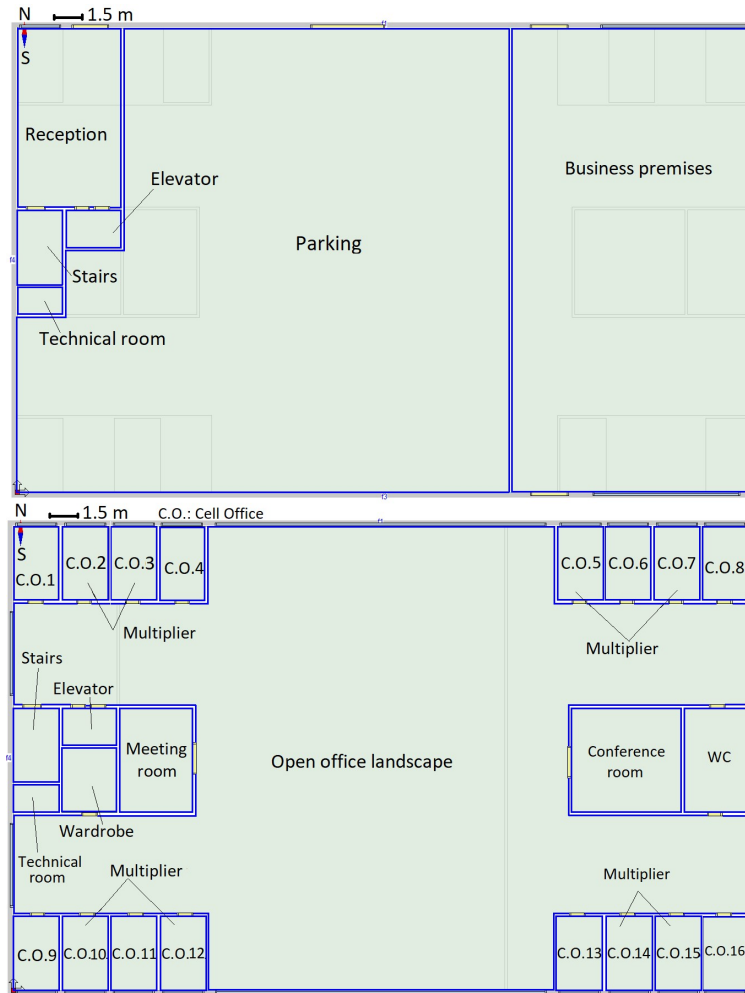


Fig. 13. Generic ground floor plan, the first floor plan (top), and the second and the third floor plans at level 3.4 m and 6.8 m (bottom) with thermal zones

Table 5 presents the building envelope properties of the reference building in this thesis. All characteristics were considered according to the Norwegian building code TEK 87. The HVAC system parameters and set points and usage profiles for the reference case are shown in Table 6. In addition, domestic hot water (DHW) use was selected according to the Norwegian standard NS 3031 [116].

Table 5. Properties of the building envelope for the reference case

Parameter, Units	Value
External wall U-value, W/(m ² K)	0.3
Roof U-value, W/(m ² K)	0.2
Floor U-value, W/(m ² K)	0.2
Window U-value, W/(m ² K)	2.4
ψ , W/(m ² K)	0.13
n_{50} , 1/h	4
External door U-value, W/(m ² K)	2
External shading strategy	Blinds on, if $Q_{sol} > 100$ W/m ²

Table 6. Characteristics of the HVAC system in the reference building

HVAC systems and operation	Features
Ventilation system type	CAV mechanical balanced ventilation system
The specific fan power (SFP) of the ventilation system	2.5 kW/(m ³ /s)
Schedules of ventilation system	Monday-Friday: 12 h/day for upper limit (6-18); other times reduces to lower limit
Supply airflow rates of the ventilation system	Primary zones: 4.32 m ³ /(m ² .h) and 19.8 m ³ /(m ² .h) for upper limit in heating and cooling seasons respectively, 0.72 m ³ /(m ² .h) for lower limit Secondary zones: 2.52 m ³ /(m ² .h) for upper limit, 0.72 m ³ /(m ² .h) for lower limit
Heating system	Central heating system, modelled in IDA-ICE using a generic electric heater with unlimited capacity and efficiency of 90%
Cooling system	Centralized water cooling system for cooling of supply air in the AHU
Heating distribution system	Water radiator system
Room temperature set point for local space heating *	19°C for heating
Control method of space heating and ventilation air heating and cooling systems	Space heating: supply water temperature as a function of outdoor temperature; Ventilation supply air temperature: as a function of outdoor temperature;
DHW use	5 kWh/(m ² .year)

* There was no local space cooling system in the zones and cooling of zones was done by the mechanical ventilation system

4. Achieving zero energy building performance of an existing office building through optimization and small retrofitting measures

In implementing the retrofitting measures, the building configuration in Section 3 was considered through two different approaches. In the first approach, the existing building characteristics were based on the Norwegian building code TEK 10 (2010 onwards), and small retrofitting measures were applied. In the second approach, the TEK 87 (1980s) building requirements were considered for the reference case and more renovation measures were included.

4.1. Reference building models

To have a building model based on TEK 10, the minimum requirements for building envelope, stated in this building code, along with the HVAC system set points specified in NS-EN 15251 were adopted [122]. The details about the building envelope, HVAC system set points, and the type of weather data used in simulations can be found in [139]. The target was not to exceed the maximum allowable delivered energy for Norwegian office buildings, 115 kWh/(m².year), and to satisfy the thermal comfort requirements based on NS-EN 15251. Regarding the building model based on TEK 87, the model met the maximum allowable specific annual energy use for office buildings set around 250 kWh/(m².year) [140] by considering the building properties described in TEK 87. It should be noted that a measurement-based data of several cell offices in an office building in Norway [112] was considered to have a realistic pattern of lighting and occupancy behavior in the TEK 87 model [133].

Fig. 14 shows the annual energy use and the variation of operative temperature for the TEK 87 and TEK 10 reference building models. In both models, the upper limit of airflow rate in the AHU was controlled so that the maximum allowable and recommended energy use in accordance with TEK 10 and TEK 87 was not exceeded. At the same time, the operative temperature, based on adaptive thermal comfort

requirements in NS-EN 15251, was satisfied for both reference building models although it was not a requirement especially for TEK 87 building case. It should be pointed out that the operative temperatures in Fig. 14 (b) have been presented for the worst zone, cell office C.O.16 in Fig. 13.

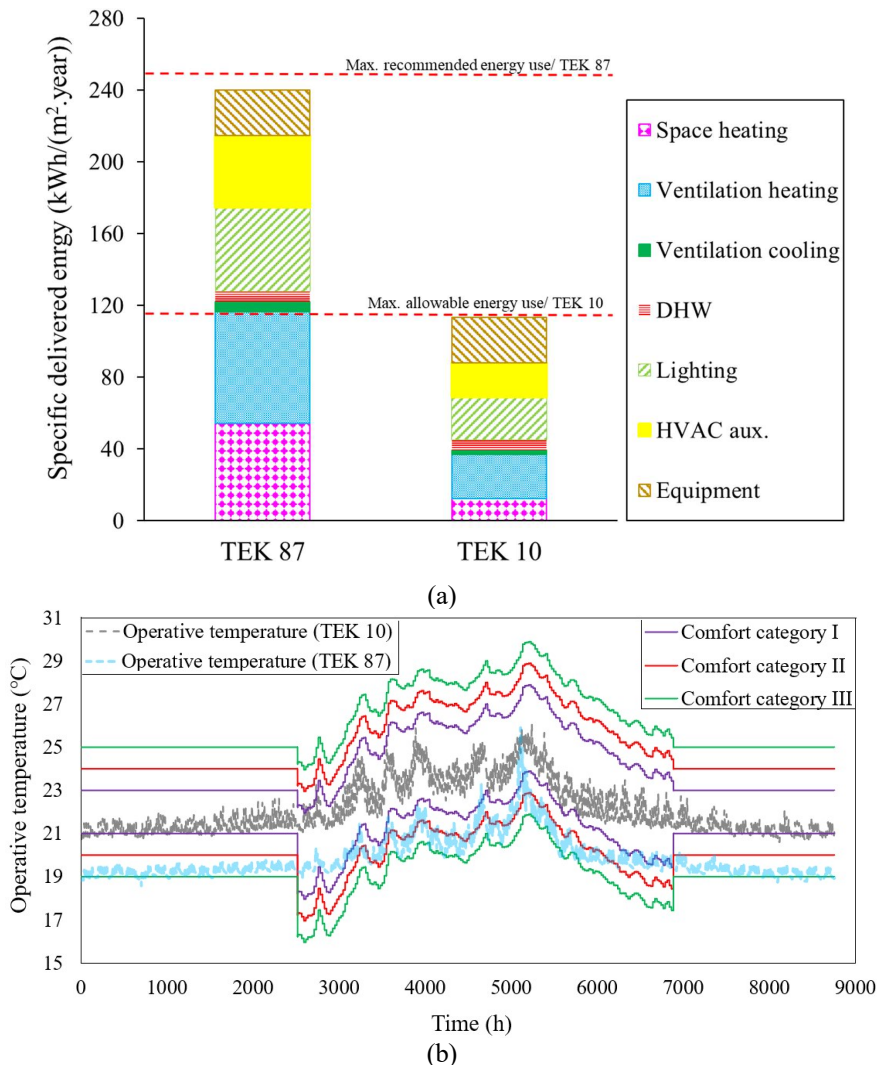


Fig. 14. Annual (a) specific energy use and (b) variation of operative temperature for the TEK 87 and TEK 10 reference building models

4.2. Minimizing delivered energy and LCC through small retrofitting

4.2.1. Input parameters, constraints, and objective functions

In this approach, the renovation measures included various types of windows, external walls, roof, ground floor, and external shading along with set points for supply air temperature and airflow rate in the AHU. In this optimization approach, two different strategies were considered for the objective functions. In the first strategy, the LCC of renovation measures was the objective and the specific energy use for space heating and space cooling was the constraint. In the second one, the delivered energy to the building was the objective and the increase in the total cost of renovation measures (5% and 10%) was the constraint. Furthermore, the maximum PPD and overheating degree hours (DH_{26}) were used as the thermal comfort constraint for both aforementioned strategies (Table 7).

Table 7. Details of constraint functions for two strategies

	First strategy			Second strategy	Description
DH_{26} (h)	(3 rd floor-Cell offices no. 16 and 09) < 50				Based on TEK 10 [7]
PPD (%)	(3 rd floor-Cell offices no. 16 and 09) < 15				Based on TEK 10 [7]
E_{SH} (kWh/(year.m ²))	Oslo	Tromsø	Stavanger	NA	Calculated based on NS 3701 standard [10]
	20.72	32.96	20		
E_{SC} (kWh/(year.m ²))	Oslo	Tromsø	Stavanger	NA	Calculated based on NS 3701 standard [10]
	9.38	2.10	4.48		
Total cost increase	NA			5% and 10%	Increase with respect to the reference case

A schematic of the implemented optimization process is shown in Fig. 15. All considered inputs were firstly added and connected to the GS module via parameter mapping to an appropriate source out of script macro (the gray boxes with the blue arrows inside the dashed red box). Switches were considered to alter different options for each group of inputs. Their associated costs were then summed using an adder representing the total amount of operational and investment costs of the building retrofitting process. Afterwards, the constraints were implemented so that if the considered parameter could not meet the constraint requirement, the objective would simply be multiplied by a large

number and, since the aim was to minimize the objective functions, the output would consequently be removed from the optimal set of solutions determined by the optimization engine; Fig. 15. The details of the optimization algorithms, parameters, and system used can be found in [139].

4.2.2. Optimization results of the first retrofitting approach

Fig. 16 and Fig. 17 show how GenOpt optimized the objective function (LCC of renovation measures) through the GS module, e.g. for the building case in Oslo. In this case, the simulation runs converged after around 140 iterations. However, GS module divided the results into two levels, one without satisfying the constraint functions (upper level in the left part of Fig. 16) and the other that satisfied all the constraint functions (lower level in the left picture as well as the right picture in Fig. 16). In other words, using the GS modules, the objective function was minimized at the two aforementioned levels since the cases that did not meet the constraints were multiplied by a large number (for example 10 000 in this thesis), while acceptable results remained unchanged during the optimization process. The same trend is observed in Fig. 17 where the all-air system was used. The convergence was achieved after around 160 iterations. The number of simulations that could not meet the constraints was higher than those in the case with the waterborne radiator space heating (RSH) system, implying that achieving the building energy use with the PH standard level while satisfying thermal comfort requirements was more critical with the AA systems.

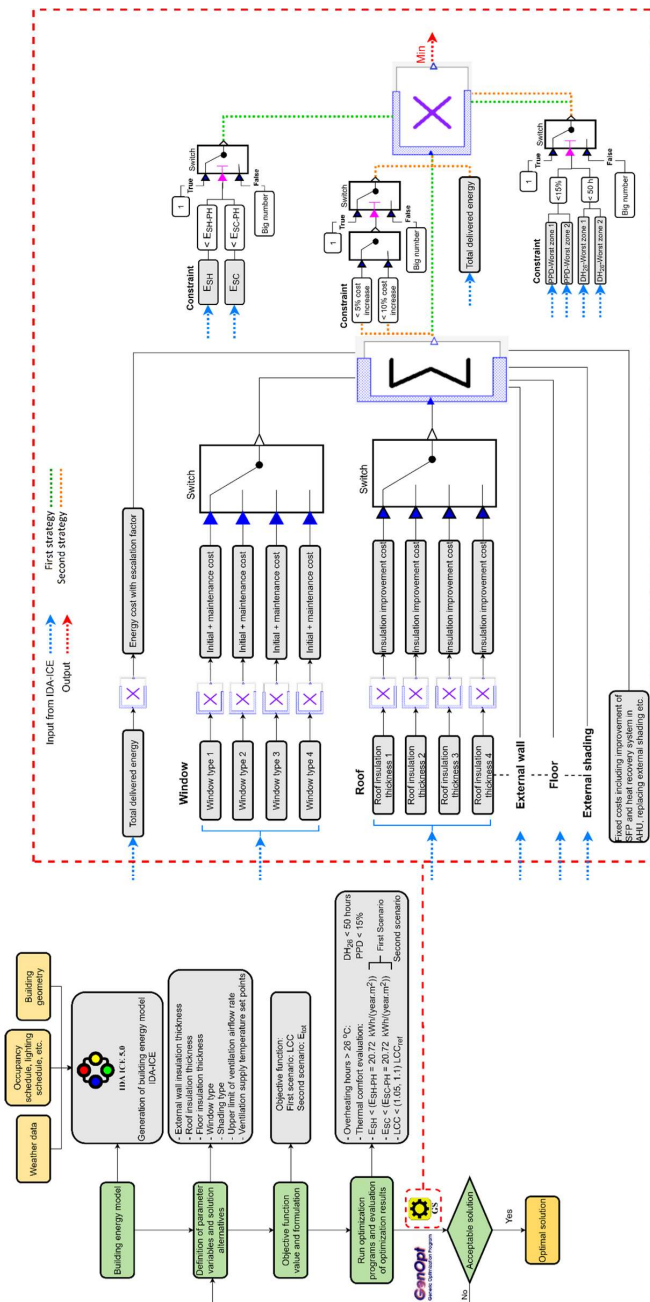


Fig. 15. Model framework and optimization process through the GS module

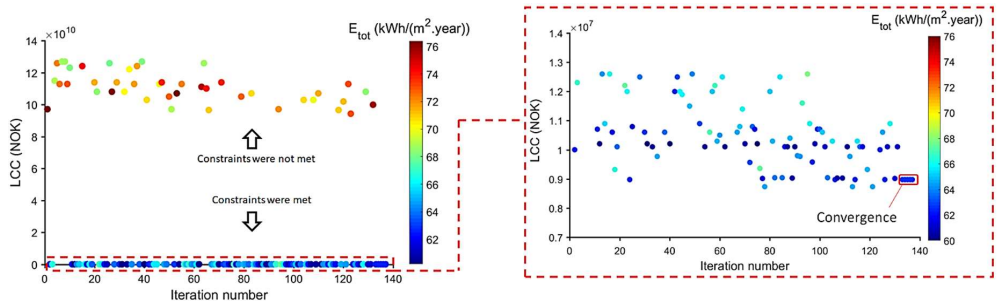


Fig. 16. Optimization results through GS module for the building case with the RSH system for Oslo climate (Minimizing LCC)

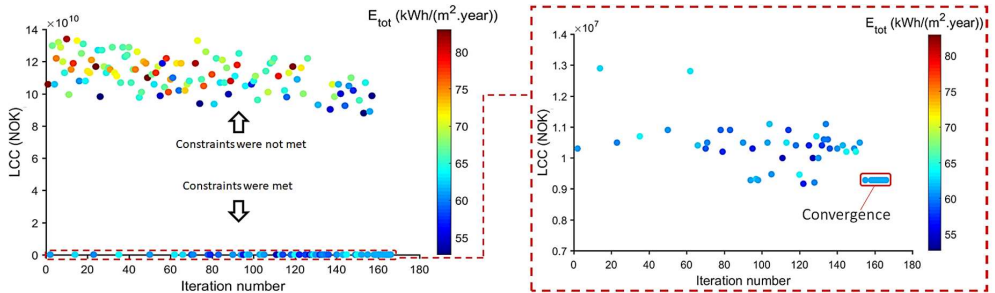
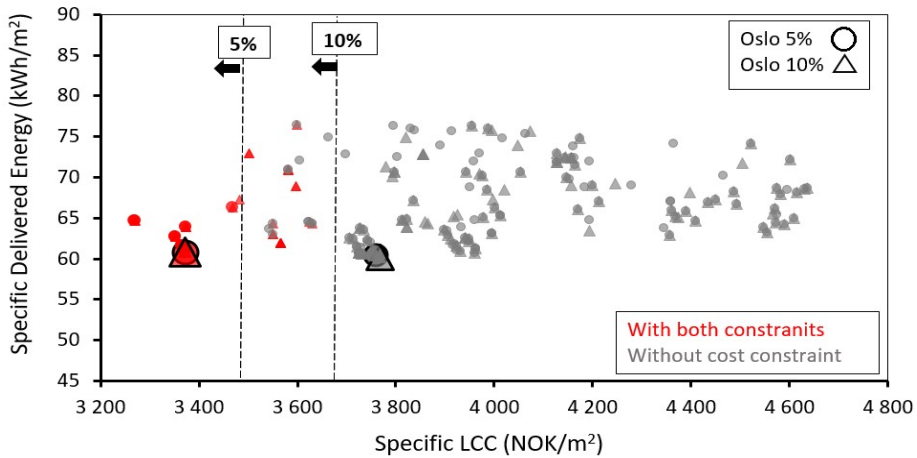


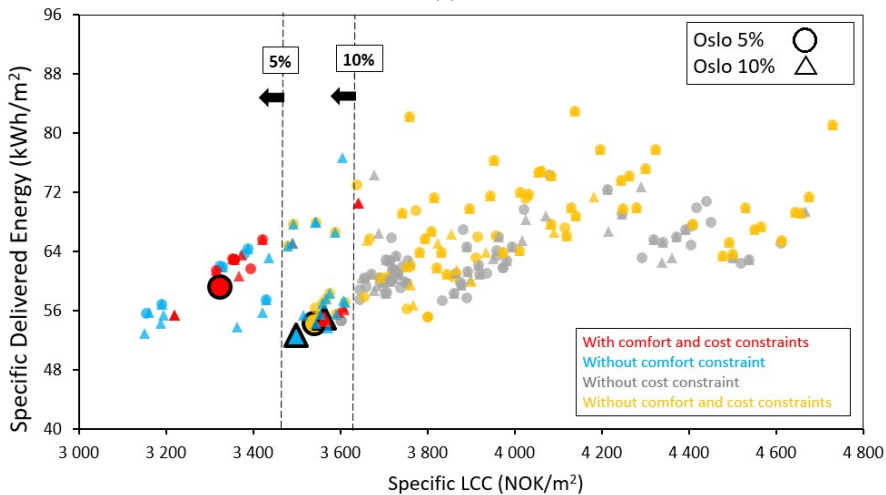
Fig. 17. Optimization results through GS module for the building case with AA system for Oslo climate (Minimizing LCC)

The effect of constraint functions on the delivered energy and the LCC of design parameters for Oslo climate (minimizing delivered energy), are shown in Fig. 18(a) and (b). In the RSH system, see Fig. 18(a), the thermal comfort constraint was satisfied for all the cases and the cost increase was the only constraint, see the vertical dashed lines in Fig. 18. Note that in Fig. 18(a), the minimum points (with and without constraint) are marked with the same symbols, but larger. The four different colors in Fig. 18(b) show the four different conditions with respect to the constraints. The global minimum energy use points (with and without constraints) for different cost increase cases are shown with the same symbols, but larger. Moreover, the specific delivered energy was almost directly proportional to the specific LCC in both Fig. 18(a) and (b). This implies that the reduction of the operational energy cost due to both adjustment of the HVAC set points and using the high performing building envelope was higher than the increase of renovations'

investment cost. A similar trend was also reported in [38] and [49] for cooling dominated and heating dominated climates respectively. Passive cooling strategies and type of heating system were the optimization parameters that substantially affected the operational energy cost in these studies. The obtained results also showed that the high quality of window and external wall was always used in all the optimized cases, but the ground floor and the roof retrofitting were the costliest options.



(a)



(b)

Fig. 18. Effect of constraint function on the optimization solutions for (a) RSH system and (b) AA system for Oslo climate (Minimizing delivered energy)

Table 8. Energy and LCC values of various optimal solutions for both strategies

	Simulation case	Specific delivered energy (kWh/m ²)	Energy saving vs reference (%)	Specific LCC (NOK/m ²)	LCC saving vs reference (%)
Reference	Ref. Oslo	113.30	NA	3311.99	NA
	Ref. Stavanger	100.20	NA	2947.34	NA
	Ref. Tromsø	126.38	NA	3676.33	NA
First strategy (Minimizing LCC)	Opt. RSH Oslo	64.50	43.1	3129.04	5.52
	Opt. RSH Stavanger	54.42	45.7	2845.98	3.44
	Opt. RSH Tromsø	70.00	44.6	3279.32	10.80
	Opt. AA Oslo	57.41	49.3	3117.69	5.87
	Opt. AA Stavanger	44.92	55.2	2927.67	0.67
Second strategy (Minimizing delivered energy)	Opt. AA Tromsø	60.43	52.2	3359.46	8.62
	Opt. RSH Oslo 5%	60.84	46.3	3370.92	-1.78
	Opt. RSH Oslo 10%	60.83	46.3	3627.97	-1.77
	Opt. RSH Stavanger 5%	52.92	47.2	3091.75	-4.51
	Opt. RSH Stavanger 10%	51.53	48.6	3091.75	-5.59
	Opt. RSH Tromsø 5%	64.46	49.0	3701.20	-0.68
	Opt. RSH Tromsø 10 %	63.80	49.5	3727.40	-1.38
	Opt. AA Oslo 5%	59.16	47.8	3564.97	-0.37
	Opt. AA Oslo 10%	54.99	51.5	3476.54	-7.64
	Opt. AA Stavanger 5%	44.56	55.5	2917.83	1.00
	Opt. AA Stavanger 10%	44.56	55.5	2917.83	1.00
PH	Opt. AA Tromsø 5%	56.97	54.9	3665.92	0.28
	Opt. AA Tromsø 10%	56.97	54.9	3665.92	0.28
	PH RSH Oslo	60.19	46.9	3627.13	-9.51
	PH RSH Stavanger	50.92	49.2	3368.81	-14.30
	PH RSH Tromsø	63.80	49.5	3727.38	-1.38
	PH AA Oslo	56.67	49.9	3668.97	-10.77
	PH AA Stavanger	46.03	54.1	3372.80	-14.43
	PH AA Tromsø	59.46	52.9	3746.54	-1.91

4.3. Improving thermal and visual comfort through optimization of fenestration, envelope, shading device, and energy supply system

4.3.1. Input parameters, constraints, and objective functions

In the second retrofitting approach, the reference building properties were based on TEK 87 and more input parameters were involved in the optimization compared to the first approach. The extra parameters included were the supply water temperature set points from the central heating system, supply/return water temperature to/from radiators (only RSH system was considered), heat exchanger efficiency in AHU, overheating of zone hot water supply in the central heating system, and window opening control and

shading device control alternatives. Additionally, the ground floor renovation was removed from the input parameters since it was not found as a cost-effective measure in the first retrofitting approach. DF was also considered as a visual comfort constraint in the optimization process. Concerning the objective function, only specific delivered energy was used and the LCC was not considered because the findings in the Section 4.2.2 showed that the reduction of operational cost was higher than the increase of investment cost due to retrofitting. Accordingly, most of extra input parameters considered in the second retrofitting approach were related to operational cost.

Regarding the window opening and shading device control methods, three control methods for window opening (including never open window), and seven control methods for shading device control methods (including never drawn shading) were considered as follow:

- Window opening (alt. 1): Indoor operative temperature control method was used for the summer and winter operation. The summer operation control was based on indoor operative temperature. The winter operation was based on CO₂ and indoor operative temperature control methods.
- Window opening (alt. 2): Indoor operative temperature control method was combined with the direct solar radiation on the façade and wind velocity control for the summer operation.

It should be mentioned that the window opening in IDA-ICE was applied according to the CELVO model, which defined the window opening area in terms of height, width, and discharge coefficient of the window [[142](#)].

- Shading control (alt. 1): Shading position control was suggested with respect to the indoor air temperature outside the working hours (zone not in use) and according to illuminance during the working hours (zone in use). It should be pointed out that this alternative was the only condition in which the shading slat angle was controlled according to illuminance and changed based on the solar azimuth angle. Otherwise, the slat angle was kept constant at 45° in other conditions. The aim was to minimize energy use and maximize comfort.

- Shading control (alt. 2): Shading position control was based on the solar radiation measured on the exterior side of windows during the working hours and according to solar radiation and indoor air temperature outside the working hours. The aim was to avoid overheating during working hours and to gain heat outside the working hours.
- Shading control (alt. 3): Shading position control was based on illuminance during the working hours and according to the indoor air temperature and the minimum solar radiation outside the working hours. The aim was to maximize comfort and minimize mechanical cooling.
- Shading control (alt. 4): Shading position control was based on the solar radiation measured on the exterior side of windows during the working hours and according to the indoor air temperature and the minimum solar radiation outside the working hours. The aim was to avoid overheating during the working hours and preserve heat gain outside the occupancy hours.
- Shading control (alt. 5) and (alt. 6): Shading position control was based on illuminance and solar radiation on the exterior side of windows all day long, respectively.

It should be stated that all the alternatives for window opening and shading device control methods were developed through detailed macros in IDA-ICE, as described in [133].

4.3.2. Optimization framework and simulation tool

Fig. 20 illustrates the proposed method for the second retrofitting approach. The method was structured in several steps.

- The pre-processing step (the green area in Fig. 20), in which the building model was generated in IDA-ICE and the input parameters for the optimization problem were defined.
- The intermediate step (the red area in Fig. 20), where the output parameters from the energy simulation software were evaluated in terms of average daylight fact

(DF_{avg}), DH_{26} , and PPD_{avg} . The first parameter, daylight factor, was considered as the visual comfort index and the two latter, discomfort hours for the indoor operative temperature greater than 26°C and the averaged predicted percentage dissatisfied, were chosen as the thermal comfort indexes. These constraints were implemented through the GS module in the same way as described in Section 4.2.1.

- The optimization step (the purple area in Fig. 20), where the objective function was iteratively assessed until an optimal solution was achieved.
- The post-processing step (the “ZEB analysis” box in Fig. 20), where the optimal solutions were elaborately analyzed further in terms of ZEB balance described in Section 2.6.

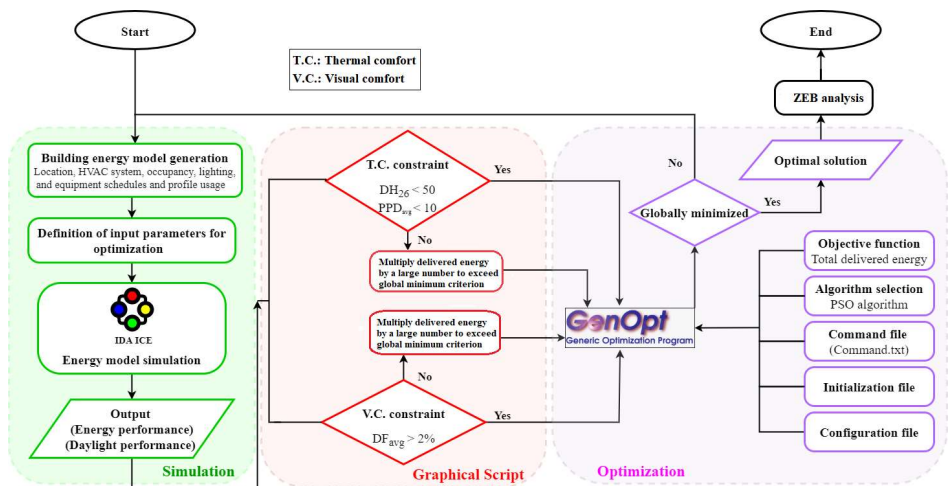


Fig. 20. Proposed framework for the optimization process in the second retrofitting method

4.3.3. Optimization results of the second retrofitting approach

4.3.3.1. Optimization results

The optimization results showed that the largest value of heat exchanger efficiency was chosen in the optimal solution. The reason was that the improvement of heat exchanger efficiency decreased the building energy use with trivial impact on the

visual and thermal comfort conditions. Regarding the window to floor area ratio, a moderate value was selected for the optimal solution implying that this parameter was a conflicting factor for maximizing visual comfort and thermal comfort and minimizing energy use, simultaneously. The external wall, window, and roof retrofitting with low U-value were prioritized for the optimal solution. Regarding shading device and window opening, the control methods based on the temperature and solar radiation set points (window opening alt. (2) and shading control alt. (6)) were the preferred options for the global optimal solution. Overall, comparison of the window opening and shading device control methods in this PhD work indicated that the solar radiation and the indoor temperature parameters were the most effective factors in controlling the dynamic shading device and the window opening. This was especially achieved when different set points were considered for the same parameter, for example solar radiation, for controlling the shading and window opening. The reason could be justified by the coincidence of solar shading and window opening activation. In fact, selecting the same parameters, but with different set points, for the control methods of shading device and window opening ascertained that the shading would not be drawn when the windows were open, and the best performance of both shading and window opening was achieved. It is worth stating that it was also observed in [86] that the strategies controlled based on solar irradiance were the most selected control methods for the optimal shading control in different investigated cases.

Fig. 21 shows the optimization results taking both visual and thermal comfort constraint functions into account. The cases with a low PPD_{avg} and high DF_{avg} values had a relatively high energy use (yellow and green points in the lower part in the acceptable solutions area).

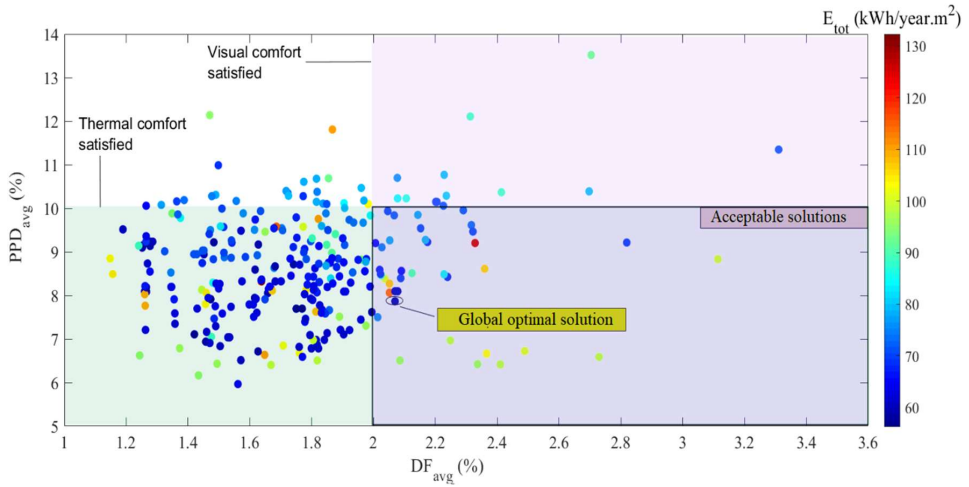


Fig. 21. Scatter plot of optimization results

However, the solutions with less energy use fell within the thermal comfort satisfied area (dark blue points in the lower part in the thermal comfort satisfied area) emphasizing the difficulty of finding an optimal solution when considering both thermal and visual comfort filters. The reason was that a fewer number of parameters (mainly window to floor area ratio and partly glazing type) affected daylight factor than the thermal comfort. Furthermore, the total delivered energy reduced dramatically after optimization by around 77% compared to the reference case. As a matter of fact, this considerable energy saving would be more limited if the cost effectiveness of retrofitting option was also taken into account. However, the proposed optimization process provides informative insights on the importance of various control methods of window opening, shading device, and HVAC set points adjustment in the improvement of building energy performance, which impose almost low investment cost during retrofitting process.

4.3.3.2. Results of ZEB balance

Fig. 22 illustrates the process to reach ZEB balance through the imported and exported primary energy balance. Firstly, a large amount of energy saving, around 81%, in primary imported energy was achieved during optimization and the ZEB balance was then achieved by exporting electricity from onsite production.

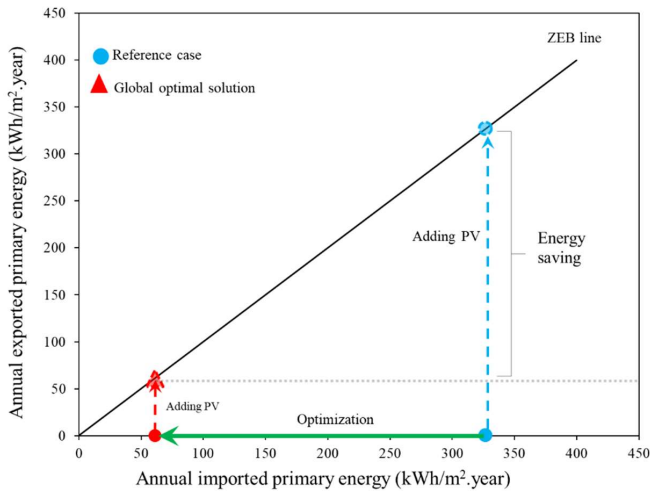
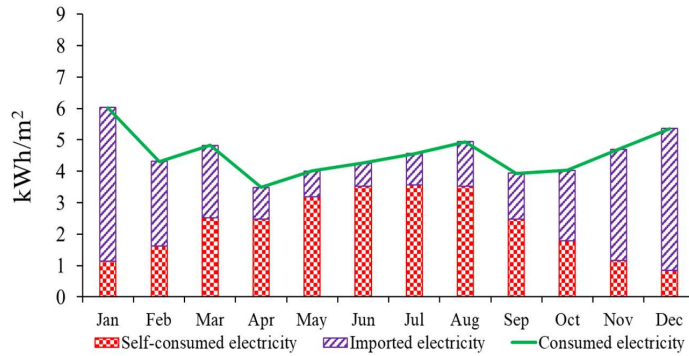


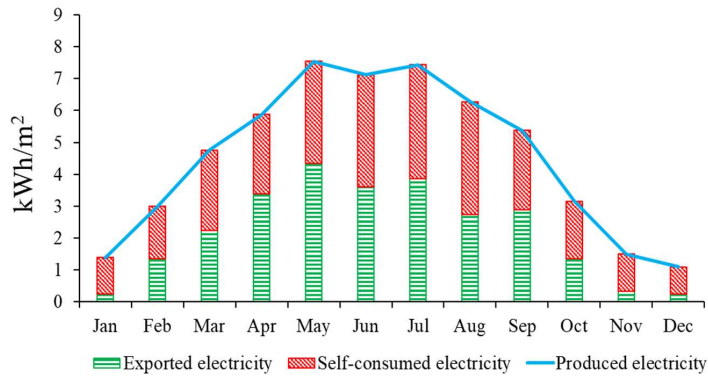
Fig. 22. ZEB analysis process in terms of exported and imported primary energy use

Therefore, the required PV panel area to reach ZEB level was around 1 352 m² for the global optimal solution and around 5 960 m² for the reference case, if no optimization was performed. Furthermore, as the roof area was around 1 000 m², these optimized PV might be placed on the roof somehow. But, without optimization, it would be completely impossible or not feasible.

Fig. 23 shows the monthly variation of electricity portion in ZEB analysis in terms of export/production and import/consumption. The maximum electricity production for both the reference and the optimized cases was achieved during summertime, due to high solar radiation intensity. Consequently, a significant amount of electricity was imported during the winter, and a high portion of electricity was exported during the summer.



(a)



(b)

Fig. 23. Monthly variation of electricity portion in ZEB analysis in terms of (a) export/production and (b) import/consumption for the global optimal solution

Additionally, there was still some amount of imported electricity even during summer, even though the electricity produced by PV was tried to be self-consumed as much as possible. It can be observed in Fig. 23 and Fig. 24 that the optimized case internally consumed nearly half of the generated electricity by PV panels. More precisely, considering the supply cover factor as defined in Eq. 20, 54% of the onsite produced electricity on a monthly basis, and 51% of that on an hourly basis, was self-consumed in the building.

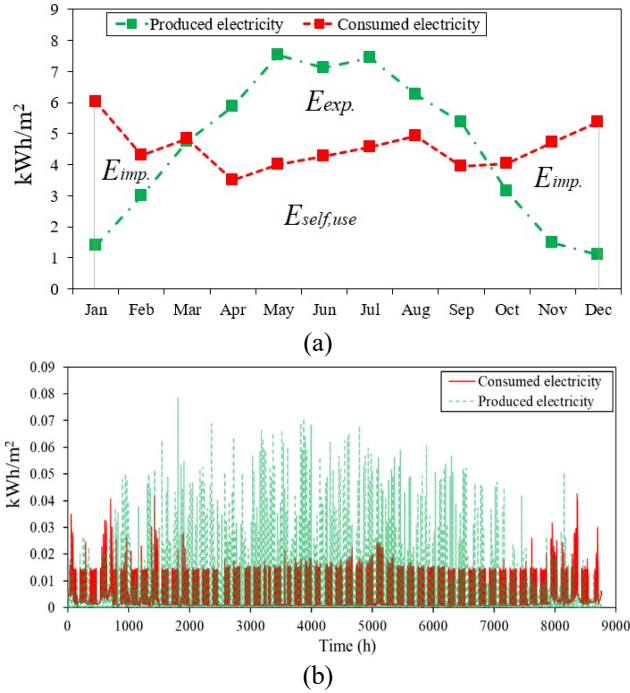


Fig. 24. (a) monthly and (b) hourly production and consumption electricity with areas for ZEB balance

An important point regarding ZEB balance is that it is economically preferable to use the generated electricity directly in the building (self-consumption) instead of exporting it to the grid. This is because the power company will only pay for the electricity price (Spot-price) plus a feed-in tariff, but not for the grid-tariff, for the exported electricity. Therefore, the price for the exported electricity will be only about the half price for the imported electricity.

4.4. CFD and daylight programs for building retrofitting

4.4.1. Simulation setups

In continuation of the second retrofitting approach described earlier in previous section (section 4.3), an AA system was also investigated besides the RSH system. The input parameters, constraint criteria, and objective functions were the same as previous section. However, the supply/return water temperature to/from radiators and overheating

of zone hot water supply in the central heating system were not considered in the optimization case equipped with AA system. Alternatively, four different types of the airflow control including variable air volume with humidity control, variable air volume with CO₂ control, variable air volume with temperature control, and variable air volume with temperature and CO₂ control were considered for the AA system equipped with DCV (Table 9).

Table 9. Various types of control methods for DCV system

System type	Control method
Variable air volume with humidity control	Maximum relative humidity set point: 60% for cooling season and 40% for heating season*
	Minimum relative humidity set point: 20% for both cooling and heating seasons*
Variable air volume with CO ₂ control	Maximum CO ₂ set point: 1100 ppm
	Minimum CO ₂ set point: 700 ppm
Variable air volume with temperature control	Maximum temperature set point: 26 °C
	Minimum temperature set point: 19 °C
Variable air volume with temperature and CO ₂ control	Combination set points for CO ₂ and temperature

* There is no specific limit value for humidity of indoor air in Norway and only recommendations to prevent dampness and mold growth [123, 143]

Furthermore, the optimization framework (BES-OPT in Fig. 25) was coupled with detailed CFD simulation and daylight simulations, as the post-processing. The CFD simulations were done in IDA-ICE by interfacing OpenFOAM CFD engine, and the daylight simulations were performed through Radiance program. However, all calculation setup and execution were performed in IDA-ICE for both CFD and daylight simulations.

Regarding the CFD process (illustrated in Fig. 25 with green boxes), firstly, coupling of BES and CFD was validated by the available experimental data [83] and our previous numerical results for a single office building [144]. Afterwards, the coupling process was implemented for the optimized solution from the BES-OPT step. In the coupling process, the required boundary conditions for CFD simulations including

surface temperature, surface convective heat flux, and ventilation air flows were exported from the IDA-ICE to OpenFOAM CFD engine. These boundary conditions were then used by the CFD program to solve the continuity, momentum, and energy equations. Moreover, for the CFD simulations, the steady state solver with the RNG k- ϵ turbulence model were selected as this model has largely been used in the simulation of indoor air flow problems [145].

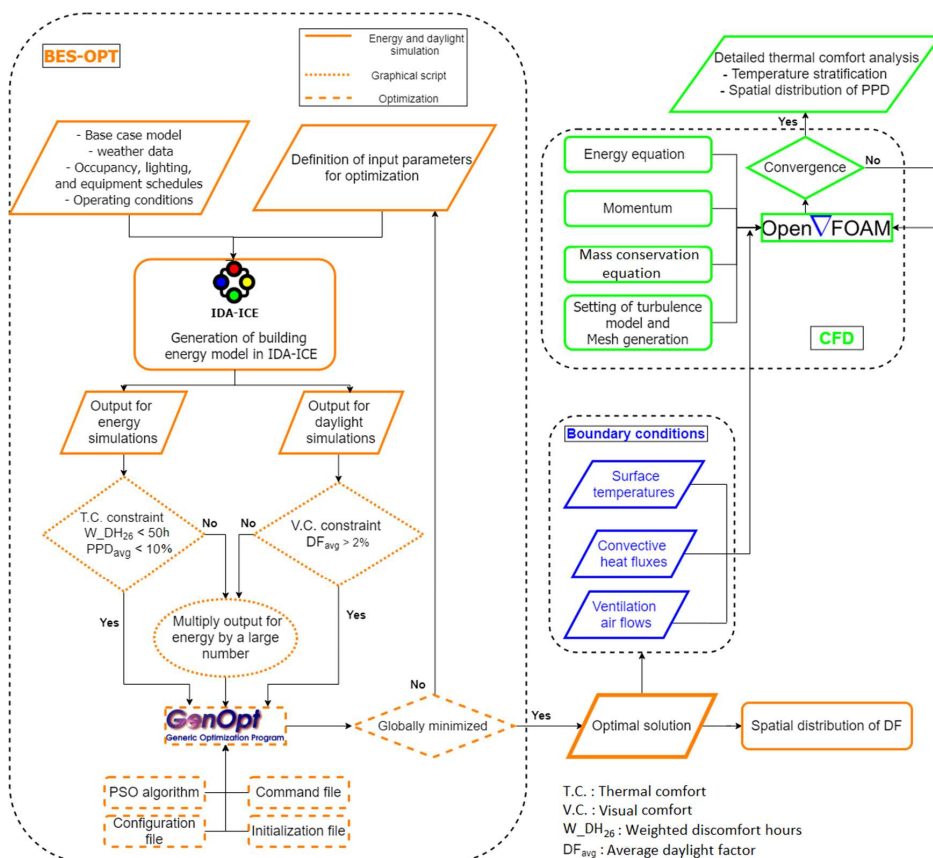


Fig. 25. Coupling framework of building energy optimization, daylight, and CFD

In accordance with the modelled geometry, a hexahedral mesh model was generated and executed in the CFD interface in IDA-ICE. Furthermore, a mesh refinement was applied to the boundary layers near the surfaces. The obtained indoor air

velocity and air temperature results from the CFD simulations were then exported to MATLAB program for PPD calculation. Fig. 26 shows the 3D Model modelled in IDA-ICE, based on the real experimental case [83], and used for the validation study. The office was equipped with radial diffuser located on the ceiling for both space heating and ventilation purposes.

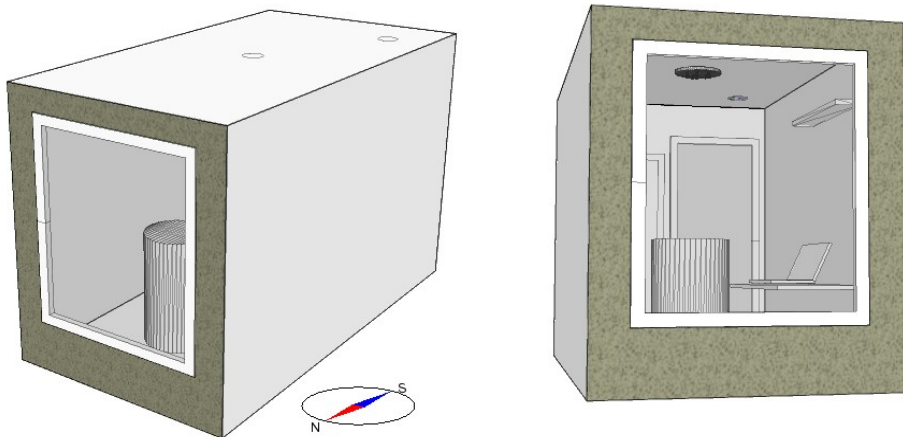


Fig. 26. Modelled configuration of the office cubicle in IDA-ICE

Concerning the detailed daylight analysis, three dynamic indexes comprised of UDI, cDA, and sDA, described in Section 2.3 were used. For UDI assessment, 100 lux and 2 000 lux were chosen as the minimum and maximum limits in Eq. (7). In evaluating cDA and sDA, the percentage of the daytime hours over 300 lux with partial credit and percentage of the occupied hours when the illuminance is equal or greater than 300 lux were considered. The daylight simulations were carried out through the Daylight-tab in IDA-ICE that uses backward raytracing and Radiance as a simulation engine. In this regard, a climate-based sky model with high precision was used in the Radiance software and a MATLAB script was used for visualizing the dynamic daylight indexes.

4.4.2. CFD and daylight simulation results for the energy optimized solution

4.4.2.1. BES-OPT analysis

Fig. 27 shows the scatter plot of optimized results filtered by both thermal and visual thermal comfort constraints. Comparing the results for RSH and AA systems (Fig. 27 (a) and Fig. 27 (b)) in the second optimization approach shows that satisfying thermal comfort requirements was more difficult in the case with AA system than in the RSH system. It can be observed with larger number of triangles and larger range of PPD_{avg} in the AA system in Fig. 27 (b).

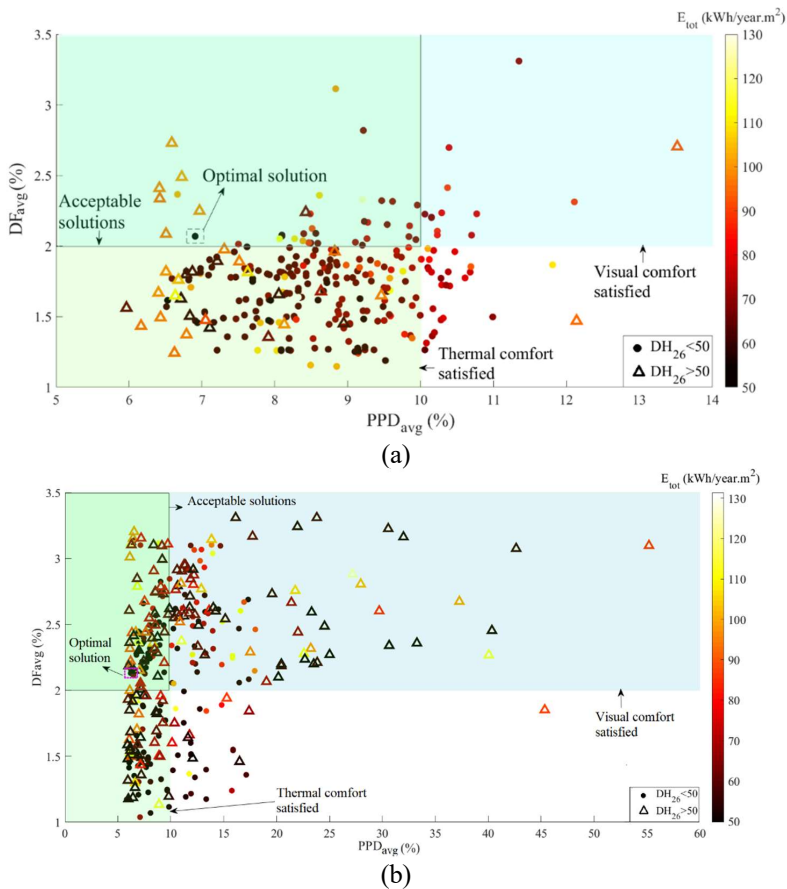


Fig. 27. Optimization results for (a) RSH system and (b) AA system in the second retrofitting approach

The reason could be more complicated control method of space heating and ventilation system in the AA case as they both functioned with a supply air terminal. Therefore, it was more challenging to find a combination of set points for the ventilation system to minimize the building energy use and achieve the thermal comfort in this case concurrently. On the contrary, the daylight factor requirement was satisfied for more cases in the AA system than in the RSH case that could be due to the type of shading control method and higher window to floor area ratio obtained in the optimal AA case. In this regard, the shading control alts. (6) and (1), described in Section 4.3.1, were chosen for the RSH system and AA system, respectively. In addition, the best quality of the window and external wall could not be selected in this case as tighter building envelope would result in larger DH_{26} than the thermal comfort constraint.

Fig. 28 shows the amount of delivered energy to the building for the reference case and two optimization cases. Optimizing the building performance could reduce the building energy use up to around 77% and 79% in the optimized RSH and AA cases respectively while satisfying both thermal and visual comfort. Less energy use in the optimized AA case proves that the AA system can be considered as a potential HVAC system in cold climate countries as it can reduce the investment and maintenance costs associated with the local space heating and cooling systems.

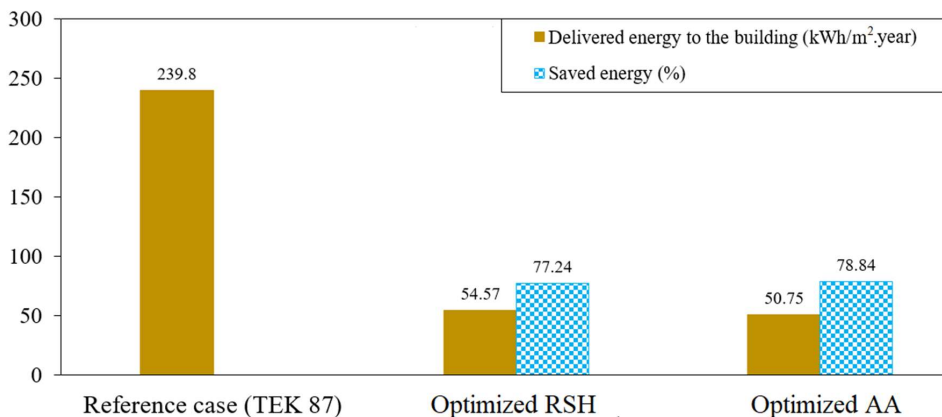
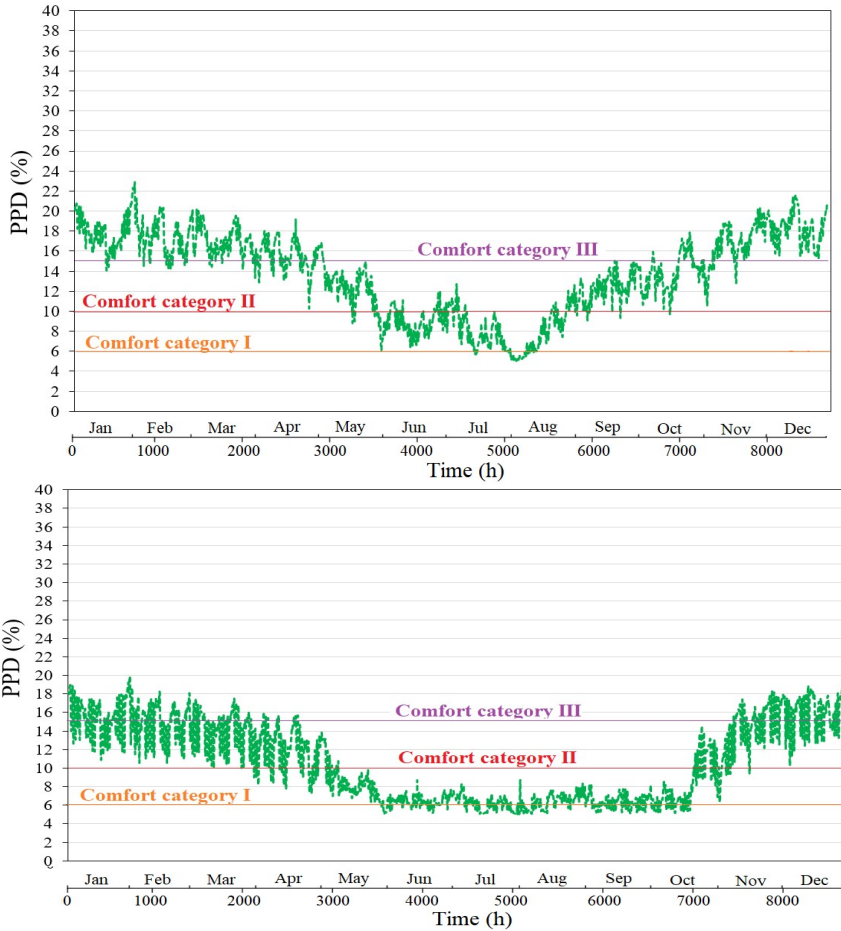


Fig. 28. Delivered energy to the building for two optimization cases

4.4.2.2. CFD and daylight assessment

Fig. 29 shows the annual variation of average PPD for the worst zone (cell office C.O.16) in terms of difficulty in meeting comfort conditions, for the reference case and the optimized RSH and AA cases. The coldest day was 2nd January, and the warmest day was 1st August, selected based on climate data for outdoor air temperature.



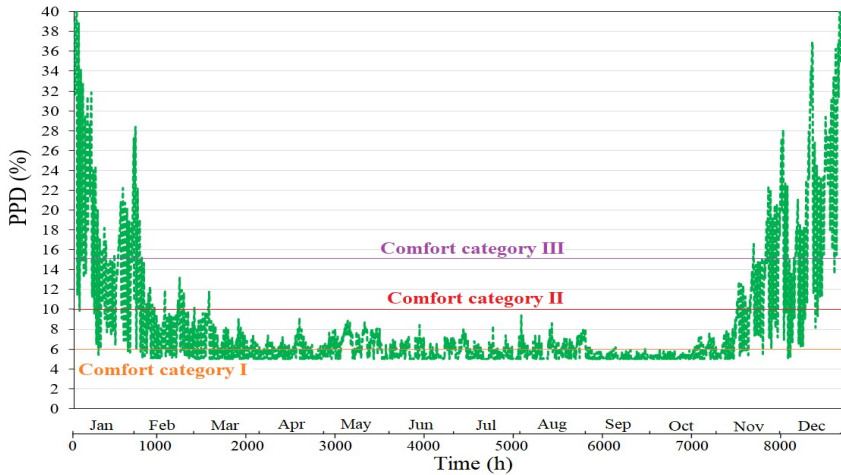


Fig. 29. Annual variation of average PPD for the cell office C.O.16 for the (a) reference case, (b) optimized RSH case (c) optimized AA case

Additionally, it was found that both optimized cases could satisfy the thermal comfort requirements, based on the comfort category II, for longer period of the year compared to the reference case. The AA optimized case showed the best performance in this respect. However, the AA system could not provide a comfortable condition, according to any of thermal comfort category, in January and December. Overall, the annual thermal comfort was improved for both optimized cases. It should be pointed out that the improvement of thermal comfort was achieved along with the reduction of delivered energy to the building more than 77%.

To examine the uniformity of air temperature distribution and the possibility of temperature stratification, the distribution of vertical air temperature difference for CFD cells between the ankle level (0.1 m above the floor) and the head level (1.1 m for a seated person), in the occupancy zone, is shown in Fig. 30. The occupancy zone was defined as the area with 0.6 m from the side walls and from 0.1 m to 1.8 m above the floor. In the coldest day of the year (Fig. 30), the majority of points met the requirements for the vertical air temperature difference, which is less than 3 K according to the second thermal comfort category for office buildings. However, a slight temperature stratification was observed covering around 50% of occupancy zone at the optimized AA in the morning at

the coldest day of the year. The reason could be due to considering a yearly average PPD as the thermal comfort constraint during optimization.

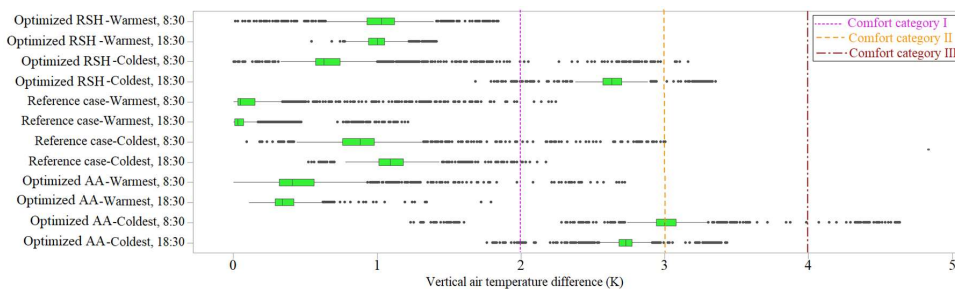


Fig. 30. Box plot of vertical air temperature difference between the ankle and head levels for the cell office C.O.16 for different cases

In addition, with respect to Fig. 29 and Fig. 30 it can be implied that a different control method for the DCV system should be adopted in the coldest periods of the year. Nevertheless, the window opening was functional for both optimized cases during summertime and no significant temperature stratification was observed, despite using rather low air flow rate compared to the reference case.

To analyze the visual comfort in detail for the optimized RSH, optimized AA, and the reference case, the spatial distribution of three common different dynamic indexes including UDI, cDA, and sDA have been shown Fig. 31. Both optimization cases showed superior performance compared to the reference case in terms of visual comfort conditions. Concerning the UDI index, more than half area of the occupancy zone could reach to almost 50% UDI, which is recommended for office building [146], after optimization in both cases. Nevertheless, the optimized AA case provided more uniform distribution of relatively high UDI in the entire area during the occupancy hours. It was even more discernible in terms of cDA and sDA indexes (Fig. 31(b) and (c) two bottom rows). As it can be seen, only a small area near the window could achieve around 35% sDA during occupancy hours in the RSH optimized case while more than 50% of the whole area in the optimized AA case could achieve 30-48% sDA. It implies that the combination of shading control method, which adopted indoor temperature and daylight

parameters, and window to floor area ratio could provide better visual comfort quality in the optimized AA case entire the year.

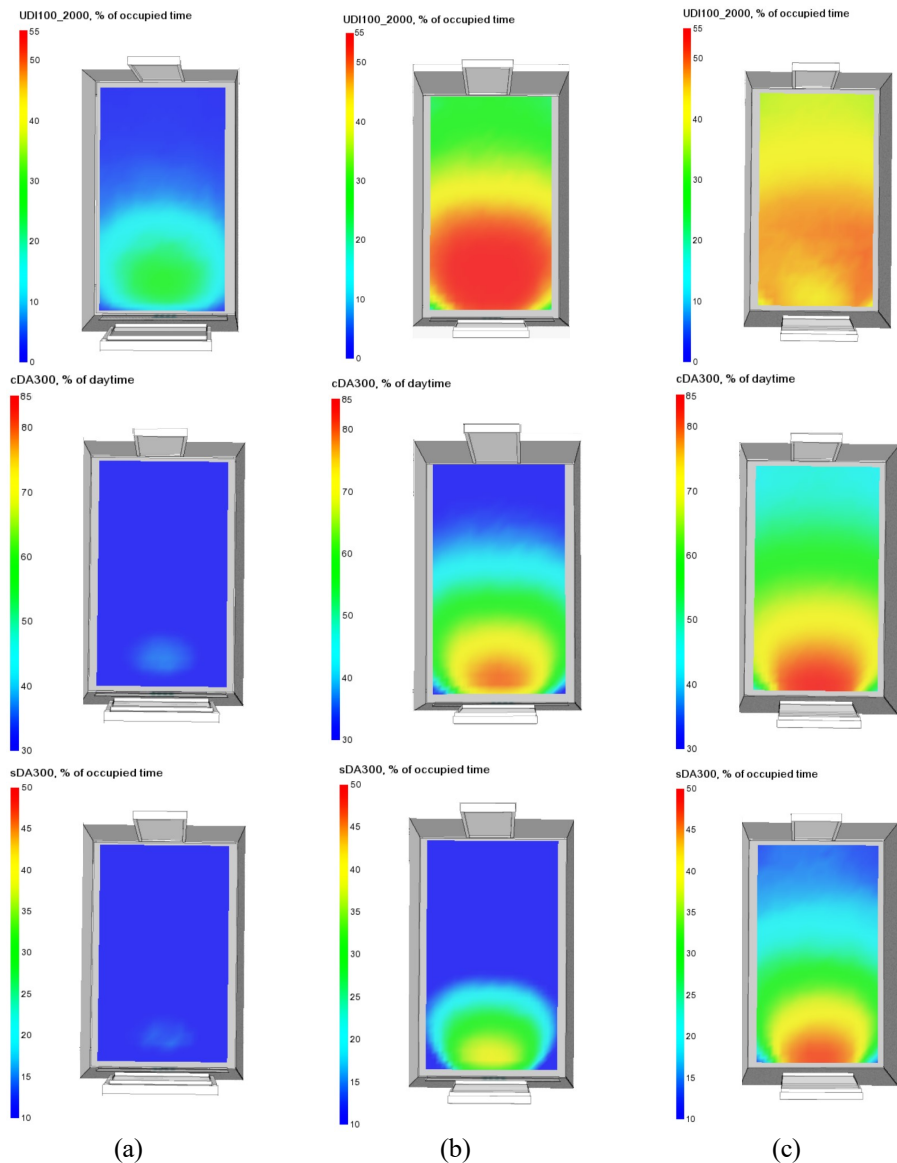


Fig. 31. Spatial distribution of three visual daylight indexes for the cell office C.O.16 for (a) reference case (b) optimized RSH, and (c) optimized AA

It is worth mentioning that although a static parameter was considered as the visual comfort constraint ($DF_{avg} > 2\%$), due to the necessity of Norwegian national requirements, the optimized design variables provided a great improvement in terms of dynamic daylight indexes compared to the reference case.

4.5. Life cycle analysis of GHG emissions from building retrofitting

Besides the energy performance and detailed thermal and visual comfort analysis of the renovation measures, their corresponding GHG emissions have also been studied through LCA method.

4.5.1. LCA framework and material emissions

Table 10 shows the quantity of extra materials and the associated carbon missions. In the PH strategies (RSH_PH and AA_PH) the extra materials were chosen to meet the standard requirements. The RSH_LCC and AA_LCC strategies were based on the Opt. AA Oslo and Opt. RSH Oslo cases described earlier in Section 4.2. The HVAC system in the RSH_PH, and RSH_LCC was the same as the reference building but with new waterborne radiators. In the AA_PH and AA_LCC, the HVAC system was an AA system with DCV control method. Furthermore, as the aim of retrofitting was to reach a nZEB level, two types of PV were used, namely Monocrystalline and Polycrystalline. The energy use for PH standard was used as the criterion to balance the total delivered energy to the building and calculate the necessary area of PV panels, which was calculated based on the method described in Section 2.6. In the OneClick LCA, in order for two types of panels to be comparable in terms of CO₂ emission, a manufacturer that produced both types of panels were chosen, which a Dutch manufacturer was. Furthermore, the lifetime of PV cells was considered 30 years and their degradation rate neglected.

Table 10. Extra materials' quantity and CO₂-eq emissions for different retrofitting strategies

Component	Materials	RSH PH		AA PH		RSH LCC		AA LCC	
		Quantity (m ² -mm)	CO ₂ -eq (kg/m ²)	Quantity	CO ₂ -eq (kg/m ²)	Quantity	CO ₂ -eq (kg/m ²)	Quantity	CO ₂ -eq (kg/m ²)
Extra insulation for external wall	Glava Extrem 32	1025-215	4.6	1025-215	4.6	1025-160	3.5	1025-160	3.5
New exterior façade (external wall)	Fiber cement board cladding	1025-22	4.3	1025-22	4.3	1025-22	4.3	1025-22	4.3
Extra insulation of the floor towards ground	Glava Extrem 32	1000-240		1000-240		1000-20		1000-20	
	Generic concrete	1000-300		1000-300		1000-300		1000-300	
	Plastic vapor barrier	1000-0.2		1000-0.2		1000-0.2		1000-0.2	
	Armouring	27000kg	116	27000kg	116	27000kg	111	27000kg	111
	Mortar	1000-3		1000-3		1000-3		1000-3	
	Epoxy floor paint	1000-0.1		1000-0.1		1000-0.1		1000-0.1	
Extra insulation of the roof	Glava Extrem 32	1000-240		1000-240		1000-20		1000-240	
	Double layer of asphalt roof membrane	1000-3.5	17.5	1000-3.5	17.5	1000-3.5	12.9	1000-3.5	17.5
	Plastic vapor barrier	1000-0.2		1000-0.2		1000-0.2		1000-0.2	
Window	Triple glazing, lifetime 30 years	280m ²	34	280m ²	34	280m ²	34	280m ²	34
External door	Existing doors were replaced by sliding door for use in exterior wall, lifetime 30 years	12.6m ²	4	12.6m ²	4	12.6m ²	4	12.6m ²	4
New waterborne radiator system	For RSH_PH, and RSH_LCC, lifetime 30 years	10755 kg	52	NA	NA	10755 kg	52	NA	NA

CO₂ emissions due to operational energy use were calculated based on the delivered energy to the building and emission factors for electricity and district heating in accordance with NS 3720. The functional unit was considered as one square meter of heated floor area over a service lifetime of 60 years [147]. The GHGs were based on the Kyoto basket gases weighted by their global warming potential (GWP) and aggregated to give total greenhouse gas emissions in terms of CO₂-eq [148]. Regarding the CO₂ emission factor related to the electricity production and transportation, 0.13 kg CO₂-eq/kWh was assumed based on production mix approach in the electricity supply (EU28 + Norge) with an expected average over 60 years and starting point based on the average for the last 3 years [131, 149]. The EU28 mix is a global power producer and the result of cooperation among the countries of the EU, where the goal is to reduce greenhouse gas emissions related to the production of electricity [149]. The CO₂ emission factor for district heating was selected 0.0138 kg CO₂-eq/kWh, which was based on the public data from Norwegian District Heating Fellowship [150].

4.5.2. LCA results of various retrofitting strategies

Fig. 32 shows the total CO₂ emissions for the reference building and retrofitting strategies for the lifetime of 60 years. An obvious decrease of CO₂-eq emissions associated with the operational energy use, around 68% and 73%, was obtained for the RSH and AA strategies. Less CO₂-eq reduction in the cases with RSH system was due to the heating distribution network for waterborne radiators, which did not exist in the cases with AA system. Another reason was using the DCV method in the AA system which assisted in higher reduction of building energy use than CAV ventilation in the RSH system. Although, due to the utilization of extra materials, the embodied CO₂ emissions increased in the retrofitting strategies compared to the reference case, around 12-19%, the reduction of CO₂ emissions was much lesser in the operational stage. Accordingly, the share of operational energy use (B6) in total CO₂ emissions was around 77% for the reference case whereas it was obtained around 43-46% for the retrofitting strategies, and 54-57% of total emissions were due to embodied emissions of extra materials. It was also shown in [109] that, applying the building retrofit measures could reduce the corresponding

environmental impacts by 56-96% for a residential building in Norway, where the largest reduction was due to renovation of energy supply in addition to building envelope retrofitting. Likewise, the results of retrofitting a Swedish residential building towards PH level, with energy use around 50 kWh/m².year, showed 50-64% reduction in the initial operation CO₂-eq/m² emission [105]. Overall, the AA_LCC produced the least CO₂ emissions, around 354 kg CO₂-eq/m², among all studied strategies, owing to less materials used in the product stage together with less emissions generated in the operational energy use stage.

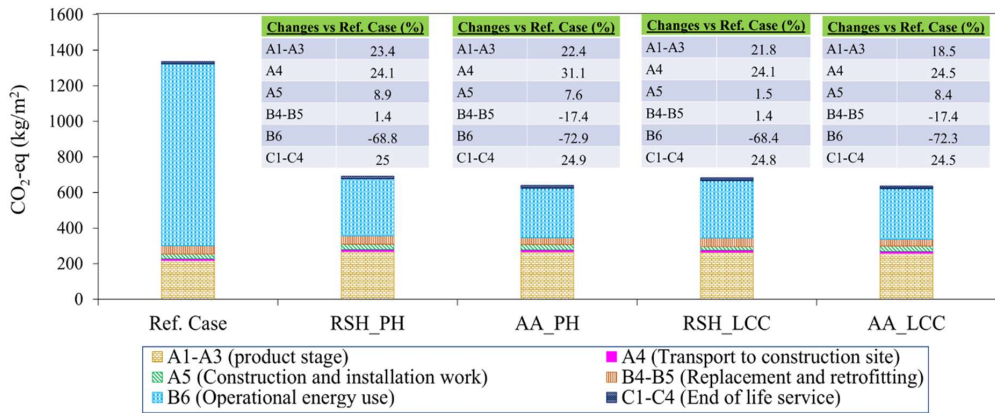


Fig. 32. Total CO₂-eq emissions related to various stages of the building life cycle for the reference building (TEK 87) and retrofitting strategies

To further compare the embodied emissions for the reference building and retrofitting strategies, the CO₂ emissions associated with different building component and materials are shown in Fig. 33. The change in the insulation thickness of the building envelope, together with replacement of various types of windows were the differences among the retrofitting strategies. The cases equipped with AA system generated less emission related to HVAC installations. In this regard, the minimum embodied CO₂ emissions from materials were produced for the AA_LCC case. Although HVAC installation generated almost the largest embodied CO₂ emissions among all building components and materials for all five cases, which was mainly due to replacement (B4-B5), the largest increase in the embodied emissions, due to retrofitting, was associated with the re-insulation of the ground floor. It was also pointed out in [151] that the

embodied emissions corresponding to the periodical maintenance of the HVAC system could be larger than the initial embodied emissions. It should be noted that, the share of produced emissions in the operational energy use which was only corresponding to re-insulation of the ground floor should also be considered to find out if this retrofit measure could compensate for the large associated embodied emissions. However, it could have been more appropriate, from an environment perspective, to further re-insulate the other parts of the building envelope instead of ground floor. It can be also observed in Fig. 33 that the emissions associated with retrofitting of exterior walls and roof were considerably lower compared to the ground floor.

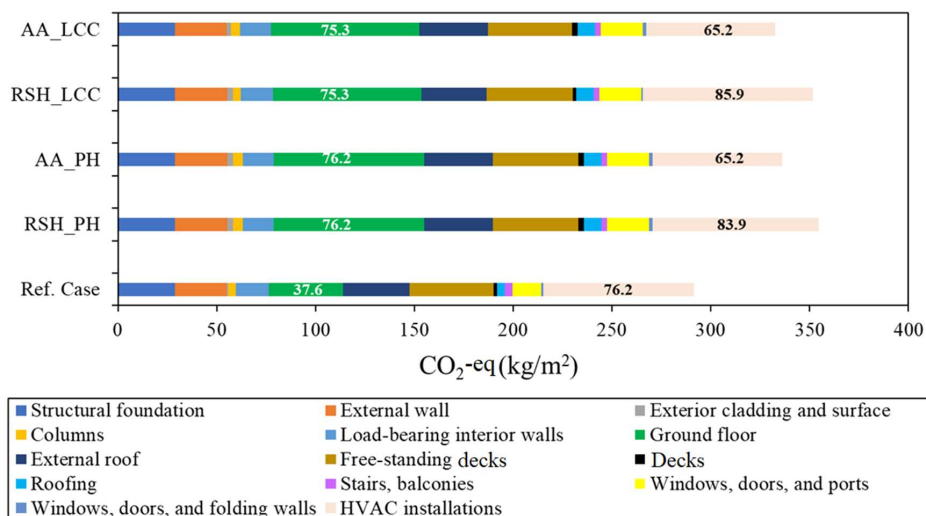


Fig. 33. Embodied CO₂-eq emissions from materials for the reference building and the retrofitting strategies

To obtain a comprehensive LCA of retrofit strategies, the CO₂ payback time was used for the studies cases, which is shown in Fig. 34. It is an important indicator for finding the retrofit strategies which have the best environmental performance during the building lifetime and determines how long it would take before the lower emissions from energy use will offset greenhouse gas emissions in connection with retrofitting. In this respect, the retrofitting strategies were compared to the reference building, spread over a 60-year period. The embodied emissions related to all building's life cycle stages, except the

replacement, have been considered at the beginning of the lifetime period, while the emissions related to the operational energy use were stacked over the building lifetime. As the results demonstrates, the CO₂ payback times for AA_LCC and RSH_LCC strategies were almost the same and equal to 3.9 years, followed by AA_PH and RSH_PH strategies with CO₂ payback times equal to 4.6 and 5.1 years, respectively. Overall, considering both the CO₂ payback times and the total CO₂ emissions generated at various stages of the building life cycle, the AA_LCC had the best environmental performance among all retrofitting strategies.

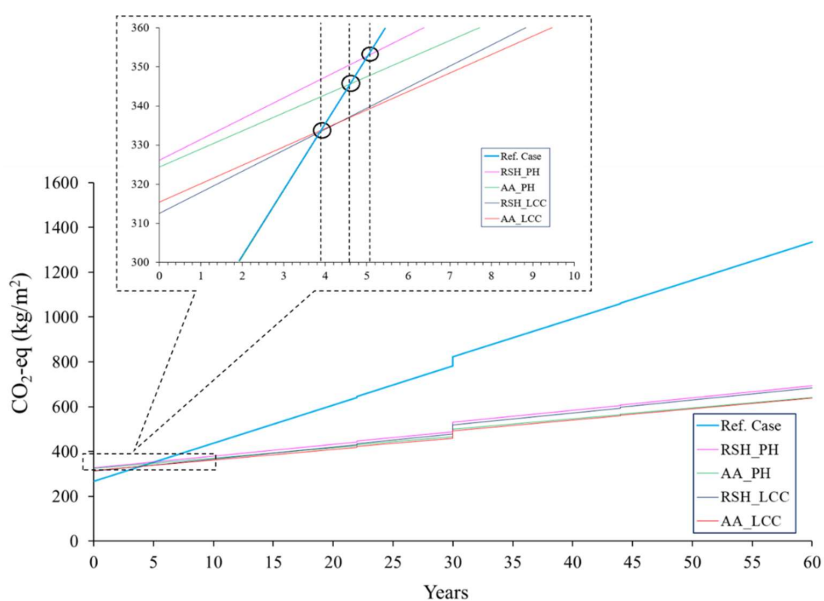


Fig. 34. Time plot of CO₂-eq for the reference case and different retrofit strategies

The nZEB level was achieved by adding PV panels to balance the total delivered energy to the building. The environmental impacts of two types of PV panels were studied for the RSH_PH strategy, which are shown in Fig. 35. Although Monocrystalline resulted in less material usage (smaller PV panel areas) to reach nZEB level, due to its higher efficiency than Polycrystalline, it generated more CO₂ emissions than Polycrystalline, especially in the product stage, replacement, and retrofitting (Fig. 35 (a)). This was due to extra Czochralski process in the production of Monocrystalline PV panels. In addition, in

both cases, the replacement and retrofitting stood for more than 49% of CO₂ emissions production. Fig. 35 (b) shows that adding PV panels to balance the delivered energy use for RSH_PH led to increase of embodied emissions around 11% and 6% when applying Monocrystalline and Polycrystalline, respectively. However, the emissions related to the operational energy use, accounting for 50% of total emissions in RSH_PH, were decreased resulting in approximately 39% and 44% net reduction of CO₂ emissions in nZEB 2 and nZEB 1 strategies, respectively.

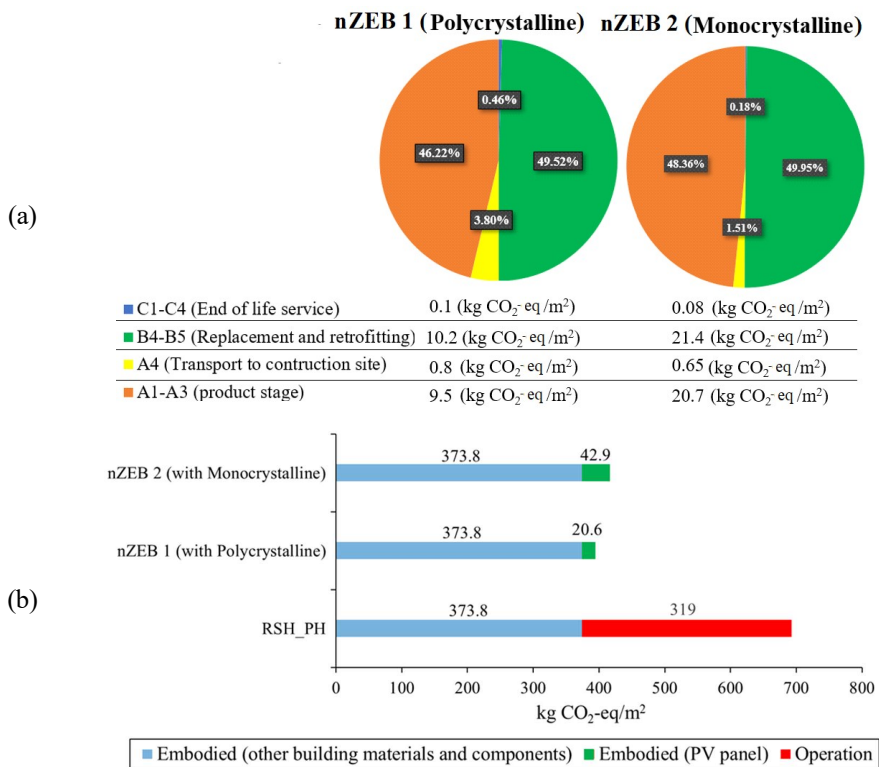


Fig. 35. (a) CO₂-eq emissions for two types of PV panels to reach nZEB level and (b) total CO₂-eq emissions for the RSH_PH and two nZEB cases

Fig. 36 shows the time profile of CO₂ emissions for RSH_PH case and two nZEB strategies over lifetime period 60 years. As it can be observed, the nZEB 1 had CO₂ payback time around 6 years while the payback time was obtained around 12 years for the nZEB 2 strategy.

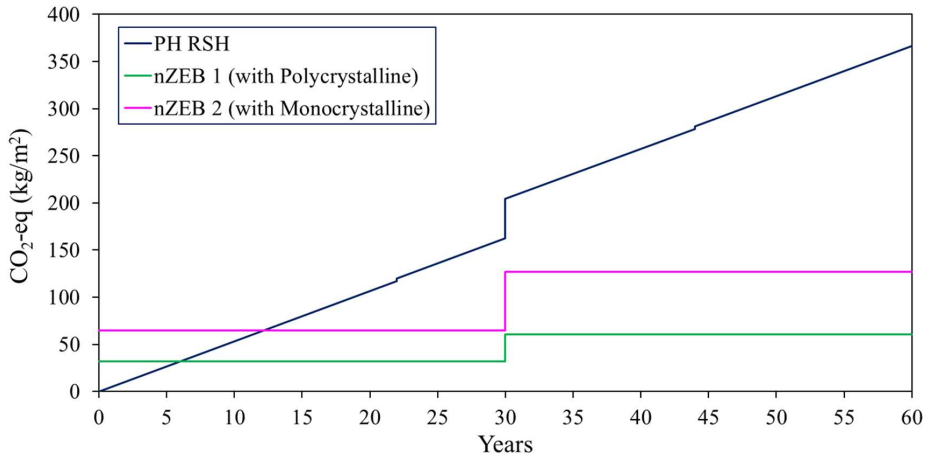


Fig. 36. Time plot of CO₂-eq for the RSH_PH and two nZEB cases

Comparing the results obtained in Fig. 35 and Fig. 36 shows that the case with Polycrystalline PV panels had better performance than Monocrystalline ones in terms of environmental impact even though a larger PV area, around 20%, was needed for the Polycrystalline PV panels to reach nZEB level. However, the high efficiency and space saving make Monocrystalline PV panels attractive on the market, as there is often limited installation space.

5. Conclusions

In this thesis, various aspects of developing sustainable building retrofitting procedures were addressed for the existing Norwegian office buildings. The approach was implemented using different numerical tools and the methods and the results provided different insights towards achieving a ZEB level.

5.1. Summary of thesis

A sustainable building retrofitting framework was implemented through two different approaches using optimization process. In the first approach, the existing building characteristics were based on the Norwegian building code TEK 10 (2010 onwards) and small retrofitting measures were applied. In the second approach, the TEK 87 (1980s) building requirements were considered for the reference case and more renovation measures were included. The optimization framework was implemented through a Graphical Script module in both approaches. Furthermore, a detailed thermal comfort and visual comfort analysis, ZEB balance evaluation, and LCA of GHG emissions associated with different retrofitting interventions were conducted for the reference cases and optimized solutions.

The results of optimization process in the first retrofitting approach showed that high-quality window and external wall were always used in the optimized solutions, but the ground floor and the roof retrofitting were the costliest options and were used only when the reduction of operational cost due to energy use was higher than the increase of investment cost. The amount of delivered energy saving for the cases equipped with the AA system was higher than the cases in which the radiator space heating system was used.

For further improvement of building energy performance towards nZEB, a large group of retrofit measures including window opening and shading device control strategies were also investigated through the second retrofitting approach. The optimization results in this approach revealed that the building energy use for space heating and space cooling could be significantly reduced through optimization process, up to 77%, compared to the reference building case modelled in compliance with the

Norwegian building regulation TEK 87. The optimal shading control method was based on solar radiation on the exterior side of the windows and the best performance regarding the window opening was attained when the control method was in accordance with indoor air temperature, direct solar radiation on the façade, and wind velocity set points, for the summer operation. Accordingly, the main factors in controlling shading devices and window opening were selected based on the indoor air temperature and the solar radiation parameters, but with different set points for these optimization input variables. The most challenging optimization design variable to select was the window to floor area ratio because it influenced the thermal and visual comfort in an opposite way. It signifies the importance of considering the combined effect of these design variables when targeting the nZEB level. In addition, the proposed optimization framework implemented through the Graphical Script empowers building engineers and architects to test such design solutions.

Detailed CFD and daylight simulation results for the optimized solutions in the second retrofitting approach showed that both the optimized RSH and AA cases could satisfy the thermal comfort requirements, based on the comfort category II, for longer period of the year compared to the reference case. The optimized AA case showed the best performance in this respect. However, the DCV system, adopted in this optimized case, could not provide a comfortable condition, according to any of three comfort categories, in extreme cold conditions in Norway. The window opening was functional for both optimized cases during summertime and no significant temperature stratification was observed, in spite of using rather low air flow rate compared to the reference case.

LCA of GHG emissions associated with the optimal building renovation solutions in the first retrofitting approach showed that applying retrofit measures increased the embodied emissions for various retrofit interventions owing to use of extra materials, their transport to construction site, and end of life service. However, compared to reference building TEK 87, the reduction of CO₂ emissions associated with the operational energy use, which were calculated around 69-73%, outweighed the embodied CO₂ emissions of extra materials. Among all retrofitting strategies, the LCC optimized case with AA system showed the best performance in terms of environmental impact so that the total

CO₂ emissions were decreased from 1336 kg CO₂-eq/m², in the reference case, to 637 kg CO₂-eq/m² in the AA_LCC strategy. The reason was that this strategy showed better energy performance with less material use, due to omitting waterborne radiators in this strategy, which resulted in less embodied and operational CO₂ emissions compared to other retrofitting strategies. The GHG emissions of two nZEB cases corresponding to use of Polycrystalline and Monocrystalline PV panels showed a considerable reduction, around 39-44%, of total CO₂ emissions compared to the PH case with RSH system.

This PhD work provides practical insights for developing sustainable retrofit interventions of Norwegian office buildings, and as demonstrated, preliminary steps for further research into implementation of low temperature all-air system to achieve ZEB level.

5.2. Future work

An essential step for future work is prolonged and onsite measurement/monitoring in buildings being modified using the considered approaches. As presented in the different sections, most of the retrofitting process was focused on various options for building envelope, fenestration, HVAC system components and set point, especially the AA system, window opening control methods, and shading device materials and control methods. However, the energy supply technologies have not been investigated. Technologies that further facilitate the efficient implementation of renewable energy mix is yet to be studied. Furthermore, it should be noted that this thesis has chiefly dealt with space heating and building electricity usage. Energy savings from DHW was not discussed. This brings up further challenges, as the most buildings are shifted to ZEB level, energy use from DHW play a key role.

The future work should be planned to address the following directions:

- Development and application of energy efficient supply technologies that take advantage of onsite renewable energy sources such as integration of solar collectors with ground source heat pump (GSHP) systems.

- Development of efficient heat recovery systems in the building stock that include both exhaust air and wastewater.
- Integration of the above-mentioned systems with the next generation of district heating system and the electricity grids and considering various climate change scenarios instead of using typical weather data.

It is worth mentioning that the data sources used in this LCA work may include some uncertainties arising from inaccuracy of available data or their dependency on the specific analyzed systems and inaccuracy of parameters modelled in this thesis. Finally, let us remind that the targets were restricted to zero energy building level. It would be more challenging to focus on zero emission building level. This could be achieved by broad use of low CO₂ emission materials and those having negative embodied carbon in the construction phase, such as tree and short-term crops, or extensive use of renewable energy sources such as PV panels, biomass combined heat and power (CHP) etc. It should target at compensating both the embodied and operational emissions during the entire building life cycle. It would be also interesting to find out which approach is more efficient, because if, for example, a scenario of low carbon electricity grid is considered, it would be more difficult to achieve a zero emission level through extensive use of PV panels.

References

- [1] Global Climate Change Indicators. National Centers for Environmental Information, National Oceanic and Atmospheric Administration, USA., (2016).
- [2] DIRECTIVE (EU) 2018/844 of the European parliament and of the council of 30 May 2018 amending Directive 2010/31/EU on the energy performance of buildings and Directive 2012/27/EU on energy efficiency (Text with EEA relevance), in, Official Journal of the European Union.
- [3] I. Artola, K. Rademackers, R. Williams, J. Yearwood, Boosting building renovation: What potential and value for Europe, Study for the iTRE Committee, Commissioned by DG for Internal Policies Policy Department A, (2016) 72.
- [4] IEA (2019), The Critical Role of Buildings, IEA, Paris, <https://www.iea.org/reports/the-critical-role-of-buildings>.
- [5] National Science and Technology Council, C. o. Federal R&D, "Federal R&D Agenda for Net Zero Energy, High-Performance Green Buildings," USA, (2008).
- [6] Energy Facts Norway, Ministry of Petroleum and Energy, Retrieved from <https://energifaktanorge.no/en/>, in, 2015.
- [7] Building Technical Regulations (TEK10) 2010, § 14-2. Requirements for energy efficiency (in Norwegian), in.
- [8] Building Technical Regulations (TEK17) 2017, § 14-2. Requirements for energy efficiency (in Norwegian), in.
- [9] D. Kolokotsa, C. Diakaki, E. Grigoroudis, G. Stavrakakis, K. Kalaitzakis, Decision support methodologies on the energy efficiency and energy management in buildings, *Advances in Building Energy Research*, 3 (1) (2009) 121-146.
- [10] NS-3701-Criteria for passive houses and low energy buildings, Non-residential buildings, in, Standard Norge, Norway, 2012.
- [11] Statistics Norway, <https://www.ssb.no/en/statbank/table/03173/tableViewLayout1/>, in, 2020.
- [12] M. Thyholt, A.G. Lien, T.H. Dokka, Kartlegging av mekanisk kjøling i nye kontor- og forretningsbygg, in, SINTEF Bygg og miljø, Trondheim, Norway, 2001, pp. 36.
- [13] THEMA Consulting Group- Energibruk i kontorbygg, Trender og drivere. Norges vassdrags- og energidirektorat (NVE), ENOVA, in, Norway, 2013.
- [14] Enova, S.F. "Enovas Byggstatistikk 2020." *Trondheim*. Enova. Accessed from <https://www.enova.no> (2020).

- [15] I. Sartori, B.J. Wachenfeldt, A.G. Hestnes, Energy demand in the Norwegian building stock: Scenarios on potential reduction, *Energy Policy*, 37 (5) (2009) 1614-1627.
- [16] E. Rosenberg, K. Espegren, A. Lind, M. Kirkengen, Future energy demand - a Norwegian overview, in, Institute for Energy Technology (IFE), Norway, 2013.
- [17] Statistics Norway, SSB, Balance of district heating (GWh) 1983 - 2019, Retrieved from <https://www.ssb.no/en/statbank/table/04727/>, in, 2020.
- [18] D. D'Agostino, L. Mazzarella, What is a Nearly zero energy building? Overview, implementation and comparison of definitions, *Journal of Building Engineering*, 21 (2019) 200-212.
- [19] A.J. Marszal, P. Heiselberg, J.S. Bourrelle, E. Musall, K. Voss, I. Sartori, A. Napolitano, Zero Energy Building – A review of definitions and calculation methodologies, *Energy and Buildings*, 43 (4) (2011) 971-979.
- [20] K. Voss, I. Sartori, R. Lollini, Nearly-zero, net zero and plus energy buildings, *REHVA Journal*, Dec, (2012).
- [21] I. Sartori, A. Napolitano, K. Voss, Net zero energy buildings: A consistent definition framework, *Energy and Buildings*, 48 (2012) 220-232.
- [22] S.M. Fufa, R.D. Schlanbusch, K. Sørnes, M. Inman, I. Andresen, A Norwegian ZEB Definition Guideline, ZEB Project report 29, in, 2016.
- [23] O. Pasichnyi, F. Levihn, H. Shahrokni, J. Wallin, O. Kordas, Data-driven strategic planning of building energy retrofitting: The case of Stockholm, *Journal of Cleaner Production*, 233 (2019) 546-560.
- [24] C. Fan, D. Yan, F. Xiao, A. Li, J. An, X. Kang, Advanced data analytics for enhancing building performances: From data-driven to big data-driven approaches, *Building Simulation*, (2020).
- [25] B. Grillone, S. Danov, A. Sumper, J. Cipriano, G. Mor, A review of deterministic and data-driven methods to quantify energy efficiency savings and to predict retrofitting scenarios in buildings, *Renewable and Sustainable Energy Reviews*, 131 (2020) 110027.
- [26] S. Touzani, J. Granderson, S. Fernandes, Gradient boosting machine for modeling the energy consumption of commercial buildings, *Energy and Buildings*, 158 (2018) 1533-1543.
- [27] M. Brown, C. Barrington-Leigh, Z. Brown, Kernel regression for real-time building energy analysis, *Journal of Building Performance Simulation*, 5 (4) (2012) 263-276.
- [28] W.N.W.M. Adnan, N.Y. Dahlan, I. Musirin, Development of hybrid artificial neural network for quantifying energy saving using measurement and verification, *Indonesian Journal of Electrical Engineering and Computer Science*, 8 (1) (2017) 137-145.

- [29] C. Chang, J. Zhao, N. Zhu, Energy saving effect prediction and post evaluation of air-conditioning system in public buildings, *Energy and Buildings*, 43 (11) (2011) 3243-3249.
- [30] J.S. Macías, C.P. Tello, A.A. Ramírez, A.L. Arista, H.M. Almaguer, P.R. Escobedo, A.R. Puente, Assessment of electrical saving from energy efficiency programs in the residential sector in Mexicali, Mexico, *Sustainable cities and society*, 38 (2018) 795-805.
- [31] P. Zangheri, R. Armani, M. Pietrobon, L. Pagliano, Identification of cost-optimal and NZEB refurbishment levels for representative climates and building typologies across Europe, *Energy Efficiency*, 11 (2) (2018) 337-369.
- [32] A. Rysanek, R. Choudhary, Optimum building energy retrofits under technical and economic uncertainty, *Energy and Buildings*, 57 (2013) 324-337.
- [33] F. Ascione, N. Bianco, C. De Stasio, G.M. Mauro, G.P. Vanoli, Artificial neural networks to predict energy performance and retrofit scenarios for any member of a building category: A novel approach, *Energy*, 118 (2017) 999-1017.
- [34] Y.-H. Lin, M.-D. Lin, K.-T. Tsai, M.-J. Deng, H. Ishii, Multi-objective optimization design of green building envelopes and air conditioning systems for energy conservation and CO₂ emission reduction, *Sustainable Cities and Society*, 64 (2021) 102555.
- [35] F. Rosso, V. Ciancio, J. Dell'Olmo, F. Salata, Multi-objective optimization of building retrofit in the Mediterranean climate by means of genetic algorithm application, *Energy and Buildings*, 216 (2020).
- [36] P. Pilechiha, M. Mahdavejad, F. Pour Rahimian, P. Carnemolla, S. Seyedzadeh, Multi-objective optimisation framework for designing office windows: quality of view, daylight and energy efficiency, *Applied Energy*, 261 (2020).
- [37] S. Longo, F. Montana, E. Riva Sanseverino, A review on optimization and cost-optimal methodologies in low-energy buildings design and environmental considerations, *Sustainable Cities and Society*, 45 (2019) 87-104.
- [38] F. Harkouss, F. Fardoun, P.H. Biwole, Passive design optimization of low energy buildings in different climates, *Energy*, 165 (2018) 591-613.
- [39] T. Niemelä, K. Levy, R. Kosonen, J. Jokisalo, Cost-optimal renovation solutions to maximize environmental performance, indoor thermal conditions and productivity of office buildings in cold climate, *Sustainable Cities and Society*, 32 (2017) 417-434.
- [40] M. Palonen, M. Hamdy, A. Hasan, MOBO a new software for multi-objective building performance optimization, in: *Proceedings of BS 2013: 13th Conference of the International Building Performance Simulation Association, France,, 2013.*
- [41] J. Hirvonen, J. Jokisalo, J. Heljo, R. Kosonen, Towards the EU emissions targets of 2050: optimal energy renovation measures of Finnish apartment buildings, *International Journal of Sustainable Energy*, 38 (7) (2018) 649-672.

- [42] V. Arabzadeh, J. Jokisalo, R. Kosonen, A cost-optimal solar thermal system for apartment buildings with district heating in a cold climate, *International Journal of Sustainable Energy*, 38 (2) (2018) 141-162.
- [43] L. Magnier, F. Haghghat, Multiobjective optimization of building design using TRNSYS simulations, genetic algorithm, and Artificial Neural Network, *Building and Environment*, 45 (3) (2010) 739-746.
- [44] E. Asadi, M.G. da Silva, C.H. Antunes, L. Dias, A multi-objective optimization model for building retrofit strategies using TRNSYS simulations, GenOpt and MATLAB, *Building and Environment*, 56 (2012) 370-378.
- [45] M. Ferrara, E. Sirombo, E. Fabrizio, Automated optimization for the integrated design process: the energy, thermal and visual comfort nexus, *Energy and Buildings*, 168 (2018) 413-427.
- [46] F.P. Chantrelle, H. Lahmidi, W. Keilholz, M.E. Mankibi, P. Michel, Development of a multicriteria tool for optimizing the renovation of buildings, *Applied Energy*, 88 (4) (2011) 1386-1394.
- [47] Y. Lu, S. Wang, Y. Zhao, C. Yan, Renewable energy system optimization of low/zero energy buildings using single-objective and multi-objective optimization methods, *Energy and Buildings*, 89 (2015) 61-75.
- [48] O.T. Karaguzel, R. Zhang, K.P. Lam, Coupling of whole-building energy simulation and multi-dimensional numerical optimization for minimizing the life cycle costs of office buildings, *Building Simulation*, 7 (2) (2013) 111-121.
- [49] Y. Schwartz, R. Raslan, D. Mumovic, Implementing multi objective genetic algorithm for life cycle carbon footprint and life cycle cost minimisation: A building refurbishment case study, *Energy*, 97 (2016) 58-68.
- [50] N. Delgarm, B. Sajadi, S. Delgarm, Multi-objective optimization of building energy performance and indoor thermal comfort: A new method using artificial bee colony (ABC), *Energy and Buildings*, 131 (2016) 42-53.
- [51] N. Delgarm, B. Sajadi, F. Kowsary, S. Delgarm, Multi-objective optimization of the building energy performance: A simulation-based approach by means of particle swarm optimization (PSO), *Applied Energy*, 170 (2016) 293-303.
- [52] K. Bamdad, M.E. Cholette, L. Guan, J. Bell, Ant colony algorithm for building energy optimisation problems and comparison with benchmark algorithms, *Energy and Buildings*, 154 (2017) 404-414.
- [53] N. Djuric, V. Novakovic, J. Holst, Z. Mitrovic, Optimization of energy consumption in buildings with hydronic heating systems considering thermal comfort by use of computer-based tools, *Energy and Buildings*, 39 (4) (2007) 471-477.
- [54] K. Grygierek, J. Ferdyn-Grygierek, Multi-Objective Optimization of the Envelope of Building with Natural Ventilation, *Energies*, 11 (6) (2018).

- [55] T. Hong, J. Kim, M. Lee, A multi-objective optimization model for determining the building design and occupant behaviors based on energy, economic, and environmental performance, *Energy*, 174 (2019) 823-834.
- [56] M. Karmellos, A. Kiprakis, G. Mavrotas, A multi-objective approach for optimal prioritization of energy efficiency measures in buildings: Model, software and case studies, *Applied Energy*, 139 (2015) 131-150.
- [57] E. Taveres-Cachat, G. Lobaccaro, F. Goia, G. Chaudhary, A methodology to improve the performance of PV integrated shading devices using multi-objective optimization, *Applied Energy*, 247 (2019) 731-744.
- [58] R. Wu, G. Mavromatidis, K. Orehounig, J. Carmeliet, Multiobjective optimisation of energy systems and building envelope retrofit in a residential community, *Applied Energy*, 190 (2017) 634-649.
- [59] M. Hamdy, A. Hasan, K. Siren, Applying a multi-objective optimization approach for Design of low-emission cost-effective dwellings, *Building and Environment*, 46 (1) (2011) 109-123.
- [60] P.E. Nilsson, Achieving the Desired Indoor Climate-Energy efficiency aspects of system design, The Commtech Group, Denmark, 2003.
- [61] P.V. Nielsen, Ventilation in Commercial and Residential Buildings, Ventilation System and Air Quality, von Karman Institute for Fluid Dynamics Brussels, Belgium, 1998.
- [62] L. Mora, Prediction of the thermo-aeraulic performances of buildings by association of models of different levels of fineness within an object-oriented environment, Université de la Rochelle, 2003.
- [63] F. Haghghat, Y. Li, A.C. Megri, Development and validation of a zonal model—POMA, *Building and environment*, 36 (9) (2001) 1039-1047.
- [64] A. Foucquier, S. Robert, F. Suard, L. Stéphan, A. Jay, State of the art in building modelling and energy performances prediction: A review, *Renewable and Sustainable Energy Reviews*, 23 (2013) 272-288.
- [65] Y. Sun, Y. Wu, R. Wilson, A review of thermal and optical characterisation of complex window systems and their building performance prediction, *Applied Energy*, 222 (2018) 729-747.
- [66] C.F. Reinhart, J. Mardaljevic, Z. Rogers, Dynamic daylight performance metrics for sustainable building design, *Leukos*, 3 (1) (2006) 7-31.
- [67] S. Carlucci, F. Causone, F. De Rosa, L. Pagliano, A review of indices for assessing visual comfort with a view to their use in optimization processes to support building integrated design, *Renewable and sustainable energy reviews*, 47 (2015) 1016-1033.
- [68] V.R.L. Verso, G. Mihaylov, A. Pellegrino, F. Pellerey, Estimation of the daylight amount and the energy demand for lighting for the early design stages: Definition of a set of mathematical models, *Energy and Buildings*, 155 (2017) 151-165.

- [69] CIE, International lighting vocabulary, Commission Internationale de l'Éclairage, CIE S 017: 2011, (2011).
- [70] H. Sabry, A. Sherif, M. Gadelhak, M. Aly, Balancing the daylighting and energy performance of solar screens in residential desert buildings: Examination of screen axial rotation and opening aspect ratio, *Solar Energy*, 103 (2014) 364-377.
- [71] U. ISO, 14040, Gestión ambiental, Análisis de ciclo de vida. Principios y marco de referencia, (2006).
- [72] AEN/CTN150, UNE-EN ISO 14044. Gestión Ambiental. Análisis de Ciclo de Vida. Requisitos y Directrices. (2006).
- [73] ISO 14020:2000, Environmental labels and declarations- General principles, in, Standard Norge, 2002.
- [74] A. Vilches, A. Garcia-Martinez, B. Sanchez-Montañes, Life cycle assessment (LCA) of building refurbishment: A literature review, *Energy and Buildings*, 135 (2017) 286-301.
- [75] A. Miller, K. Ip, Sustainable Construction Materials, in: *Sustainability, Energy and Architecture*, 2013, pp. 341-358.
- [76] EN 15978- Sustainability of construction works- Assessment of environmental performance of buildings- Calculation method, in, Standard Norge, Norway, 2011.
- [77] X. Oregi, P. Hernandez, C. Gazulla, M. Isasa, Integrating Simplified and Full Life Cycle Approaches in Decision Making for Building Energy Refurbishment: Benefits and Barriers, *Buildings*, 5 (2) (2015) 354-380.
- [78] Z. Wang, W. Liu, J. Yin, Driving forces of indirect carbon emissions from household consumption in China: an input–output decomposition analysis, *Natural Hazards*, 75 (2) (2015) 257-272.
- [79] I. Blom, L. Itard, A. Meijer, Environmental impact of building-related and user-related energy consumption in dwellings, *Building and Environment*, 46 (8) (2011) 1657-1669.
- [80] E. Meex, A. Hollberg, E. Knapen, L. Hildebrand, G. Verbeeck, Requirements for applying LCA-based environmental impact assessment tools in the early stages of building design, *Building and Environment*, 133 (2018) 228-236.
- [81] Y. Li, X. Chen, X. Wang, Y. Xu, P.-H. Chen, A review of studies on green building assessment methods by comparative analysis, *Energy and Buildings*, 146 (2017) 152-159.
- [82] T. Sartori, R. Drogemuller, S. Omrani, F. Lamari, A schematic framework for Life Cycle Assessment (LCA) and Green Building Rating System (GBRS), *Journal of Building Engineering*, (2021).

- [83] A. Cablé, M. Mysen, K. Thunshelle, Can demand controlled ventilation replace space heating in office buildings with low heating demand?, in: Indoor Air conference, Hong Kong, 2014.
- [84] W.J. Fisk, D. Faulkner, D. Sullivan, F. Bauman, Air change effectiveness and pollutant removal efficiency during adverse mixing conditions, 7 (1) (1997) 55-63.
- [85] F.J. Offermann, D. Int-Hout, Ventilation effectiveness measurements of three supply/return air configurations, Environment International, 15 (1) (1989) 585-592.
- [86] E. Naderi, B. Sajadi, M.A. Behabadi, E. Naderi, Multi-objective simulation-based optimization of controlled blind specifications to reduce energy consumption, and thermal and visual discomfort: Case studies in Iran, Building and Environment, 169 (2020).
- [87] K. Lakhdari, L. Sriti, B. Painter, Parametric optimization of daylight, thermal and energy performance of middle school classrooms, case of hot and dry regions, Building and Environment, 204 (2021) 108173.
- [88] A. Katsifaraki, B. Bueno, T.E. Kuhn, A daylight optimized simulation-based shading controller for venetian blinds, Building and Environment, 126 (2017) 207-220.
- [89] G. Yun, K.C. Yoon, K.S. Kim, The influence of shading control strategies on the visual comfort and energy demand of office buildings, Energy and Buildings, 84 (2014) 70-85.
- [90] M. Thalfeldt, J. Kurnitski, External shading optimal control macros for 1-and 2-piece automated blinds in European climates, in: Building Simulation, Springer, 2015, pp. 13-25.
- [91] F. Stazi, F. Naspi, G. Ulpiani, C. Di Perna, Indoor air quality and thermal comfort optimization in classrooms developing an automatic system for windows opening and closing, Energy and Buildings, 139 (2017) 732-746.
- [92] H.B. Rijal, P. Tuohy, M.A. Humphreys, J.F. Nicol, A. Samuel, J. Clarke, Using results from field surveys to predict the effect of open windows on thermal comfort and energy use in buildings, Energy and Buildings, 39 (7) (2007) 823-836.
- [93] M.J. Alonso, H.M. Mathisen, R. Collins, Ventilative cooling as a solution for highly insulated buildings in cold climate, Energy Procedia, 78 (2015) 3013-3018.
- [94] T. Psomas, M. Fiorentini, G. Kokogiannakis, P. Heiselberg, Ventilative cooling through automated window opening control systems to address thermal discomfort risk during the summer period: Framework, simulation and parametric analysis, Energy and Buildings, 153 (2017) 18-30.
- [95] D.B. Crawley, J.W. Hand, M. Kummert, B.T. Griffith, Contrasting the capabilities of building energy performance simulation programs, Building and Environment, 43 (4) (2008) 661-673.
- [96] P.V. Nielsen, Fifty years of CFD for room air distribution, Building and Environment, 91 (2015) 78-90.

- [97] P.V. Nielsen, F. Allard, H.B. Awbi, L. Davidson, A. Schälín, Computational fluid dynamics in ventilation design REHVA guidebook No 10, in, Taylor & Francis, 2007.
- [98] A. Novoselac, Combined airflow and energy simulation program for building mechanical system design, (2004).
- [99] W. Tian, X. Han, W. Zuo, M.D. Sohn, Building energy simulation coupled with CFD for indoor environment: A critical review and recent applications, *Energy and Buildings*, 165 (2018) 184-199.
- [100] M. Rodríguez-Vázquez, I. Hernández-Pérez, J. Xamán, Y. Chávez, M. Gijón-Rivera, J.M. Belman-Flores, Coupling building energy simulation and computational fluid dynamics: An overview, *Journal of Building Physics*, 44 (2) (2020) 137-180.
- [101] X. Shan, N. Luo, K. Sun, T. Hong, Y.-K. Lee, W.-Z. Lu, Coupling CFD and Building Energy Modelling to Optimize the Operation of a Large Open Office Space for Occupant Comfort, *Sustainable Cities and Society*, (2020).
- [102] B. Pandey, R. Banerjee, A. Sharma, Coupled EnergyPlus and CFD analysis of PCM for thermal management of buildings, *Energy and Buildings*, 231 (2021) 110598.
- [103] F. Asdrubali, I. Ballarini, V. Corrado, L. Evangelisti, G. Grazieschi, C. Guattari, Energy and environmental payback times for an NZEB retrofit, *Building and Environment*, 147 (2019) 461-472.
- [104] R. Moschetti, H. Brattebø, M. Sparrevik, Exploring the pathway from zero-energy to zero-emission building solutions: A case study of a Norwegian office building, *Energy and Buildings*, 188-189 (2019) 84-97.
- [105] C. Piccardo, A. Dodoo, L. Gustavsson, Retrofitting a building to passive house level: A life cycle carbon balance, *Energy and Buildings*, 223 (2020).
- [106] X. Chen, K. Qu, J. Calautit, A. Ekambaram, W. Lu, C. Fox, G. Gan, S. Riffat, Multi-criteria assessment approach for a residential building retrofit in Norway, *Energy and Buildings*, 215 (2020).
- [107] S.K. Pal, A. Takano, K. Alanne, K. Siren, A life cycle approach to optimizing carbon footprint and costs of a residential building, *Building and Environment*, 123 (2017) 146-162.
- [108] T.F. Kristjansdóttir, A. Houlihan-Wiberg, I. Andresen, L. Georges, N. Heeren, C.S. Good, H. Brattebø, Is a net life cycle balance for energy and materials achievable for a zero emission single-family building in Norway?, *Energy and Buildings*, 168 (2018) 457-469.
- [109] B. Wrålsen, R. O'Born, C. Skaar, Life cycle assessment of an ambitious renovation of a Norwegian apartment building to nZEB standard, *Energy and Buildings*, 177 (2018) 197-206.
- [110] N. Llantoy, M. Chàfer, L.F. Cabeza, A comparative life cycle assessment (LCA) of different insulation materials for buildings in the continental Mediterranean climate, *Energy and Buildings*, 225 (2020).

- [111] L. Luo, Y. Chen, Carbon emission energy management analysis of LCA-Based fabricated building construction, *Sustainable Computing: Informatics and Systems*, 27 (2020).
- [112] Y. Fang, Y. Ding, N. Nord, Data-driven analysis of occupancy and lighting patterns in office building in Norway, *REHVA Journal*, (2019) 64-69.
- [113] ANSI/ASHRAE Standard 55, “Thermal Environmental Conditions for Human Occupancy.” American Society of Heating, Refrigerating and Air-Conditioning Engineers., in, 2013.
- [114] European Commission, “Energy roadmap 2050.” European Union, in, 2012.
- [115] N.H. Sandberg, I. Sartori, O. Heidrich, R. Dawson, E. Dascalaki, S. Dimitriou, T. Vimm-r, F. Filippidou, G. Stegnar, M. Šijanec Zavrl, H. Brattebø, Dynamic building stock modelling: Application to 11 European countries to support the energy efficiency and retrofit ambitions of the EU, *Energy and Buildings*, 132 (2016) 26-38.
- [116] NS 3031, Calculation of energy performance of buildings - Method and data, in, Standard Norge, 2014, pp. 100.
- [117] NS-EN ISO 52000-1, energy performance of buildings, overarching EPB assessment. Part 1: General framework and procedures in, Standard Norge, Norway, 2017.
- [118] Validation of IDA Indoor Climate and Energy 4.0 with Respect to CEN Standards EN 15255-2007 and EN 15265-2007, , in, Equa Simulation Finland Oy, 2010 <http://www.equa.se/en/ida-ice/validation-certifications>.
- [119] M. Wetter, GenOpt (R), generic optimization program, User Manual, Version 2.0.0, (2003).
- [120] N. Hashempour, R. Taherkhani, M. Mahdikhani, Energy performance optimization of existing buildings: A literature review, *Sustainable Cities and Society*, 54 (2020).
- [121] NS-EN ISO 7730- 2006, Ergonomics of the thermal environment - Analytical determination and interpretation of thermal comfort using calculation of the PMV and PPD indices and local thermal comfort criteria, in, Standard Norge, Norway.
- [122] NS-15251-2014, Indoor environmental input parameters for design and assessment of energy performance of buildings addressing indoor air quality, thermal environment, lighting and acoustics, in, Standard Norge, Norway.
- [123] Arbeidstilsynet, <https://www.arbeidstilsynet.no/tema/utforming-av-arbeidsplassen/rad-ved-tilbakeforing-til-arbeid-for-kontorarbeidsplasser/>, in, 15th May, 2020.
- [124] G. Ward, R. Shakespeare, *Rendering with Radiance: the art and science of lighting visualization*, (1998).
- [125] Calculation of average daylight factor and glass area (in Norwegian), SINTEF Byggforsk 421.626, in, 2004.

- [126] I. LM, Approved method: IES spatial Daylight autonomy (sDA) and annual sunlight exposure (ASE), (2013).
- [127] Z. Rogers, D. Goldman, Daylighting metric development using daylight autonomy calculations in the sensor placement optimization tool, Boulder, Colorado, USA: Architectural Energy Corporation: http://www.archenergy.com/SPOT/SPOT_Daylight%20Autonomy%20Report.pdf, (2006).
- [128] A. Hasan, M. Vuolle, K. Sirén, Minimisation of life cycle cost of a detached house using combined simulation and optimisation, *Building and Environment*, 43 (12) (2008) 2022-2034.
- [129] Statistics Norway, Electricity prices, <https://www.ssb.no/en/energi-og-industri/statistikker/elkraftpris>, (2019).
- [130] Norsk Prisbok, in, Norconsult Informasjonssystemer AS, <https://www.norskprisbok.no/WhatIsNP.aspx>, 2019.
- [131] NS 3720- Method for greenhouse gas calculations for buildings (in Norwegian), in, Norsk standard, 2018.
- [132] Bionova. 2020. Calculate your environmental impacts in minutes [Online]. <https://www.oneclicklca.com/>. Accessed date: 03.05.2020., in.
- [133] M. Rabani, H. Bayera Madessa, N. Nord, Achieving zero-energy building performance with thermal and visual comfort enhancement through optimization of fenestration, envelope, shading device, and energy supply system, *Sustainable Energy Technologies and Assessments*, 44 (2021) 101020.
- [134] Byggeforskrift- TEK 87, 1987, in.
- [135] F. Noris, E. Musall, J. Salom, B. Berggren, S.Ø. Jensen, K. Lindberg, I. Sartori, Implications of weighting factors on technology preference in net zero energy buildings, *Energy and Buildings*, 82 (2014) 250-262.
- [136] G.N. Tiwari, R.K. Mishra, S.C. Solanki, Photovoltaic modules and their applications: A review on thermal modelling, *Applied Energy*, 88 (7) (2011) 2287-2304.
- [137] H.B. Madessa, Performance Analysis of Roof-mounted Photovoltaic Systems – The Case of a Norwegian Residential Building, *Energy Procedia*, 83 (2015) 474-483.
- [138] Grini Catherine, Sartori Igor, Haase Matthias, Wigenstad Tore, Mathisen Hans-Martin, Wøhlk Helle, Sørensen Jæger, Pettersen Arnkell, B. Ida, LECO - Energibruk i fem kontorbygg i Norge, in, SINTEF Byggeforsk, Norway, 2010, pp. 165.
- [139] M. Rabani, H. Bayera Madessa, O. Mohseni, N. Nord, Minimizing delivered energy and life cycle cost using Graphical script: An office building retrofitting case, *Applied Energy*, 268 (2020).
- [140] N. Nord, Building Energy Efficiency in Cold Climates, in: *Encyclopedia of Sustainable Technologies*, 2017, pp. 149-157.

- [141] J. Hirvonen, J. Jokisalo, J. Heljo, R. Kosonen, Towards the EU Emission Targets of 2050: Cost-Effective Emission Reduction in Finnish Detached Houses, *Energies*, 12 (22) (2019).
- [142] A. Bring, P. Sahlin, M. Vuolle, Models for Building Indoor Climate and Energy Simulation, in, Dept. of Building Sciences, KTH, Stockholm, Sweden, 1999.
- [143] The Director General of the National Archival Services of Norway, Requirements for archive premises-Guidelines for public bodies, 2007, in.
- [144] M. Rabani, H.B. Madessa, N. Nord, P. Schild, M. Mysen, Performance assessment of all-air heating in an office cubicle equipped with an active supply diffuser in a cold climate, *Building and Environment*, 156 (2019) 123-136.
- [145] T. van Hooff, P.V. Nielsen, Y. Li, Computational fluid dynamics predictions of non-isothermal ventilation flow-How can the user factor be minimized?, *Indoor Air*, 28 (6) (2018) 866-880.
- [146] C.F. Reinhart, D.A. Weissman, The daylit area – Correlating architectural student assessments with current and emerging daylight availability metrics, *Building and Environment*, 50 (2012) 155-164.
- [147] A.G. Hestnes, N.L. Eik-Nes, Zero emission buildings, Fagbokforlaget Bergen, 2017.
- [148] L.A. Wright, S. Kemp, I. Williams, ‘Carbon footprinting’: towards a universally accepted definition, *Carbon Management*, 2 (1) (2011) 61-72.
- [149] R. Turconi, A. Boldrin, T. Astrup, Life cycle assessment (LCA) of electricity generation technologies: Overview, comparability and limitations, *Renewable and Sustainable Energy Reviews*, 28 (2013) 555-565.
- [150] Norsk fjernvarme. 2020. Energikilder- Retrieved April, 2020 <https://www.fjernvarme.no/fakta/energikilder>, in.
- [151] M. Medas, D. Cheshire, A. Cripps, J. Connaughton, M. Peters, Towards BIM-integrated, resource-efficient building services, *Product Lifetimes And The Environment*, (2015).

Selected Papers

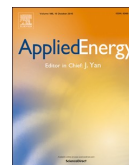
Paper 1

M. Rabani, H. Bayera Madessa, O. Mohseni, N. Nord, Minimizing delivered energy and life cycle cost using Graphical script: An office building retrofitting case, *Applied Energy*, 268 (2020).



Contents lists available at ScienceDirect

Applied Energy

journal homepage: www.elsevier.com/locate/apenergy

Minimizing delivered energy and life cycle cost using Graphical script: An office building retrofitting case

Mehrdad Rabani^{a,c,*}, Habtamu Bayera Madessa^a, Omid Mohseni^b, Natasa Nord^c

^a Department of Civil Engineering and Energy Technology, Oslo Metropolitan University, Norway

^b Norconsult AS, Norway

^c Department of Energy and Process Engineering, Norwegian University of Science and Technology, Norway

HIGHLIGHTS

- Graphical script method was used for optimization of an office building.
- Two scenarios were considered to minimize the delivered energy and life cycle cost.
- Performance of all air heating and radiator-based heating systems were studied.
- Office building retrofitting through optimization led to an energy saving up to 55%
- Optimizing all air heating system may lead to lower energy use than passive house.

ARTICLE INFO

Keywords:

Building retrofitting
Optimization process
Graphical script
Passive house level
Nearly zero energy building
Life cycle cost

ABSTRACT

Selecting the most cost-effective retrofit interventions to achieve a significant reduction of energy use and CO₂ emissions in the building sectors is challenging, because a large number of possible retrofitting options should be analyzed. To remedy this and simplify the decision-making process, optimization may be adopted. This study developed an iterative optimization process by coupling a dynamic energy simulation software, IDA-ICE, and a generic optimization engine, GenOpt, through the Graphical Script module. This optimization process was applied to an office building located in the Nordic climate. Two scenarios were considered. In the first scenario, the optimal designs were achieved by minimizing the life cycle cost of retrofitting measures over a span of 60 years, while the building energy use for space heating and cooling were the constraints to satisfy the Norwegian passive house standard level. In the second scenario, the delivered energy to the building was minimized and the life cycle cost of retrofitting was limited to a predefined value. Two different space heating systems were used, radiator space heating and all-air systems. The optimization parameters included building envelope elements and heating and cooling set points (in the case of all-air system). The results showed that the specific life cycle cost could be reduced up to 11%, while the energy use for the space heating and space cooling was met according to the Norwegian passive house standards. The delivered energy to the building could be decreased by up to 55% in the second scenario.

1. Introduction

Energy efficiency measures in building stock play a significant role in the reduction of total energy use. Among all users, existing non-residential buildings account for a large portion of energy use and greenhouse gas (GHG) emissions. For instance, in Norway, non-residential buildings form around 62% of the total building stock [1], emphasizing the essential need for improving the energy performance of this building type. In cold climate countries, the building energy

efficiency is even more challenging due to cold climate conditions and high heating needs, which accounts for between 40% and 60% of the total energy use [2]. Apart from the energy use, the importance of indoor air quality (IAQ) in well-being and productivity of occupants in non-residential buildings, e.g. offices, cannot be ignored since the occupants spend a lot of their time in the indoor environment. Therefore, building retrofitting is a viable solution in improving the existing building stock's energy performance and IAQ.

Building retrofitting is a means of upgrading existing building

* Corresponding author at: Department of Civil Engineering and Energy Technology, Oslo Metropolitan University, Norway.
E-mail address: Mehrdad.Rabani@oslomet.no (M. Rabani).

<https://doi.org/10.1016/j.apenergy.2020.114929>

Received 16 October 2019; Received in revised form 26 January 2020; Accepted 28 March 2020

0306-2619/© 2020 The Author(s). Published by Elsevier Ltd. This is an open access article under the CC BY license (<http://creativecommons.org/licenses/by/4.0/>).

Nomenclature*Roman symbols*

AA	all-air
ACOR	ant colony optimization
AHU	air handling unit
ANN	artificial neural network
$A_{\text{total-window}}$	total window area (m^2)
$A_{\text{total-heated floor}}$	total heated floor area (m^2)
a	discount factor for escalation of energy price
CAV	constant air volume
CHP	combined heat and power
DCV	demand control ventilation
DHW	domestic hot water
DH_{26}	overheating degree hours (h)
dLCC	profitability of the retrofitting measures (NOK)
E	simulated annual energy use ($\text{kWh}/(\text{m}^2\cdot\text{year})$)
$E_{\text{SC,PH}}$	energy use for space cooling for passive house ($\text{kWh}/(\text{m}^2\cdot\text{year})$)
$E_{\text{SH,PH}}$	energy use for space heating for passive house ($\text{kWh}/(\text{m}^2\cdot\text{year})$)
E_{tot}	total delivered energy to the building ($\text{kWh}/(\text{m}^2\cdot\text{year})$)
e	increase in the electric energy price
e_p	energy price (NOK/kWh)
f	inflation rate
GA	genetic algorithm
GS	graphical script
GHG	greenhouse gas
GPS	generalized pattern search
HVAC	heating, ventilation, air conditioning system
IAQ	indoor air quality
IC_m	investment cost of building envelope renovation (NOK)
i	nominal interest rate
iMOO	integrated multi-objective optimization
LCC	life cycle cost (NOK)

LCC_e	annual cost due to building operation (NOK)
LCC_r	life cycle cost of the reference case (NOK)
LCCF	life cycle carbon footprint
LEB	low energy building
LTH	low temperature heating
MOBO	multi-objective building optimization
MOO	multi-objective optimization
MOABC	multi-objective artificial bee colony
MINLP	multi-objective mixed-integer non-linear problem
NPV	net present value
NSGA-II	multi-objective genetic algorithm
n	number of years in the building lifetime
n_{50}	airtightness (1/h)
nZEB	nearly zero energy/emission building
PDH	min total occupant hours dissatisfaction
PH	passive house
PMV	predicted mean vote
PPD	predicted percentage dissatisfied
PSO	particle swarm optimization
PV	photovoltaic
RC	replacement cost of various parameters (NOK)
RSH	radiator space heating system
r_e	real interest rate
SC	space cooling
SHGC	solar heat gain coefficient
SH	space heating
SFP	specific fan power ($\text{kW}/(\text{m}^3/\text{s})$)
VAV	variable air volume
U	total heat transfer heat coefficient ($\text{W}/(\text{m}^2\cdot\text{K})$)
WWR	window to wall ratio
ZEB	zero energy building

Greek symbols

Ψ	normalized thermal bridge
--------	---------------------------

performance in order to decrease the building energy use, reduce the GHG emissions, and provide a comfortable indoor environment for occupants. Potential retrofit interventions are commonly applied to building envelope and design aspects, building systems and installations, and building control and management tools [3]. However, the majority of retrofitting strategies focus on the building envelope and ventilation system. To improve the building envelope properties, the following technologies are widely applied: (1) enhancing wall, ceiling, and floor thermal resistances, (2) improving airtightness, (3) enhancing the solar heat gain coefficient (SHGC) of window glazing, and (4) using shading components. To improve the ventilation system performance, replacing constant air volume (CAV) by variable air volume (VAV) for the ventilation control system and improving the efficiency of the heat recovery system are the actions frequently applied [4–7]. Another group of measures often considered in building retrofitting process are the parameters dealing mostly with the heating distribution system. Low temperature heating (LTH), systems such as a LTH radiator [8–10] or an under-floor LTH [11,12], connected to district heating, heat pump, or combined heat and power (CHP) supply systems are some practical examples used in cold climate areas. Nevertheless, the challenge that arises here is that the integration of all these high-ranking retrofit options at their best level would not yield a desirable reduction of building energy use, because of simultaneous effects. A case in this point is the ventilation system, where the improvement of heat recovery efficiency with a reduction in ventilation airflow rate does not decrease the energy use for heating as much as expected [6]. As a result, selecting a proper set of building retrofitting measures that can minimize

the building energy use and the related costs, while satisfying IAQ in the long term remains the main challenge. Therefore, it will be even more challenging when a stricter target such as nearly zero energy/emission building (nZEB) level is chosen as a target energy level [13]. Note that nZEB has been defined differently based on energy use or emissions either from energy use or the total emissions from both energy use and building production phase [14–16]. Regardless of different definitions, there is not yet any internationally or standard definition for nZEB, except that these buildings are characterized by high energy efficient components and energy supply from renewable energy sources [2,13]. Hence, building retrofitting to the low-energy or the passive house (PH) level can be considered as the ambitious level on a transitional way towards nZEB. The building envelope in PHs is upgraded so that an airtight, highly insulated building may require little or no energy for space heating (SH) or cooling (SC). This may raise doubts about choice of building service systems and consequently their sizes and investment justification.

Considering the above mentioned challenges and the approach towards nZEB, we adopted an optimization method, as suggested in [17,18], to cope with the challenge of selecting a proper set of retrofitting measures.

2. Literature review on building optimization

One of the most prevalent methods in exploring optimal solutions for retrofitting projects is based on integrating the building performance simulation tools such as EnergyPlus, DOE-2, IDA-ICE, and

Table 1
Summary of literature about the optimization of building energy performance tools.

Ref.	Model	Optimization and energy simulation tool	Objective function(s) and constraints	Input parameters
[25]	Multi-objective optimization	<ul style="list-style-type: none"> Artificial Neural Network (ANN) with multi-objective Genetic Algorithm (NSGA-II) TRNSYS 	<ul style="list-style-type: none"> Max thermal comfort in building energy use Number of discomfort hours (constraint) 	<ul style="list-style-type: none"> Set points for cooling, heating, and relative humidity Supply air flow rate Window surface area Wall insulation thickness Roof insulation materials Window type Wall insulation thickness and material type Solar collector type Wall construction topology Roof construction topology Glass type and size Insulation thickness of external wall Absorption coefficient of wall's outer face Shading depth External and internal partition wall type Roof type Floor type Window type PV size Wind turbine size Bio-diesel generator
[26]	Multi-objective optimization	<ul style="list-style-type: none"> GenOpt and a Tchebycheff optimization method developed in MATLAB TRNSYS 	<ul style="list-style-type: none"> Min retrofit cost Min energy saving Min number of discomfort hours 	
[27]	Single-objective optimization	<ul style="list-style-type: none"> GenOpt TRNSYS 	<ul style="list-style-type: none"> Min primary energy use Indoor operative temperature (constraint) Daylight factor (constraint) 	
[28]	Single and multi-objective optimization	<ul style="list-style-type: none"> NSGA-II algorithm developed in MATLAB TRNSYS 	<ul style="list-style-type: none"> Min energy use Min cost Min life cycle GHG Min thermal discomfort 	
[17]	Single-objective and multi-objective optimization	<ul style="list-style-type: none"> GA NSGA-II algorithm developed in MATLAB TRNSYS 	<ul style="list-style-type: none"> Min total cost Min carbon dioxide emission Min grid inter-action index of reference building Low energy building (LEB) (constraint) Zero energy building (ZEB) (constraint) 	
[20]	Multi-objective optimization	<ul style="list-style-type: none"> NSGA-II in Multi-Objective Building Optimization tool (MOBO) TRNSYS 	<ul style="list-style-type: none"> Min energy use for cooling Min energy use for heating well Min life cycle cost 	<ul style="list-style-type: none"> External walls thermal transmittance Roof thermal transmittance Ground thermal transmittance Window to wall ratio (WWR) at each façade Glazing type at each façade External wall thermal insulation Roof thermal insulation Glass type Exterior insulation thickness Panel insulation thickness Bricks thickness Thermal bridges insulation WWR Building orientation Window size Glazing properties Wall thermal properties Overhang depth and tilt angle Heating set point temperature Cooling set point temperature Wall thermal properties Glazing properties Building rotation Roof thermal properties Wall insulation thickness Window size Overhang depth Heating set point Cooling set point Building orientation Building envelope insulation thickness Supply-water temperature set points Heat exchange area of the radiators Glazing type Windows Area Roof insulation thickness Ground floor insulation thickness Building orientation Temperatures difference in infiltration controller Air change value rate in infiltration controller Heating and cooling set point Window type Ventilation/window opening type
[29]	Single-objective optimization	<ul style="list-style-type: none"> GenOpt EnergyPlus 	<ul style="list-style-type: none"> Min LCC 	
[30]	Multi-objective optimization	<ul style="list-style-type: none"> jEPlus + EA tool EnergyPlus 	<ul style="list-style-type: none"> Min embodied CO₂/operational CO₂ Min LCC/ LCCF (Life cycle carbon footprint) Min annual energy consumption/ annual energy spending 	
[31]	Multi-objective optimization	<ul style="list-style-type: none"> jEPlus tool MATLAB EnergyPlus 	<ul style="list-style-type: none"> Min annual cooling electricity Min annual heating electricity Min annual lighting electricity 	
[32]	Single-objective and multi-objective optimization	<ul style="list-style-type: none"> Multi-objective artificial bee colony (MOABC) developed in MATLAB jEPlus tool EnergyPlus 	<ul style="list-style-type: none"> Min total annual building electricity consumption Min Predicted Percentage of Dissatisfied (PPD) 	
[33]	Single-objective optimization	<ul style="list-style-type: none"> Ant Colony Optimization (ACOR) developed in MATLAB GenOpt EnergyPlus 	<ul style="list-style-type: none"> Min annual building energy use 	
[34]	Single-objective optimization	<ul style="list-style-type: none"> GenOpt EnergyPlus 	<ul style="list-style-type: none"> Min total cost PPD (constraint) 	
[35]	Multi-objective optimization	<ul style="list-style-type: none"> NSGA-II algorithm developed in MATLAB EnergyPlus 	<ul style="list-style-type: none"> Min LCC Max thermal comfort 	
[36]	Multi-objective optimization	<ul style="list-style-type: none"> Integrated multi-objective optimization (iMOO) tool NSGA-II algorithm developed in MATLAB EnergyPlus 	<ul style="list-style-type: none"> Min Predicted Mean Vote (PMV) Min initial investment Cost Min thermal Energy Consumption Min Net Present Value (NPV) Global warming potential 	

(continued on next page)

Table 1 (continued)

Ref.	Model	Optimization and energy simulation tool	Objective function(s) and constraints	Input parameters
[37]	Multi-objective optimization	<ul style="list-style-type: none"> ● MATLAB ● multi-objective mixed-integer non-linear problem (MINLP) 	<ul style="list-style-type: none"> ● Min total annual primary energy consumption ● Min total investment cost 	<ul style="list-style-type: none"> ● Window type ● Door type ● Wall insulation type and thickness ● Floor structure ● Ceiling structure ● Electricity equipment power ● Angle of louvre blades ● Z coordinate of the center point of each individual blade
[38]	Multi-objective optimization	<ul style="list-style-type: none"> ● Multi-objective optimization (MOO) tool ● Grasshopper ● EnergyPlus 	<ul style="list-style-type: none"> ● Min total annual net energy electricity use ● Max energy converted into electricity by the PV cells ● Max daylighting level in the zone measured as the continuous daylight autonomy 	<ul style="list-style-type: none"> ● Operating strategies for energy conversion and storage technologies including heat pumps, solar panels, biomass, oil boilers and thermal storage
[39]	Multi-objective and simultaneous optimization	<ul style="list-style-type: none"> ● Epsilon-constrained mixed integer linear program (MILP) using the CPLEX ● EnergyPlus 	<ul style="list-style-type: none"> ● Min Annualized costs ● Min life cycle GHG emissions 	
[40]	Modified multi-objective optimization	<ul style="list-style-type: none"> ● Genetic algorithm PR_GA_RF developed in MATLAB ● IDA-ICE 	<ul style="list-style-type: none"> ● Min carbon dioxide equivalent (CO₂-eq) emissions ● Min investment cost ● Summer overheating degree-hour (constraint) 	<ul style="list-style-type: none"> ● Insulation thickness of wall, roof, and floor ● Window type ● Heat recovery type in air handling unit ● Shading type ● Heating/cooling system types
[22]	Multi-objective optimization	<ul style="list-style-type: none"> ● Pareto Archive NSGA-II algorithm in MOBO ● IDA-ICE 	<ul style="list-style-type: none"> ● Min additional investment cost ● Min annual space heating energy ● Additional investment cost (constraint) 	<ul style="list-style-type: none"> ● Insulation thickness of wall, roof, and floor ● Heat recovery efficiency ● Window type
[23]	Multi-objective optimization	<ul style="list-style-type: none"> ● NSGA-II algorithm and parallel computation in MOBO ● IDA-ICE 	<ul style="list-style-type: none"> ● Min LCC ● Min annual CO₂ emission 	<ul style="list-style-type: none"> ● Window U-value ● Wall and door U-value ● Floor U-value ● Solar thermal area and PV capacity ● Type of building energy source
[24]	Multi-objective optimization	<ul style="list-style-type: none"> ● Pareto Archive NSGA-II algorithm and in MOBO ● IDA-ICE 	<ul style="list-style-type: none"> ● Min LCC ● Min annual district heating energy use 	<ul style="list-style-type: none"> ● Solar collector area ● Storage Tank volume ● Tilt angle of solar collector ● PV-panels area
[21]	Multi-objective optimization	<ul style="list-style-type: none"> ● Pareto Archive NSGA-II algorithm and in MOBO ● IDA-ICE 	<ul style="list-style-type: none"> ● Min CO₂ emission of delivered energy to the building ● Min NPV of the 15-year LCC ● Min total occupant hours dissatisfaction (PDH) ● Maximum ventilation airflow rate (constraint) 	<ul style="list-style-type: none"> ● Insulation thickness of wall and roof ● Window type ● Type of lighting system ● Type of cooling and ventilation systems ● Dimensioning output power of ground source heat pump

TRNSYS, etc., with optimization engines including custom programming and general optimization tools such as MOBO, GenOpt, jEPlus, BeOpt, and MultiOpt, etc. [19]. The approaches, which automate the search process in finding optimal solutions with less effort, have largely been studied. Table 1 summarizes these studies and their features including modelling approach, type of tools, objective functions and design parameters used in the optimization procedure. Findings from the literature review show that the following features are included in most of the retrofitting projects for single/multi-objective optimization of building performance.

- **Input parameters:** Insulation thickness of the building envelope elements, surface area and type of glazing, overhang tilt angle, overhang depth, and type of shading are mainly considered as the optimization input parameters for the building envelope. In addition, size of photovoltaic (PV) panel, solar thermal collector area, type of energy source, and heating and cooling temperature set points are selected as the major optimization input parameters for the building HVAC system.
- **Objective functions and constraints:** Building energy use, life cycle cost (LCC), life cycle GHG, and thermal comfort of occupants are the most selected targets as the optimization objective functions. The number of discomfort hours and daylight are also chosen as the thermal and visual constraint functions in the optimization process. In some researches [20,21], no constraint function was used, but a post processing analysis of thermal comfort was instead performed

to visualize the comfortable conditions for the optimized cases.

- **Optimization and building energy performance simulation tools:** GenOpt, MOBO, and jEPlus tools as well as Genetic algorithm (GA) and NSGA-II algorithm developed in MATLAB are often chosen as the optimization tool. TRNSYS and EnergyPlus are used as the energy simulation tool for single/multi-objective optimization process. Furthermore, several researchers integrated optimization tools such as MOBO with IDA-ICE energy simulation software [21–24].

The present study considered a different optimization approach for building retrofitting towards nZEB. Our method aimed at integrating the GenOpt optimization tool with IDA-ICE building performance simulation software through the Graphical Script (GS) approach, which implements an algorithm through an illustrative framework. This approach was implemented with two goals. Firstly, to evaluate the possibility in reducing the LCC of the energy retrofitting measures, the LCC was minimized, while the energy use for SH and SC was defined according to the Norwegian PH standard. Secondly, to investigate the extent to which it is possible to reduce the annual delivered energy to the building, the delivered energy was minimized, while the LCC of the energy retrofitting measures was limited. In both approaches, the retrofitting measures were determined so that the thermal comfort criteria were satisfied.

The remainder of the paper is organized as follows. Section 3 describes the proposed framework and methodology to assess the optimal configurations. For this purpose, in the first part of this section, the

details of the case study including building geometry, specifications of building envelope, energy source and HVAC system are presented and discussed. In the second part, detailed information about the optimization procedure and how the GS implemented the necessary inputs, constraints, and objective functions in IDA-ICE and linked them to the GenOpt tool is provided. Section 4 presents the obtained results of the application of the optimization method to the case study and provides a critical assessment of the results. Finally, Section 5 summarizes the conclusions and findings of this study and suggests a framework for future work.

3. Methodology

3.1. Case building selection and its specifications

The aim of this study was to determine the techno-economic retrofitting measures of a typical office building located in a cold climate region. The case building examined in this paper was a generic office building located in Norway. In order to select a reference office building with an appropriate total floor area, the statistics of office building stock in Norway was analyzed, as shown in Fig. 1.

From Fig. 1, it may be noted that the most of the office buildings in Norway [41] were built in the 1980s with a total heated floor area of less than 10 000 m². Therefore, an office building with roughly 3 000 m² total heated floor area was chosen as the case building in this study to both facilitate the computations of the optimization process and address the total heated floor area of a typical office building in Norway. As a case study in the present work, it was also assumed that the reference office building met the Norwegian building code TEK 10 that is similar to the low energy building level [42].

The multi-story generic office building used for the dynamic simulations is shown in Fig. 2. The office building had a compact square design with a total volume of 9 062 m³ and consisted of three floors with a total heated floor area of 2 940 m². The total external wall area was 1 326 m² with doors covering a total of 21 m². Regarding windows size, the Norwegian building code, TEK 10, imposes a maximum requirement for windows relating the window U-value and area as follows:

$$\frac{U_{\text{window}} \cdot A_{\text{total-window}}}{A_{\text{total-heated floor}}} \leq 0.24 \quad (1)$$

Eq. (1) implies that if a larger window area is needed, a lower window U-value should be selected to meet the national building code

TEK 10. According to this building code, the ratio should be considered in order to avoid a high building energy use for space heating and cooling due to window oversizing and to not compromise the daylight effect due to window undersizing at the same time. Therefore, regarding the minimum required U-value for windows of 1.6 W/(m²·K) for energy calculations, based on the Norwegian building code TEK 10, a ratio of 0.2 corresponding to a total window area of 367 m² was considered for the reference case building.

Simulation of the building energy performance was conducted using IDA-ICE version 4.8 software in this study. The simulation tool has already been validated by ASHRAE 140-2004 CEN 13791, CEN 15255, and CEN 15265 (2007) [43].

Fig. 3 shows the thermal zones and floor plans in the simulation model. Zoning of each floor was done with respect to a realistic scenario of possible solutions in office buildings. Zones were designed to comply with the area requirement in the Norwegian standard NS 3031 [44], which states that the area for the primary zones (with occupancy) should be at least 65% and the maximum of 35% for the secondary zones (without occupancy and equipment). The total area of primary zones was around 2 230 m². The first floor included a reception with a separate entrance and access to elevator and stairs, parking garage, and a designated section for business premises. The second and the third floors comprised of 16 cell offices, open plan office area, and meeting and conference rooms. The office building also had elevators, technical spaces, and toilets. In addition, the IDA-ICE zone multiplier function was used to simplify the duplicate cell offices in the second and the third floors to reduce the computational time of simulations.

The building envelope properties of the reference building are indicated in Table 2. All properties were considered based on the Norwegian building code, TEK 10. In addition, the features of the main HVAC system in the reference case are presented in Table 3. The technical specifications are typical for the office buildings built during the 1980s and renovated to the TEK 10 level. The domestic hot water (DHW) use was selected according to the standard NS 3031 using the standardized value for the office building category [44].

The internal heat gains were considered according to the Norwegian standard NS 3031. Table 4 shows the internal heat gain values and profiles used in the simulation software. Furthermore, the heat gains in the primary zones were due to occupancy, lighting, and equipment, while for the secondary zones only heat gain due to the lighting was considered.

To run the simulations over the period of one year, the typical climate data from the ASHRAE IWEC 2 database were used for three cities

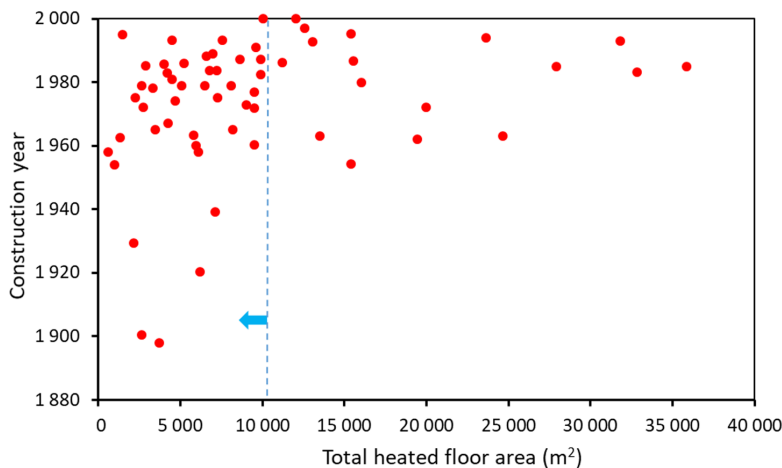


Fig. 1. Total heated floor area vs. construction year of office buildings equipped with cooling plant in Norway.

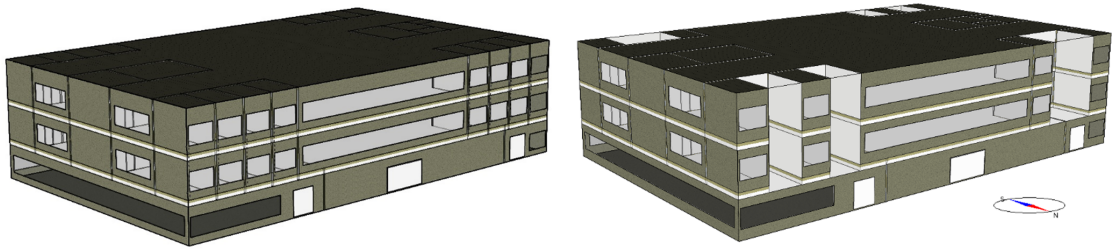


Fig. 2. 3D representation of the three floors of the case building as modeled in IDA-ICE simulation tool without (left) and with (right) zone multiplier.

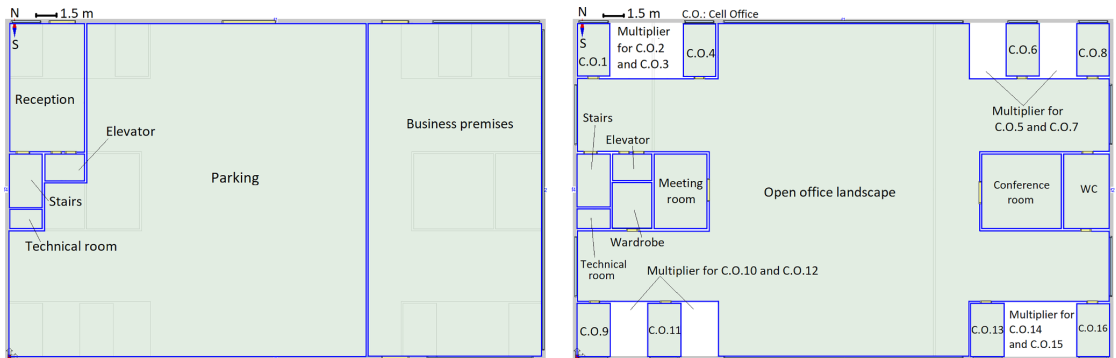


Fig. 3. Generic ground floor plan, the first floor plan (left), and the second and the third floor plans at level 3.4 m and 6.8 m (right) with thermal zones.

Table 2
Building envelope properties used as input values in IDA-ICE.

Parameter, Units	Value	Note
External wall U-value, W/(m ² ·K)	0.22	Minimum requirement
Roof U-value, W/(m ² ·K)	0.18	Minimum requirement
External floor U-value, W/(m ² ·K)	0.18	Minimum requirement
Window U-value, W/(m ² ·K)	1.60	Minimum requirement
Normalized thermal bridge ψ , W/(m ² ·K)	0.06	Minimum requirement
Airtightness n_{50} , 1/h	3	Minimum requirement
Internal wall U-value, W/(m ² ·K)	0.62	
Story separator U-value, W/(m ² ·K)	0.17	Calculated using [45]
External door U-value, W/(m ² ·K)	1.60	Minimum requirement
External shading strategy	Blinds on, if $Q_{sol} > 100 \text{ W/m}^2$	

in Norway: Oslo, Stavanger, and Tromsø. The annual mean outdoor temperatures were around 6.3 °C, 8.4 °C, and 2.9 °C, and the space heating design outdoor temperatures in the present work were around -20 °C, -13.5 °C, and -14.6 °C for Oslo, Stavanger, and Tromsø, respectively. The details of climatic condition for these three locations can be found in ASHRAE classification [47].

3.2. Model framework and optimization method

In this study, in order to further improve the energy performance of the building with minimum associated cost, two different scenarios were implemented using an optimization process. The proposed framework in the retrofitting process is shown in Fig. 4. Furthermore, two different HVAC systems were considered for retrofitting of the building. The first system was the same as the one used in the reference case and was a radiator SH (RSH) system with a CAV ventilation system. The second system was an all-air (AA) system where both space heating and cooling were done using a demand control ventilation (DCV) system and local heating/cooling devices were avoided. The DCV system was controlled by CO₂ and temperature. The supply air temperature set

points (in AHU) were considered as a function of return air temperature to the AHU and CO₂ set points were limited between 700 and 1 100 ppm. The lower limit of the air flow rate was set to 0.2 l/s and the upper limit was determined during the optimization process. However, in the secondary zones the CAV system was still used with the same amount of air flow rate as the first scenario.

3.2.1. Input parameters in the optimization process

In the model framework, shown in Fig. 4, the building model was firstly generated in IDA-ICE as explained in Section 3.1. Afterwards, the optimization sequence initiated. In this stage, the input parameters for the optimization process were determined based on the most selected parameters in the literature. Table 5 indicates the input parameters with their corresponding costs. Note that the cost values in Table 5 are given in NOK¹. The U-value of the building envelope was set to satisfy the Norwegian PH standard NS 3701 [48]. The air temperature set points (only for AA cases) represented the points of the supply air

¹The current currency ratio is 1 NOK ~0.1 EUR.

Table 3
Main features of the HVAC systems of the reference office building.

HVAC systems and operation	Features
Ventilation system strategy	Mechanical balanced ventilation system with rotary heat recovery system with efficiency 70%
The specific fan power (SFP) of the ventilation system	2.5 kW/(m ³ /s)
Schedules of ventilation system operation based on the realistic use of the building	Monday-Friday: 12 h/day for upper limit (6–18); other times reduces to lower limit
Supply airflow rates of the ventilation system	Primary zones: 2.3 l/(m ² ·s) and 4 l/(m ² ·s) for upper limit in heating and cooling seasons respectively, 0.2 l/(m ² ·s) for lower limit Secondary zones: 0.7 l/(m ² ·s) for upper limit, 0.2 l/(m ² ·s) for lower limit
Heating system	District heating system, modelled in IDA-ICE using a generic top heater with unlimited capacity and efficiency of 88% considering heat loss during distribution according to NS 3031
Cooling system	Centralized water cooling system for cooling of supply air in AHU
Heating distribution system	Water radiator system
Room temperature set point for heating and cooling	21 °C for heating and 24 °C for cooling
Control method of SH and ventilation air heating and air cooling systems	Space heating: supply water temperature as a function of outdoor temperature; Ventilation supply air: supply air temperature control according to the return air temperature to AHUs
DHW use	5 kWh/(m ² ·year)

temperature profile as a function of return air temperature to AHU. The prices were taken from the price list from the Norwegian Price Book year 2019 [49]. In addition, the details of shading properties can be found in Appendix A. It should be noted that the U-values of the reference building envelope, given in Table 2, were also considered as optimization input parameters.

3.2.2. Objective functions and constraints

After determining the input parameters, two objective functions were considered in order to evaluate the possibilities for different combinations of retrofitting measures. In the first scenario, the LCC was defined as the objective function to be minimized, while in the second scenario the delivered energy to the building was the objective function to be minimized.

The LCC, given in Eq. (2), included the following elements: (1) the total building cost, which represented the annual building operational cost (LCC_e), (2) the investment cost of building envelope renovation and improvement of SFP due to change of ventilation system from CAV to DCV (IC_m), and (3) replacement cost of various parameters (RC). As such,

$$LCC = LCC_e + IC_m + RC \quad (2)$$

where RC was the cost associated with replacing the old windows and replacement of necessary HVAC elements due to maintenance.

The profitability of the retrofitting measures was calculated using Eq. (3) as suggested in [50],

$$dLCC_i = LCC_i - LCC_r \quad (3)$$

where $dLCC_i$ is the difference between the LCC for every case (LCC_i) and for the reference case (LCC_r). Furthermore, LCC_e in this research was calculated using the NPV of the operational costs during the building lifetime as shown in Eqs. (4) and (5).

$$LCC_e = ae_p E \quad (4)$$

$$a = \frac{1 - (a + r_e)^{-n}}{r_e} \quad (5)$$

Table 4
Internal heat gains values and usage profiles from occupants, lighting.

Internal heat gain source and usage profile	Note
- Occupants, the usage profile is: Monday-Friday: 0.067 occupant/m ² during 6–18 o'clock, no usage at other times including weekends and holidays as well as in the secondary zones	Each person occupies around 15 m ² of floor area, considering activity level is 1.2 met [46], which is equal to 108 W/person, the internal gain from occupants equals to 7.2 W/m ² , which is equal to approximately 0.067 occupant/m ²
- Lighting, the usage profile has the same trend as occupants	8 W/m ² (25 kWh/(m ² ·year))
- Office equipment, the usage profile has the same trend as occupants, no usage in the secondary zones	11 W/m ² (34 kWh/(m ² ·year))

$$r_e = \left(\frac{i - f}{1 + f} \right) - \frac{e}{1 + e} \quad (6)$$

The value of these factors for this study have been explained in Appendix B. It should be mentioned that only electricity price was considered, because district heating price in Norway is often following the electricity price and is lower.

In this study, different constraints were imposed for the two optimization scenarios. The constraint criteria, PPD and overheating degree hours (DH_{26}), defined as the number of hours during which the operative temperature was higher than 26 °C, were considered for both optimization scenarios and for both AA and RSH systems. Specific energy use for SH and SC were considered as the constraints in the first optimization scenario. The rate of increase in the total retrofitting cost with respect to the reference case was considered in the second optimization scenario. Details of different constraints and their use are shown in Table 6. It should be mentioned that the maximum PPD was considered as the constraint criterion during the optimization process for the worst zones, because these zones experienced a higher temperature range during the year in the reference case.

3.2.3. GS module and optimization algorithm

The optimization process was implemented through the GS module. This module is an available option in IDA-ICE 4.8 in which different sets of optimization input parameters, objectives, and constraints can be considered through an illustrative way by inserting and connecting components. It should be noted that the GS module is executed by IDA modeler without starting the IDA solver and it makes the manipulation of constraint functions, input parameters, and objective functions more understandable and convenient. Its principle can also be implemented in various energy simulation tools. Therefore, the novelty of this study is the carefully developed and implemented objective and constraint functions through GS module in this specific optimization problem in order to develop a general knowledge on the improvement/retrofitting of an office building.

A schematic of the implementing process is shown in Fig. 4. In this study, all mentioned inputs in Table 5 were firstly added and connected

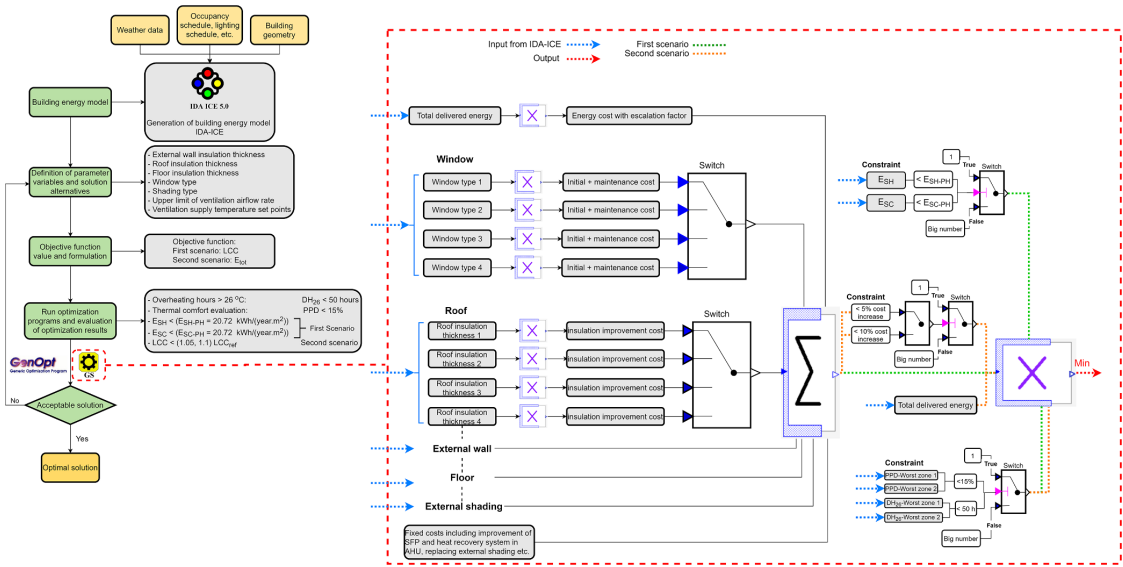


Fig. 4. Model framework and optimization process through the GS module.

Table 5
Input parameters used for the optimization process.

Variable	Value	Insulation/demolition -maintenance cost (NOK/m ²)	Description
Window type (U-value W/(m ² ·K))	1.4	3285.5/849.04–219.41	Retrofitting was after 20 and 40 years
	1.2	3472/897.23–231.86	
	1.0	3749.5 /968.94–250.39	
	0.8 (NS 3701)	4027/1040.65–268.92	
External wall type (U-value W/(m ² ·K))	0.20	1272/493.944	250 mm: insulation thickness
	0.17	1394/543.152	300 mm: insulation thickness
	0.15	1451/583.456	350 mm: insulation thickness
	0.13	1652/676.408	400 mm: insulation thickness
	0.12 (NS 3701)	1832/772.312	450 mm: insulation thickness
Ground floor type (U-value W/(m ² ·K))	0.16	1057	250 mm: insulation thickness
	0.13	1091	300 mm: insulation thickness
	0.10	1193	350 mm: insulation thickness
	0.08 (NS 3701)	1227	400 mm: insulation thickness
	0.16	798/79	230 mm: insulation thickness
Roof type (U-value W/(m ² ·K))	0.13	884/410	300 mm: insulation thickness
	0.10	1008/548	400 mm: insulation thickness
	0.08 (NS 3701)	1126/623	500 mm: insulation thickness
	1	1751	Black-Sunworker M391
External shading type	2	1751	Bronze-Sunworker M393
	3	1751	Gray-Sunworker M654
	2.0	NA	For AA system
	2.5		
3.0			
3.5			
4.0			
4.5			
5.0			
1st point of supply temperature profile for AA system (°C)	(23, 24, 25, 26)	NA	Return temperature to AHU = 10
2nd point of supply temperature profile for AA system (°C)	(23, 24, 25, 26)	NA	Return temperature to AHU = 22
3rd point of supply temperature profile for AA system (°C)	(14, 15, 16)	NA	Return temperature to AHU = 24
4th point of supply temperature profile for AA system (°C)	(14, 15, 16)	NA	Return temperature to AHU = 40

Table 6
Details of constraint functions for two scenarios.

	First scenario			Second scenario	Description
DH ₂₆ (h)	(3rd floor-Cell offices no. 08 and 01) < 50				Based on TEK 10 [42]
PPD (%)	(3rd floor-Cell offices no. 08 and 01) < 15				Based on TEK 10 [42]
E _{SH} (kWh/(year·m ²))	Oslo	Tromsø	Stavanger	NA	Calculated based on NS 3701 standard [48]
	20.72	32.96	20		
E _{SC} (kWh/(year·m ²))	Oslo	Tromsø	Stavanger		
	9.38	2.10	4.48		
Total cost increase	NA			5% and 10%	Increase with respect to the reference case

to the GS module via parameter mapping to an appropriate source out of script macro (the gray boxes with the blue arrows inside the dashed red box). Switches were considered to alter different options for each group of inputs. Their associated costs were then summed using an adder representing the total amount of operational and investment costs of the building retrofitting process. Afterwards, the constraints were implemented so that if the considered parameter could not meet the constraint requirement, the objective would simply be multiplied by a large number and, since the aim was to minimize the objective functions, the output would consequently be removed from the optimal set of solutions determined by the optimization engine; see Fig. 4.

In this study, GenOpt was employed as the optimization engine. Since only a limited number of retrofitting measures and dimensions were offered by the market, it was possible to investigate the building elements variables in a discrete space. Furthermore, the hybrid algorithm Particle Swarm Optimization (PSO) and a Generalized Pattern Search (GPS) coupled with Hooke-Jeeves algorithm was chosen to deal with discrete values and to benefit from the global features of the PSO algorithm with the convergence properties of the GPS algorithm [51]. The details of parameters selected for the optimization algorithm are described in Appendix C. The simulations were performed on a 32 GB RAM of a Windows-based workstation (2.20 GHz) with Intel (R) Xeon (R) Gold 5120 CPU with 14 parallel cores and lasted for 36 h for each optimization case, and 648 h in total for 18 optimization cases. It should be noted that, the optimization of two extra heated floor areas of 5000 m² and 7000 m² were also tested: each simulation took around 83 h and 119 h, respectively, which implies that a total of 1494 h and 2142 h, respectively, would be needed to complete all the 18 optimization cases.

4. Results and discussions

In this section, the results of the optimization process are presented, both for the first scenario in which the LCC function was minimized, see Section 4.1, and for the second scenario with annual delivered energy to the building as the minimized objective, see Section 4.2.

4.1. First optimization scenario: Minimizing the LCC function

Fig. 5 shows how GenOpt optimized the objective function through the GS module, e.g. for the building case in Oslo. In this case, the simulation runs converged after around 140 iterations. However, GS module divided the results into two levels, one without satisfying the constraint functions (upper level in the left part of Fig. 5) and the other that satisfied all the constraint functions (lower level in the left picture as well as the right picture in Fig. 5). In other words, using the GS modules, the objective function was minimized at the two aforementioned levels since the cases that did not meet the constraints were multiplied by a large number (for example 10 000 in this study), while acceptable results remained unchanged during the optimization process. The same trend is observed in Fig. 6 where the AA HVAC system was used. The convergence was achieved after around 160 iterations. The number of simulation runs that could not meet the constraints was higher than those in the case with the RSH system, implying that achieving the building energy use with the PH standard level while satisfying thermal comfort requirements was more critical with the AA systems.

The optimal cost solution data points for the RSH and AA systems in Figs. 5 and 6 (right pictures) correspond to a set of input parameters. Fig. 7 illustrates, for example, the design options for the AA system for the global optimal point and all the other solutions satisfying the constraints highlighted in red (optimal neighborhood). Each profile in this diagram corresponds to a set of decision parameters. Furthermore, each input parameter of the optimization problem is specified on a polar axis. The minimum and maximum values of the polar axis for the building envelope components, the supply air temperature, and the ventilation air flow rate correspond to the values in Table 5. Comparing the different configurations showed a variation in using different options for each parameter, except for the window parameter. This means that high performing windows were inevitable in order to reach the PH standard level even with minimum cost.

A similar diagram is shown in Fig. 8 for the global optimal point for the RSH and AA systems. Combined analysis of Fig. 8 and the results in Fig. 9 shows that using the low U-values for the building envelope

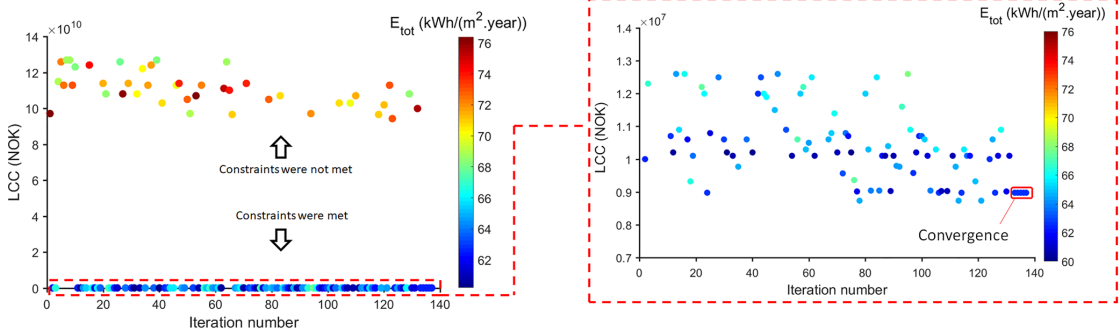


Fig. 5. Optimization results through GS module for the building case with the RSH system for Oslo climate.

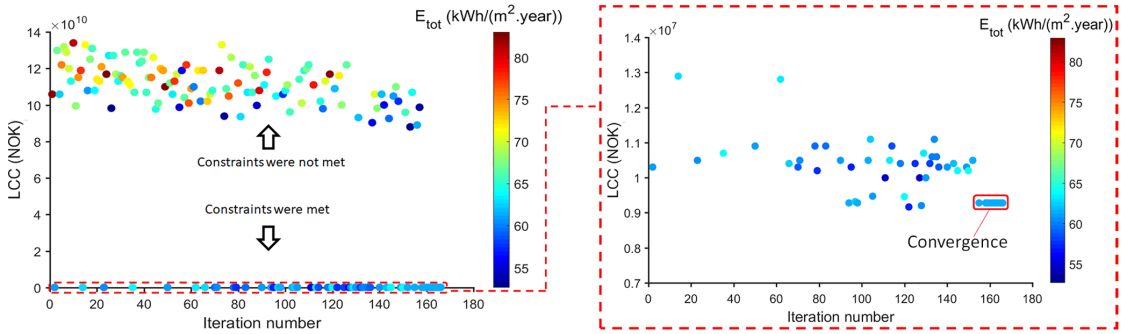


Fig. 6. Optimization results through GS module for the building case with AA system for Oslo climate.

elements did not lead to the PH standard level with minimum LCC. In this regard, the U-values for the ground floor and the roof for the RSH system (see Fig. 8a) as well as the U-values for the ground floor for the AA system (see Fig. 8c) were not changed during optimization. For the RSH system, the high quality building envelope elements in Oslo and Stavanger and the low quality ones in Tromsø (see Fig. 8b), except for the window that was low quality in all three cities, caused a maximum LCC. The reason could be found in Fig. 9b, in which the operational cost in Tromsø was higher than investment cost, while the investment cost in Stavanger and Oslo was higher. In other words, although using the low quality building envelope in Tromsø gave lower investment cost, this resulted in a high operational cost due to high energy use for RSH, leading the total maximum LCC to occur in this case. Comparing the minimum and maximum LCC, see Fig. 9a and b, for the AA system indicated that the best performance in terms of the LCC could be achieved using the low values of the maximum airflow rate for the upper limit of air ventilation. It was followed by selecting the high performing external wall and window in all three cities, while satisfying the energy use for the PH standard and thermal comfort at the same time.

In Fig. 10, the results of the optimization runs were compared to both the reference case building and the PH standard building, equipped with both the RSH and the AA systems, for the PH standard [48]. Regarding the LCC, the maximum savings compared to the reference case were achieved around 6%, 4%, and 11% for the optimized RSH case in Oslo, Stavanger, and Tromsø, respectively. The maximum energy savings obtained were around 51%, 55%, and 54% for the PH AA case in Oslo, Stavanger, and Tromsø, respectively. It is worth noting that the optimization process did not only decrease the total delivered energy by at least 44%, but also reduced the LCC up to 11% compared to the reference building for the cases with the AA system. However, no

LCC saving was achieved for the PH standard cases.

Fig. 11 shows the monthly variation of average operative temperature in one of the worst zones, the cell office 8 in Fig. 3, for the global optimal solution point in different cases throughout the year. In Fig. 11, it may be observed that adopting the thermal constraint functions for the overheating temperature and the PPD could provide the acceptable indoor temperature level for all cases during the year. Furthermore, the high temperature range, 24–25 °C as well as temperature fluctuations were experienced in the cases equipped with the AA system, especially the PH cases, indicating that the indoor temperature control in this type of the HVAC system was more challenging. Especially, when the system operated with low air flow rate there might be a high vertical temperature gradient and a stationary air region in the occupancy zone of the room as reported by [52,53].

4.2. Second optimization scenario: Minimizing delivered energy

For the second scenario, as mentioned before, a 5% and 10% increase with respect to the operational cost of the reference case was considered as a constraint criteria in addition to the thermal comfort constraints. The objective was to minimize the delivered energy to the building. Fig. 12 depicts the different configurations of optimization input parameters in the minimum energy use point for the RSH and AA systems. In the case of the RSH system with 5% cost increase, the high performing window and the external wall were used for all the cases. However the high performing roof was only used in Oslo and Tromsø. The best quality of ground floor could not be used in any case. Likewise, these parameters were chosen for the global optimum cases with 10% increase, except in Tromsø where all the high performing design parameters were used in the global optimum point. For the AA system, the high performing roof, the window, and the external wall were used

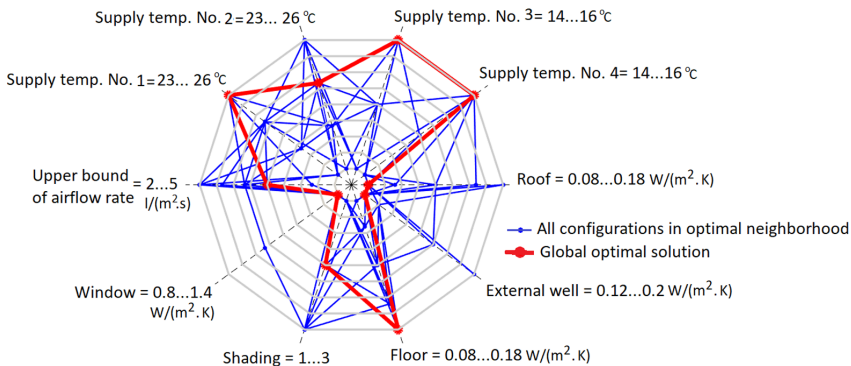


Fig. 7. All possible configurations of design parameters that satisfied the constraint functions for the AA system in Oslo.

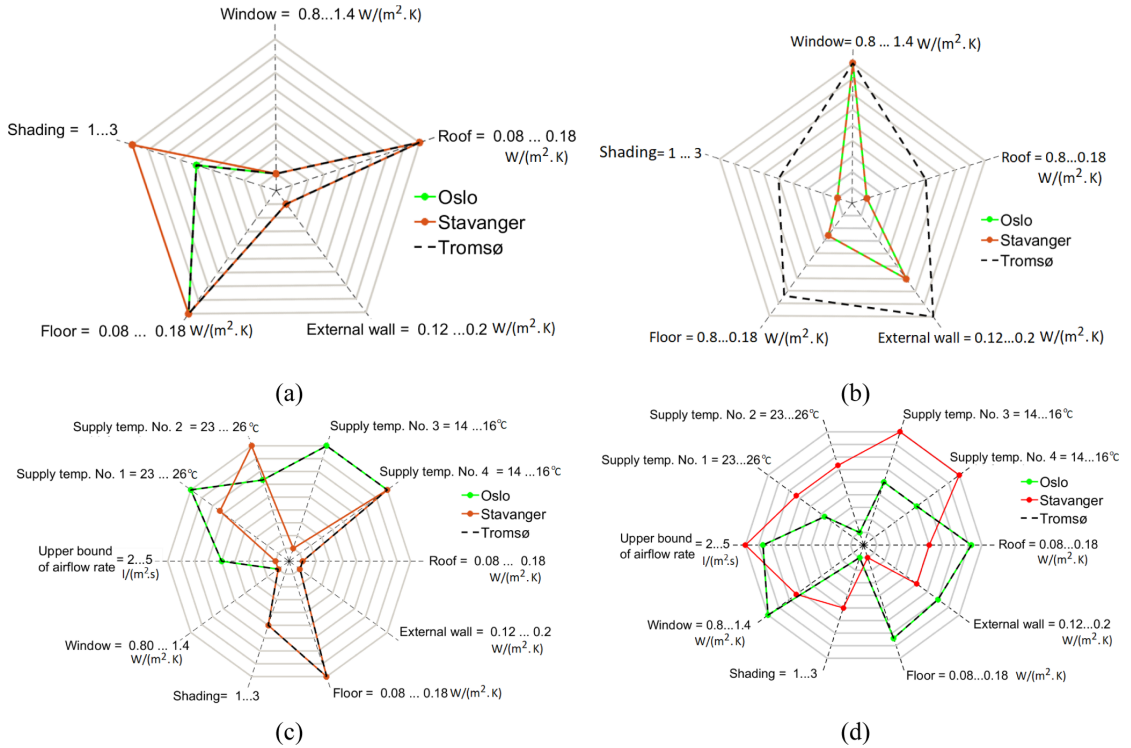


Fig. 8. Design parameter configurations in the global optimal point for RSH: (a) minimum and (b) maximum total costs, and for AA system: (c) minimum and (d) maximum total costs.

in all cities with both 5% and 10% cost increase. In addition, comparing Fig. 8 and Fig. 12 revealed that almost similar quality of building envelope components resulted in the minimum LCC and the delivered energy for the AA system in the first and second scenarios respectively. However, the combination of the HVAC set points was different indicating the importance of selecting appropriate set points when targeting the PH level through different approaches.

The effect of constraint functions on the delivered energy and the LCC of design parameters, illustrated in Fig. 12, are shown in Figs. 13 and 14. In the RSH system, see Fig. 13, the thermal comfort constraint was satisfied for all the cases and the cost increase was the only constraint, see the vertical dashed lines in Fig. 13. Note that in Fig. 13, the minimum points (with and without constraint) are marked with the

same symbols, but larger. The minimum energy point for the cases in Oslo and Stavanger was lower when there was no cost constraint (see in Fig. 13a and 13b two big gray triangles and circles), because all high performing design parameters could not be used for the global minimum point in these cases (see Fig. 12a). However, the amount of increase in the retrofitting LCC was much higher than the energy reduction when the cost constraint was not used, implying that refurbishment of the roof and the ground floor should not be prioritized in the retrofitting. Comparing the minimum points with and without the constraint for Tromsø 5% and Tromsø 10% also showed the fact that with the ground floor refurbishment no significant energy reduction was achieved (the big gray circle and triangle in Fig. 13c).

For the cases with the AA system in Fig. 14, the optimization process

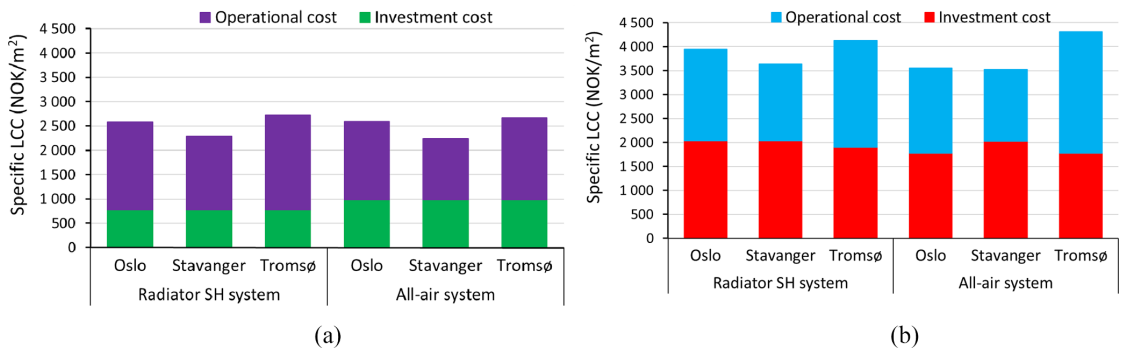


Fig. 9. Ratio of the operational cost to the investment cost for (a) minimum and (b) maximum LCC.

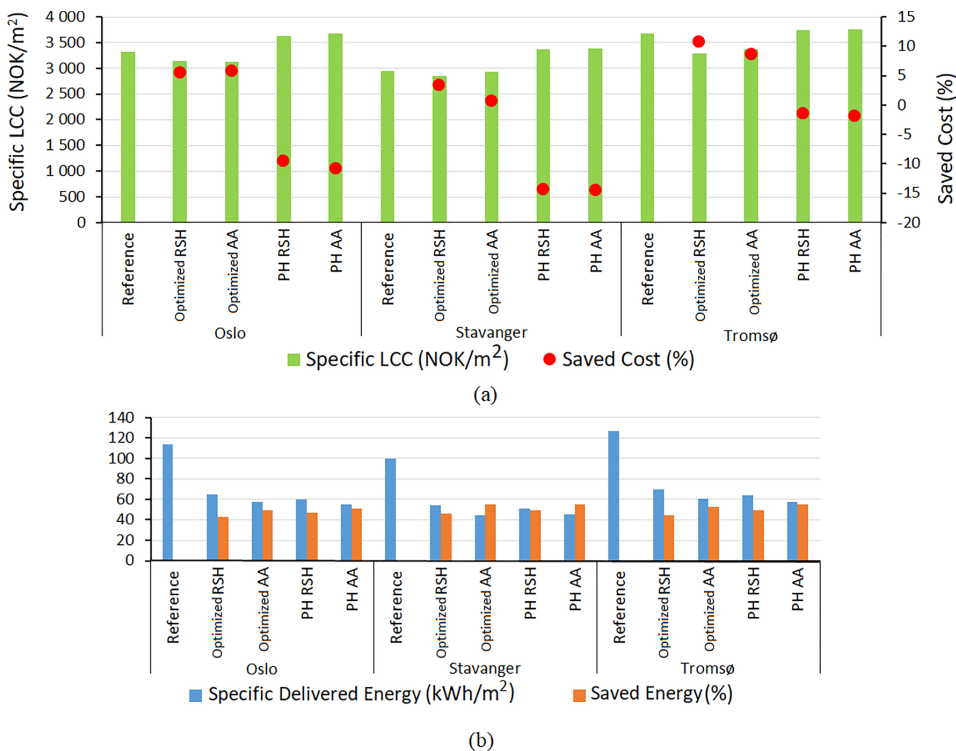


Fig. 10. Comparison of (a) specific LCC and (b) specific delivered energy for the reference, optimized, and PH standard cases.

was more challenging since the thermal comfort was not satisfied in some cases. The four different colors in Fig. 14 show the four different conditions with respect to the constraints. The global minimum energy use points (with and without constraints) for different cost increase cases are shown with the same symbols, but larger. Furthermore, in Fig. 14, it can be noted that for the cases of Stavanger 5% and 10%, the minimum energy use point was around 43.2 kWh/m² for the case without cost increase constraint. For the cases of Oslo 5% and 10%, the minimum energy use was achieved around 53 kWh/m² and 52.5 kWh/m², respectively when both thermal comfort and cost increase constraints were not considered. Nevertheless, for the cases of Tromsø 5% and 10%, around 53.9 kWh/m² was obtained for the case without the thermal comfort constraint. Comparing these cases implied that when the nZEB is the main target, the cost-effective options should always be taken into account and not the ones with minimum energy use. The reason is that a little energy saving may result in a large increase in the total retrofitting LCC (for example, compare the big red triangle and circle with gray ones in Fig. 14a).

Fig. 15 shows the optimized supply air temperature profiles, defined as a function of return air temperature to AHU, for the AA system. These profiles are associated with the global minimum LCC solution in the first scenario and the global minimum delivered energy solution in the second scenario.

Finally, the trade-off of optimal solutions for two retrofitting scenarios between the specific delivered energy and the specific LCC is qualitatively shown in Fig. 16 and is quantitatively described in Table 7. Compared to the reference case buildings, the energy saving

potential of the retrofitting measures was 43–56% in various cases. In spite of considering 5% and 10% cost increase in the second scenario, the LCC saving for the minimum delivered energy point, compared to the reference case, was still achieved around 1% for the AA Stavanger case and 0.28% for the AA Tromsø case. In addition, the ground floor retrofitting was the most expensive option. However, the optimized solution including the ground floor retrofitting for the cases equipped with the AA system could reduce the delivered energy even more than the PH standard level (see the point for PH AA in Fig. 16) thanks to the HVAC set point adjustments by the optimization process. The corresponding cost was also less than the PH AA case, because the reduction of the operational cost due to both adjustment of the HVAC set points and using the high performing building envelope was lower than the investment cost. Comparing these two scenarios showed that all the cases in the second scenario could almost satisfy the energy use for the PH standard level. However, energy saving was achieved only for the AA Stavanger and the AA Tromsø cases in this scenario.

5. Conclusion

This article dealt with a design methodology to facilitate the selection of cost-effective building retrofitting measures using an optimization approach, developed to improve the energy performance of an office building, located in a Nordic climate, towards nearly zero energy/emission building by targeting the passive house level as the first step. The optimization framework was processed through the Graphical Script module making the implementation of the constraints and objective

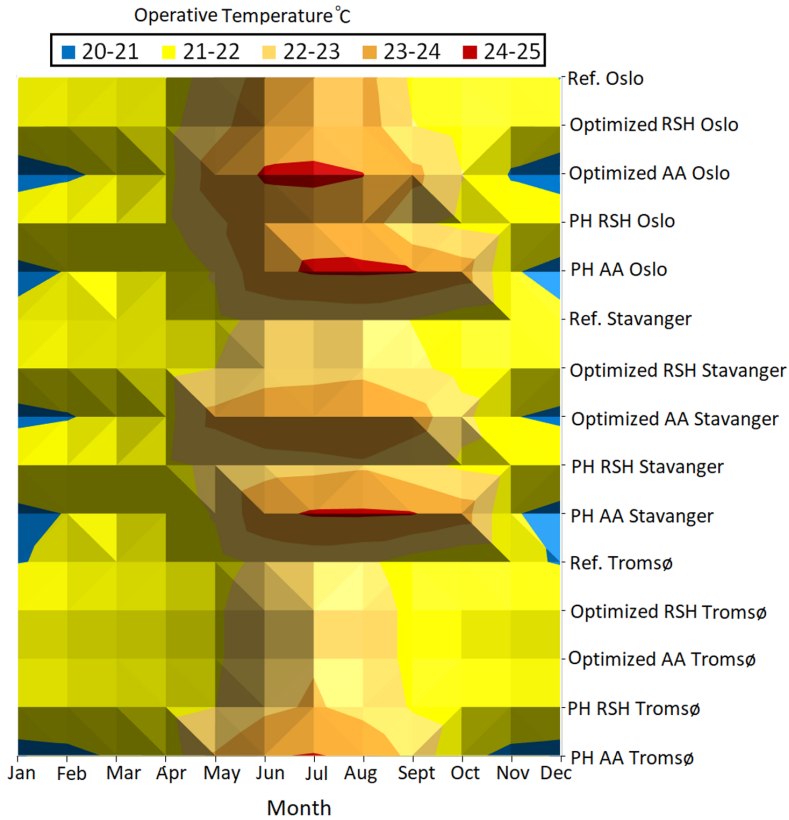


Fig. 11. Monthly variation of average operative temperature of the worst zone for global optimal solutions in various cases during the year in the first scenario.

functions more understandable by using an illustrative approach.

The findings of the analysis were compared to the reference cases through two optimization scenarios and the results showed a large energy saving potential for all optimized cases. High quality window and external wall were always used in all the optimized cases, but the ground floor and the roof retrofitting were the most costly options and were used only when the reduction of operational cost due to energy use was lower than the investment cost. The amount of delivered

energy saving for the cases equipped with the all-air system was higher than the cases in which the radiator space heating system was used.

In the second scenario, in which the delivered energy was considered as the objective function, the all-air systems could reach even lower energy use than the passive house standard level due to optimizing supply temperature and the air flow rate set points. In the first scenario, when the life cycle cost of retrofit interventions was considered as the objective, the maximum saving in the life cycle cost over

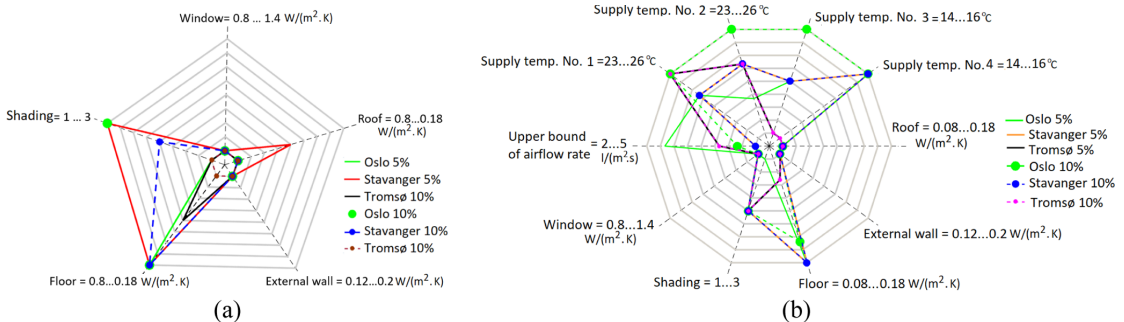


Fig. 12. Design parameter configurations in the minimum energy use point for (a) RSH system and (b) AA system in the second scenario.

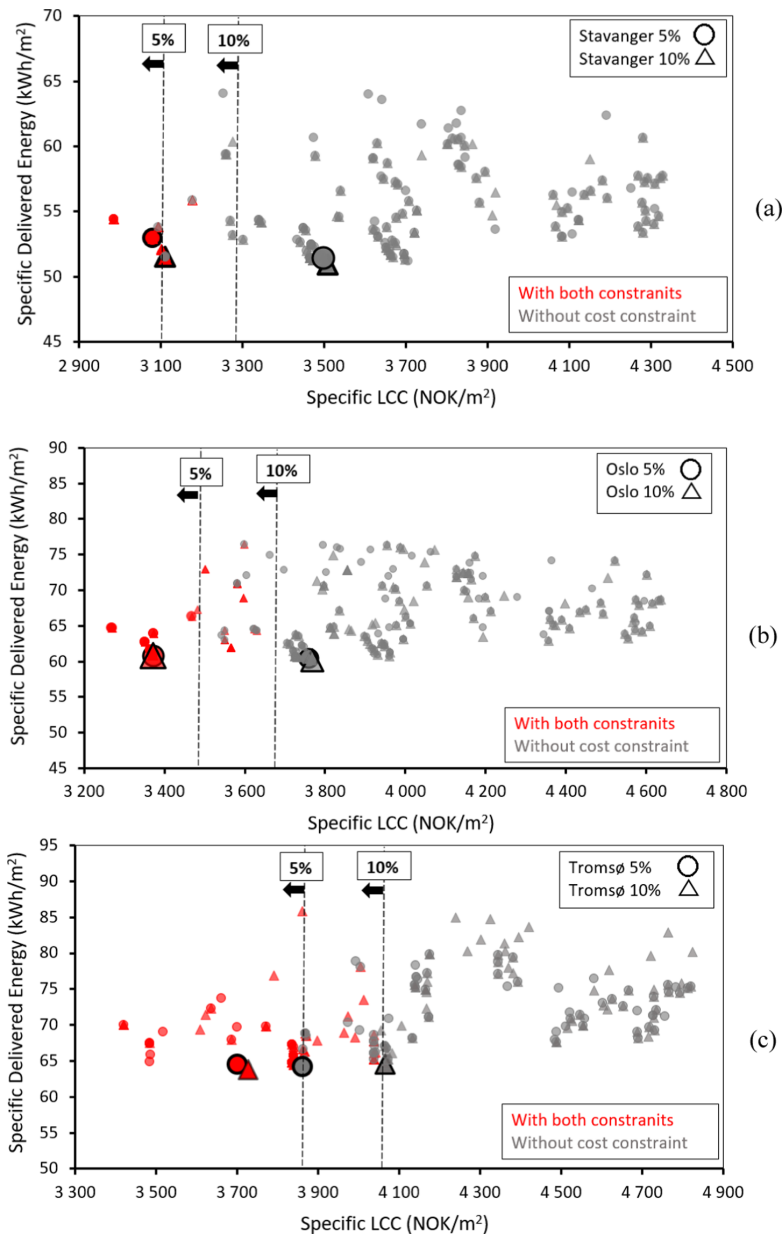


Fig. 13. Effect of constraint function on the optimization solutions for RSH system in (a) Stavanger (b) Oslo and (c) Tromsø in the second scenario.

a period of 60 years was up to 11% for the radiator space heating Tromsø case, while still meeting the space heating and space cooling needs according to the Norwegian passive house standard level. It is worth mentioning that the thermal comfort for occupants was satisfied for all the cases in both scenarios.

Future work on the optimization process through Graphical Script module presented in this work could follow the second step in achieving nearly zero energy/emission building level. This step can take

advantage of onsite production of renewable energy through integration of photovoltaic cells to the roof top or facade in order to balance the total amount of building energy use. In addition, since the indoor temperature control in the all-air system is challenging, a detailed analysis of the system performance in terms of air distribution and air temperature stratification would make an interesting investigation. It can be achieved by involving the coupling of energy simulation with computational fluid dynamic simulation software.

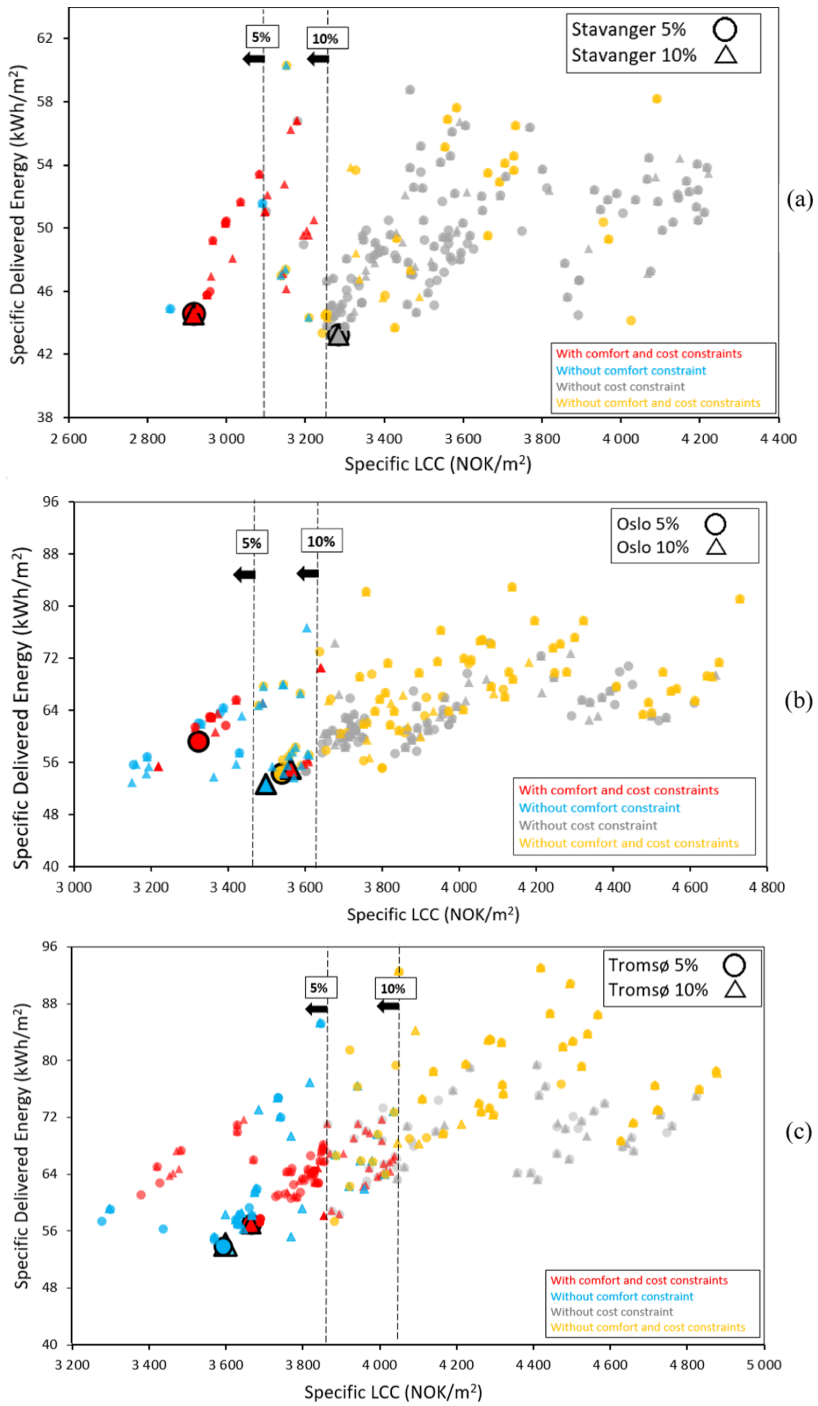


Fig. 14. Effect of constraint function on the optimization solutions for AA system in (a) Stavanger (b) Oslo and (c) Tromsø in the second scenario.

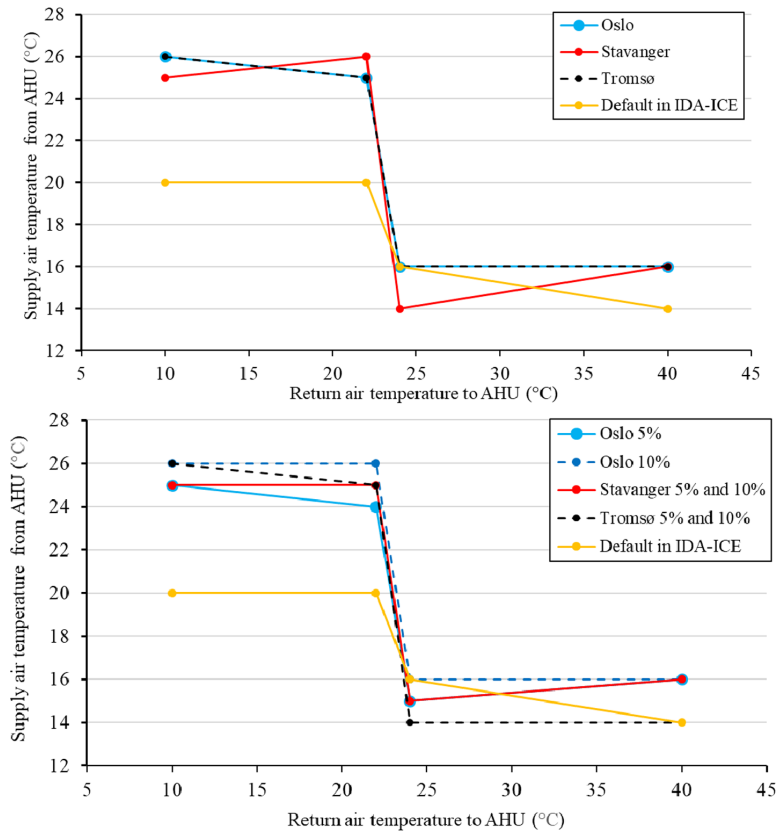


Fig. 15. Optimized supply temperature profile as a function of return temperature to AHU in the first scenario (top) and the second scenario (bottom).

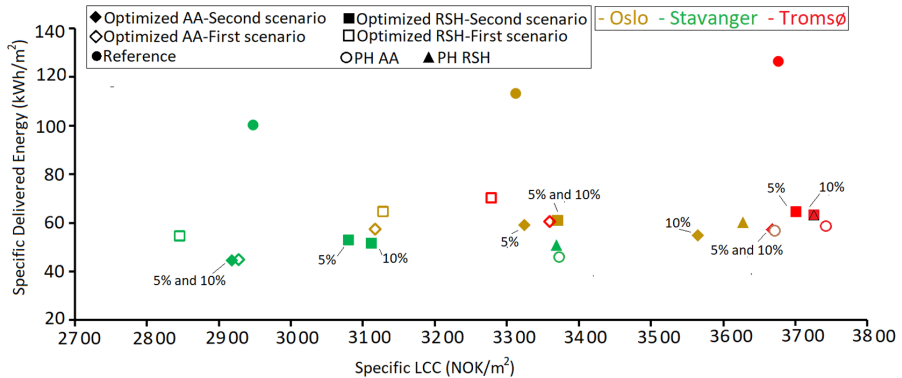


Fig. 16. Trade-off of optimal solutions considering both specific delivered energy and specific LCC for two scenarios.

Table 7
Energy and LCC values of various optimal case solutions for both scenarios.

	Simulation case	Specific delivered energy (kWh/m ²)	Energy saving vs reference (%)	Specific LCC (NOK/m ²)	LCC saving vs reference (%)
Reference	Ref. Oslo	113.30	NA	3311.99	NA
	Ref. Stavanger	100.20	NA	2947.34	NA
	Ref. Tromsø	126.38	NA	3676.33	NA
First Scenario	Opt. RSH Oslo	64.50	43.1	3129.04	5.52
	Opt. RSH Stavanger	54.42	45.7	2845.98	3.44
	Opt. RSH Tromsø	70.00	44.6	3279.32	10.80
	Opt. AA Oslo	57.41	49.3	3117.69	5.87
	Opt. AA Stavanger	44.92	55.2	2927.67	0.67
	Opt. AA Tromsø	60.43	52.2	3359.46	8.62
Second Scenario	Opt. RSH Oslo 5%	60.84	46.3	3370.92	-1.78
	Opt. RSH Oslo 10%	60.83	46.3	3627.97	-1.77
	Opt. RSH Stavanger 5%	52.92	47.2	3091.75	-4.51
	Opt. RSH Stavanger 10%	51.53	48.6	3091.75	-5.59
	Opt. RSH Tromsø 5%	64.46	49.0	3701.20	-0.68
	Opt. RSH Tromsø 10%	63.80	49.5	3727.40	-1.38
	Opt. AA Oslo 5%	59.16	47.8	3564.97	-0.37
	Opt. AA Oslo 10%	54.99	51.5	3476.54	-7.64
	Opt. AA Stavanger 5%	44.56	55.5	2917.83	1.00
	Opt. AA Stavanger 10%	44.56	55.5	2917.83	1.00
	Opt. AA Tromsø 5%	56.97	54.9	3665.92	0.28
	Opt. AA Tromsø 10%	56.97	54.9	3665.92	0.28
PH	PH RSH Oslo	60.19	46.9	3627.13	-9.51
	PH RSH Stavanger	50.92	49.2	3368.81	-14.30
	PH RSH Tromsø	63.80	49.5	3727.38	-1.38
	PH AA Oslo	56.67	49.9	3668.97	-10.77
	PH AA Stavanger	46.03	54.1	3372.80	-14.43
	PH AA Tromsø	59.46	52.9	3746.54	-1.91

CRedit authorship contribution statement

Mehrdad Rabani: Methodology, Software, Writing - original draft, Writing - review & editing. **Habtmu Bayera Madessa:** Conceptualization, Supervision, Writing - review & editing. **Omid Mohseni:** Methodology, Software. **Natasa Nord:** Supervision, Writing - review & editing.

Declaration of Competing Interest

The authors declare that they have no known competing financial interests or personal relationships that could have appeared to influence the work reported in this paper.

Appendix

A. Shading type and properties

Table 8 presents the shading properties used as the input parameters in the optimization process. The solar factor in this table shows the percentage of solar heat which is blocked in the summer by glazing and outdoor solar protection type.

Table 8
External shading properties for the optimization process.

Shading type	Solar factor	Solar transmission	Solar reflection	Solar absorption
(Type 1) Black Sunworker M391	0.12	0.06	0.05	0.89
(Type 2) Bronze Sunworker M393	0.12	0.07	0.08	0.85
(Type 3) Gray Sunworker M654	0.13	0.14	0.47	0.39

B. Specifications of LCC factors

Table 9 shows the details of factors used for the calculation of LCC model for a lifetime period 60 years. It should be noted that the energy price value in this table includes the grid fee.

Table 9
Input parameters for LCC calculations.

Variables in the LCC model	Expression	Value	Unit
Lifetime	n	60	Year
Inflation	f	2	%
Escalation rate	e	1	%
Energy price [54]	e_p	1.2	NOK/kWh
Nominal interest rate	i	7	%

C. Specifications of optimization algorithm

Table 10 elaborates the selected values for the hybrid optimization algorithm. The first part is for the PSO algorithm and the last entries are for the GPS implementation of the Hooke-Jeeves algorithm.

Table 10
Hybrid algorithm parameters for the optimization process.

Algorithm type	Algorithm parameter	Value	
PSO	Neighbourhood topology	Von Neumann	
	Neighbourhood size	5	
	Number of particles	10	
	Seed	50	
	Number of generations	10	
	Cognitive acceleration	2.8	
	Social acceleration	1.3	
	Maximum velocity discrete	4	
	Constriction gain	0.5	
	GPS and Hooke-Jeeves	Mesh size divider	2
		Initial mesh size exponent	0
Mesh size exponent increment		1	
Number of step reduction		4	

References

- https://www.ssb.no/en/bygg-bolig-og-endom/statistikker/bygningsmasse/aar. Statistics Norway; 2019.
- Nord N. Building energy efficiency in cold climates. *Encyclopedia Sustain Technol* 2017;149–57.
- Kolokotsa D, Diakaki C, Grigoroudis E, Stavarakis G, Kalaitzakis K. Decision support methodologies on the energy efficiency and energy management in buildings. *Adv Build Energy Res* 2009;3:121–46.
- Zhou Z, Zhang S, Wang C, Zuo J, He Q, Rameezdeen R. Achieving energy efficient buildings via retrofitting of existing buildings: a case study. *J Cleaner Prod* 2016;112:3605–15.
- Jung N, Pailho S, Shemeikka J, Lahdelma R, Airaksinen M. Energy performance analysis of an office building in three climate zones. *Energy Build* 2018;158:1023–35.
- Wang Q, Holmberg S. A methodology to assess energy-demand savings and cost effectiveness of retrofitting in existing Swedish residential buildings. *Sustain Cities Soc* 2015;14:254–66.
- Liu G, Liu B, Wang W, Zhang J, Athalye R, Moser D, et al. *Advanced Energy Retrofit Guide Office Buildings*: Pacific Northwest National Laboratory and PECC With assistance from the U.S. Department of Energy; 2011.
- Wang Q, Ploskić A, Holmberg S. Retrofitting with low-temperature heating to achieve energy-demand savings and thermal comfort. *Energy Build* 2015;109:217–29.
- Wang Q, Laurenti R, Holmberg S. A novel hybrid methodology to evaluate sustainable retrofitting in existing Swedish residential buildings. *Sustain Cities Soc* 2018;156:24–38.
- Homfray N. *Analysis of Potential Building Retrofits to Accommodate the Shift to Low Temperature Heating*: University of Strathclyde; 2018.
- Hesarakı A, Holmberg S. Energy performance of low temperature heating systems in five new-built Swedish dwellings: a case study using simulations and on-site measurements. *Build Environ* 2013;64:85–93.
- Mindykowski D. Optimization of heating and cooling system for a passive house equipped with heat pump and heat storage [Master of Science]. Trondheim, Norway: Norwegian University of Science and Technology (NTNU); 2016.
- DIRECTIVE (EU) 2018/844 of the European parliament and of the council of 30 May 2018 amending Directive 2010/31/EU on the energy performance of buildings and Directive 2012/27/EU on energy efficiency (Text with EEA relevance). *Official Journal of the European Union*; 2018.
- Berardi U. *Handbook of Energy Efficiency in Buildings: A Life Cycle Approach*. ZEB and NZEB (Definitions, Design Methodologies, Good Practices, and Case Studies). 2018:88.
- Andresen I. *Handbook of Energy Systems in Green Buildings. Definitions, Targets, and Key Performance Indicators for New and Renovated Zero Emission Buildings*. 2018:35–60.
- Wiik MK, Fufa SM, Kristjansdottir T, Andresen I. Lessons learnt from embodied GHG emission calculations in zero emission buildings (ZEBs) from the Norwegian ZEB research centre. *Energy Build* 2018;165:25–34.
- Lu Y, Wang S, Zhao Y, Yan C. Renewable energy system optimization of low/zero energy buildings using single-objective and multi-objective optimization methods. *Energy Build* 2015;89:61–75.
- Harkouss F, Fardoun F, Biwole PH. Multi-objective optimization methodology for net zero energy buildings. *J Build Eng* 2018;16:57–71.
- Longo S, Montana F, Riva Sanseverino E. A review on optimization and cost-optimal methodologies in low-energy buildings design and environmental considerations. *Sustain Cities Soc* 2019;45:87–104.
- Harkouss F, Fardoun F, Biwole PH. Passive design optimization of low energy buildings in different climates. *Energy* 2018;165:591–613.
- Niemelä T, Levy K, Kosonen R, Jokisalo J. Cost-optimal renovation solutions to maximize environmental performance, indoor thermal conditions and productivity of office buildings in cold climate. *Sustain Cities Soc* 2017;32:417–34.
- Palonen M, Hamdy M, Hasan A. *MOBO a new software for multi-objective building performance optimization*; 2013.
- Hirvonen J, Jokisalo J, Heljo J, Kosonen R. Towards the EU emissions targets of 2050: optimal energy renovation measures of Finnish apartment buildings. *Int J Sustain Energ* 2018;38:649–72.
- Arabzadeh V, Jokisalo J, Kosonen R. A cost-optimal solar thermal system for apartment buildings with district heating in a cold climate. *Int J Sustain Energ* 2018;38:141–62.
- Magnier L, Haghghat F. Multiobjective optimization of building design using TRNSYS simulations, genetic algorithm, and Artificial Neural Network. *Build Environ* 2010;45:739–46.
- Asadi E, da Silva MG, Antunes CH, Dias L. A multi-objective optimization model for building retrofit strategies using TRNSYS simulations GenOpt and MATLAB. *Build Environ* 2012;56:370–8.
- Ferrara M, Siroambo E, Fabrizio E. Automated optimization for the integrated design process: the energy, thermal and visual comfort nexus. *Energy Build* 2018;168:413–27.
- Chantrelle FP, Lahmidi H, Keilholz W, Mankibi ME, Michel P. Development of a multicriteria tool for optimizing the renovation of buildings. *Appl Energy* 2011;88:1386–94.
- Karaguzel OT, Zhang R, Lam KP. Coupling of whole-building energy simulation and multi-dimensional numerical optimization for minimizing the life cycle costs of office buildings. *Build Simul* 2013;7:111–21.
- Schwartz Y, Raslan R, Mumovic D. Implementing multi objective genetic algorithm for life cycle carbon footprint and life cycle cost minimisation: a building refurbishment case study. *Energy* 2016;97:58–68.
- Delgarm N, Sajadi B, Delgarm S. Multi-objective optimization of building energy performance and indoor thermal comfort: a new method using artificial bee colony (ABC). *Energy Build* 2016;131:42–53.
- Delgarm N, Sajadi B, Kowsary F, Delgarm S. Multi-objective optimization of the building energy performance: a simulation-based approach by means of particle swarm optimization (PSO). *Appl Energy* 2016;170:293–303.
- Bamdad K, Cholette ME, Guan L, Bell J. Ant colony algorithm for building energy optimisation problems and comparison with benchmark algorithms. *Energy Build* 2017;154:404–14.
- Djuric N, Novakovic V, Holst J, Mitrovic Z. Optimization of energy consumption in buildings with hydronic heating systems considering thermal comfort by use of computer-based tools. *Energy Build* 2007;39:471–7.
- Grygierek K, Ferdyn-Grygierek J. Multi-Objective Optimization of the Envelope of Building with Natural Ventilation. *Energies*. 2018;11.
- Hong T, Kim J, Lee M. A multi-objective optimization model for determining the building design and occupant behaviors based on energy, economic, and environmental performance. *Energy* 2019;174:823–34.
- Karmellos M, Kiprakis A, Mavrotas G. A multi-objective approach for optimal prioritization of energy efficiency measures in buildings: model, software and case studies. *Appl Energy* 2015;139:131–50.
- Taveres-Cachat E, Lobaccaro G, Goia F, Chaudhary G. A methodology to improve the performance of PV integrated shading devices using multi-objective optimization. *Appl Energy* 2019;247:731–44.
- Wu R, Mavromatidis G, Orehoung K, Carmeliet J. Multiobjective optimisation of energy systems and building envelope retrofit in a residential community. *Appl Energy* 2017;190:634–49.
- Hamdy M, Hasan A, Siren K. Applying a multi-objective optimization approach for Design of low-emission cost-effective dwellings. *Build Environ* 2011;46:109–23.

- [41] Thyholt M, Dokka AGLoTH. Kartlegging av mekanisk kjøling i nye kontor- og forretningsbygg. Trondheim, Norway: SINTEF Bygg og miljø; 2001. p. 36.
- [42] Direktoratet for Byggkvalitet, Byggteknisk forskrift - TEK 10. 2010.
- [43] Validation of IDA Indoor Climate and Energy 4.0 with Respect to CEN Standards EN 15255-2007 and EN 15265-2007. Equa Simulation Finland Oy, 2010 <http://www.equa.se/en/ida-ice/validation-certifications>.
- [44] NS 3031, Calculation of energy performance of buildings - Method and data. Standard Norge; 2014. p. 100.
- [45] Betongelement Foreningen, http://betongelementboka.betongelement.no/betongapp/BookE.asp?isSearch=0&liID=34&DocumentId=BindE/Del_1/E3/3_4_U_verdi_for_etasjeskiller.pdf&BookId=E. 2008.
- [46] ASHRAE. Thermal environmental conditions for human occupancy, ANSI/ASHRAE Standard 55e2010. Atlanta, Georgia: American Society of Heating, Refrigerating and Air Conditioning Engineers; 2010.
- [47] ANSI/ASHRAE/IESNA. Standard 90.1e2007 normative Appendix B: building envelope climate criteria. 2007.
- [48] NS-3701-Criteria for passive houses and low energy buildings, Non-residential buildings. Norway: Standard Norge; 2012.
- [49] Norsk Prisbok. Norconsult Informasjonssystemer AS, <https://www.norskprisbok.no/WhatsNP.aspx>; 2019.
- [50] Hasan A, Vuolle M, Sirén K. Minimisation of life cycle cost of a detached house using combined simulation and optimisation. *Build Environ* 2008;43:2022–34.
- [51] Wetter M. GenOpt (R), generic optimization program, User Manual, Version 2.0. 0. 2003.
- [52] Krajčák M, Simone A, Olesen BW. Air distribution and ventilation effectiveness in an occupied room heated by warm air. *Energy Build* 2012;55:94–101.
- [53] Rabani M, Madessa HB, Nord N, Schild P, Mysen M. Performance assessment of all-air heating in an office cubicle equipped with an active supply diffuser in a cold climate. *Build Environ* 2019;156:123–36.
- [54] Statistics Norway, Electricity prices, <https://www.ssb.no/en/energi-og-industri/statistikker/elkraftpris>. 2019.

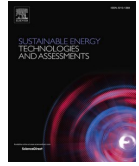
Paper 2

M. Rabani, H. Bayera Madessa, N. Nord, Achieving zero-energy building performance with thermal and visual comfort enhancement through optimization of fenestration, envelope, shading device, and energy supply system, *Sustainable Energy Technologies and Assessments*, 44 (2021) 101020



Contents lists available at ScienceDirect

Sustainable Energy Technologies and Assessments

journal homepage: www.elsevier.com/locate/seta

Achieving zero-energy building performance with thermal and visual comfort enhancement through optimization of fenestration, envelope, shading device, and energy supply system

Mehrdad Rabani^{a,b,*}, Habtamu Bayera Madessa^a, Natasa Nord^b^a Department of Civil Engineering and Energy Technology, Oslo Metropolitan University, Norway^b Department of Energy and Process Engineering, Norwegian University of Science and Technology, Norway

ARTICLE INFO

Keywords:

Building retrofitting
 Optimization process
 Shading control method
 Window opening control method
 Zero energy building

ABSTRACT

Building retrofitting towards nearly zero energy building (nZEB) with comfortable visual and thermal conditions, requires a comprehensive parametric analysis of building retrofit measures. This paper presented an optimization method to automate the procedure of finding the best combination of measures minimizing the building energy use and achieving the nZEB target while enhancing both thermal and visual comfort conditions. The study was performed by coupling of an Indoor climate and energy simulation software (IDA-ICE) and a generic optimization tool (GenOpt) through a Graphical Script interface and the optimization was applied to a typical office building located in Norway. The adopted method allowed the concurrent optimization of building envelope, building energy supply, fenestration, and shading device material, and control methods. Two constraint functions including visual and thermal comfort criteria were considered. Afterwards, PV panels were integrated with the building site for on-site production of electricity towards ZEB level. Findings demonstrated that the inclusive optimization approach could significantly decrease the building energy use, up to 77%, and improve both the thermal and visual comfort simultaneously. Furthermore, the best performance for the optimal solution was achieved when the shading device and window opening control methods functioned with solar radiation and indoor air temperature setpoints.

1. Introduction

Buildings account for a large share of total energy use and significantly contribute to global warming. In the EU, building sector stands for 40% of total energy use [1] and releasing approximately 40% of all GHG emissions [2]. As the total energy use is expected to increase in the future, [3] energy efficiency measures should be considered in different areas such as building sector so that a widespread sustainable development can be achieved. In this regard, the latest update of EPBD requires all EU member states to develop a roadmap for the energy retrofitting of existing buildings [4]. Especially, when the energy savings potential on a national level is the matter of concern, it is essential to investigate the existing building stock due to substantially worse energy performance in older buildings than newer ones [5].

While considering the energy efficiency in buildings, thermal comfort and well-being of occupants are aspects of great significance, especially in office buildings. However, improving both indoor climate

and visual conditions may lead to increase in the energy use. It is even more challenging when the target is to improve the building energy performance towards nZEB and to provide thermal and visual comfort at the same time [6,7]. Therefore, a large number of studies have investigated the impact of applying various retrofit measures on the building energy performance through different approaches such as data-driven methods, [8,9] optimization techniques, [10,11] or combination of both approaches [12,13]. Data-driven methods, which are also referred as grey-box or black-box models, take advantage of statistical analysis to find the relationships between the building input and output variables without detailed knowledge of building physical behavior [12]. However, optimization approaches adopt machine learning techniques and algorithms such as genetic algorithm, particle swarm optimization, and sequential search to find the optimal set of building retrofit measures through an iterative process, [14] which was considered in this study.

* Corresponding author at: Department of Civil Engineering and Energy Technology, Oslo Metropolitan University, Norway.

E-mail addresses: Mehrdad.Rabani@oslomet.no (M. Rabani), Habtamu-Bayera.Madessa@oslomet.no (H. Bayera Madessa), natasa.nord@ntnu.no (N. Nord).<https://doi.org/10.1016/j.seta.2021.101020>

Received 23 September 2020; Received in revised form 16 December 2020; Accepted 12 January 2021

2213-1388/© 2021 The Author(s). Published by Elsevier Ltd. This is an open access article under the CC BY license (<http://creativecommons.org/licenses/by/4.0/>).

Nomenclature	
<i>Roman symbols</i>	
A	area of each zone (m ²)
A _{eff}	effective area of the window opening (m ²)
AHU	air handling unit
ANN	artificial neural network
C _d	discharge coefficient
CAV	constant air volume
CFD	computational fluid dynamics
DF _{avg}	average daylight factor
DH ₂₆	discomfort hours for the indoor operative temperature more than 26 °C during occupancy (h)
DHW	domestic hot water
E _{el,prod}	produced electricity by PV cells (kWh)
E _{el,use}	energy use due to lighting, equipment, HVAC system and domestic hot water (kWh)
E _{imp}	imported energy (kWh)
E _{exp}	delivered energy to the grid (kWh)
E _{p,exp}	primary exported energy (kWh)
E _{p,imp}	primary imported energy (kWh)
E _{self,use}	self-consumption of generated electricity (kWh)
E _{tot}	specific total delivered energy to the building on annual basis (kWh/(m ² ·year))
EPBD	energy performance of buildings directive
EU	European Union
GA	genetic algorithm
GenOpt	generic optimization program
GHG	greenhouse gas
GS	graphical script
GSHP	ground-source heat pump
H	window height (m)
HVAC	heating, ventilation, air conditioning system
i	type of energy carrier
k	zone counter
LCC	life cycle cost
MOBO	multi-objective building optimization
m	monthly/hourly counter
N	total number of zones
NSGAI	non-dominated sorting genetic algorithm II
n ₅₀	airtightness
nZEB	nearly zero energy building
PDH	total occupant hours dissatisfaction
PH	passive house
PMV	predicted mean vote
PPD	predicted percentage dissatisfied (%)
PPD _{avg}	annual average of predicted percentage dissatisfied during total occupied hours (%)
PR	performance ratio relating the actual and the theoretical energy output of the PV system
PSO	particle swarm optimization
PV	photovoltaic
Q _{sol}	solar radiation for controlling shading (W/m ²)
SFP	specific fan power (kW/(m ³ /s))
U	total heat transfer heat coefficient (W/(m ² ·K))
UDI	useful daylight illuminance
VAV	variable air volume
W	window width (m)
W _{DH₂₆}	weighted discomfort hours
W _{PPD}	weighted predicted percentage of dissatisfied
w	weighting factors/metrics for primary energy
ZEB	zero energy building
<i>Greek symbols</i>	
ψ	normalized thermal bridge (W/(m ² ·K))
γ	mismatch factor/supply cover factor (%)

2. Literature review on the optimization of building energy performance

2.1. Building envelope and HVAC setpoints

In order to facilitate the process of finding the optimal set of building retrofit measures, many studies have suggested an optimization approach. In this respect, numerous studies focused on the optimization of building envelope, façade parameters, and the setpoints for space heating, space cooling, and ventilation system. Table 1 shows a summary of these parameters applied in the most recent studies.

2.2. Parameters of building energy supply system

Studies in the literature also showed that optimizing the type and parameters of the building energy supply system could improve the building performance. Lu et al. [27] investigated single and multi-objective optimization of PV cell size, wind turbine size and power, and the capacity of bio-diesel generator in order to minimize the total cost of renovations, CO₂ emissions, and building-grid interaction index. Wu et al. [28] optimized the operation strategies for energy conversion and storage technologies including heat pumps, solar panels, biomass, oil boilers and thermal storage in order to minimize the annualized costs and life cycle GHG emissions of typical residential buildings. Hirvonen et al. [29] performed a multi-objective optimization process to minimize the LCC and CO₂ emissions due to the renovation of four Finish reference buildings. In addition to building envelope characteristics and window type, they considered energy system parameters including type and capacity of heat pump, PV size, and the type of sewage heat recovery

system from wastewater. The results showed that utilizing the GSHP as the energy supply system was the most cost-effective renovation measure. Ferrara et al. [30] investigated the optimization of building envelope and energy supply system in order to minimize the global cost during the entire life cycle of the building. The energy supply parameters consisted of the choice of generator terminals, auxiliary heaters for domestic hot water, PV type, dimension of water storage, and the percentage of building roof area covered by PV and thermal solar collectors.

2.3. Visual comfort parameters

Since optimizing building fenestration and glazing is always accompanied by compromising the occupants' visual comfort, some studies investigated the optimization of the visual comfort either by maximizing it as an objective function or considering it as a constraint function. Taveres-Cachat et al. [31] optimized the angle of louver blades and their center point coordinate in a PV integrated shading system to minimize the total net energy use, maximize the daylight level and the energy converted by the PV material. Fang and Cho [32] conducted an optimization study including the combined effects of window size, skylight size and location, and length of horizontal fixed sun louver on the maximization and minimization of UDI and energy use intensity, respectively. Pilechiha et al. [33] proposed an optimization framework for maximizing the daylight and minimizing the building energy use. The size of windows and room dimensions were altered during the optimization. The results showed a possibility of providing satisfactory quality of view for more than 80% of the reference room points, considering maximizing and minimizing the building daylight and energy use, respectively [20]. Kirmat et al. [34] presented a detailed

Table 1
Type of building envelope, façade parameters, and HVAC setpoints included in the optimization design variables in recent scientific studies.

Authors	Description	Design variables
Rosso et al. [15]	A multi-objective optimization was proposed to minimize building energy use, construction and energy costs, and CO ₂ emission. EnergyPlus was coupled with Python for the novel genetic algorithm aNSGA-II.	<ul style="list-style-type: none"> • Glazing system • Radiative properties of finishing layer • Vertical and horizontal insulation thickness • Presence or absence of solar shading • Change open balconies into glazed, movable sun spaces, closed during the cold season
Lu et al. [16]	A reliability analysis was conducted on the optimization of office buildings under uncertainties in the envelope and occupancy parameters. Rhinoceros, EnergyPlus, and the genetic algorithm were integrated for this purpose.	<ul style="list-style-type: none"> • U-value of walls • Visible transmittance of window
Ascione et al. [17]	A tailored rating assessment approach, comprised of optimization, validation, analysis and planning of requalification interventions, was carried out to improve the performance of an industrial building in terms of primary energy consumption and global cost. The optimization was done through coupling between EnergyPlus and MATLAB.	<ul style="list-style-type: none"> • Type of window • Presence and absence of solar screen • Heating temperature setpoint schedule • HVAC air flow rates
Chang et al. [18]	A multi-objective optimization framework was developed to minimize the energy use, indoor thermal discomfort, CO ₂ emissions, and payback period in residential buildings. EnergyPlus was coupled with GA, which modelled in MATLAB, for optimization process.	<ul style="list-style-type: none"> • Vertical façade option including Trombe wall, double skin façade, solar PV, PCM integrated in wood-lightweight concrete, and Algae façade • Roof options including exterior metal roof, green roof, solar PV, and cool coated roof
Li and Wang [19]	A coordinated multi-stage optimizations of building design and energy systems was proposed as a computation cost-effective method for zero/low energy buildings. An ANN model and a GA-based using EnergyPlus was adopted.	<ul style="list-style-type: none"> • Roof solar absorptance • Window-to-wall ratio • Wall solar absorptance • Overhang projection ratio
Si et al. [20]	A multi-objective optimization was applied to the design of a newly built complex building. The aim was to minimize annual energy demand and average predicted percentage dissatisfied. Simulations were done using EnergyPlus integrated with modeFRONTIER for automatic runs and parallel simulations.	<ul style="list-style-type: none"> • Exterior wall insulation thickness and conductivity • Roof insulation thickness and conductivity • Exterior window type • Cooling and heating temperature setpoints
Ascione et al. [21]	A multi-objective optimization was implemented through coupling between EnergyPlus and MATLAB to minimize the building primary energy use and global cost of retrofit measures in two different climates.	<ul style="list-style-type: none"> • Roof insulation thickness • Vertical walls insulation thickness • Window type • Position of the shading systems • Percentage of the roof covered by photovoltaic panels
Ascione et al. [22]	A multi-optimization framework was proposed to minimize the daily running cost of space heating and maximum PPD over a specific day via	<ul style="list-style-type: none"> • Heating setpoint temperature during a hourly interval of the investigated day for different thermal zone type

Table 1 (continued)

Authors	Description	Design variables
	weather-data-based control for residential buildings. EnergyPlus and MATLAB were coupled for this purpose.	
Ilbeigi et al. [23]	A single-objective optimization was carried out to minimize the energy use of an office building by coupling EnergyPlus with Galapagos plugin based on a Genetic Algorithm.	<ul style="list-style-type: none"> • Wall U-value • Infiltration rate • Roof U-value
Bui et al. [24]	An optimization of building performance was carried out to minimize the energy use of a simple office model by applying an adaptive facade. EnergyPlus was linked to Eppy toolkit in Python.	<ul style="list-style-type: none"> • Adaptive façade using an electrochromic window. • Window visible transmittance • Window U-value
Nasruddin et al. [25]	A two-objective optimization approach was implemented to minimize building energy use and maximize thermal comfort through the improvement of HVAC system. IESVE software (for energy simulation and PPD calculations) was coupled with ANN and a multi-objective GA.	<ul style="list-style-type: none"> • Cooling setpoint • Relative humidity setpoint • Supply air flow rate (VAV system) • Window area • Wall thickness • Supply air temperature (VAV system) • Supply radiant temperature (radiant system) • Supply radiant flow rate (radiant system) • Starting and stopping thermostat delay
Guo et al. [26]	An optimization framework was developed to minimize the total building cooling energy use and maintain the PPD at certain level through improvement of night ventilation system control. EnergyPlus was linked to Omni-optimizer.	<ul style="list-style-type: none"> • Night venting duration • Minimum indoor temperature setpoint • Night air change rate setpoint • Activation threshold temperature • Internal thermal mass area • Specific fan power

optimization study on the design alternatives of a shading device with amorphous cells in order to minimize the total energy use and maximize the UDI of a test room model. For each shading panel, the shading distance from the window, movement point and rotation angle of shading slats were optimized. Yi [35] performed an optimization study on the geometry elements of an amorphous building façade to improve its daylighting performance. The aim was to find the best user’s design preference in order to qualitatively and quantitatively improve the building visual performance and aesthetic value simultaneously. Naderi et al. [36] optimized the architectural features and control parameters of a smart shading blind in a simple room to improve both visual and thermal comfort conditions. The design parameters included the slat width, angle, thickness, and reflectance, blind distance to the glass, shading location (interior, exterior), and shading control strategies. They adopted average discomfort glare index as the objective function for visual comfort.

2.4. Thermal comfort parameters

Occupant’s thermal comfort is also another conflicting barrier in improving the building energy performance and it has been addressed in various ways. Magnier and Haghghat [37] considered thermal comfort as an objective function to be maximized along with the total energy use to be minimized simultaneously. They used average and absolute PMV as the thermal comfort objective. Hong et al. [38] used PMV also as the thermal comfort objective function to be minimized along with the energy use, the net present value, and the global warming potential of building renovation measures. Grygierek and Ferdyn-Grygierek [39] conducted an optimization study to minimize the life cycle cost of

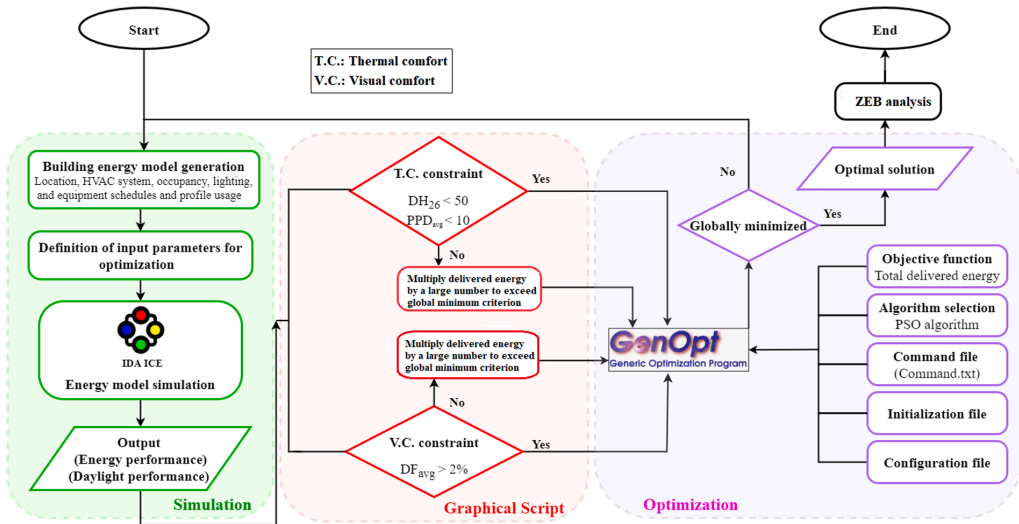


Fig. 1. Proposed framework for the optimization process.

building retrofitting measures and maximize the thermal comfort of occupants at the same time. Maximizing the thermal comfort of occupants was, in fact, done by minimizing the number of thermal discomfort hours. Niemelä et al. [40] proposed a multi-objective optimization to minimize the three objectives: CO₂ emissions due to delivering energy to the building, the net present value of its life cycle cost, and the PDH. Sghouri et al. [41] performed an optimization study to minimize an area-weighted mean discomfort degree-hours by modifying the overhangs projections of a building case. Ascione et al. [11,42,43] in three different multi-optimization frameworks considered the annual percentage of discomfort hours over occupied hours as the thermal comfort objective function to be minimized along with other objectives. The discomfort hours were assessed when PPD was higher than 20%.

2.5. Building energy simulation and optimization tools

There are several building energy performance and optimization tools frequently used in literature for building performance and optimization purposes. Regarding optimization tool, Tian et al. [44] carried out a review on the existing optimization tools, namely, GenOpt, [45] MOBO, [46] jEPlus + EA, [36,47] BEopt, [48] and MultiOpt [49] tools. These tools were integrated with building energy performance simulation tools such as EnergyPlus, [50–52] TRNSYS, [7,49,53] and IDA-ICE [29,40,54].

The aforementioned studies highlighted the importance of considering a hybrid set of building envelope and HVAC system parameters in the optimization process in order to improve the building energy performance and satisfy the visual and thermal comfort of occupants at the same time. Nevertheless, various shading and window opening control strategies, and HVAC setpoints were not studied together during optimizations in the literature. Therefore, the novelty of our paper was to investigate the interaction of window opening and shading device automatic control methods and parameters with other important design variables through optimization process, which was missing in the literature. Various control strategies and setpoints for shading devices, window opening and HVAC system can be conflicting when reducing building energy use and satisfying thermal and visual comfort conditions simultaneously. This was accomplished by integrating the IDA Indoor Climate and Energy (IDA-ICE) software and optimization tool (GenOpt) in order to improve the energy performance of a typical

existing office building and to find out what the minimum energy use would be considering both visual and thermal comfort conditions.

In the following sections, the proposed simulation-based method for a typical Norwegian office building is described. In this respect, the base case design configuration, conditions, and HVAC system, and setpoints are introduced. Afterwards, a wide range of parameters including building envelope, window glazing type, window to floor area ratio, and control strategies and setpoints for shading devices, window opening, and HVAC system are given. Besides, a PV is added in order to balance the total building energy use to achieve the ZEB level in the optimal solutions. Afterwards, the obtained results for the optimal cases are presented and commented. Finally, the main conclusions are summarized and the possibilities for the future work are discussed.

3. Method

Fig. 1 illustrates the proposed method for this study. The method was structured in several steps:

- The pre-processing step (the green area in Fig. 1), in which the building model was generated in IDA-ICE and the input parameters for the optimization problem were defined.
- The intermediate step (the red area in Fig. 1), where the output parameters from the energy simulation software were evaluated in terms of DF_{avg} , DH_{26} , and PPD_{avg} . The first parameter, daylight factor, was considered as the visual comfort index and the two latter, discomfort hours for the indoor operative temperature more than 26 °C and predicted percentage dissatisfied, were chosen as the thermal comfort indexes.
- The optimization step (the purple area in Fig. 1), where the objective function was iteratively assessed until an optimal solution was achieved.
- The post-processing step (the “ZEB analysis” box in Fig. 1), where the optimal solutions were elaborately analyzed in terms of ZEB balance.

3.1. Pre-processing step

In the pre-processing stage, the building energy model was generated in IDA-ICE software.

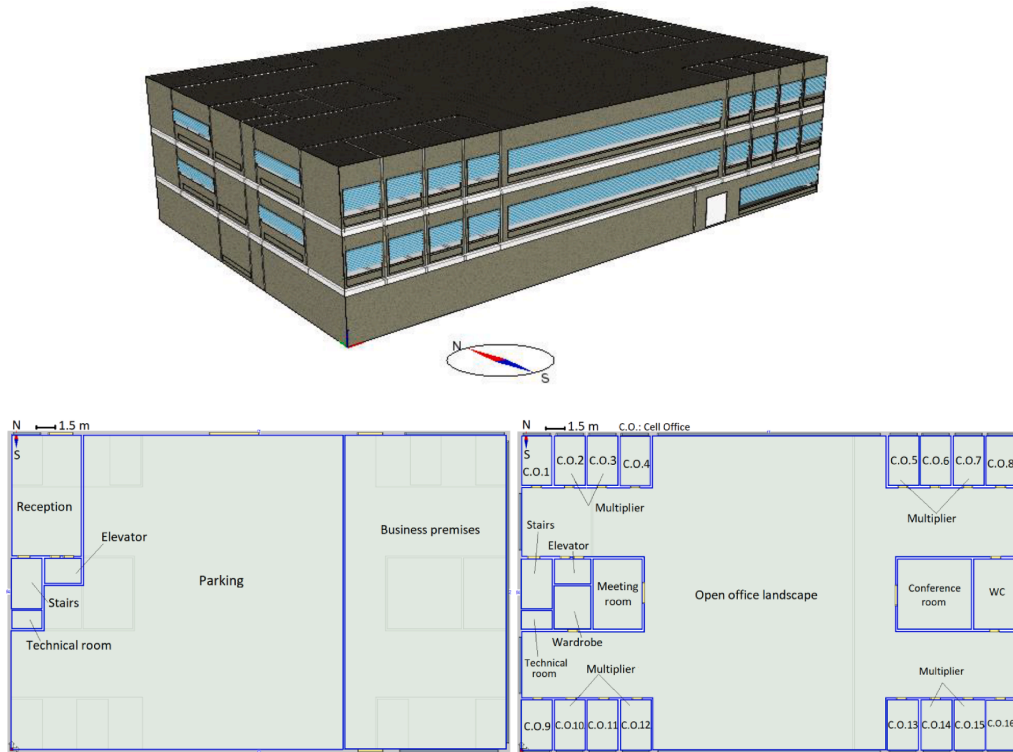


Fig. 2. Office building configuration (top), the first floor plan (bottom-left), and the second and the third floor plans at level 3.4 m and 6.8 m (bottom right).

Table 2
General building information on the reference case.

Parameter	Value/Feature
Building orientation	North-South
Number of floors	3
Floor height (m)	2.9
Total building height (m)	10.5
Total heated floor area (m ²)	2 940
Total building volume (m ³)	9 062
Total window area (m ²)	286.2
Total door area (m ²)	21

Table 3
Properties of the building envelope for the reference case.

Parameter, Units	Value
External wall U-value, W/(m ² K)	0.3
Roof U-value, W/(m ² K)	0.2
Floor U-value, W/(m ² K)	0.2
Window U-value, W/(m ² K)	2.4
ψ , W/(m ² K)	0.13
n_{50} , 1/h	4
External door U-value, W/(m ² K)	2
External shading strategy	Blinds on, if $Q_{sol} > 100 \text{ W/m}^2$ [57]

3.1.1. Case study and building energy model generation

We considered a case study model representing the configuration of typical office buildings located in Norway. According to the statistics of office building stock in Norway, most of office buildings were built in the 1980 s with a total heated floor area between 2,500 to 10,000 m² [55]. Therefore, as a case study, a reference office building with 3,000 m² total heated floor area was considered for the simulations in this study. The building envelope characteristics, lighting system, and HVAC system, and setpoints were chosen for a typical office building constructed in 1987 satisfying the Norwegian building code TEK87 [56]. Fig. 2 shows the office building model developed in the simulations in this study. Fig. 2 presents the zone multiplier, which is an available function in IDA-ICE, used to simplify the duplicate cell offices in the second and the third floors in order to reduce the simulation computational time. Furthermore, the type of shading device for the windows was an exterior venetian blind. The general building information about the reference case building are given in Table 2. The total window area was selected based on TEK87, so that the window to floor area ratio did not exceed

15%.

Table 3 presents the building envelope properties of the reference building. All characteristics were considered according to the Norwegian building code TEK87. The HVAC system parameters and setpoints and usage profiles for the reference case are shown in Table 4. In addition, DHW use was selected according to the Norwegian standard NS 3031 [57].

Table 5 presents the internal heat gains due to occupancy, lighting, and equipment along with their usage profiles. As the reference building was built in 1987 and is currently in use, the internal heat gain due to equipment and its usage profile was implemented in IDA-ICE according to the Norwegian standard NS 3031. Furthermore, a measurement-based data of several cell offices in an office building in Norway [58] was considered to have a realistic pattern of lighting and occupancy behavior, as shown in Fig. 3.

The simulations were run over a period of one year with the typical weather data taken from the ASHRAE IWEC 2 database for Oslo, Norway climate. The annual mean outdoor temperature was around 6.3°C and

Table 4
Characteristics of the HVAC system in the reference building.

HVAC systems and operation	Features
Ventilation system type	CAV mechanical balanced ventilation system
The SFP of the ventilation system	2.5 kW/(m ³ /s)
Schedules of ventilation system	Monday-Friday: 12 h/day for upper limit (6–18); other times reduces to lower limit
Supply airflow rates of the ventilation system	Primary zones: 4.32 m ³ /(m ² .h) and 19.8 m ³ /(m ² .h) for upper limit in heating and cooling seasons respectively, 0.72 m ³ /(m ² .h) for lower limit Secondary zones: 2.52 m ³ /(m ² .h) for upper limit, 0.72 m ³ /(m ² .h) for lower limit
Heating system	Central heating system, modelled in IDA-ICE using a generic electric heater with unlimited capacity and efficiency of 90%
Cooling system	Centralized water cooling system for cooling of supply air in the AHU
Heating distribution system	Water radiator system
Room temperature setpoint for local space heating *	19°C for heating
Control method of space heating and ventilation air heating and cooling systems	Space heating: supply water temperature as a function of outdoor temperature; Ventilation supply air temperature: as a function of outdoor temperature;
DHW use	5 kWh/(m ² .year)

* There was no local space cooling system in the zones and cooling of zones was done by the mechanical ventilation system.

Table 5
Internal heat gains and usage profiles due to occupancy, lighting, and equipment.

Usage profile of internal heat gains	Source values of internal heat gains
- Occupants, the usage profile was considered based on measurement data.	Each person occupies around 10 m ² of floor area, with activity level is 1.2 met, which is equal to 0.1 occupant/m ²
- Lighting, the usage profile was considered based on measurement data.	8 W/m ²
- Office equipment, the usage profile was: Monday-Friday: usage during 6–18o'clock, no usage at other times including weekends and holidays. No equipment for secondary zones	11 W/m ²

the space heating design outdoor temperature was considered around -20°C. Further detail about the climatic condition for this city can be found in ASHRAE classification [59]. It should be underlined that the building model in this study matched the requirements of Norwegian building code TEK 87 for specific annual energy needs of office buildings, as reported in [5].

3.1.2. Definition of input parameters for optimization

In total, 15 input variables in three main categories were considered for the optimization as shown in Table 6. The first group of variables associated with the building envelope were chosen based on the most relevant parameters in the literature. The insulation materials, applied for the external wall and the roof, were replaced by new insulation materials with different thickness, as shown in Table 6. The second group in the variables corresponded to the HVAC parameters and set-points. It should be mentioned that overheating in Table 6 means that the supply water temperature for the space heating at central heating system was slightly increased in the morning to avoid a very high peak load. The third group of variables consisted of different control methods for shading devices and window opening. To recall, the optimization latter variables in combination was missing in literature and none of the studies considered the combined control of these two types of variables for the optimization process. The shading material properties are explained in detail in the Appendix (see Table 8). It should be underlined

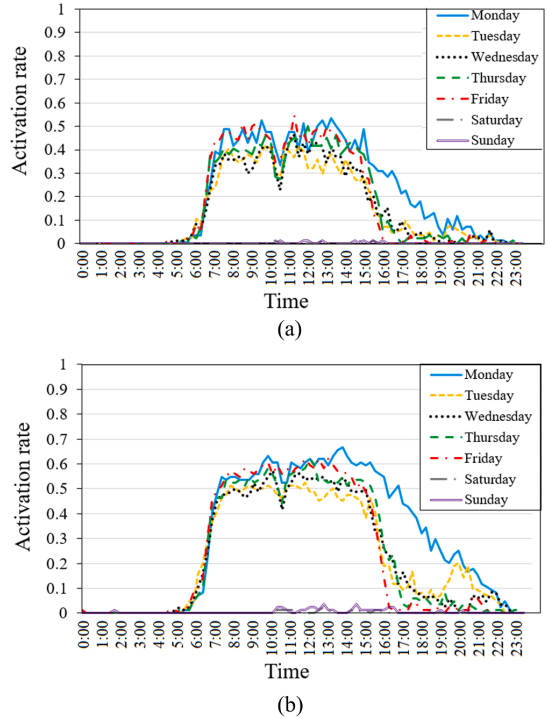


Fig. 3. Average (a) occupancy and (b) lighting patterns for weekdays and weekends.

that in order to implement the window to floor area ratio as a single parameter and place all the windows in the center of the walls, the window coordinates were calculated and adjusted by linking them to this ratio through the GS interface. This was important as the daylight and energy simulations were simultaneously performed in each iteration during the optimization.

The two control methods for the window opening and the six control methods for shading device are illustrated in detail in Fig. 4. It should be noted that both window opening and shading device control methods were controlled and operated automatically. In the window opening control method, the following principles were implemented:

- Condition (a): Indoor air temperature control method was used for the summer and winter operation. The summer operation control was based on indoor operative temperature. The winter operation was based on CO₂ and indoor operative temperature control methods.
- Condition (b): Indoor air temperature control method was combined with the direct solar radiation on the façade and wind velocity control for the summer operation.

It has to be stressed that the window opening in IDA-ICE was applied according to the CELVO model, which defined the window opening area in terms of height, width, and discharge coefficient of the window [60]. The corresponding equation is elaborated in the Appendix (Eq. (10)).

In the shading control methods, the control parameters and rules were implemented as follows:

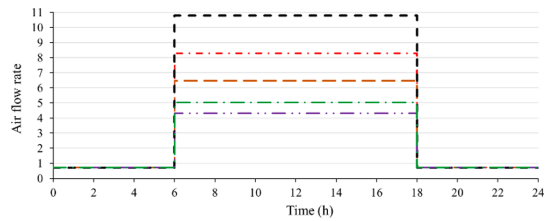
- Condition (c): Shading position control was suggested with respect to the indoor air temperature outside the working hours (zone not in use) and according to illuminance during the working hours (zone in

Table 6
Optimization parameters considered for the optimization process.

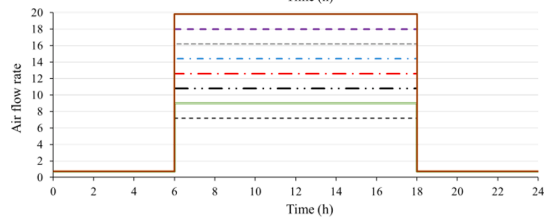
Parameter	Value	Description
<i>Glazing and building envelope</i>		
Window to floor area ratio	(10–24)	Interval: 2.8
Window type (U-value W/(m ² .K))	(2.4, 2.2, 2.0, 1.8, 1.6, 1.4, 1.2, 1.0, 0.8, 0.6)	2.4 based on TEK87 and 0.8 based on NS 3701
Roof type (U-value W/(m ² .K))	0.20 0.18 0.16 0.13 0.10 0.08 0.06	180 mm EPS S80 insulation 200 mm EPS S80 insulation 230 mm EPS S80 insulation 280 mm EPS S80 insulation 370 mm EPS S80 insulation 460 mm EPS S80 insulation 620 mm EPS S80 insulation
External wall type (U-value W/(m ² .K))	0.30 0.28 0.26 0.24 0.22 0.20 0.17 0.15 0.13 0.12 0.10	30 mm Mineral Wool insulation 63 mm Mineral Wool insulation 73 mm Mineral Wool insulation 83 mm Mineral Wool insulation 93 mm Mineral Wool insulation 118 mm Mineral Wool insulation 150 mm Mineral Wool insulation 170 mm Mineral Wool insulation 180 mm Mineral Wool insulation 230 mm Mineral Wool insulation 280 mm Mineral Wool insulation

HVAC parameters and setpoints

Profile of supply air temperature set points in AHU (°C)



Profile of supply water temperature setpoints from the central heating system (°C)



Supply/return water temperature to/from radiators (°C)

(45, 55, 65, 70)/(25, 30, 35, 40)
Sixteen combinations of supply/return temperatures are possible

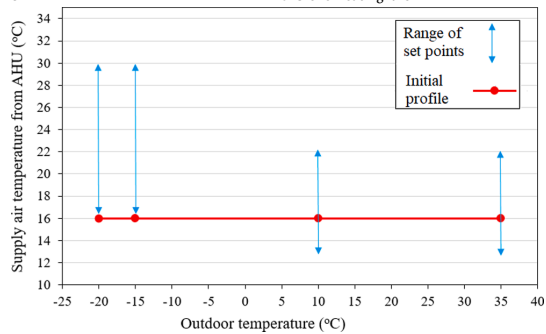
Heat exchanger efficiency in AHU

(0.55, 0.75, 0.85)

Overheating of zone hot water supply in the central heating system (°C)

- 1 Always off
- 2 5°C overheating 5–6 AM
- 3 9°C overheating 5–6 AM
- 4 5°C overheating 4–6 AM
- 5 9°C overheating 4–6 AM

Upper/lower limit of ventilation supply airflow rate during heating season (m³/(h.m²))



Upper/lower limit of ventilation supply airflow rate during cooling season (m³/(h.m²))

(continued on next page)

Table 6 (continued)

Parameter	Value	Description
<i>Shading device and window opening control methods</i>		
Window opening control alternatives	1	Never open
	2	Seasonal opening with temperature and CO ₂ control, in Fig. 4 (a)
	3	Opening with temperature and solar radiation control, in Fig. 4 (b)
<i>Shading device control alternatives</i>		
	1	Never drawn
	2	Daylight-Sun-Min energy, in Fig. 4 (c)
	3	Sun-Get heat, in Fig. 4 (d)
	4	Daylight-Get heat-Min cool, in Fig. 4 (e)
	5	Sun-Get heat-Preserve heat, in Fig. 4 (f)
	6	Daylight control, in Fig. 4 (g)
	7	Solar radiation control, in Fig. 4 (h)
<i>Other parameters</i>		
Lighting rate (W/m ²)	(7, 11, 30)	NA
Shading material type	1	Generic outside blind slat
	2	Marine venetian blind slat
	3	Celery venetian blind slat
	4	Opaque light-dark colored slat
	5	Pewter venetian blind slat
	6	Opaque white colored slat
	7	Mocha venetian blind slat
	8	Bisque venetian Blind slat
	9	White venetian Blind slat

use). It should be pointed out that Condition (c) was the only condition in which the shading slat angle was controlled according to illuminance and changed based on the solar azimuth angle. Otherwise, the slat angle was kept constant at 45° in other conditions. The aim was to minimize energy use and maximize comfort.

- Condition (d): Shading position control was based on the solar radiation measured on the exterior side of windows during the working hours and according to solar radiation and indoor air temperature outside the working hours. The aim was to avoid overheating during working hours and to gain heat outside the working hours.
- Condition (e): Shading position control was based on illuminance during the working hours and according to the indoor air temperature and the minimum solar radiation outside the working hours. The aim was to maximize comfort and minimize mechanical cooling.
- Condition (f): Shading position control was based on the solar radiation measured on the exterior side of windows during the working hours and according to the indoor air temperature and the minimum solar radiation outside the working hours. The aim was to avoid overheating during the working hours and preserve heat gain outside the occupancy hours.
- Conditions (g) and (h): Shading position control was based on illuminance and solar radiation on the exterior side of windows all day long, respectively.

It should be stated that all the algorithms were developed through detailed macros in IDA-ICE as shown in Fig. 4.

3.1.3. Daylight and energy simulation tools

The energy simulations of the optimization analyses were carried out by using the IDA-ICE dynamic simulation. The daylight simulations were performed in the Radiance tool, [61] which was already integrated with IDA-ICE software through the Daylight-tab in the software. In this regard, IDA-ICE employed the Radiance’s genBSDF program to assess the solar bidirectional properties of the complex fenestration system with controllable shading. Furthermore, the daylight factor index was used in the simulations with high precision, and the daylight was measured at desktop level. It should be clarified that both energy and daylight simulations in each iteration during optimization process were performed simultaneously in IDA-ICE.

3.2. Intermediate step

3.2.1. GS interface

In implementing the optimization process, an intermediate step was applied in order to arrange the results according to the thermal and visual comfort constraints. The process was done through the GS interface, which is an available option in IDA-ICE (see the central red part in Fig. 1). This module gives the possibility to manipulate the data in an illustrative way by inserting and connecting different components [62]. It should be mentioned that the GS module is executed by IDA modeler without running the IDA solver. In the present work, it was adopted to check the constraint functions during optimization process. If the results of daylight and thermal comfort simulations obtained from IDA to ICE did not satisfy the visual and thermal comfort constraints, the total

Table 7
Optimized input parameters, except HVAC setpoint at AHU and central heating system, for different optimized cases.

Parameters	Min W_PPD when W_DH ₂₆ < 50	Min E _{tot} when W_DH ₂₆ < 50	Max DF _{avg} when DF _{avg} > 2%	Min E _{tot} when DF _{avg} > 2%	Global optimal solution
Window to floor area ratio	14.18	14.57	24.00	14.96	14.96
Window (U-value, W/(m ² K))	1.0	0.6	0.6	0.6	0.6
Roof (U-value, W/(m ² K))	0.06	0.06	0.2	0.08	0.08
External wall (U-value, W/(m ² K))	0.1	0.1	0.3	0.1	0.1
Supply/return water temperature to/from radiators (°C)	65/30	70/40	65/35	70/30	70/30
Heat exchanger efficiency in AHU	0.85	0.85	0.85	0.85	0.85
Overheating of zone hot water supply in the central heating system (alternative number in Table 6)	2	2	1	5	5
Window opening control (alternative number in Table 6)	1	3	1	3	3
Shading device control (alternative number in Table 6)	2	5	7	7	7
Lighting rate (W/m ²)	7	7	7	7	7
Shading material type (alternative number in Table 6)	9	9	7	8	8

delivered energy, E_{tot}, would be multiplied by a large number. Therefore, the undesirable results were removed from the acceptable set of solutions as the objective was to minimize the total delivered energy to the building. In addition, this simple method could expedite the process of finding the optimized set of input parameters, selected by the GenOpt tool in each iteration.

3.2.2. Constraint functions implementation

For the purpose of this study, a single objective function, which was E_{tot}, along with two constraint functions for thermal comfort and one for visual comfort were considered for optimization. The constraint functions were DF_{avg}, considered as the visual comfort requirement, and W_DH₂₆ and W_PPD, selected as the thermal comfort criteria. The two latter were calculated as follows:

$$W_DH_{26} = \frac{\sum_{k=1}^N A_k \cdot DH_{26k}}{\sum_{k=1}^N A_k} < 50 \text{ hours} \tag{1}$$

$$W_PPD = \frac{\sum_{k=1}^N A_k \cdot PPD_{avg,k}}{\sum_{k=1}^N A_k} < 10\% \tag{2}$$

It should be emphasized that PPD in Eq. (1) was calculated as an average value for each thermal zone in IDA-ICE. Furthermore, the 50 h and 10% criteria in Eqs. (1) and (2) are considered based on the current

requirement for the Norwegian building code TEK17 [63] and the requirement for indoor air quality according to the comfort category II [64]. The criterion for average daylight factor was considered DF_{avg} > 2%, according to the Norwegian building code TEK17 [63] and it was calculated and averaged for the office cubicles. It should be noted that the technical requirements in the Norwegian building code TEK17 are similar as for the PH standard [5].

3.3. Optimization method and tool

In this stage, the optimization process was initiated in the GenOpt engine. Regarding the optimization specifications, in the present study, PSO algorithm was chosen from the GenOpt algorithm library to handle both continuous and discrete input parameters and benefit the global features of the PSO algorithm [45]. The details of parameters for the optimization algorithm are described in the Appendix (see Table 9). The optimization simulations were run on a 32 GB RAM of a Windows-based workstation (2.20 GHz) with Intel (R) Xeon (R) Gold 5120 CPU with 14 parallel cores and lasted for around 40 days to accomplish the whole optimization case.

3.4. Post-processing step

After finding the optimal solution, a ZEB analysis was performed. There are already several ZEB definitions. However, a common approach for all definitions is the annual balance between the weighted demand and the weighted supply [65,66] and it is generally done by integrating PV cells to the building façade and roof. The weighted demand and supply can be calculated in different ways; the export/import balance, load/generation balance, and monthly net balance, which is the combination of two other methods [66,67]. In the present work, the export/import balance method was selected and calculated as follows:

$$ZEB = |E_{p,exp}| - |E_{p,imp}| \approx 0 \tag{3}$$

$$E_{p,imp} = \sum_i E_{imp}(i) \times w(i) \tag{4}$$

$$E_{p,exp} = \sum_i E_{exp}(i) \times w(i) \tag{5}$$

where w is the weighting factors/metrics used in this paper as the primary energy factor and i refers to different type of energy carrier. It should be mentioned that the export/import balance in this study took into consideration the self-consumption of generated electricity, and afterwards created a balance between the need for exported and imported energy as follows:

$$\begin{cases} E_{exp} = \left| \sum_{m=1}^{12} (E_{el,use} + E_{el,prod.}) \right| & \text{if } \sum_{m=1}^{12} (E_{el,use} + E_{el,prod.}) < 0 \\ E_{exp} = 0 & \text{if } \sum_{m=1}^{12} (E_{el,use} + E_{el,prod.}) \geq 0 \end{cases} \tag{6}$$

$$\begin{cases} E_{self,use} = \left| \sum_{m=1}^{12} E_{el,prod} \right| & \text{if } \sum_{m=1}^{12} (E_{el,use} + E_{el,prod.}) > 0 \\ E_{self,use} = \sum_{m=1}^{12} E_{el,use} & \text{if } \sum_{m=1}^{12} (E_{el,use} + E_{el,prod.}) \leq 0 \end{cases} \tag{7}$$

$$E_{imp} = \sum_{m=1}^{12} E_{el,use} - E_{self,use} \tag{8}$$

where m is the number of months or hours for monthly or hourly calculations, respectively.

Finally, the mismatch factor or so called supply cover factor, was calculated as follows [68]:

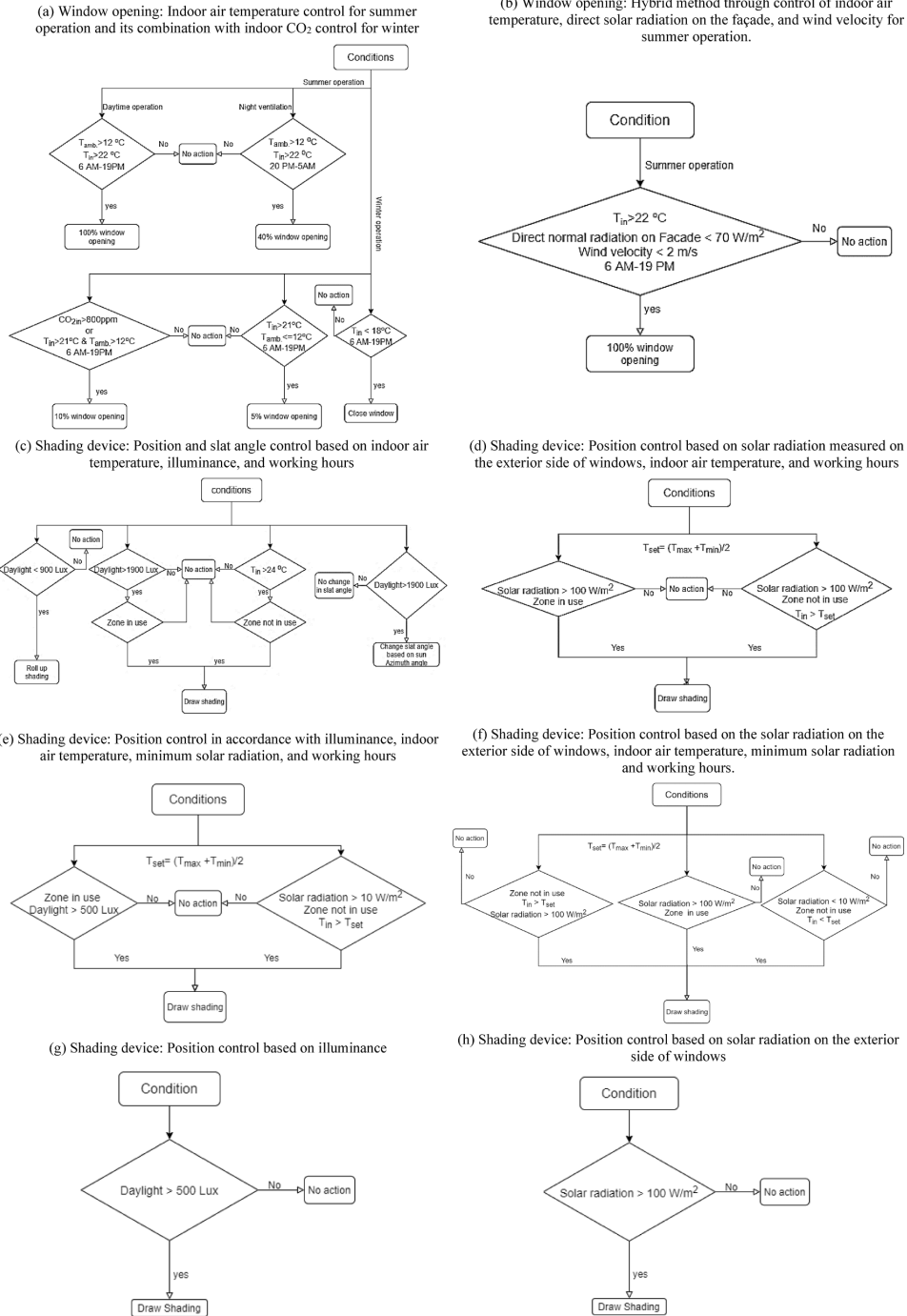


Fig. 4. Flow diagram of different control methods for automatic window opening and control of the shading device.

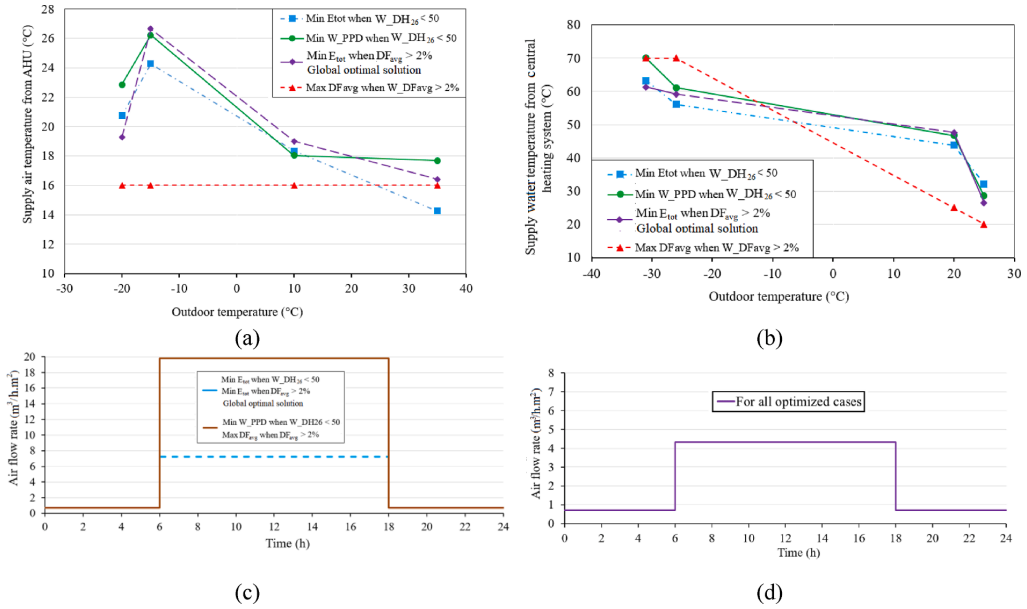


Fig. 5. Optimal (a) supply air temperature profile from AHU, (b) supply water temperature, (c) ventilation supply airflow rate during the cooling season, and (d) ventilation supply airflow rate during the heating season.

$$\gamma = \frac{\text{self-consumption of generated electricity}}{\text{on-site electricity generation}} = \frac{E_{self,use}}{\sum_{m=1}^{12} E_{el,prod.}} \quad (9)$$

In the above-mentioned equations, the absolute sign was used, because the produced energy was given a negative sign and the used energy was given a positive sign. For hourly calculations, the number of samples was changed to 8760 for the entire year. The PV module had an average efficiency of 18% for monocrystalline PV cells [69]. Furthermore, a tilt angle of 35°, the optimal PV tilt angle in Oslo climate, [70] module quality loss of 1.2%, and inverter operation loss of 8% were considered for the PV system, which gives a yearly average PR of 67% [70]. The weighting factor 2.3 [71] was also considered for imported and exported primary energy for ZEB balance calculations.

It is worth mentioning that an important point regarding the ZEB calculations in this study was to significantly take advantage of the self-consumption of generated electricity on-site. It is economically preferable to use the generated electricity directly in the building instead of exporting it to the grid. This is because the grid owner would only pay the electricity price (spot-price) plus a feed-in tariff, but not the grid-tariff, for the exported electricity. Therefore, the price of the sold electricity would only be about half the total price for the imported electricity.

4. Results

4.1. Optimization results

In the first part of this section, the optimization results are presented and analyzed considering thermal comfort and visual comfort constraint functions. Afterwards, the ZEB analysis was conducted for the optimal solution.

Table 7 shows the best set of input parameters after the optimization. Lighting performance and heat exchanger efficiency were always set to the lowest and the largest values for all the optimization scenarios, respectively. The reason was that the improvement of lighting system and heat exchanger efficiency decreased the building energy use with

trivial impact on the visual and thermal comfort conditions. Regarding the window to floor area ratio, the maximum possible value was chosen during optimization when the visual comfort was the matter of concern. However, a moderate value was selected for the minimum energy use and the maximum thermal comfort cases implying that this parameter was a conflicting factor for maximizing visual comfort and thermal comfort and minimizing energy use simultaneously. Among the U-values of building façade, external wall retrofitting with low U-value was prioritized for all the scenarios, except the case with the maximum visual comfort as this parameter did not have any impact on the daylight. The roof renovation to lowest U-value was the preference of the scenarios with thermal comfort satisfaction.

Regarding shading device and window opening, the control methods based on the temperature and solar radiation setpoints (Condition (b) and Condition (h) in Fig. 4) were the preferred options for the global optimal solution, while none of control methods for window opening was desirable in terms of providing the best thermal comfort conditions. It is also interesting to note that the simple control method (Condition (h) in Fig. 4) for shading device was selected in the majority of the optimization cases except the cases concerning discomfort hours inferring that a complicated control method did not necessarily ensure an indoor comfort condition. Overall, comparison of the window opening and the shading device control methods indicate that the solar radiation and the indoor temperature parameters were the most effective factors in controlling the dynamic shading device and the window opening. This was especially achieved when different setpoints were considered for the same parameter, for example solar radiation, for controlling the shading and window opening. The reason could be justified by the coincidence of solar shading and window opening activation. In fact, selecting the same parameters, but with different setpoints, for the control methods of shading device and window opening ascertained that the shading would not be drawn when the windows were open, and the best performance of both shading and window opening was achieved.

Fig. 5 shows the optimal supply air temperatures and supply airflow rate setpoints in the AHU and the supply water temperature from the central heating system. A different trend is observed in the Max DF_{avg}

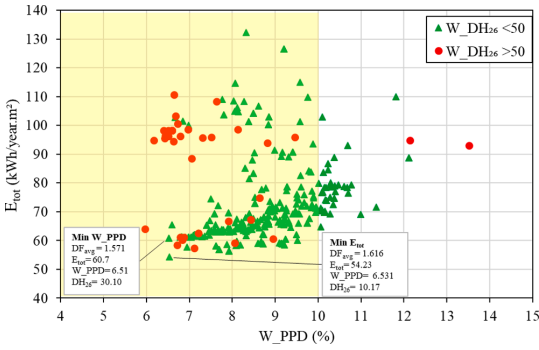


Fig. 6. Scatter plot of optimization solutions filtered only by thermal comfort constraint.

case because modifying the supply air temperature setpoints did not affect maximizing visual comfort (see Fig. 5(a) and (b)). However, for other cases in which minimizing the energy use and maximizing the

thermal comfort were the primary optimization objectives, a similar variation patterns of the supply air temperature from the AHU, and the supply water temperature from the central heating system were selected for various cases after the optimization of the reference building (Fig. 5 (a) and (b)).

Furthermore, the lowest air flow rate was chosen for the cases in which minimizing the building energy use was the primary goal, while the highest air flow rate was selected for visual and thermal comfort as the main objective during the cooling season, as shown in Fig. 5 (c). The same air flow rate, as the reference case, was chosen for all the cases in heating season, as shown in Fig. 5 (d). It implies that adjusting the supply air temperature in the AHU could both minimize the building energy use and satisfy the thermal comfort requirement for all the cases resulting in no change in the air flow rate pattern during the heating season.

Fig. 6 shows all the simulated cases after optimization when the thermal comfort was the only constraint. Most of the cases could satisfy both the thermal discomfort hours and the average PPD requirements. The minimum energy use when the thermal comfort was the only constraint was obtained around 54 kWh/(m².year) and the energy use for the case with the minimum W_PPD was achieved around 61 kWh/

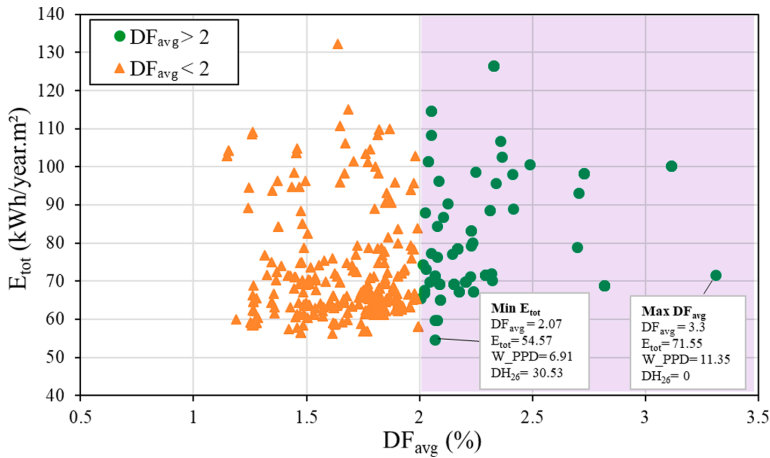


Fig. 7. Scatter plot of optimization solutions filtered only by visual comfort constraint.

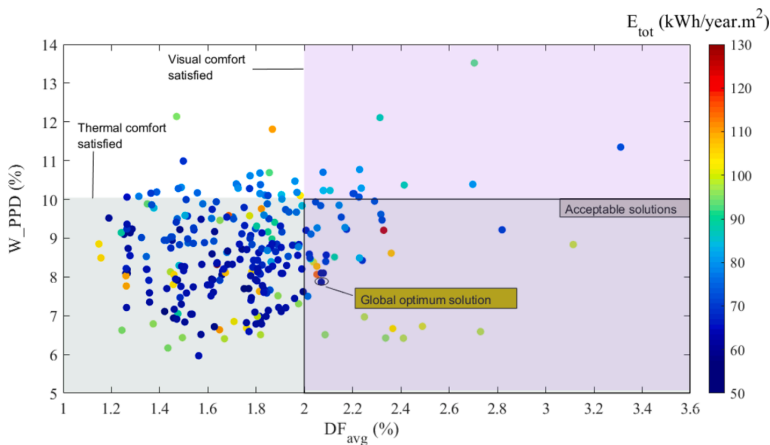


Fig. 8. W_PPD vs DF_{avg} for different values of E_{tot} objective function.

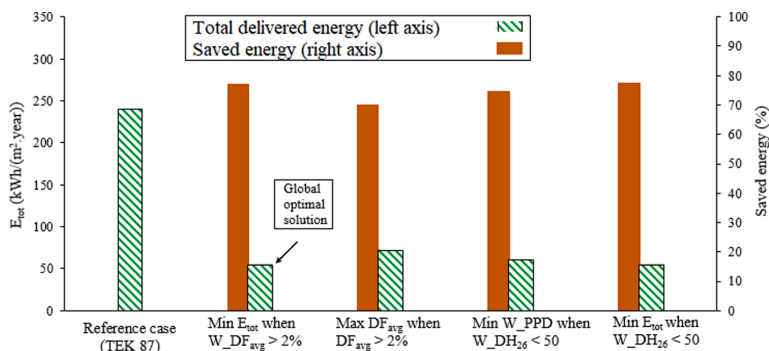


Fig. 9. Total delivered energy for different optimized scenarios.

(m².year). Comparing the optimized set of input variables for these two specific cases, see Table 6, may justify the results. The best quality of window (the lowest U-value) could not be used to reach the minimum average PPD due to increase of discomfort hours during the summer. In this respect, a slight decrease in the minimum average PPD in the Min W_{PPD} case resulted in a dramatic increase in the overheating hours, around 3 times, and the cooling energy use, around 1.2 times more than the Min E_{tot} case. This can support the importance of performing optimization to find an optimal solution in retrofitting studies.

Fig. 7 shows the scatter plot related to the energy use of all the optimized solutions considering only daylight factor constraint. Compared to the thermal comfort (see Fig. 6), fewer solutions could satisfy the daylight factor requirements implying that achieving visual comfort was more challenging than thermal comfort when retrofitting a building. It also indicates that the thermal comfort and visual comfort are two conflicting factors to reach low building energy use. For example, the selection of window to floor area ratio in different scenarios was the most important parameter on the daylight factor. This infers that a larger ratio was more desirable in terms of daylight factor (visual comfort condition) whereas smaller ratio was more favorable when the thermal comfort was the matter of concern. This in turn could affect the choice of other input parameters by the optimization engine in order to achieve the minimum building energy use. Fig. 7 also displays that, The minimum total energy use was obtained around 55 kWh/(m².year) when the results were only filtered by the visual comfort. Referring the optimized input parameters in Table 6, it infers that window to floor area ratio was the most sensitive parameter to be optimized so that a small increase to satisfy the visual comfort (Min E_{tot} when $DF_{avg} > 2\%$) led to the change in all other input parameters including shading device control methods to reach the minimum possible energy use. The consequence was, however, a significant increase in the discomfort hours (see Fig. 7).

Taking both visual and thermal comfort constraint functions into account, fewer solutions fell within the acceptable solution area (see Fig. 8). The global optimal solution was the same as the case with minimum energy use filtered by the average daylight factor (Min E_{tot} when $DF_{avg} > 2\%$). It is interesting to point out that the cases with a low W_{PPD} and high DF_{avg} values had a relatively high energy use (yellow and green points in the lower part in the acceptable solutions area). However, the solutions with less energy use fell within the thermal comfort satisfied area (dark blue points in the lower part in the thermal comfort satisfied area) emphasizing the difficulty of finding an optimal solution when considering both thermal and visual comfort filters. The reason was that a fewer number of parameters (mainly window to floor area ratio and partly glazing type) affected daylight factor than the thermal comfort.

The corresponding energy use for different optimized scenarios is presented in Fig. 9. Compared to the reference case, the total delivered

energy reduced dramatically after optimization, 77.4% for the case with the minimum E_{tot} filtered by discomfort hours (regardless visual comfort) and 77.2% for the global optimal solution. As a matter of fact, this considerable energy saving would be more limited if the cost effectiveness of retrofitting option was also taken into account. However, the proposed optimization process in this paper provides informative insights on the importance of various control methods of window opening, shading device, and HVAC setpoints adjustment in the improvement of building energy performance, which impose almost low investment cost during retrofitting process.

Fig. 10 shows the annual operative temperature variation in one of the worst zones, for example, C.O.16 cell office see Fig. 2, in terms of the indoor operative temperature fluctuation before and after the optimization and according to NS-EN 15251:2007 comfort categories for office buildings [64]. The three categories limits in Fig. 10 were implemented according to the standard for acceptable indoor operative temperature in office buildings equipped with a cooling system. In addition to a large energy saving after the optimization, see Fig. 9, the operative temperature was also improved during both winter and summer operation. In this regard, the number of hours met the comfort category II (recommended for office buildings) considerably increased after the optimization, up to 10 times more than the reference case. Comparing different cases show that the best operative temperature profile, in terms of number of hours met the comfort category II, occurred in the Min W_{PPD} (Case (c) in Fig. 10) with around 6,573 h. The consequence was a higher delivered energy and higher number of discomfort hours ($W_{DH_{26}}$), especially during September and October, than the Min E_{tot} , $DH_{26} < 50$ (case (b) in Fig. 10). Furthermore, referring to Table 7, it can be noted that a shading control method based on the combination control of solar radiation, daylight, and the indoor temperature setpoints led to the best performance in terms of satisfactory operative temperature.

4.2. Results of ZEB balance

Fig. 11 illustrates the process to reach ZEB balance through the imported and exported primary energy balance. Firstly, a large amount of energy saving, around 81%, in primary imported energy was achieved during optimization and the ZEB balance was then achieved by exporting electricity from onsite production.

Therefore, the required PV panel area to reach ZEB level was around 1,352 m² for the global optimal solution and around 5,960 m² for the reference case, if no optimization was performed. Furthermore, as the roof area was around 1,000 m², these optimized PV might be placed on the roof somehow. But, without optimization, it would be completely impossible or not feasible.

Fig. 12 shows the monthly variation of electricity portion in ZEB analysis in terms of export/production and import/consumption. The maximum electricity production for both the reference and the

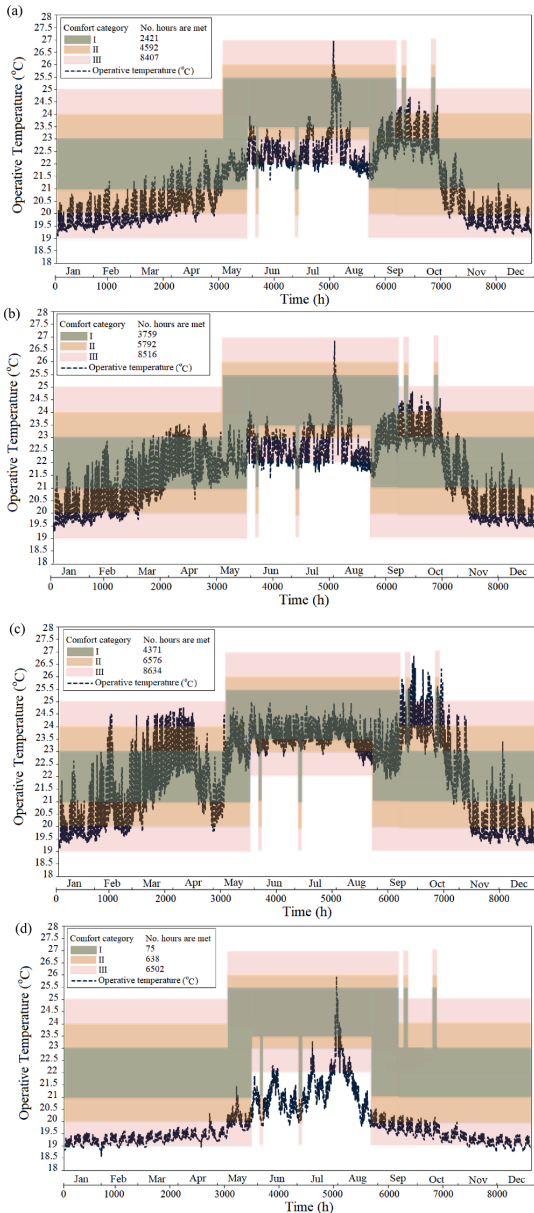


Fig. 10. Thermal comfort analysis in terms of operative temperature according to NS-EN 15251:2007 for (a) Min E_{tot} when $DF_{avg} > 2\%$, (b) Min E_{tot} when $DH_{26} < 50$, (c) Min W_{PPD} when $DH_{26} < 50$, and (d) reference cases for the C. O.16 cell office located in the third floor.

optimized cases was achieved during summer time, due to high solar radiation intensity. Consequently, a significant amount of electricity was imported during the winter, and a high portion of electricity was exported during the summer.

Additionally, there was still some amount of imported electricity even during summer, even though the electricity produced by PV was tried to be self-consumed as much as possible. It can be observed in Fig. 13 that the optimized case internally consumed nearly half of the

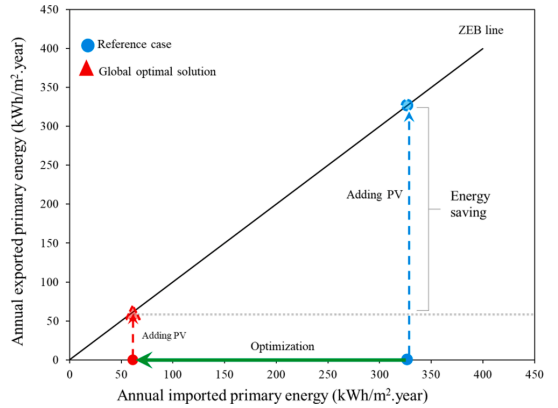


Fig. 11. ZEB analysis process in terms of exported and imported primary energy use.

generated electricity by PV panels. More precisely, considering the supply cover factor as defined in Eq. (9), 54% of the on-site produced electricity on a monthly basis, and 51% of that on an hourly basis, was self-consumed in the building.

An important point regarding ZEB balance is that it is economically preferable to use the generated electricity directly in the building (self-consumption) instead of exporting it to the grid. This is because the power company will only pay for the electricity price (Spot-price) plus a feed-in tariff, but not for the grid-tariff, for the exported electricity. Therefore, the price for the exported electricity will be only about the half price for the imported electricity.

5. Discussion

The findings in the result section pose some issues for discussion about the optimization process, both with respect to the adopted method and to the obtained results.

Employing IDA-ICE provided the possibility to implement all optimization input parameters, including the shading and window opening control methods, and the constraint and objective function through the parametric tab and GS interface in the software, which take advantage of a graphical user interface for applying functions and parameters. In addition, adopting the PSO algorithm, coupled with GS interface of the dynamic simulation IDA-ICE software, allowed decreasing the number of simulations by excluding those that did not meet the visual and thermal comfort constraint criteria. In this regard, all combinations of the 15 considered parameters, each of them with different alternatives, were in total 1.07×10^{18} cases. By using the optimization, such a vast number of simulation cases were dropped to only 1,900 cases, which were performed by IDA-ICE software. Nevertheless, since both energy and daylight simulations were run for each case with complicated window opening and shading control methods, the computational time increased remarkably.

With regard to the findings related to the energy savings due to the building retrofit measures, it is interesting to also discuss about the cost effectiveness of the building retrofit interventions. Since a substantial reduction of building energy use was achieved, compared to the reference building, through the optimization process, the operational cost would also decrease. This noticeable energy saving might not be reached if the cost effectiveness of retrofit measures was also taken into consideration, due to the investment costs of using extra systems and materials. However, we proposed a large group of retrofit measures, including various control methods of window opening, shading device, and HVAC setpoints adjustment, which could improve the building energy performance with almost low investment cost during retrofitting

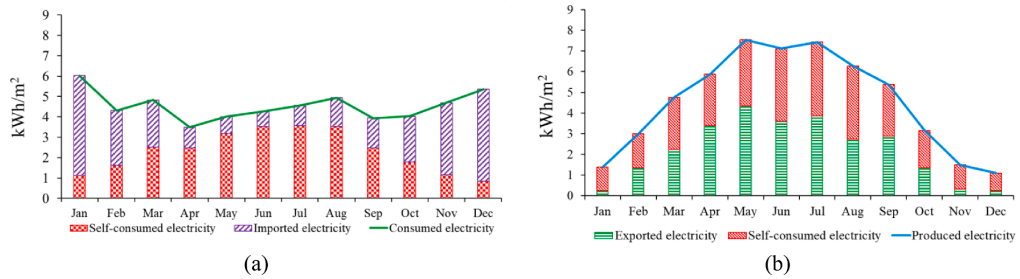


Fig. 12. Monthly variation of electricity portion in ZEB analysis in terms of (a) export/production and (b) import/consumption for the global optimal solution.

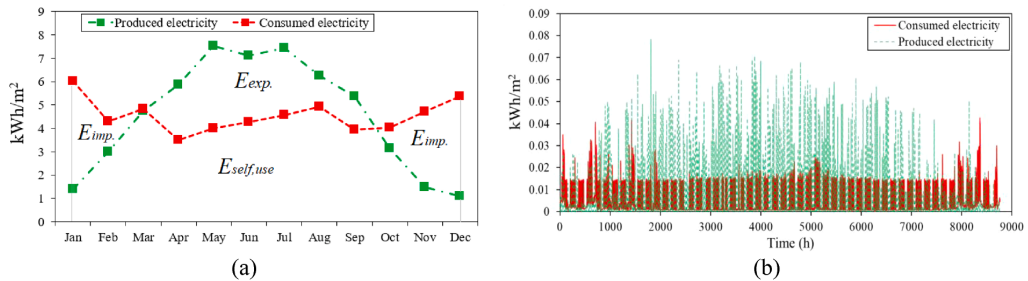


Fig. 13. (a) Monthly and (b) hourly production and consumption electricity with areas for ZEB balance.

process. This could imply that the reduction of operational cost due to enhancement of building energy performance might be dominant in the life cycle cost of the building retrofiting.

6. Conclusion

This paper focused on the retrofiting of building performance in terms of energy use and thermal comfort and visual comfort criteria. For this purpose, an inclusive optimization approach integrating building envelope, glazing parameters, HVAC setpoints, shading device, and window opening control methods was adopted. The shading and window opening control strategies were implemented using various control methods including the indoor air temperature, the CO₂ level, the daylight level, the wind velocity, and direct solar radiation on the façade. All these control methods were developed through the control macros in IDA-ICE, while the visual and thermal comfort constraints were implemented and linked to GenOpt (optimization tool) using Graphical Script interface in IDA-ICE. The main aim was to minimize the delivered energy to an office building, located in the Nordic climate, while meeting the thermal and visual comfort requirements at the same time. Afterwards, a ZEB analysis was performed by integrating PV panels in the building site for on-site production of electricity.

The findings showed that the building energy use for space heating and space cooling could be significantly reduced through optimization process, up to 77%, compared to the reference building case modelled in compliance with the Norwegian building regulation TEK87. Moreover, both visual and thermal comfort requirements, according to the Norwegian building regulation TEK17 and the standard NS-EN 15251:2007, were satisfied. In this regard, the optimal shading control method was based on solar radiation on the exterior side of the windows and the best performance regarding the window opening was attained when the control method was in accordance with indoor air temperature, direct solar radiation on the façade, and wind velocity setpoints, for the summer operation. Accordingly, the main factors in controlling shading devices and window opening were selected based on the indoor air temperature and the solar radiation parameters, but with different

setpoints for these optimization input variables. The optimal shading material was Bisque venetian Blind slat. The other input parameters obtained for the global optimal solution included the best quality of envelope, except for the roof, and the highest efficiency of heat exchanger in the AHU. It was followed by the adjustment of the ventilation supply air temperature and the flow rate in the AHU and the supply water temperatures from the central heating plant to the local radiators. However, the most challenging optimization design variable to select was the window to floor area ratio because it influenced the thermal and visual comfort in an opposite way. In other words, it was difficult to find an optimal ratio satisfying both thermal and visual comfort requirements because it would affect the selection of other design variables such as window opening and shading control methods, which had impact on the thermal comfort and building energy use. This could signify the role of optimization methods in feasible studies of building retrofiting with large number of design variables. Furthermore, the ZEB analysis revealed that for the optimal solution, the required PV panel area was around 1,352 m² and for the reference case it was around 5,960 m² if no retrofiting was performed.

Future work on the optimization process can investigate the improvement of building performance equipped with all-air system in terms of energy use and thermal and visual comfort criteria. Additionally, thermal comfort and visual comfort can be assessed in further detail through conducting daylight and CFD simulations as a post processing step. It is an interesting case to compare the spatial distribution of thermal and visual comfort indexes instead of only evaluating an average value of these parameters before and after optimization. It is specifically important that a dynamic visual comfort index such as daylight autonomy or useful daylight illuminance is applied, as using the average daylight factor is not an appropriate way to optimize the position of shading device.

Declaration of Competing Interest

Hereby, the authors confirm that the paper does not have any conflicts of interest and any financial and personal relationships with other

people or organizations.

Appendix

The window opening in IDA-ICE was modelled based on the following equation [60]:

$$A_{eff} = C_d \cdot W \cdot H \tag{10}$$

where the discharge coefficient, C_d , was selected as default value set to 0.65. It should be noted that the window opening percentage was associated with the effective opening area of the window in Eq. (10).

Table 8
Optical properties of various shading device materials.

Shading slat materials	Visible transmittance	Visible outside reflectance	Visible inside reflectance	Emissivity
Generic outside blind slat	0	0.35	0.35	0.9
Marine venetian blind slat	0	0.0725	0.0725	0.9
Celery venetian blind slat	0	0.331	0.331	0.9
Opaque light-dark colored slat	0	0.7	0.4	0.9
Pewter venetian blind slat	0	0.364	0.364	0.9
Opaque white colored slat	0	0.7	0.7	0.9
Mocha venetian blind slat	0	0.323	0.323	0.9
Bisque venetian blind slat	0	0.549	0.549	0.9
White venetian blind slat	0	0.743	0.743	0.9

Table 9
Algorithm parameters for the optimization process.

Algorithm type	Algorithm parameter	Value
PSO	Neighbourhood topology	Von Neumann
	Neighbourhood size	5
	Number of particles	10
	Seed	50
	Number of generations	20
	Cognitive acceleration	2.8
	Social acceleration	1.3
	Maximum velocity discrete	4
	Constriction gain	0.5

References

[1] I. Artola, K. Rademakers, R. Williams, J. Yearwood, Boosting building renovation: What potential and value for Europe, Study for the iTRE Committee, Commissioned by DG for Internal Policies Policy Department A (2016) 72.
 [2] Y. Saheb, A. Saussay, C. Johnson, A. Blyth, A. Mishra, T. Gueret, Modernising Building Energy Codes, (2013).
 [3] O.d.c.e.d.d. économiques, Transition to sustainable buildings: strategies and opportunities to 2050, OECD Publishing 2013.
 [4] DIRECTIVE (EU) 2018/844 of the European parliament and of the council of 30 May 2018 amending Directive 2010/31/EU on the energy performance of buildings and Directive 2012/27/EU on energy efficiency (Text with EEA relevance), Official Journal of the European Union, 2018.
 [5] Nord N. Building energy efficiency in cold climates. *Encyclopedia of Sustainable Technologies* 2017:149–57.

[6] Ferrara M, Filippi M, Sirombo E, Cravino V. A simulation-based optimization method for the integrative design of the building envelope. *Energy Proc* 2015;78: 2608–13.
 [7] Ferrara M, Sirombo E, Fabrizio E. Automated optimization for the integrated design process: the energy, thermal and visual comfort nexus. *Energy Build* 2018; 168:413–27.
 [8] Pasichnyi O, Levihn F, Shahroki H, Wallin J, Kordas O. Data-driven strategic planning of building energy retrofitting: the case of Stockholm. *J Cleaner Prod* 2019;233:546–60.
 [9] Fan C, Yan D, Xiao F, Li A, An J, Kang X. Advanced data analytics for enhancing building performances: from data-driven to big data-driven approaches. *Build Simul* 2020.
 [10] Hashempour N, Taberkhani R, Mahdikhani M. Energy performance optimization of existing buildings: a literature review. *Sustain Cities Soc* 2020;54.
 [11] Ascione F, Bianco N, Mauro GM, Vanoli GP. A new comprehensive framework for the multi-objective optimization of building energy design: Harlequin. *Appl Energy* 2019;241:331–61.
 [12] Grillone B, Danov S, Sumper A, Cipriano J, Mor G. A review of deterministic and data-driven methods to quantify energy efficiency savings and to predict retrofitting scenarios in buildings. *Renew Sustain Energy Rev* 2020;131:110027.
 [13] Ali U, Shamsi MH, Bohacek M, Hoare C, Purcell K, Mangina E, et al. A data-driven approach to optimize urban scale energy retrofit decisions for residential buildings. *Appl Energy* 2020;267:114861.
 [14] Lin Y-H, Lin M-D, Tsai K-T, Deng M-J, Ishii H. Multi-objective optimization design of green building envelopes and air conditioning systems for energy conservation and CO2 emission reduction. *Sustain Cities Society* 2021;64:102555.
 [15] Rosso F, Ciancio V, Dell’Omo J, Salata F. Multi-objective optimization of building retrofit in the Mediterranean climate by means of genetic algorithm application. *Energy Build* 2020;216.
 [16] Lu S, Li J, Lin B. Reliability analysis of an energy-based form optimization of office buildings under uncertainties in envelope and occupant parameters. *Energy Build* 2020;209.
 [17] Ascione F, Bianco N, Iovane T, Mauro GM, Napolitano DF, Ruggiano A, et al. A real industrial building: modeling, calibration and Pareto optimization of energy retrofit. *J Build Eng* 2020;29:101186.
 [18] Chang S, Castro-Lacouture D, Yamagata Y. Decision support for retrofitting building envelopes using multi-objective optimization under uncertainties. *J Build Eng* 2020;32:101413.
 [19] Li H, Wang S. Coordinated optimal design of zero/low energy buildings and their energy systems based on multi-stage design optimization. *Energy* 2019;189: 116202.
 [20] Si B, Wang J, Yao X, Shi X, Jin X, Zhou X. Multi-objective optimization design of a complex building based on an artificial neural network and performance evaluation of algorithms. *Adv Eng Inf* 2019;40:93–109.
 [21] Ascione F, Bianco N, Mauro GM, Napolitano DF. Retrofit of villas on Mediterranean coastlines: Pareto optimization with a view to energy-efficiency and cost-effectiveness. *Appl Energy* 2019;254:113705.
 [22] Ascione F, Bianco N, Mauro GM, Napolitano DF, Vanoli GP. Weather-data-based control of space heating operation via multi-objective optimization: application to Italian residential buildings. *Appl Therm Eng* 2019;163:114384.
 [23] Ilbeigi M, Ghomeishi M, Dehghanbanadaki A. Prediction and optimization of energy consumption in an office building using artificial neural network and a genetic algorithm. *Sustain Cities Soc* 2020;61:102325.
 [24] Bui D-K, Nguyen TN, Ghazlan A, Ngo N-T, Ngo TD. Enhancing building energy efficiency by adaptive façade: a computational optimization approach. *Appl Energy* 2020;265:114797.
 [25] Nasruddin Sholahudin, Satrio P, Mahlia TMI, Giannetti N, Saito K. Optimization of HVAC system energy consumption in a building using artificial neural network and multi-objective genetic algorithm. *Sustain Energy Technol Assess* 2019;35:48–57.
 [26] Guo R, Heiselberg P, Hu Y, Zhang C, Vasilevskis S. Optimization of night ventilation performance in office buildings in a cold climate. *Energy Build* 2020; 225:110319.
 [27] Lu Y, Wang S, Zhao Y, Yan C. Renewable energy system optimization of low/zero energy buildings using single-objective and multi-objective optimization methods. *Energy Build* 2015;89:61–75.
 [28] Wu R, Mavromatis G, Orehounig K, Carmeliet J. Multiobjective optimisation of energy systems and building envelope retrofit in a residential community. *Appl Energy* 2017;190:634–49.

- [29] Hirvonen J, Jokisalo J, Heljo J, Kosonen R. Towards the EU emissions targets of 2050: optimal energy renovation measures of Finnish apartment buildings. *Int J Sustain Energy* 2018;38(7):649–72.
- [30] Ferrara M, Rolfo A, Prunotto F, Fabrizio E. EDeSSOpt – Energy Demand and Supply Simultaneous Optimization for cost-optimized design: application to a multi-family building. *Appl Energy* 2019;236:1231–48.
- [31] Taveres-Cachat E, Lobaccaro G, Goia F, Chaudhary G. A methodology to improve the performance of PV integrated shading devices using multi-objective optimization. *Appl Energy* 2019;247:731–44.
- [32] Fang Y, Cho S. Design optimization of building geometry and fenestration for daylighting and energy performance. *Sol Energy* 2019;191:7–18.
- [33] P. Pilechiha, M. Mahdavinjad, F. Pour Rahimian, P. Carnemolla, S. Seyedzadeh, Multi-objective optimisation framework for designing office windows: quality of view, daylight and energy efficiency, *Applied Energy* 261 (2020).
- [34] Kirmat A, Krejcar O, Ekici B, Fatih Tasgetiren M. Multi-objective energy and daylight optimization of amorphous shading devices in buildings. *Sol Energy* 2019; 185:100–11.
- [35] Yi YK. Building facade multi-objective optimization for daylight and aesthetical perception. *Build Environ* 2019;156:178–90.
- [36] Naderi E, Sajadi B, Behabadi MA, Naderi E. Multi-objective simulation-based optimization of controlled blind specifications to reduce energy consumption, and thermal and visual discomfort: case studies in Iran. *Build Environ* 2020;169.
- [37] Magnier L, Haghghat F. Multiobjective optimization of building design using TRNSYS simulations, genetic algorithm, and Artificial Neural Network. *Build Environ* 2010;45(3):739–46.
- [38] Hong T, Kim J, Lee M. A multi-objective optimization model for determining the building design and occupant behaviors based on energy, economic, and environmental performance. *Energy* 2019;174:823–34.
- [39] Grygierek K, Ferdyn-Grygierek J. Multi-objective optimization of the envelope of building with natural ventilation. *Energies* 2018;11(6).
- [40] Niemelä T, Levy K, Kosonen R, Jokisalo J. Cost-optimal renovation solutions to maximize environmental performance, indoor thermal conditions and productivity of office buildings in cold climate. *Sustain Cities Soc* 2017;32:417–34.
- [41] Sghoui H, Mezrab A, Karkri M, Naji H. Shading devices optimization to enhance thermal comfort and energy performance of a residential building in Morocco. *J Build Eng* 2018;18:292–302.
- [42] Ascione F, Bianco N, Maria Mauro G, Napolitano DF. Building envelope design: Multi-objective optimization to minimize energy consumption, global cost and thermal discomfort. Application to different Italian climatic zones. *Energy* 2019; 174:359–74.
- [43] Ascione F, Bianco N, De Masi RF, Mauro GM, Vanoli GP. Energy retrofit of educational buildings: transient energy simulations, model calibration and multi-objective optimization towards nearly zero-energy performance. *Energy Build* 2017;144:303–19.
- [44] Tian ZC, Chen WQ, Tang P, Wang JG, Shi X. Building energy optimization tools and their applicability in architectural conceptual design stage. *Energy Procedia* 2015; 78:2572–7.
- [45] M. Wetter, GenOpt (R), generic optimization program, User Manual, Version 2.0. 0, (2003).
- [46] M. Palonen, M. Hamdy, A. Hasan, MOBO a new software for multi-objective building performance optimization, BS2013, France, 2013.
- [47] Y. Zhang, Use jEPlus as an efficient building design optimisation tool, CIBSE ASHRAE Technical Symposium, Imperial College, London UK 2012.
- [48] C. Christensen, R. Anderson, S. Horowitz, A. Courtney, J. Spencer, BEopt™ Software for Building Energy Optimization: Features and Capabilities, National Renewable Energy Lab. (NREL), Golden, CO (United States), United States, 2006.
- [49] Chantrelle FP, Lahmidi H, Keilholz W, Mankibi ME, Michel P. Development of a multicriteria tool for optimizing the renovation of buildings. *Appl Energy* 2011;88 (4):1386–94.
- [50] Schwartz Y, Raslan R, Mumovic D. Implementing multi objective genetic algorithm for life cycle carbon footprint and life cycle cost minimisation: a building refurbishment case study. *Energy* 2016;97:58–68.
- [51] Karaguzel OT, Zhang R, Lam KP. Coupling of whole-building energy simulation and multi-dimensional numerical optimization for minimizing the life cycle costs of office buildings. *Build Simul* 2013;7(2):111–21.
- [52] Delgarm N, Sajadi B, Delgarm S. Multi-objective optimization of building energy performance and indoor thermal comfort: a new method using artificial bee colony (ABC). *Energy Build* 2016;131:42–53.
- [53] Asadi E, da Silva MG, Antunes CH, Dias L. A multi-objective optimization model for building retrofit strategies using TRNSYS simulations, GenOpt and MATLAB. *Build Environ* 2012;56:370–8.
- [54] Arabzadeh V, Jokisalo J, Kosonen R. A cost-optimal solar thermal system for apartment buildings with district heating in a cold climate. *Int J Sustain Energy* 2018;38(2):141–62.
- [55] Statistics Norway, 2019, <https://www.ssb.no/en/bygg-bolig-og-eiendom/statistikker/bygningsmasse/aar>. (Accessed 2019).
- [56] Byggeforskrift- TEK 87, 1987.
- [57] NS 3031, 2014, Calculation of energy performance of buildings - Method and data, Standard Norge, p. 100.
- [58] Fang Y, Ding Y, Nord N. Data-driven analysis of occupancy and lighting patterns in office building in Norway. *REHVA J* 2019:64–9.
- [59] ANSI/ASHRAE/IESNA.2007, Standard 90.1e2007 normative Appendix B: building envelope climate criteria.
- [60] Bring A, Sahlin P, Vuolle M. Models for Building Indoor Climate and Energy Simulation. KTH, Stockholm, Sweden: Dept. of Building Sciences; 1999.
- [61] G. Ward, R. Shakespeare, Rendering with Radiance: the art and science of lighting visualization, (1998).
- [62] M. Rabani, H. Bayera Madessa, O. Mohseni, N. Nord, Minimizing delivered energy and life cycle cost using Graphical script: An office building retrofitting case, *Applied Energy* 268 (2020).
- [63] Building Technical Regulations (TEK17) 2017, with guidance (in Norwegian), § 13-4. Thermal indoor climate.
- [64] NS-EN 15251:2007- Indoor environmental input parameters for design and assessment of energy performance of buildings addressing indoor air quality, thermal environment, lighting and acoustics, Standard Norge, 2007.
- [65] Sartori I, Napolitano A, Voss K. Net zero energy buildings: a consistent definition framework. *Energy Build* 2012;48:220–32.
- [66] K. Voss, I. Sartori, R. Lollini, Nearly-zero, net zero and plus energy buildings, *REHVA Journal*, Dec (2012).
- [67] I. Sartori, S.V. Løtveit, K.S. Skeie, Guidelines on energy system analysis and cost optimality in early design of ZEB, 2018, p. 65.
- [68] Noris F, Musall E, Salom J, Berggren B, Jensen SO, Lindberg K, et al. Implications of weighting factors on technology preference in net zero energy buildings. *Energy Build* 2014;82:250–62.
- [69] Tiwari GN, Mishra RK, Solanki SC. Photovoltaic modules and their applications: a review on thermal modelling. *Appl Energy* 2011;88(7):2287–304.
- [70] Madessa HB. Performance analysis of roof-mounted photovoltaic systems – the case of a norwegian residential building. *Energy Proc* 2015;83:474–83.
- [71] NS-EN ISO 52000-1, Energy performance of buildings Overarching EPB assessment, Part 1: General framework and procedures, Standard Norge, 2017, p. 144.

Paper 3

M. Rabani, H. Bayera Madessa, N. Nord, Building retrofitting through coupling of building energy simulation-optimization tool with CFD and Daylight programs, *Energies* 14(8) (2021) 2180.

Article

Building Retrofitting through Coupling of Building Energy Simulation-Optimization Tool with CFD and Daylight Programs

Mehrdad Rabani ^{1,2,*}, Habtamu Bayera Madessa ¹ and Natasa Nord ² 

¹ Department of Civil Engineering and Energy Technology, Oslo Metropolitan University, 0130 Oslo, Norway; habama@oslomet.no

² Department of Energy and Process Engineering, Norwegian University of Science and Technology, 7491 Trondheim, Norway; natasa.nord@ntnu.no

* Correspondence: mehrab@oslomet.no

Abstract: Simultaneous satisfaction of both thermal and visual comfort in buildings may be a challenging task. Therefore, this paper suggests a comprehensive framework for the building energy optimization process integrating computational fluid dynamics (CFD) daylight simulations. A building energy simulation tool, IDA Indoor Climate and Energy (IDA-ICE), was coupled with three open-source tools including GenOpt, OpenFOAM, and Radiance. In the optimization phase, several design variables i.e., building envelope properties, fenestration parameters, and Heating, Ventilation and Air-Conditioning (HVAC) system set points, were selected to minimize the total building energy use and simultaneously improve thermal and visual comfort. Two different scenarios were investigated for retrofitting of a generic office building located in Oslo, Norway. In the first scenario a constant air volume (CAV) ventilation system with a local radiator in each zone was used, while an all-air system equipped with a demand control ventilation (DCV) was applied in the second scenario. Findings showed that, compared to the reference design, significant reduction of total building energy use, around 77% and 79% in the first and second scenarios, was achieved respectively, and thermal and visual comfort conditions were also improved considerably. However, the overall thermal and visual comfort satisfactions were higher when all-air system was applied.

Keywords: building retrofitting; building performance optimization; CFD; daylight analysis; thermal and visual comfort



Citation: Rabani, M.; Bayera Madessa, H.; Nord, N. Building Retrofitting through Coupling of Building Energy Simulation-Optimization Tool with CFD and Daylight Programs. *Energies* **2021**, *14*, 2180. <https://doi.org/10.3390/en14082180>

Academic Editor: Darya Nemova

Received: 18 March 2021

Accepted: 12 April 2021

Published: 14 April 2021

Publisher's Note: MDPI stays neutral with regard to jurisdictional claims in published maps and institutional affiliations.



Copyright: © 2021 by the authors. Licensee MDPI, Basel, Switzerland. This article is an open access article distributed under the terms and conditions of the Creative Commons Attribution (CC BY) license (<https://creativecommons.org/licenses/by/4.0/>).

1. Introduction

It is estimated that building stock accounts for approximately 28%, on a global scale [1], and 40%, in the European Union, of total energy use [2]. Therefore, retrofitting existing buildings is considered as a crucial step to reach energy goals and to thoroughly decarbonize the building stock in Europe by 2050 [3]. A tailored approach in this respect applies building performance optimization techniques by using optimization algorithms to find the best set of retrofit measures based on simulation results and proposed objectives [4]. Many researchers, designers, and engineers have used this well-developed technique to improve building energy efficiency due to its capability in automating design tasks in various aspects in the last decade. These aspects concern four main elements, namely, objective functions, design variables, simulation, and optimization tools. Regarding objective functions, various parameters dealing with energy, visual, and acoustic performance of buildings are selected. For example, Djuric et al. [5], Rabani et al. [6], Karaguzel et al. [7], Chantrelle et al. [8] and Ferrara et al. [9] conducted a single objective optimization and considered the retrofitting costs or the building energy use (the two latter studies) as the objective. Several studies such as those of Mangnier and Haghghat [10], Harkouss et al. [11], Asadi et al. [12], Niemelä et al. [13], Wu et al. [14], Hamdy et al. [15], and Palonen et al. [16]

conducted multi objective optimization to improve building performance. The objectives in the aforementioned studies dealt with building energy use, CO₂ emissions, investment and operational costs, and thermal comfort indexes such as predicted percentage dissatisfied (PPD), predicted mean vote (PMV), and discomfort hours. In some studies, such as [17], the optimization objective was the improvement of renewable technologies such as minimizing the dependency on the nearby energy grid and maximizing the self-consumption of photo-voltaic (PV) panels. In addition to these objectives, several studies such as those of Zhang et al. [18], Kiritat et al. [19], and Fang and Cho [20] focused mainly on daylight performance. In this regard, Naderi et al. [21] focused on the discomfort glare index (DGI) as the visual comfort indicator to be minimized. Some studies such as those of Bassuet et al. [22] and Saksela et al. [23] chose acoustic parameters as the objective function in the optimization process.

Most of the input design variables corresponded the building envelope and façade and service systems. For example, Chantrelle et al. [8], Grygierek and Ferdyn-Grygierek [24], Delgarm et al. [25], Schwartz et al. [26], and Harkouss et al. [11] optimized the window to wall ratio, façade U-values and thermal properties, roof topology, and glazing types. Djuric et al. [5], Mangnier and Haghghat [10], Delgarm et al. [27], Arabzadeh et al. [28], Bamdad et al. [29], and Lu et al. [30] focused on the set points for cooling and heating, supply air flow rates, solar collector and PV area and tilt angle, storage tank volume, the supply water temperature and the heat exchange area of the radiators as the input design variables. Operating strategies for heat storage and energy conversion techniques such as use of heat pump, solar panel, biomass, and oil boiler were optimized in the study by Wu et al. [14]. Furthermore, solar shading devices for windows were also optimized in terms of distance from glazing, movement point and rotation angle of panel, and the angle of louver blades [19,31,32]. Some research studies such as [33,34] introduced a holistic platform so that the energy conservation measures (ECMs) and input design variables were not constrained to those to be applied at building level, but also considered district level measures. These sets of measures included: (1) passive ECMs relying on the increase of envelope thermal resistance or the current windows replacement, and upgrades of the façade, floor, roof, and openings; (2) renewable retrofitting strategies based on the installation of sustainable energy sources such as: wind, sun, water, and geothermal; (3) active ECMs including the replacement of existing energy supply systems by new ones such as biomass boilers, natural gas Combined Heat Power (CHP) units, and heat pumps; and (4) control ECMs which are related practically to the selected active ECMs such as system scheduling, optimal start-up and shut-down, weather compensation, load following, and sequencing control.

Until now, various tools and software packages have been developed for the optimization of building performance. With respect to building energy simulation (BES), EnergyPlus [7,25–27], TRNSYS [8,11,12,30], and IDA-ICE [13,15,28,35] were widely applied. Moreover, Radiance software was employed for daylight simulations in several studies [18–20]. Regarding optimization tools, several algorithms, software systems, and platforms have been commonly integrated with building performance tools. For example, GenOpt [5–7,29], MOO [31,36], GAMS [37], jEPlus [25–27], Rhinoceros [38], MATLAB [15,39,40], non-dominated sorting genetic algorithm II (NSGA II) [13,28,35], and CPLEX algorithm [14,41] are among the widespread optimization tools and platforms. A recent study has shown that the integration of artificial neural networks such as Multilayer Feedforward Neural Networks (MFNN) with metaheuristic algorithms such as NSGA II and Multi-Objective Particle Swarm Optimization (MOPSO) can minimize the computation time [42].

Nevertheless, optimizing building energy performance using the aforementioned BES software still cannot ensure desirable indoor air conditions. The reason is that these software systems adopt a multi-zone approach to model the indoor airflow behavior in order to facilitate the implementation of simulation models and reduce the computational time [43]. In other words, each building zone in this approach is considered as a node with

uniform distribution of temperature, humidity, concentration, etc. [44,45]. As the air is assumed to be well mixed in the zone, this method may not be effective and can fail to accurately predict the air flow behavior when a ventilation strategy functioning with a high vertical gradient (stratified) of air flow distribution is applied. This is important when controlling Heating, Ventilation, and Air-Conditioning (HVAC) systems for simulating thermal comfort distribution in the occupancy area [46].

Unlike the multi-zone modelling approach, the computational fluid dynamics (CFD) method has shown great potential in predicting indoor air flow behavior [47]. In this method, the building zone is divided into a large number of control volumes and Navier-Stokes equations are solved in these control volumes to precisely predict the air flow characteristics in the space [48]. Therefore, coupling BES software with the CFD method can improve the quality of results and provide detailed information about the thermal load, building energy use, spatial air temperature and thermal comfort distributions. There are two methods of coupling BES and CFD, namely one-step and two-step coupling; the first method only provides CFD with the boundary conditions obtained by BES, while the latter also returns the simulated boundary conditions from CFD to BES. In this regard, several researchers have investigated the coupling of BES and CFD.

Novoselac [49] developed a new tool for accurate analysis of building energy use and thermal comfort. Different coupling methods for exchanging data between BES and CFD were evaluated through a two-step method. It was found that delivering heat flux to CFD as boundary conditions and giving surface temperature back to BES can provide more accurate calculation of surface heat flux than log-law wall functions in CFD. Tian et al. [50] made a comprehensive review of the methods and applications of integrating CFD with BES. They compared different one-step and two-step methods in terms of limitations, accuracy, stability, convergence, and speed for the co-simulation. Rodríguez-Vázquez et al. [51] reviewed the research studies in which BES–CFD coupling was used to investigate building systems, building components, and urban configurations of buildings. Their findings show that the integration of the BES and CFD methods provides an improvement that ranges between 10% and 50% for predicting building energy requirements. Furthermore, the analysis showed that the computation time for implementing the CFD method could be reduced by importing the information from the BES. Shan et al. [52] coupled EnergyPlus for BES with FLUENT software for CFD simulation of air temperature and PMV field. Furthermore, the air flow rates across the virtual partition walls between two adjacent subzones obtained from CFD were given to EnergyPlus for use as inter-zone air flow. The aim was to find the optimal temperature set points for the subzones in order to achieve a uniform occupant thermal comfort and avoid overcooling in a large open office. Pandey et al. [53] also coupled the EnergyPlus and Ansys Fluent tools for BES-CFD simulations of phase change material (PCM) in the built environment and compared the results with those obtained from EnergyPlus. Their findings highlighted that the coupled simulation has better prediction accuracy than the BES tool for active and passive use of PCM under forced convection. However, the BES tool is recommended for modeling the passive use of PCM during natural convection. Yamamoto et al. [54] developed a coupling two-step method combining BES and CFD. The aim was to assess the accuracy of coupling by analyzing the obtained temperature distribution in an environment where natural convection by floor heating is dominant. Colombo et al. [55] considered the application of coupling the thermal network, using IDA-ICE software, with an external CFD tool, using Star-CCM+ tool, for a double-skin glazed façade over a warm day cycle. In their iterative process, the surface temperatures obtained from the BES tool were used as boundary conditions for the CFD simulation and the heat fluxes to and from the façade components computed by CFD were used to improve the BES tool estimation. Zhang and Mirzaei [56] proposed a new framework to substantially reduce the computation cost of the dynamic coupling procedure of CFD and BES. In their approach, a high-resolution CFD model (CFD_f) provides the boundary conditions, including the flow patterns, to a low-resolution CFD model (CFD_c) at the

openings in the form of the mass flow information to BES, in order to start the iterative process. Afterwards, the CFD_c and BES domains implement a fully dynamic external coupling to deliver an accurate energy simulation.

The optimization of building energy performance, by integrating different optimization and BES tools, to achieve a nearly zero energy building (nZEB) level has been extensively investigated in the literature, but only a few studies have considered the coupling of optimization, BES tool, and CFD software. In this paper, an inclusive methodology is introduced to couple the BES software, IDA-ICE [57], to the optimization tool, GenOpt, and the CFD software, OpenFOAM [58] (integrated in IDA-ICE), in order to reach a nZEB level with satisfactory thermal and visual comfort conditions. In the optimization process, both energy and daylight simulations were implemented simultaneously. Furthermore, a detailed post-analysis of thermal and visual comfort was performed through detailed CFD and dynamic daylight simulations.

2. Methodology

Figure 1 shows the coupling of optimization and CFD simulation framework.

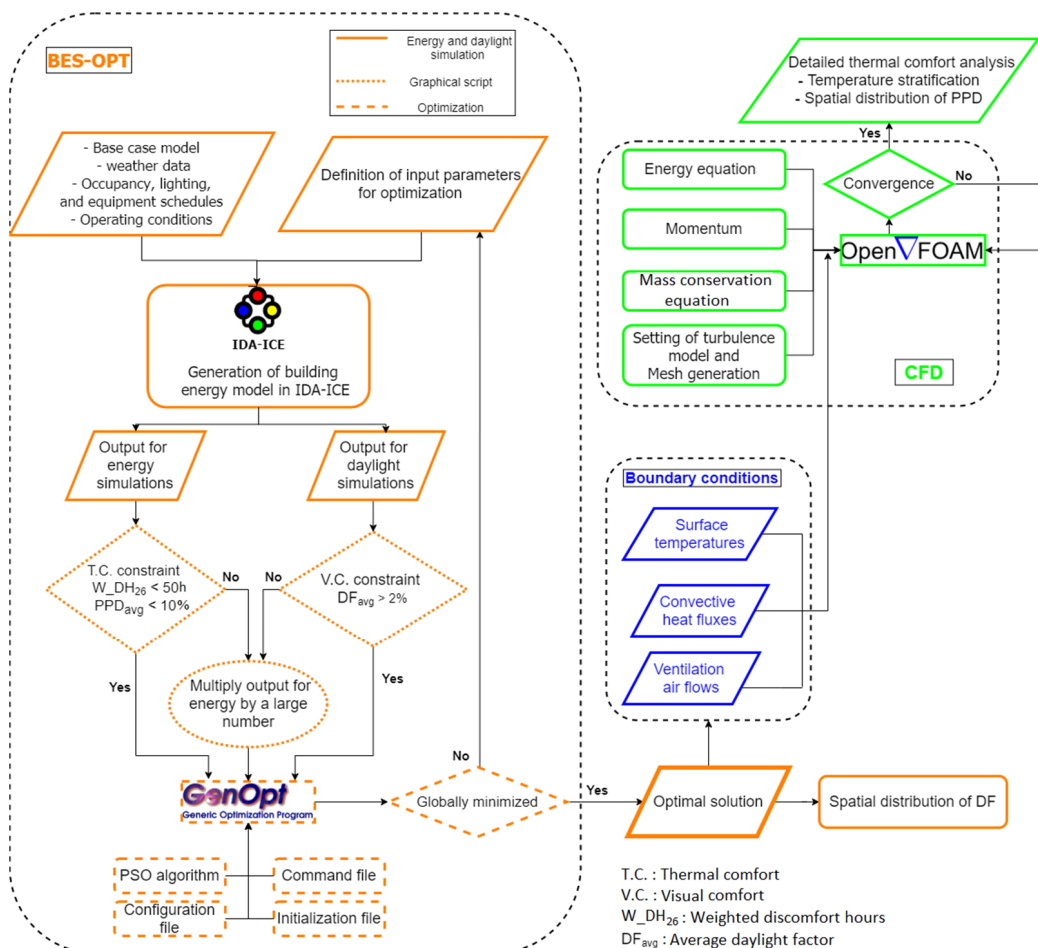


Figure 1. Building energy optimization, daylight, and computational fluid dynamics (CFD) framework.

In the first step, the reference building model was generated in IDA-ICE and the optimization input parameters for daylight and energy simulations were described in the building energy simulation-optimization process (BES-OPT). The obtained results from both simulation types were evaluated in terms of average daylight factor (DF_{avg}), discomfort hours (DH_{26}), and average predicted percentage of dissatisfied (PPD_{avg}) through Graphical Script (GS) interface in IDA-ICE. Afterwards, the simulation results were transferred to the optimization tool to iteratively assess the objective function until an optimal solution was reached. Finally, a post-processing step analyzed the optimal solutions in detail in terms of thermal comfort and daylight quality using the CFD and detailed daylight simulations.

2.1. BES-OPT Process

In this stage, the reference building energy model was first generated using IDA-ICE software (solid orange objects in Figure 1). This was a typical office building located in Norway. The total heated floor area of the building was selected at around 3000 m² as the majority of office buildings were constructed in the 1980s with a total heated floor area of between 2500 to 10,000 m² [59]. The building envelope properties, technical system specifications and set points were chosen for a general office building constructed in 1987 meeting the Norwegian building code TEK87 [60], as explained in our previous work [61].

The optimization process was implemented by coupling IDA-ICE software with a GS interface and GenOpt tool. GS interface is an available option in IDA-ICE (dotted orange objects in Figure 1) considered as an intermediate step to manipulate the outputs from IDA-ICE regarding the thermal and visual comfort constraints. Details of GS interface functions can be found in the work done by Rabani et al. [6].

Regarding optimization scenarios, two different cases were considered. In the first case, it was assumed that the space heating and ventilation systems remained as the same type as the reference building and in the second scenario, an all-air system was used instead. An all-air system means that the ventilation, space heating and cooling in different zones were performed using a demand control ventilation (DCV) system without applying any means of local heating or cooling units, e.g., a radiator, in the zones. Therefore, two different set of parameters were considered as the optimization input variables. However, the input parameters corresponding to glazing and building envelope, shading device and window opening control methods, and shading materials and lighting rates were common input variables for both scenarios. The common parameters were as follows:

- Window-to-floor ratio (%): the ratio of window-to-floor varied in the range of 10–24% with a 2.8% interval. To alter the size of all the windows with a correct coordinate at the same time as the ratio was changed, a coordinate calculator was developed through GS in IDA-ICE.
- Window U-values $W/(m^2 \cdot K)$: the values were changed from 0.6 (based on Norwegian building code TEK87) to 2.4 (based on Norwegian passive standard for non-residential buildings NS 3701) with an interval of 0.2 [62]. It should be noted that better window U-values are also associated with shifting from single glazed to triple glazed windows, which results in higher investment cost.
- Roof U-values $W/(m^2 \cdot K)$: the values were improved from U-value 0.2 to U-value 0.06 by adding an EPS S80 insulation layer increasing from a thickness of 180 mm to 620 mm, respectively.
- External wall U-values $W/(m^2 \cdot K)$: the values were improved by adding Mineral Wool insulation layer, from a thickness of 30 mm, corresponding to U-value 0.3, to 280 mm, corresponding to U-value 0.1.
- Window opening control method: three opening control methods included closed windows, seasonal opening with temperature and CO₂ control, and opening with temperature, wind velocity, and solar radiation control. Details of window opening control methods are elaborated in our previous work [61].

- Shading device control method: seven control methods were considered. The main parameters in these control methods were solar radiation, daylight level, and indoor operative temperature. The performance of these control methods was elaborated in our previous work. Details of shading control methods are also explained in our previous work [61].
- Heat exchanger efficiency in (air handling unit) AHU: three values 0.55, 0.75, and 0.85 were considered.
- Shading materials: Generic outside, Marine, Celery, Pewter, Mocha, Bisque, and White venetian blind slats as well as Opaque white colored and light-dark colored slats were selected for the slats of the integrated window shading [61].
- Lighting rate (W/m^2): three lighting rates 7, 11, and $30 W/m^2$ were selected.
- Supply air temperature profile in the AHU: the profile was considered as a function of outdoor temperature and was described at four points, shown in Table 1.

Table 1. Supply air temperature profile in the air handling unit (AHU) in both scenarios.

Point Number in the Profile	Range-Interval ($^{\circ}C$)	Corresponding Outdoor Temperature ($^{\circ}C$)
1st point	(16–30)-1.6	−20
2nd point	(16–30)-1.6	−15
3rd point	(13–22)-1.6	10
4th point	(13–22)-1.6	35

The parameters used only in the first optimization scenario (CAV) were the followings:

- Supply hot water temperature profile for radiators used for space heating: the profile was described in the same manner as the supply air temperature in AHU, shown in Table 2.

Table 2. Supply hot water temperature profile for space heating from central heating system in the first scenario.

Point Number in the Profile	Range-Interval ($^{\circ}C$)	Corresponding Outdoor Temperature ($^{\circ}C$)
1st point	(45–90)-1.6	−31
2nd point	(45–90)-1.6	−26
3rd point	(25–60)-1.6	20
4th point	(14–40)-1.6	25

- Supply/return water temperature to/from radiators: 16 combinations of four supply temperature set points 45, 55, 65, 70 ($^{\circ}C$) and return temperature set points 25, 30, 35, 40 ($^{\circ}C$).
- Upper/lower limit of ventilation supply airflow rate during heating and cooling seasons. Five profiles for heating season and eight profiles for cooling season, illustrated in Figure 2.

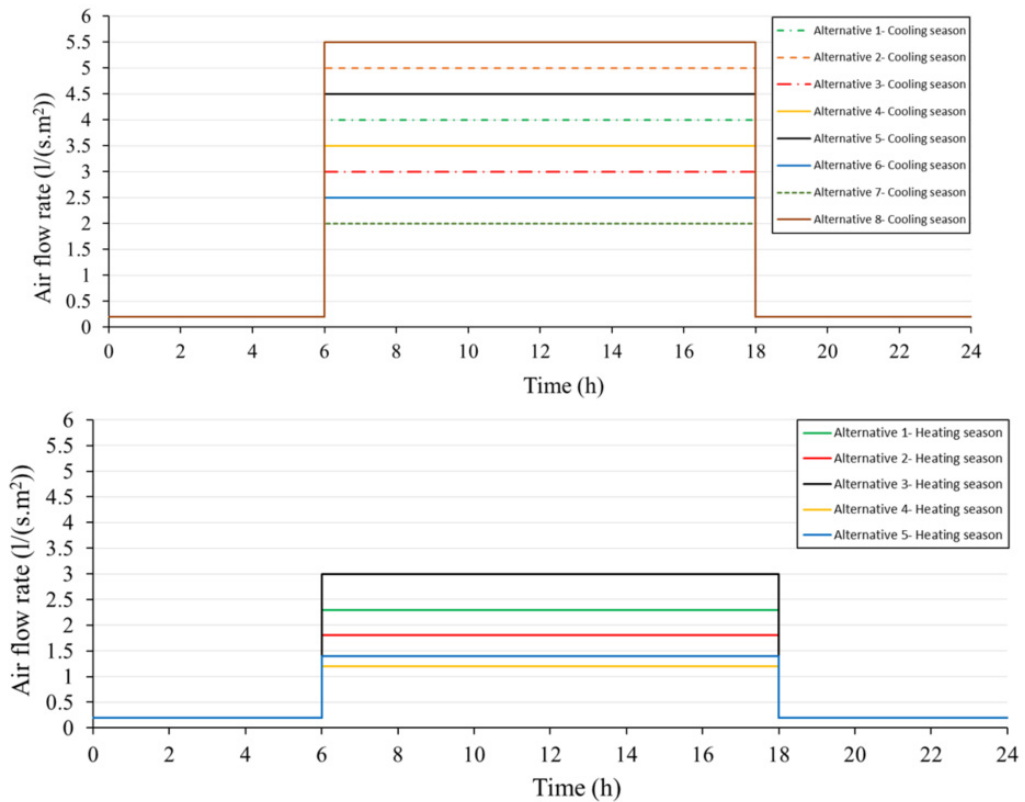


Figure 2. Ventilation air flow rates for cooling (top) and heating (bottom) seasons in the first optimization scenario.

The parameters used only in the second optimization scenario (all-air system) were as follows:

- Type of DCV system: four types of airflow control listed in Table 3.

Table 3. Various types of control method for DCV system in the second scenario.

System Type	Control Method
Variable air volume with humidity control	Maximum relative humidity set point: 60% for cooling season and 40% for heating season ¹ Minimum relative humidity set point: 20% for both cooling and heating seasons ¹
Variable air volume with CO ₂ control	Maximum CO ₂ set point: 1100 ppm Minimum CO ₂ set point: 700 ppm
Variable air volume with temperature control	Maximum temperature set point: 26 °C Minimum temperature set point: 19 °C
Variable air volume with temperature and CO ₂ control	Combination set points for CO ₂ and temperature

¹ There is no specific limit value for humidity of indoor air in Norway, only recommendations to prevent dampness and mold growth [63,64].

Maximum air flow rate set point: the air flow rate varied between 2 to 6 L/(s.m²) with interval 0.27 L/(s.m²).

The objective of the optimization process was to minimize the total delivered energy to the building (E_{tot}) meaning that the problem was a single objective optimization. The constraint parameters were visual comfort index, assessed using average daylight factor (DF_{avg}), and thermal comfort indexes, evaluated using weighted average PPD (W_PPD_{avg})

and weighted discomfort hours over 26 °C ($W_{DH_{26}}$) [61]. According to the current requirements for Norwegian building code TEK17 [65], the DF_{avg} was set greater than or equal to 2%. Regarding the thermal comfort, building comfort category II [66] was considered stating that $W_{PPD_{avg}}$ and $W_{DH_{26}}$ should be less than 10% and 50 h, respectively.

In the present study, the optimization Particle Swarm Optimization (PSO) algorithm was selected in GenOpt to deal with both continuous and discrete input parameters and benefit from the global features of the PSO algorithm [61,67]. Furthermore, both energy and daylight simulations were simultaneously carried out in IDA-ICE on 32 GB RAM of a Windows-based workstation (2.20 GHz) with Intel (R) Xeon (R) Gold 5120 CPU with 14 parallel cores, and lasted for around 40 days to finish each optimization case. Combinations of the input parameters were in total 1.07×10^{18} cases. By using the optimization, a large number of simulation cases were reduced to only 1900 cases, using IDA-ICE software. Nevertheless, since both energy and daylight simulations were run for each case with complicated window opening and shading control methods, the computational time increased considerably.

2.2. Boundary Conditions and CFD Process

After finding the optimal solution, as the first step detailed CFD and daylight simulations were performed for optimal solutions to investigate thermal and visual comfort in further detail. The CFD simulations were done in IDA-ICE by interfacing with the OpenFOAM CFD engine, and the daylight simulations were performed through the Radiance program [68]. However, calculation setup and execution were performed in IDA-ICE for both CFD and daylight simulations.

Regarding the CFD process, the one-way approach was considered. Firstly, coupling of BES and CFD was validated by the available experimental data and our previous numerical study for a single office building [69,70], in which we used Star-CCM+ software for performing CFD simulations [69]. Afterwards, the coupling method was applied to the optimal solutions, as illustrated in Figure 1 (blue and green objects). In the coupling process, the required boundary conditions for CFD simulations including surface temperature, surface convective heat flux, and ventilation air flows were exported from the IDA-ICE to the OpenFOAM CFD engine. These boundary conditions were then used by the CFD program to solve the continuity, momentum, and energy equations. Moreover, for the CFD simulations, the steady state solver with the RNG $k-\epsilon$ turbulence model were selected, as this model has been used extensively in the simulation of indoor air flow problems [71]. In accordance with the modelled geometry, a hexahedral mesh model was generated and executed in the CFD interface in IDA-ICE. Furthermore, a mesh refinement was applied to the boundary layers near the surfaces. The obtained indoor air velocity and air temperature results from the CFD simulations were then exported to the MATLAB program for PPD calculation.

Figure 3 shows a real office cubicle fitted with measuring devices and its corresponding 3DModel modelled in IDA-ICE, used for the validation study. The office was equipped with an active supply diffuser located on the ceiling for both space heating and ventilation purposes. The details of experimental conditions including room dimensions, location of supply and exhaust terminals on the ceiling, and supply air temperature and flow rate were reported in [69,70].

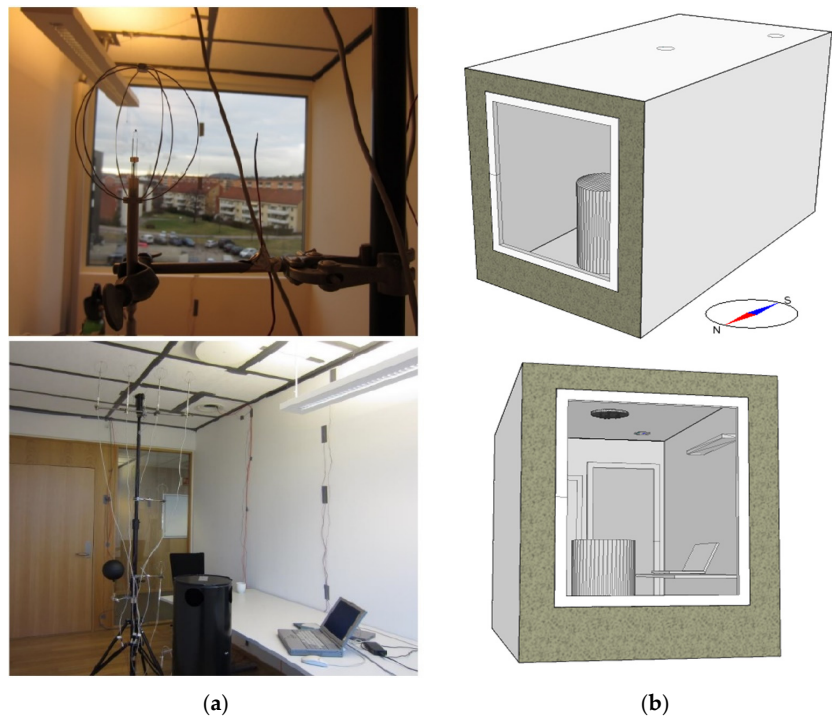


Figure 3. (a) Experimental setup [70] and (b) modelled configuration of the office cubicle in IDA-ICE.

2.3. Daylight Analysis

To obtain an overview of visual comfort throughout the year, three dynamic daylight indexes including Useful Daylight Illuminance (UDI), continuous Daylight Autonomy (cDA), and spatial Daylight Autonomy (sDA) were calculated (see Appendix A for details) and visualized for two optimization scenarios and the reference case. UDI describes how many hours or the percentage of the occupancy hours in which daylight levels are within the desired interval [72]. In this study, 100 lux and 2000 lux were selected as the minimum and maximum limits, respectively. cDA represents the percentage of the workhours when the illuminance is over or under a predefined threshold. In the present study, the percentage of daytime hours over 300 lux with partial credit was considered [73]. Furthermore, sDA shows the percentage of the occupied hours when the illuminance is equal or greater than 300 lux [74].

The daylight simulations were carried out through the Daylight-tab in IDA-ICE that uses backward raytracing and Radiance as a simulation engine. In this regard, a climate-based sky model with high precision was used in the Radiance software and a MATLAB script was used for visualizing the dynamic daylight indexes.

3. Results and Discussion

In this section, the results obtained from BES-OPT are presented for both scenarios. Afterwards, a detailed analysis of CFD and daylight simulations for the optimal solutions are described.

3.1. BES-OPT Analysis

Figure 4 shows the scatter plot of optimized results filtered by both thermal and visual comfort constraints. The triangles show the simulation cases where the discomfort hours were larger than 50 and the circles show those cases with discomfort hours smaller than 50. Furthermore, the dark symbols (both triangles and circles) represent the

simulation cases with low total delivered energy to the building (E_{tot}) while those with higher E_{tot} are demonstrated with lighter colors. Comparing the first (Figure 4a) and the second (Figure 4b) scenarios shows that satisfying thermal comfort requirements was more difficult in the second scenario than in the first scenario during the optimization process, which can be observed by the larger number of triangles and larger range of W_PPD_{avg} in the second scenario. The reason could be the more complicated control method of space heating and the ventilation system in the second scenario as they both functioned with a supply air terminal in an all-air system. Therefore, it was more challenging to find a combination of set points for the ventilation system to minimize building energy use and achieve thermal comfort concurrently in the second scenario. On the contrary, the daylight factor requirement was satisfied for more cases in the second than in the first scenario which could be due to the shading control method and higher window-to-floor ratio in the second scenario.

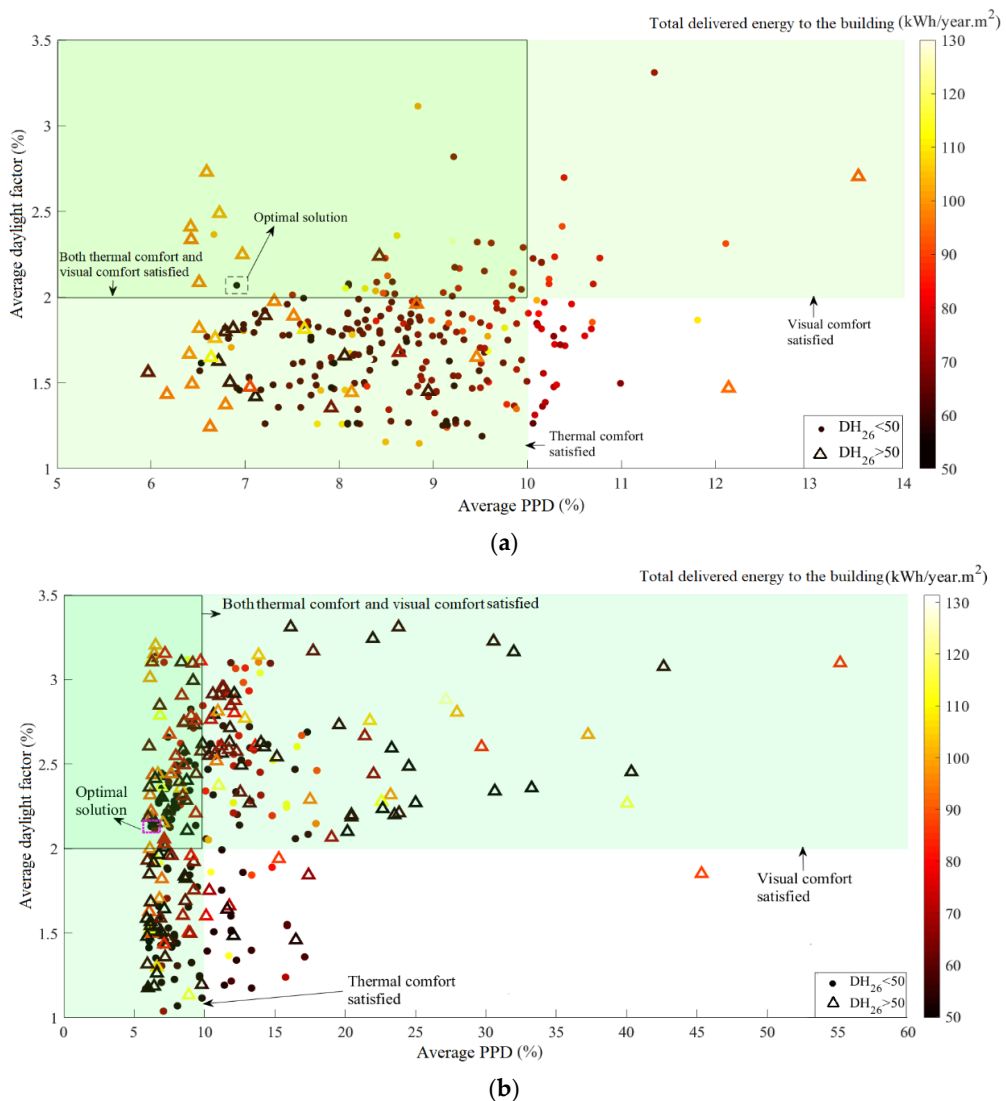


Figure 4. Optimization results for the first scenario (a) and the second scenario (b).

The optimized input parameters for both scenarios are shown in Table 4. Different window-to-floor ratio, U-value of building envelope, and shading control methods were required to satisfy both thermal and visual comfort in both scenarios. As was also observed in Figure 4, satisfying thermal comfort, especially DH_{26} , was more difficult in the second scenario than in the first. Thus, the best quality of window and external wall could not be selected in the second scenario as a tighter building envelope would result in larger DH_{26} and consequently reduce thermal comfort. The best performance and efficiency of the lighting system and heat exchanger were selected for both scenarios, as enhancing their efficiency could decrease the building’s energy use with trivial impact on the visual and thermal comfort conditions.

The percentile distribution of delivered energy use to the building, filtered by either and then both thermal and visual comfort conditions, is shown in Figure 5 for all solutions. Adopting an all-air system in the second scenario could result in overall less energy use compared to the CAV system. In this regard, around 75% of the simulated cases had less energy use in the second scenario than the 50% in the first scenario. However, in both scenarios, the cases filtered only by thermal comfort could arrive at less energy use with less distribution than by visual comfort, implying that achieving low-level building energy use with thermal comfort is easier than with visual comfort. The reason is that the number of input parameters influencing visual comfort were fewer than for thermal comfort.

Table 4. Optimized input parameters for both scenarios.

Parameters	First Scenario	Second Scenario
Common parameters		
Window-to-floor ratio	14.96	17.72
Window (U-value)	0.6	0.8
Roof (U-value)	0.08	0.06
External wall (U-value)	0.1	0.12
Heat exchanger efficiency in air handling unit (AHU)	0.85	0.85
Window opening control method	By indoor temperature, solar radiation, and wind velocity	
Shading device control method	By solar radiation	By daylight and indoor temperature
Lighting rate (W/m^2)	7	7
Shading material type	Bisque venetian Blind slat	Celery venetian blind slat

Supply air temperature profile in the AHU

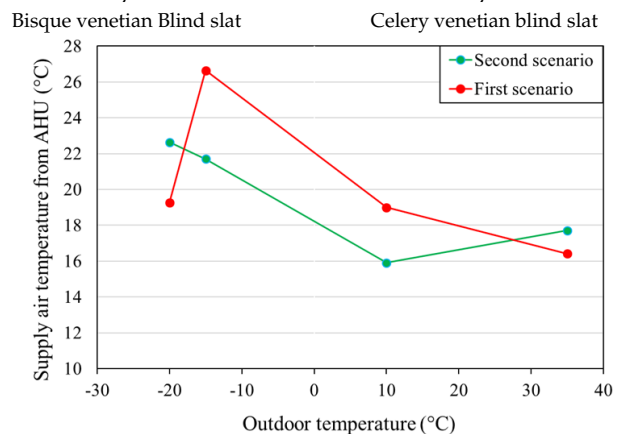


Table 4. Cont.

Parameters	First Scenario	Second Scenario
	Only in the first scenario	
Upper/lower limit of ventilation supply airflow rate during heating and cooling seasons (l/(s.m ²))		
Supply hot water temperature profile for space heating from central heating system		
Supply/return water temperature to/from radiators (°C)	70/30	
	Only in the second scenario	
Type of demand control ventilation (DCV) system	Variable air volume with temperature control	
Maximum air flow rate set point (l/s.m ²)	3.39	

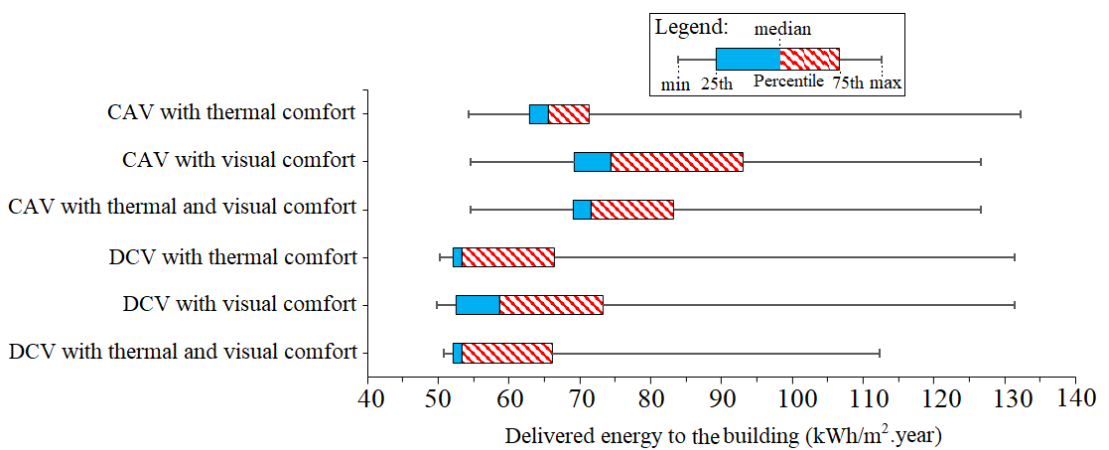


Figure 5. Percentile distribution of annual delivered energy to the building.

Figure 6 shows the amount of delivered energy to the building for the reference case and two optimization scenarios. Optimizing the building performance could reduce building energy use by up to approximately 77% and 79% in the first and second scenarios, respectively, while satisfying both thermal and visual comfort. The reasons were better building envelope quality, appropriate window-to-floor ratio, and proper control methods for shading device and window opening that were selected through the optimization process in both scenarios. Less energy use in the second scenario than in the first could mainly be due to the type of ventilation in the all-air system, for which the DCV method could adjust the air flow rate according to the considered control parameters for indoor conditions (see Table 3). However, the CAV ventilation method in the first scenario maintained a constant air flow rate during working hours, disregarding indoor conditions. This proves that an all-air system can be considered as a potential HVAC system in cold climate countries as it can reduce the investment and maintenance costs associated with local space heating and cooling systems.

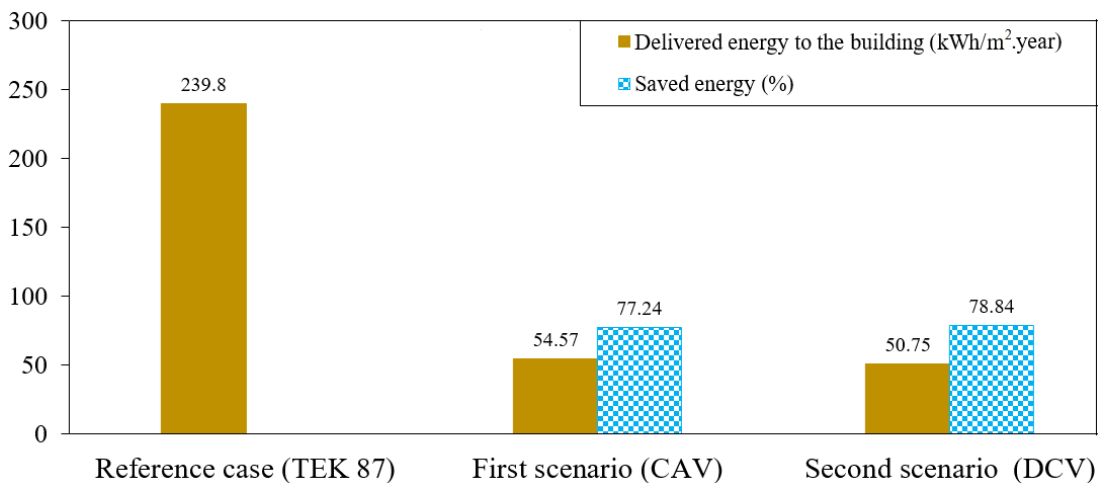


Figure 6. Delivered energy to the building for two optimization scenarios.

3.2. CFD and Daylight Assessment

Figure 7 shows the variation of indoor air temperature and air velocity along the measurement line in the vertical plane defined in the experimental work [70]. As can be seen, both temperature and velocity variations obtained in the present study were in good agreement with our previous numerical study and were also within the uncertainty range of the experimental data. The RNG $k-\epsilon$ turbulence model, used in this study, and the Standard $K-\epsilon$ model, used in our previous numerical study [69], indicated almost the same trend and followed the experimental data with good agreement, except in the proximity of the ceiling (Figure 7a). However, the RNG $k-\epsilon$ turbulence model could predict air velocity better than the Standard $K-\epsilon$ model near the floor, and followed the experimental data less well than Standard $K-\epsilon$ at the middle height of the room (Figure 7b).

Figures 8 and 9 show, respectively, the annual variation of average PPD and spatial distribution of PPD for the worst zone, in terms of difficulty in meeting comfort conditions, for the reference case and two optimization scenarios. More precisely, the worst zone in this study was defined as the zone in the building experiencing the highest operative temperature in summer and largest temperature fluctuations throughout the year. The coldest day was 2nd January ($T_{\text{outdoor}} = -19\text{ }^{\circ}\text{C}$), and the warmest day was 1st August ($T_{\text{outdoor}} = 31\text{ }^{\circ}\text{C}$), selected based on climate data for outdoor air temperature. Looking at the annual average variation of PPD, it is found that both optimized scenarios could satisfy the thermal comfort requirements, based on the comfort category II, for a longer period of

the year compared to the reference case. The second optimized scenario showed the best performance in this respect. However, the all-air system (second optimized scenario) could not provide comfortable conditions, according to any of the thermal comfort categories, in January and December. This can also be observed in the spatial distribution of PPD on the coldest day, when a rather high degree of discomfort was experienced in the occupancy area (the black rectangle) in the second scenario (Figure 9c). On the warmest day, both optimized scenarios showed an acceptable performance in the occupancy area in spite of window opening. Although two optimized scenarios could not provide as acceptable thermal comfort conditions as the reference case on the coldest and warmest days, the annual thermal comfort was, in general, improved for both optimized scenarios. It should be pointed out that the improvement of thermal comfort was achieved along with the reduction of delivered energy to the building by more than 77%.

To examine the uniformity of air temperature distribution and the possibility of temperature stratification, the distribution of vertical air temperature difference for CFD cells between the ankle level (0.1 m above the floor) and the head level (1.1 m for a seated person), in the occupancy area, is shown in Figure 10. The occupancy area was defined as the area 0.6 m from the side walls and from 0.1 m to 1.8 m above the floor. On the coldest day of the year (Figure 10), the majority of points met the requirements for vertical air temperature difference, which is less than 3 K according to the second thermal comfort category for office buildings [75]; however, a slight temperature stratification was observed covering around 50% of the occupancy area at the second scenario on the morning of the coldest day of the year. This could be due to considering yearly average PPD as the thermal comfort constraint during optimization. In addition, with respect to Figures 8c, 9c and 10, it can be implied that a different control method for the DCV system should be adopted in the coldest periods of the year. Nevertheless, the window opening was functional for both optimized scenarios during summertime and no significant temperature stratification was observed, despite using a rather low air flow rate compared to the reference case.

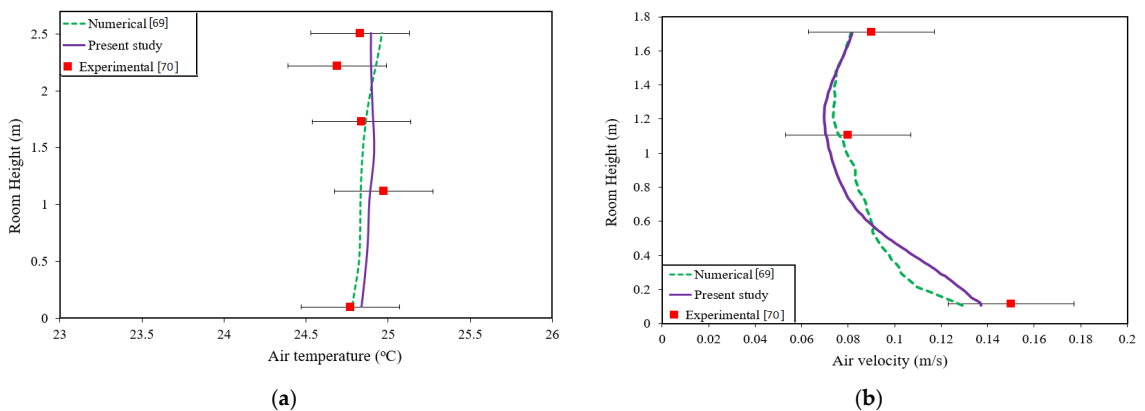


Figure 7. Variation of (a) air temperature and (b) air velocity in the validation study.

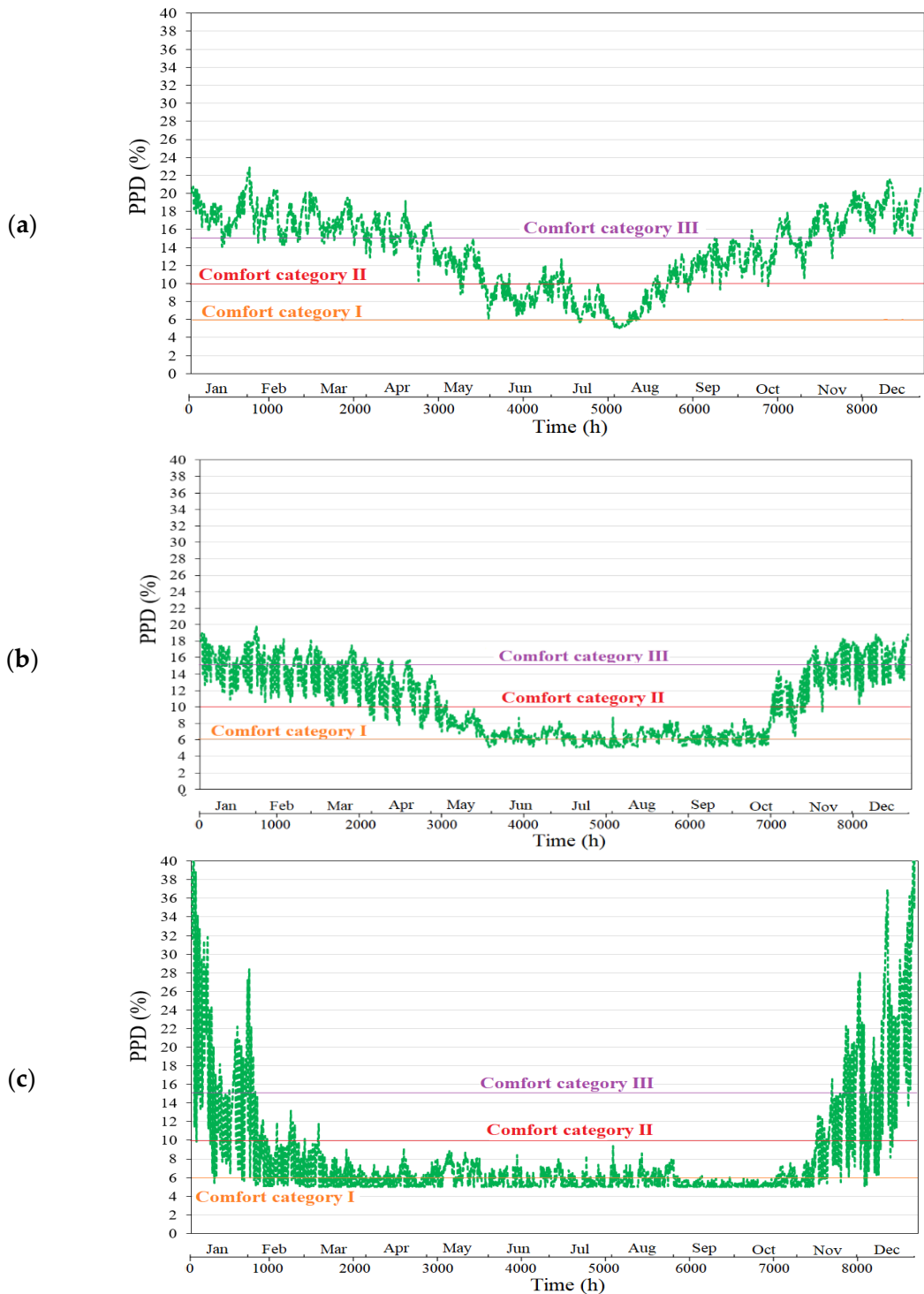


Figure 8. Annual variation of average predicted percentage dissatisfied (PPD) for the cell office C.O.16 for the (a) reference case, (b) first optimized scenario (c) second optimized scenario.

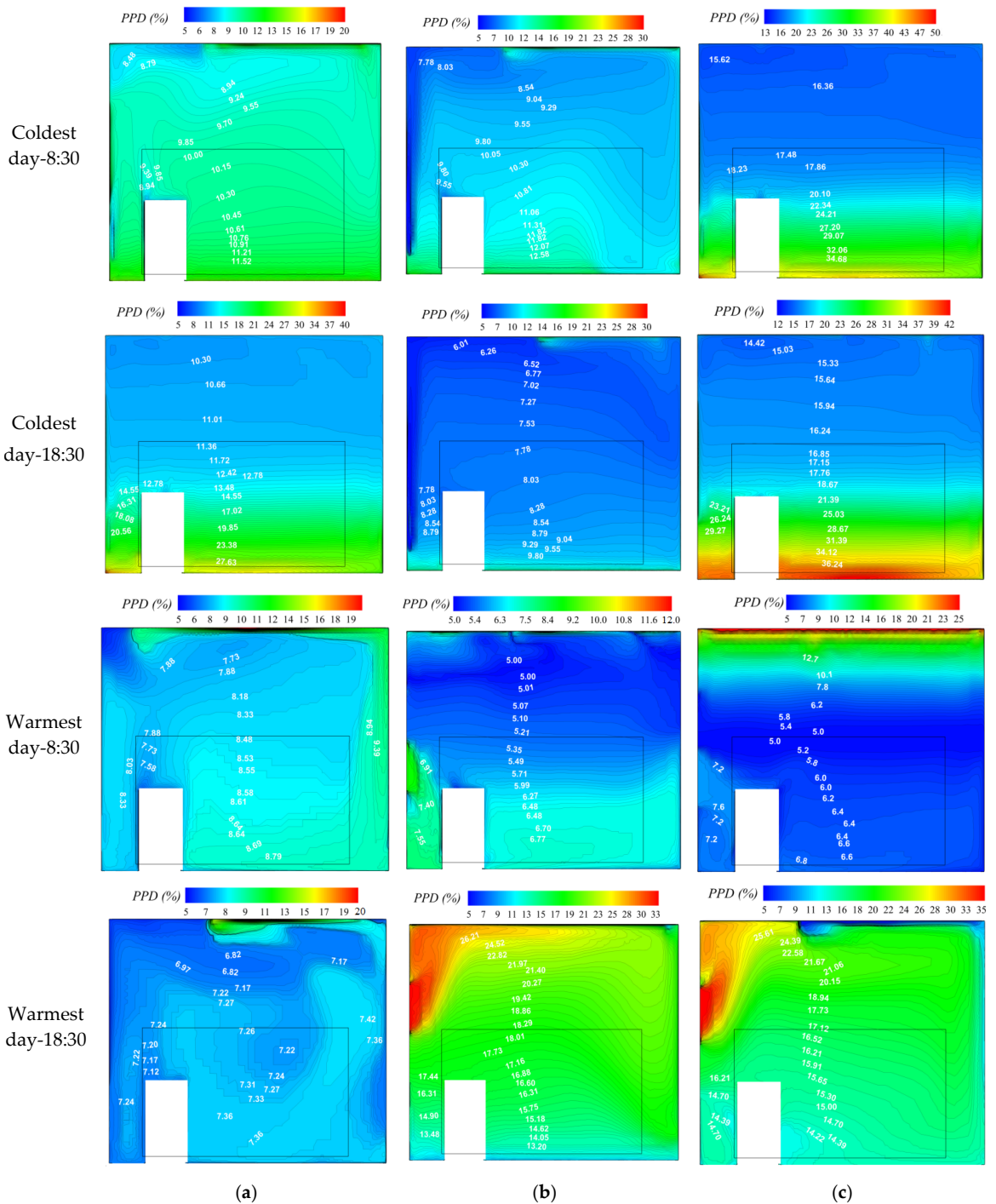


Figure 9. Spatial distribution of PPD in a vertical cross section passing through the window and occupancy area for the cell office C.O.16 for the (a) reference case, (b) first optimized scenario (c) second optimized scenario.

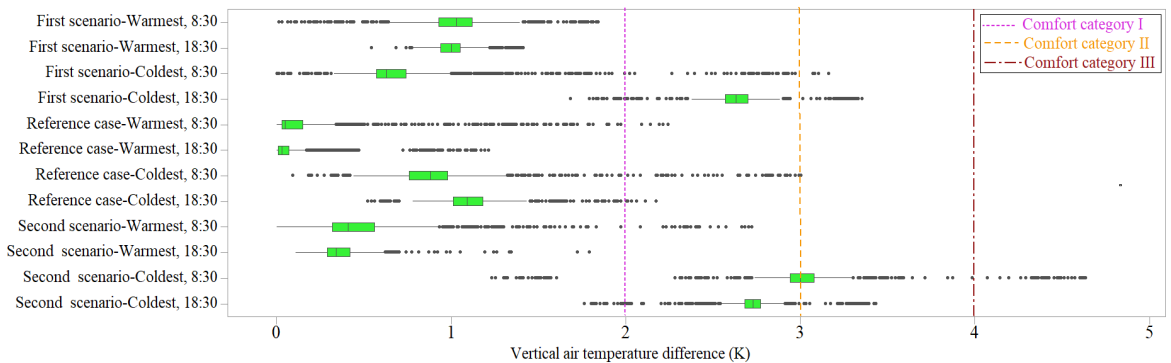


Figure 10. Box plot of vertical air temperature difference between the ankle and head levels for the cell office C.O.16 for different cases.

To analyze the visual comfort in detail for the two optimization scenarios and the reference case, the spatial distribution of three different common dynamic indexes including UDI, cDA, and sDA are shown in Figure 11. Both optimization scenarios showed superior performance compared to the reference case in terms of visual comfort conditions. Concerning the UDI index, more than half of the occupancy area could reach almost 50% UDI, which is recommended for office buildings [76], after optimization in both scenarios. Nevertheless, the second scenario provided more uniform distribution of relatively high UDI in the entire area during the occupancy hours. This was even more discernible in terms of cDA and sDA indexes (Figure 11b, two bottom rows) so that only a small area near the window could achieve around 35% sDA during occupancy hours in the first optimization scenario while a larger range of sDA, 30%–48%, covered more than 50% of the whole area. This implies that the combination of shading control method, which adopted indoor temperature and daylight parameters, and window-to-floor ratio could provide better visual comfort quality in the second scenario for the entire year. It is worth mentioning that although a static parameter was considered as the visual comfort constraint ($DF_{avg} > 2\%$), due to the necessity of Norwegian national requirements, the optimized design variables provided a great improvement in terms of dynamic daylight indexes compared to the reference case.

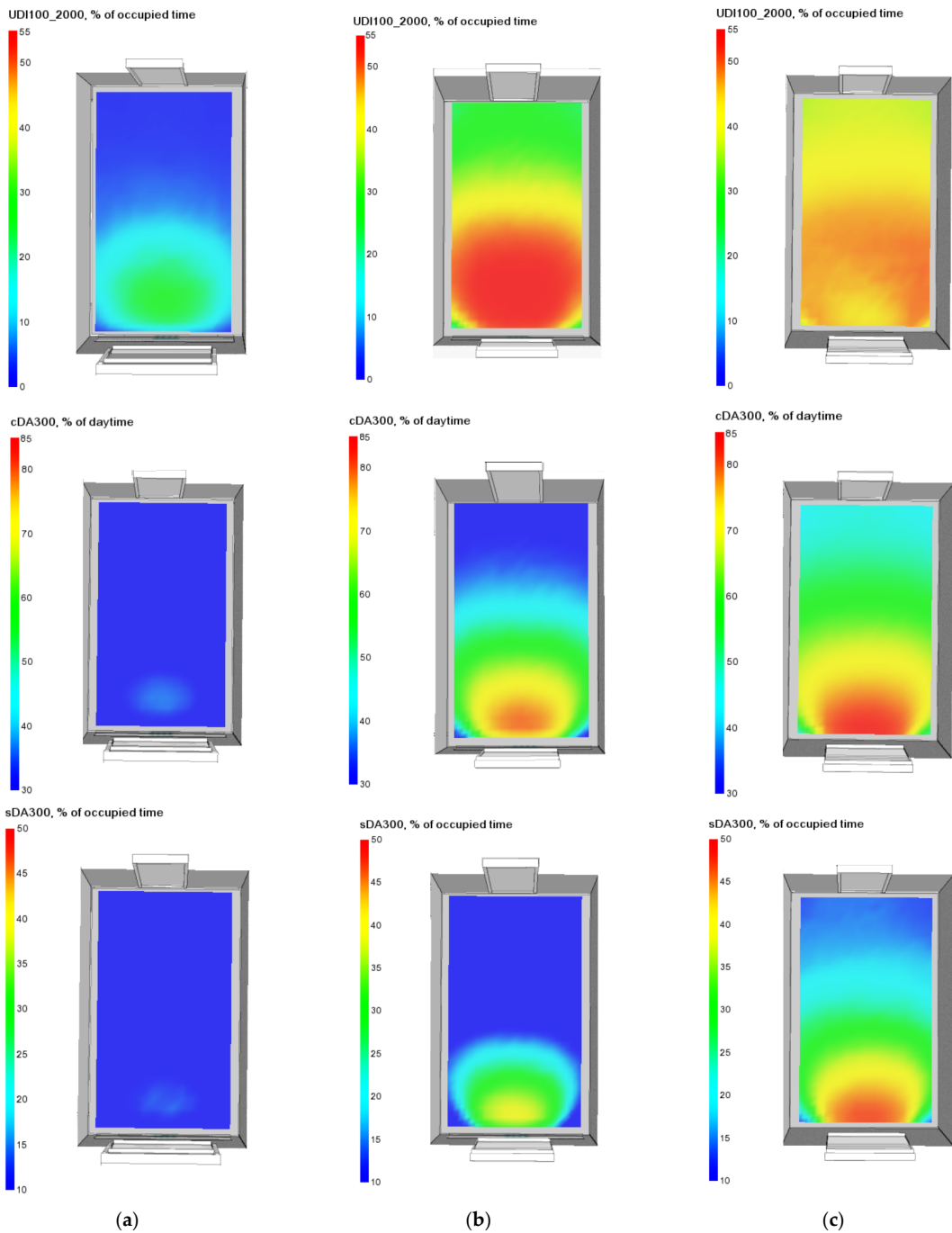


Figure 11. Spatial distribution of three visual daylight indexes for the cell office C.O.16 for (a) reference case (b) first optimized scenario, and (c) second optimized scenario.

4. Conclusions

In this study, a framework to take advantage of coupling the building energy simulation-optimization process with CFD and daylight simulations was presented. The aim of the proposed framework was to refine the efficiency of feasible studies concerning the retrofitting of building performance.

The objectives were to reduce the building energy use and improve thermal and visual comfort, to be achieved together with the best possible configuration of building envelope, fenestration, shading device and window opening control methods and parameters, and HVAC system set points and control methods. Two different optimization scenarios were considered; (i) a CAV ventilation system with hydronic heating system with radiators and (ii) an all-air system equipped with a DCV system for space heating, space cooling, and ventilation of different zones. The optimization process was carried out using the dynamic building energy simulation software IDA-ICE coupled with GenOpt as the optimization engine. Furthermore, a detailed thermal and visual comfort analysis of all scenarios was conducted through coupling of IDA-ICE with OpenFOAM, which is open source CFD software, and Radiance, which is an open-source daylight simulation engine. This could provide better insights regarding the improvement of thermal and visual comfort throughout the year.

The first part of the results regarding the building energy simulation-optimization (BES-OPT) process revealed that:

- Satisfying thermal comfort requirements was more difficult in an all-air system than in a CAV system during the optimization process. However, as visual comfort was only controlled by window-to-floor ratio and shading device control methods and materials, it was generally more challenging to reach low-level building energy use satisfying visual comfort requirements than thermal comfort conditions.
- The building energy use reduced up to by around 77% and 79% in the first and second scenarios respectively while satisfying both thermal and visual comfort.

The second part of the results regarding the detailed thermal comfort and visual comfort analysis are as follows:

- Both optimized scenarios could satisfy thermal comfort requirements, based on comfort category II, for longer periods of the year compared to the reference case, and the second optimized scenario showed the best performance in this respect. However, the DCV system adopted in this scenario could not provide comfortable conditions, according to any of three comfort categories, in extreme cold.
- Concerning the vertical temperature stratifications, most points in the occupancy area met the thermal comfort requirements on the coldest day of the year, which is less than 3K according to the second thermal comfort category for office buildings. However, a slight temperature stratification was observed covering around 50% of the occupancy area at the second scenario in the morning of the coldest day of the year.
- The window opening was functional for both optimized scenarios during summertime and no significant temperature stratification was observed, in spite of using a rather low air flow rate compared to the reference case.
- Regarding the daylight indexes, more than half of the occupancy area could arrive at almost 50% UDI after optimization in both scenarios. Nevertheless, the second scenario provided more uniform distribution of relatively high UDI in the entire area during the occupancy hours. This was even more discernible in terms of cDA and sDA indexes.

Overall assessment of both BES-OPT process and detailed CFD and daylight analysis proved that the DCV system (all-air system in the second scenario) can be considered as a potential HVAC system in cold climate countries as it can reduce the investment and maintenance costs associated with local space heating and cooling systems. Moreover, the current framework could suggest a paved method for better evaluation of building retrofitting measures through detailed and plausible studies.

Future developments can also focus on the evaluation of the application of such a method by expanding the possible design variables and objective functions by including the life cycle cost and CO₂ footprint of retrofitting measures in the optimization process. In this regard, it is also important to consider the impact of HVAC plant refurbishment in the optimization process as this would have a substantial effect on the total building energy reduction and its corresponding cost and CO₂ emissions. Furthermore, the effect of other phenomena such as urban heat island and climate change could be considered in the optimization process as it could have significant impacts on building energy use by increasing space cooling demand and decreasing space heating demand.

Author Contributions: Conceptualization, M.R., H.B.M. and N.N.; methodology, M.R., H.B.M. and N.N.; software, M.R.; validation, M.R.; formal analysis, M.R.; investigation, M.R., H.B.M. and N.N.; writing—original draft preparation, M.R.; writing—review and editing, M.R., H.B.M. and N.N.; supervision, M.R. and N.N.; All authors have read and agreed to the published version of the manuscript.

Funding: This research received no external funding

Institutional Review Board Statement: Not applicable.

Informed Consent Statement: Not applicable.

Conflicts of Interest: The authors declare no conflict of interest.

Appendix A

The dynamic daylight indexes including UDI, cDA, and sDA were calculated as follows, respectively:

$$UDI(Pt_i) = \frac{1}{n} \sum_{j=1}^n H(L(Pt_i, j)) \times 100, H(x) = \begin{cases} 1 & \text{Min} \leq x \leq \text{Max} \\ 0 & \text{out of range} \end{cases} \quad (A1)$$

$$cDA(Pt_i) = \frac{1}{m} \sum_{j=1}^m H(L(Pt_i, j)) \times 100, H(x) = \begin{cases} 1 & x \geq L_{Limit} \\ \frac{x}{L_{Limit}} & x < L_{Limit} \end{cases} \quad (A2)$$

$$sDA(Pt_i) = \frac{1}{n} \sum_{j=1}^n H(L(Pt_i, j)) \times 100, H(x) = \begin{cases} 1 & x \geq L_{Limit} \\ 0 & x < L_{Limit} \end{cases} \quad (A3)$$

where n and m referred to total occupancy and daytime hours, respectively. Furthermore, $L(Pt_i, j)$ represented the daylight simulation results at point i (Pt_i) and time step j , and $H(x)$ was a function representing the illuminance value.

References

1. IEA. *The Critical Role of Buildings*; IEA: Paris, France, 2019; Available online: <https://www.iea.org/reports/the-critical-role-of-buildings> (accessed on 10 November 2020).
2. Artola, I.; Rademaekers, K.; Williams, R.; Yearwood, J. *Boosting Building Renovation: What Potential and Value for Europe*; Study for the iTRE Committee, Commissioned by DG for Internal Policies Policy Department A: Brussels, Belgium, 2016; Volume 72.
3. Directive (EU) 2018/844 of the European parliament and of the council of 30 May 2018 amending Directive 2010/31/EU on the energy performance of buildings and Directive 2012/27/EU on energy efficiency (Text with EEA relevance). *Off. J. Eur. Union* **2018**, *156*, 75.
4. Hashempour, N.; Taherkhani, R.; Mahdikhani, M. Energy performance optimization of existing buildings: A literature review. *Sustain. Cities Soc.* **2020**, *54*. [[CrossRef](#)]
5. Djuric, N.; Novakovic, V.; Holst, J.; Mitrovic, Z. Optimization of energy consumption in buildings with hydronic heating systems considering thermal comfort by use of computer-based tools. *Energy Build.* **2007**, *39*, 471–477. [[CrossRef](#)]
6. Rabani, M.; Madessa, H.B.; Mohseni, O.; Nord, N. Minimizing delivered energy and life cycle cost using Graphical script: An office building retrofitting case. *Appl. Energy* **2020**, *268*. [[CrossRef](#)]
7. Karaguzel, O.T.; Zhang, R.; Lam, K.P. Coupling of whole-building energy simulation and multi-dimensional numerical optimization for minimizing the life cycle costs of office buildings. *Build. Simul.* **2013**, *7*, 111–121. [[CrossRef](#)]

8. Chantrelle, F.P.; Lahmidi, H.; Keilholz, W.; Mankibi, M.E.; Michel, P. Development of a multicriteria tool for optimizing the renovation of buildings. *Appl. Energy* **2011**, *88*, 1386–1394. [[CrossRef](#)]
9. Ferrara, M.; Sirombo, E.; Fabrizio, E. Automated optimization for the integrated design process: The energy, thermal and visual comfort nexus. *Energy Build.* **2018**, *168*, 413–427. [[CrossRef](#)]
10. Magnier, L.; Haghighat, F. Multiobjective optimization of building design using TRNSYS simulations, genetic algorithm, and Artificial Neural Network. *Build. Environ.* **2010**, *45*, 739–746. [[CrossRef](#)]
11. Harkouss, F.; Fardoun, F.; Biwole, P.H. Passive design optimization of low energy buildings in different climates. *Energy* **2018**, *165*, 591–613. [[CrossRef](#)]
12. Asadi, E.; da Silva, M.G.; Antunes, C.H.; Dias, L. A multi-objective optimization model for building retrofit strategies using TRNSYS simulations, GenOpt and MATLAB. *Build. Environ.* **2012**, *56*, 370–378. [[CrossRef](#)]
13. Niemelä, T.; Levy, K.; Kosonen, R.; Jokisalo, J. Cost-optimal renovation solutions to maximize environmental performance, indoor thermal conditions and productivity of office buildings in cold climate. *Sustain. Cities Soc.* **2017**, *32*, 417–434. [[CrossRef](#)]
14. Wu, R.; Mavromatidis, G.; Orehounig, K.; Carmeliet, J. Multiobjective optimisation of energy systems and building envelope retrofit in a residential community. *Appl. Energy* **2017**, *190*, 634–649. [[CrossRef](#)]
15. Hamdy, M.; Hasan, A.; Siren, K. Applying a multi-objective optimization approach for Design of low-emission cost-effective dwellings. *Build. Environ.* **2011**, *46*, 109–123. [[CrossRef](#)]
16. Palonen, M.; Hamdy, M.; Hasan, A. MOBO a new software for multi-objective building performance optimization. In Proceedings of the BS 2013: 13th Conference of the International Building Performance Simulation Association, Chambéry, France, 26–28 August 2013.
17. Mohammadi, Z.; Hoes, P.J.; Hensen, J.L.M. Simulation-based design optimization of houses with low grid dependency. *Renew. Energy* **2020**, *157*, 1185–1202. [[CrossRef](#)]
18. Zhang, L.; Zhang, L.; Wang, Y. Shape optimization of free-form buildings based on solar radiation gain and space efficiency using a multi-objective genetic algorithm in the severe cold zones of China. *Sol. Energy* **2016**, *132*, 38–50. [[CrossRef](#)]
19. Kirimtat, A.; Krejcar, O.; Ekici, B.; Fatih Tasgetiren, M. Multi-objective energy and daylight optimization of amorphous shading devices in buildings. *Sol. Energy* **2019**, *185*, 100–111. [[CrossRef](#)]
20. Fang, Y.; Cho, S. Design optimization of building geometry and fenestration for daylighting and energy performance. *Sol. Energy* **2019**, *191*, 7–18. [[CrossRef](#)]
21. Naderi, E.; Sajadi, B.; Behabadi, M.A.; Naderi, E. Multi-objective simulation-based optimization of controlled blind specifications to reduce energy consumption, and thermal and visual discomfort: Case studies in Iran. *Build. Environ.* **2020**, *169*. [[CrossRef](#)]
22. Bassuet, A.; Rife, D.; Dellatorre, L. Computational and Optimization Design in Geometric Acoustics. *Build. Acoust.* **2014**, *21*, 75–85. [[CrossRef](#)]
23. Saksela, K.; Botts, J.; Savioja, L. Optimization of absorption placement using geometrical acoustic models and least squares. *J. Acoust. Soc. Am.* **2015**, *137*, EL274–EL280. [[CrossRef](#)]
24. Ferdyn-Grygierek, J.; Grygierek, K. Optimization of Window Size Design for Detached House Using Trnsys Simulations and Genetic Algorithm. *Arch. Civ. Eng. Environ.* **2018**, *10*, 133–140. [[CrossRef](#)]
25. Delgarm, N.; Sajadi, B.; Delgarm, S. Multi-objective optimization of building energy performance and indoor thermal comfort: A new method using artificial bee colony (ABC). *Energy Build.* **2016**, *131*, 42–53. [[CrossRef](#)]
26. Schwartz, Y.; Raslan, R.; Mumovic, D. Implementing multi objective genetic algorithm for life cycle carbon footprint and life cycle cost minimisation: A building refurbishment case study. *Energy* **2016**, *97*, 58–68. [[CrossRef](#)]
27. Delgarm, N.; Sajadi, B.; Kowsary, F.; Delgarm, S. Multi-objective optimization of the building energy performance: A simulation-based approach by means of particle swarm optimization (PSO). *Appl. Energy* **2016**, *170*, 293–303. [[CrossRef](#)]
28. Arabzadeh, V.; Jokisalo, J.; Kosonen, R. A cost-optimal solar thermal system for apartment buildings with district heating in a cold climate. *Int. J. Sustain. Energy* **2018**, *38*, 141–162. [[CrossRef](#)]
29. Bamdad, K.; Cholette, M.E.; Guan, L.; Bell, J. Ant colony algorithm for building energy optimisation problems and comparison with benchmark algorithms. *Energy Build.* **2017**, *154*, 404–414. [[CrossRef](#)]
30. Lu, Y.; Wang, S.; Zhao, Y.; Yan, C. Renewable energy system optimization of low/zero energy buildings using single-objective and multi-objective optimization methods. *Energy Build.* **2015**, *89*, 61–75. [[CrossRef](#)]
31. Taveres-Cachat, E.; Lobaccaro, G.; Goia, F.; Chaudhary, G. A methodology to improve the performance of PV integrated shading devices using multi-objective optimization. *Appl. Energy* **2019**, *247*, 731–744. [[CrossRef](#)]
32. Yi, Y.K. Building facade multi-objective optimization for daylight and aesthetical perception. *Build. Environ.* **2019**, *156*, 178–190. [[CrossRef](#)]
33. Tommasi, L.D.; Ridouane, H.; Giannakis, G.; Katsigarakis, K.; Lilis, G.N.; Rovas, D. Model-Based Comparative Evaluation of Building and District Control-Oriented Energy Retrofit Scenarios. *Buildings* **2018**, *8*, 91. [[CrossRef](#)]
34. García-Fuentes, M.A.; Hernández, G.; Serna, V.; Martín, S.; Álvarez, S.; Lilis, G.N.; Giannakis, G.; Katsigarakis, K.; Mabe, L.; Oregi, X.; et al. OptEEMAL: Decision-Support Tool for the Design of Energy Retrofitting Projects at District Level. *IOP Conf. Ser. Earth Environ. Sci.* **2019**, *290*, 012129. [[CrossRef](#)]
35. Hirvonen, J.; Jokisalo, J.; Heljo, J.; Kosonen, R. Towards the EU emissions targets of 2050: Optimal energy renovation measures of Finnish apartment buildings. *Int. J. Sustain. Energy* **2019**, *38*, 649–672. [[CrossRef](#)]

36. Hong, T.; Kim, J.; Lee, M. A multi-objective optimization model for determining the building design and occupant behaviors based on energy, economic, and environmental performance. *Energy* **2019**, *174*, 823–834. [[CrossRef](#)]
37. Pazouki, M.; Rezaie, K.; Bozorgi-Amiri, A. A fuzzy robust multi-objective optimization model for building energy retrofit considering utility function: A university building case study. *Energy Build.* **2021**, *241*, 110933. [[CrossRef](#)]
38. Lu, S.; Li, J.; Lin, B. Reliability analysis of an energy-based form optimization of office buildings under uncertainties in envelope and occupant parameters. *Energy Build.* **2020**, *209*, 109707. [[CrossRef](#)]
39. Karmellos, M.; Kiprakis, A.; Mavrotas, G. A multi-objective approach for optimal prioritization of energy efficiency measures in buildings: Model, software and case studies. *Appl. Energy* **2015**, *139*, 131–150. [[CrossRef](#)]
40. Caldas, L.; Santos, L. Painting with light: An interactive evolutionary system for daylighting design. *Build. Environ.* **2016**, *109*, 154–174. [[CrossRef](#)]
41. Sameti, M.; Haghghat, F. Optimization approaches in district heating and cooling thermal network. *Energy Build.* **2017**, *140*, 121–130. [[CrossRef](#)]
42. Chegari, B.; Tabaa, M.; Simeu, E.; Moutaouakkil, F.; Medromi, H. Multi-objective optimization of building energy performance and indoor thermal comfort by combining artificial neural networks and metaheuristic algorithms. *Energy Build.* **2021**, *239*, 110839. [[CrossRef](#)]
43. Fouquier, A.; Robert, S.; Suard, F.; Stéphan, L.; Jay, A. State of the art in building modelling and energy performances prediction: A review. *Renew. Sustain. Energy Rev.* **2013**, *23*, 272–288. [[CrossRef](#)]
44. Axley, J. Multizone Airflow Modeling in Buildings: History and Theory. *HVAC&R Res.* **2007**, *13*, 907–928. [[CrossRef](#)]
45. Tian, W.; Sevilla, T.A.; Zuo, W.; Sohn, M.D. Coupling fast fluid dynamics and multizone airflow models in Modelica Buildings library to simulate the dynamics of HVAC systems. *Build. Environ.* **2017**, *122*, 269–286. [[CrossRef](#)]
46. Crawley, D.B.; Hand, J.W.; Kummert, M.; Griffith, B.T. Contrasting the capabilities of building energy performance simulation programs. *Build. Environ.* **2008**, *43*, 661–673. [[CrossRef](#)]
47. Nielsen, P.V. Fifty years of CFD for room air distribution. *Build. Environ.* **2015**, *91*, 78–90. [[CrossRef](#)]
48. Nielsen, P.V.; Allard, F.; Awbi, H.B.; Davidson, L.; Schälén, A. Computational Fluid Dynamics in Ventilation Design REHVA guidebook No 10. *Int. J. Vent.* **2007**, *6*, 291–294. [[CrossRef](#)]
49. Novoselac, A. Combined Airflow and Energy Simulation Program for Building Mechanical System Design. Ph.D. Thesis, The Pennsylvania State University, State College, PA, USA, 2004.
50. Tian, W.; Han, X.; Zuo, W.; Sohn, M.D. Building energy simulation coupled with CFD for indoor environment: A critical review and recent applications. *Energy Build.* **2018**, *165*, 184–199. [[CrossRef](#)]
51. Rodríguez-Vázquez, M.; Hernández-Pérez, I.; Xamán, J.; Chávez, Y.; Gijón-Rivera, M.; Belman-Flores, J.M. Coupling building energy simulation and computational fluid dynamics: An overview. *J. Build. Phys.* **2020**, *44*, 137–180. [[CrossRef](#)]
52. Shan, X.; Luo, N.; Sun, K.; Hong, T.; Lee, Y.-K.; Lu, W.-Z. Coupling CFD and Building Energy Modelling to Optimize the Operation of a Large Open Office Space for Occupant Comfort. *Sustain. Cities Soc.* **2020**. [[CrossRef](#)]
53. Pandey, B.; Banerjee, R.; Sharma, A. Coupled EnergyPlus and CFD analysis of PCM for thermal management of buildings. *Energy Build.* **2021**, *231*, 110598. [[CrossRef](#)]
54. Yamamoto, T.; Ozaki, A.; Lee, M.; Kusumoto, H. Fundamental study of coupling methods between energy simulation and CFD. *Energy Build.* **2018**, *159*, 587–599. [[CrossRef](#)]
55. Colombo, E.; Zwahlen, M.; Frey, M.; Loux, J. Design of a glazed double-façade by means of coupled CFD and building performance simulation. *Energy Procedia* **2017**, *122*, 355–360. [[CrossRef](#)]
56. Zhang, R.; Mirzaei, P.A. Fast and dynamic urban neighbourhood energy simulation using CFDf-CFDc-BES coupling method. *Sustain. Cities Soc.* **2021**, *66*, 102545. [[CrossRef](#)]
57. Björnell, N.; Bring, A.; Eriksson, L.; Grozman, P.; Lindgren, M.; Sahlin, P.; Shapovalov, A.; Vuolle, M. IDA indoor climate and energy. In Proceedings of the 6-th IBPSA Conference, Kyoto, Japan, 13–15 September 1999; pp. 1035–1042.
58. OpenFOAM Foundation. 2018. Available online: <https://github.com/OpenFOAM/OpenFOAM-dev> (accessed on 20 October 2020).
59. Statistics Norway. 2019. Available online: <https://www.ssb.no/en/bygg-bolig-og-eiendom/statistikker/bygningsmasse/aar> (accessed on 30 December 2019).
60. Byggeforskrift-TEK 87, 1987. Available online: https://dibk.no/globalassets/byggeregler/tidligere_regelverk/historisk-arkiv-1949---1987/byggeforskrift-1987.pdf (accessed on 15 November 2020).
61. Rabani, M.; Bayera Madessa, H.; Nord, N. Achieving zero-energy building performance with thermal and visual comfort enhancement through optimization of fenestration, envelope, shading device, and energy supply system. *Sustain. Energy Technol. Assess.* **2021**, *44*, 101020. [[CrossRef](#)]
62. Standard Norge. *NS-3701-Criteria for Passive Houses and Low Energy Buildings, Non-Residential Buildings, 2012*; Standard Norge: Oslo, Norway, 2012.
63. Arbeidstilsynet. Available online: <https://www.arbeidstilsynet.no/tema/utforming-av-arbeidsplassen/rad-ved-tilbakeforing-til-arbeid-for-kontorarbeidsplasser/> (accessed on 15 November 2020).

64. The Director General of the National Archival Services of Norway, Requirements for Archive Premises—Guidelines for Public Bodies, 2007. Available online: https://www.arkivverket.no/om-oss/vare-publikasjoner/riksarkivarens-rapporter-og-retningslinjer/_/attachment/download/04cc2705-d572-41e7-8810-a6e4f19f5f31:d24e6e9c694a8dc844695d015e544baea21e4351/Requirements%20for%20archive%20premises.pdf (accessed on 15 November 2020).
65. Building Technical Regulations (TEK17) 2017, § 14-2. Requirements for Energy Efficiency. Available online: <https://dibk.no/regelverk/byggteknisk-forskrift-tek17/14/14-2/> (accessed on 13 April 2021). (In Norwegian).
66. NS-15251-2014, *Indoor Environmental Input Parameters for Design and Assessment of Energy Performance of Buildings Addressing Indoor Air Quality, Thermal Environment, Lighting and Acoustics*; Standard Norge: Oslo, Norway, 2014.
67. Wetter, M. *GenOpt (R), Generic Optimization Program, User Manual, Version 2.0.0*; Lawrence Berkeley National Laboratory: Berkeley, CA, USA, 2003.
68. Ward, G.; Shakespeare, R. *Rendering with Radiance: The art and science of lighting visualization*; Morgan Kaufmann Publishers: San Francisco, CA, USA, 1998.
69. Rabani, M.; Madessa, H.B.; Nord, N.; Schild, P.; Mysen, M. Performance assessment of all-air heating in an office cubicle equipped with an active supply diffuser in a cold climate. *Build. Environ.* **2019**, *156*, 123–136. [[CrossRef](#)]
70. Cablé, A.; Mysen, M.; Thunshelle, K. Can demand controlled ventilation replace space heating in office buildings with low heating demand? In Proceedings of the 2014-13th Indoor Air Conference, Hong Kong, China, 7–12 July 2014.
71. van Hooff, T.; Nielsen, P.V.; Li, Y. Computational fluid dynamics predictions of non-isothermal ventilation flow—How can the user factor be minimized? *Indoor Air* **2018**, *28*, 866–880. [[CrossRef](#)] [[PubMed](#)]
72. Nabil, A.; Mardaljevic, J. Useful daylight illuminance: A new paradigm for assessing daylight in buildings. *Light. Res. Technol.* **2005**, *37*, 41–57. [[CrossRef](#)]
73. Rogers, Z.; Goldman, D. *Daylighting Metric Development Using Daylight Autonomy Calculations in the Sensor Placement Optimization Tool*; Architectural Energy Corporation: Boulder, CO, USA, 2006; Available online: http://www.archenergy.com/SPOT/SPOT_Daylight%20Autonomy%20Report.pdf (accessed on 15 November 2020).
74. LM, I. *Approved Method: IES Spatial Daylight Autonomy (sDA) and Annual Sunlight Exposure (ASE)*; IES Standard LM-83–12; Illuminating Engineering Society of North America: New York, NY, USA, 2012.
75. NS-EN ISO 7730-2006. *Ergonomics of the Thermal Environment—Analytical Determination and Interpretation of Thermal Comfort Using Calculation of the PMV and PPD Indices and Local Thermal Comfort Criteria*; Standard Norge: Oslo, Norway, 2006.
76. Reinhart, C.F.; Weissman, D.A. The daylight area—Correlating architectural student assessments with current and emerging daylight availability metrics. *Build. Environ.* **2012**, *50*, 155–164. [[CrossRef](#)]

Paper 4

M. Rabani, H. Bayera Madessa, M. Ljungström, L. Aamodt, S. Løvvold, N. Nord, Life cycle analysis of GHG emissions from retrofitting of building: The case of a Norwegian office building, *Building and Environment*, 24 (2021) 108159.



Contents lists available at ScienceDirect

Building and Environment

journal homepage: www.elsevier.com/locate/buildenv

Life cycle analysis of GHG emissions from the building retrofitting: The case of a Norwegian office building

Mehrdad Rabani^{a,b,*}, Habtamu Bayera Madessa^a, Malin Ljungström^c, Lene Aamodt^d, Sandra Løvvold^b, Natasa Nord^b

^a Department of Civil Engineering and Energy Technology, Oslo Metropolitan University, Norway

^b Department of Energy and Process Engineering, Norwegian University of Science and Technology, Norway

^c Norconsult AS, Norway

^d Erichsen & Horgen AS, Norway

ARTICLE INFO

Keywords:

Building retrofitting
Zero energy building
Zero emission building
LCA
Embodied CO₂-eq
CO₂-eq payback time

ABSTRACT

Through a systematic study, this paper conducted a life cycle assessment (LCA) consisting of evaluation of both embodied and operational emissions of different building retrofitting scenarios for a typical office building, located in Norway. LCA analysis was performed via the OneClick LCA tool. The emissions associated with the operational energy use were evaluated for both the reference and optimized building energy models developed in the IDA-ICE models from our previous studies. These models included two different HVAC systems: an all-air (AA) system equipped with a demand control ventilation (DCV) and a hydronic system with the radiator space heating (RSH) and a constant air volume (CAV) ventilation system. The findings showed that, through retrofitting measures, the net total emissions could be reduced up to 52%, from 1336–637 kg carbon dioxide equivalent (CO₂-eq)/m², which was achieved for the life cycle cost (LCC) optimal scenario equipped with the AA system. The share of operational energy use (B6) in the total CO₂-eq emissions was around 77% for the reference case, whereas it was around 43–46% for the retrofitting scenarios. The most embodied CO₂-eq emitted stages of the LCA through retrofitting concerned the product stage (19–23%), transport to construction site (24–31%), and the end-of-life service (around 25%). The findings confirmed that it was more environmentally friendly to further re-insulate the other parts of the building envelope instead of ground floor, as the latter retrofitting scenario was accompanied with a large increase of embodied emissions.

1. Introduction

According to the Intergovernmental Panel on Climate Change (IPCC), the global temperature has risen by roughly 1 °C since the industrial age, because of human actions. It is also expected that the temperature will increase further, by 1.5 °C, if the current situation is prolonged [1]. Greenhouse gas (GHG) emissions are considered to be one of the main sources for the climate change, and there has been already introduced a GHG abatement curve in order to maintain the global temperature rise below 2 °C by 2030 [2].

It has been reported that around 30–40% of global CO₂ emissions are produced in the building stock [3]. Since the 80–90% of the existing buildings will still be in operation in 2050 [4,5], it is apparent that building retrofitting would substantially mitigate the total GHG emissions in the building sector. Building retrofitting has been broadly

studied to cope with the climate change issue, but to achieve the target of EU's Policy, the renovation rate should further increase [6]. According to Statistics Norway (SSB), the amount of CO₂ emissions in non-residential buildings, which form the largest part of building stock in Norway (around 58%), has decreased around 39% from 2015 to 2019 due to improvement of building energy performance [7]. However, there must be additional attention to this matter if the goal is to reach a carbon neutral level in Norway by 2030. Retrofitting towards the zero energy buildings (ZEB) signifies a purposeful step in this regard, resulting in reduction of forthcoming buildings energy use. The retrofitting process can include renovation measures with regard to building envelope and façade, technical system, and utilization of renewable energy technologies [8–10]. Furthermore, there are several ZEB definitions and some of them only focus on the energy use during building operation and ignore the energy utilized for the production and manufacturing of material and systems when shifting to ZEB level, or so

* Corresponding author. Department of Civil Engineering and Energy Technology, Oslo Metropolitan University, Norway.
E-mail address: mra@erichsen-horgen.no (M. Rabani).

<https://doi.org/10.1016/j.buildenv.2021.108159>

Received 3 March 2021; Received in revised form 3 July 2021; Accepted 14 July 2021

Available online 16 July 2021

0360-1323/© 2021 The Authors. Published by Elsevier Ltd. This is an open access article under the CC BY license (<http://creativecommons.org/licenses/by/4.0/>).

Nomenclature

Roman symbols

AA	all-air
CAV	constant air volume
CHP	combined heat and power
CO ₂	carbon dioxide
CO ₂ -eq	carbon dioxide equivalent
COP	coefficient of performance
DCV	demand control ventilation
EU	European union
EPD	environmental performance declaration
GHG	greenhouse gas
GSHp	ground source heat pump

GWP	global warming potential
HVAC	heating, ventilation, air conditioning system
IPCC	intergovernmental panel on climate change
LCA	life cycle assessment
LCC	life cycle cost
n ₅₀	airtightness (1/h)
nZEB	nearly zero energy building
PH	passive house
PV	photovoltaic
RSH	radiator space heating
ZEB	zero energy building

Greek symbols

ψ	normalized thermal bridge (W/(m ² ·K))
--------	---

called embodied energy [11,12]. The concepts of the zero energy building and embodied energy have proposed the idea to replace the former concepts by the zero emission building and embodied emissions, in which the balance is applied in terms of GHG emissions [13,14]. In this regard, to reach the greatest level of the zero emission building in the retrofiting process, it is necessary to conduct a life cycle assessment (LCA) on how to compensate the embodied emissions of additional materials during the whole life cycle. The balancing can be done using the GHG emissions of produced energy from renewable sources such as the use of solar energy via photovoltaic (PV) panels [15].

A broad range of embodied CO₂ emission from buildings has been reported in literature. De Wolf et al. [16] signified this by analyzing the data obtained from over 200 buildings and the results showed that the amount of building embodied CO₂ emission equivalent (CO₂-eq) varies in the range of 150–600 kg CO₂-eq/m² per year of building lifetime. Simonen et al. [17] state also a significant change of buildings' contribution in CO₂-eq emissions, which is in the range of 10–1082 kg CO₂-eq/m² per year by evaluating 1150 buildings. These variations are pointed out regarding several parameters such as building type, materials, geometry, and other design variables. So far, several studies on the life cycle assessment (LCA) of GHG emissions related to both new and refurbished buildings have already addressed the impact of the aforementioned parameters. Some of them consider only the building use phase, but others also consider the other stages of building life cycle including the production, construction, and end-of-life.

Asdrubali et al. [18] evaluated the energy use and carbon payback time of different retrofit scenarios for a school building in Northern Italy. They applied the LCA method for calculating environmental impact of the building for lifetime of 50 years. Their findings show that a cost optimal case, in which the total specific building energy use was around 70 kWh/m²·year, had a carbon payback time around 3.2 years. Opher et al. [19] conducted a LCA, using OneClick LCA tool, to assess the embodied emissions associated with the renovation of an existing building. By assuming a 60-year lifetime, the results show that the installation of renewable energy systems and the raised concrete floor are responsible for 31% and 26% of the embodied CO₂-eq. Rodriguez et al. [20] assessed the embodied carbon emissions associated with the mechanical, electrical, and plumbing systems (MEP) in an office building in the Pacific Northwest, USA and Canada. Various heating, ventilation, and air conditioning (HVAC) systems such as variable air volume (VAV) air handling unit (AHU), parallel fan terminals, water-source heat pump, dedicated outdoor air system, variable refrigerant flow, and energy recovery ventilator were evaluated. The results showed that the embodied carbon estimates ranged from 40 to 75 kg CO₂-eq/m² for MEP. García-Sanz-Calcedo et al. [21] quantified the embodied carbon of HVAC systems installed in healthcare centers in the region of Extremadura, Spain. The results showed that the embodied carbon considering a 15-year lifetime of HVAC installations, is around 48.95 kg CO₂-eq/m².

This was equivalent to the CO₂ emitted for 2.3 years in the operation phase. Ylmén et al. [22] investigated the embodied and operational carbon emissions from HVAC systems in an office building in Sweden and the results showed that 38 kg CO₂-eq/m² was emitted in the production phase and 100 kg CO₂-eq/m² in the operation phase. Shuo [23] analyzed the embodied emissions associated with three different HVAC installations, including a VAV system, a chilled beam system, and an underfloor air distribution in an office building in Australia. The total embodied carbon emission was reported 21.01 kg CO₂-eq/m², 42.70 kg CO₂-eq/m², and 9.2 kg CO₂-eq/m², respectively. Kiamili et al. [24] performed a detailed LCA for HVAC systems based on building information modelling (BIM) of a newly built office building in Switzerland. The results indicated that the embodied impact of HVAC systems was in the range of 15–36% of the total embodied impact of office buildings. However, Medas et al. [25] indicated that recurring embodied carbon of MEP from 30 years of maintenance and replacement might be much larger than the initial embodied carbon.

Moschetti et al. [26] investigated alternative design solutions for a zero energy office building, located in Norway, in order to achieve a zero emission one. The building model was run using SimaPro tool, and the results revealed that it was difficult to totally balance the life cycle GHG emissions from materials by renewable energy, even with widespread use of PV panels, and hence the embodied emissions from the materials should come into the sharp focus. Piccardo et al. [27] conducted the LCA of a retrofitted building to passive house level. They considered various scenarios including using covering different building materials and different electricity production cases. They pointed out that a careful choice of building materials might result in maximum 68% reduction of the net CO₂-eq in the retrofitted building than in the reference case, notably when selecting the wood material for building frames. Chen et al. [28] presented a multi-criteria evaluation approach for retrofit of a residential building to reduce the primary energy, global costs, payback period and the CO₂ emission. Regarding the environmental impact, an CO₂-eq factor, corresponding to the emissions from different GHGs generated only during building operation, was considered on the time frame of 100 years. The results showed the CO₂-eq can drop up to 10.4 kg CO₂-eq/m² in the case of applying extensive retrofits of building envelope and use of renewable measures. Pal et al. [29] proposed a LCA optimization approach to find the carbon-cost optimal solutions in terms of both operational and embodied CO₂ emissions. The results showed that when the carbon optimal solution was the matter of concern, the contribution of carbon embodied emissions in the LCA process was 39%, while in the cost optimal solution, its share was 28% in the LCA. Kristjansdottir et al. [30] studied the feasibility of achieving a zero emission building level, in terms of the life cycle energy and the material emission balance, through redesigning a single family pilot building located in Norway, which was constructed based on previous concept of zero greenhouse gas emission building [31,32]. The findings revealed that

the embodied emissions can be compensated up to 60% using the new model. However, an optimization framework is necessary to reach the balance of the life cycle energy and material emissions. Llantoy et al. [33] developed a comparative LCA by focusing on different building insulation materials including polyurethane, extruded polystyrene, and mineral wool. The results showed that although all insulation materials demonstrated a net positive benefit over 55 year's lifetime, the highest environmental impact was corresponding to the polystyrene insulation material and the lowest one was for the mineral wool. Echarri-Iribarren et al. [34] proposed a Life Cycle Construction Assessment of Envelopes (LCCA-e) method for analysis of constructive improvements derived from the application of ceramic panels and aluminum in a building façade located in Spain. The results showed 65.6% and 67.7% reduction in the global energy resources (GER) and global warming potential (GWP) indicators in the production phase and a reduction of these indicators by 87.1% and 86.8% respectively in the complete LCA. Chang et al. [35] performed a life cycle energy assessment of several academic buildings in Singapore. Their findings showed that 90% of the total life cycle energy is due to operational energy while the remaining 10% is from embodied energy. Sierra-Pérez et al. [36] used an integrated life cycle and thermal dynamic simulation assessment to identify the adequacy of each renovation alternative regarding the post-renovation energy performance of a commercial building, located in Spain. Their method included an evaluation of using a renewable insulation material in a low-energy building, especially a particular cork solution. The results showed that the renovation process of the low energy building results in an increase in the embodied impacts in the building, mainly for the large amount of insulation material. Furthermore, adopting cork did not fit the requirements for competing with the common non-renewable insulation materials as it did not lead to a better environmental performance in buildings. Luo and Chen [37] established a LCA of a residential building in different areas and the results showed that the amount of CO₂ emissions in server cold area and hot summer and warm winter area are the largest and the smallest, respectively. Wrålsen et al. [38] studied the LCA of retrofitting a residential building block from 1960s to nearly Norwegian passive house standard level over a 30 years period. The results of upgrading showed that all environmental impact categories reduced around 56–96% compared to the reference case, and the carbon payback period was 1.09 year. Shirazi and Ashuri [39] carried out a systematic LCA comparison of different retrofit measures and their associated payback time for a single family residential building. The investigation results showed that the foundation wall insulation significantly contributed to the carbon and smog potential for the building constructed before 1970s. The replacement of windows and the HVAC system had the next highest environmental impact. However, for after 1970s, HVAC replacement had the highest contribution to the carbon and smog potential.

Some studies focused on the uncertainty of parameters, methods, and scenarios in LCA process as it is a long-time frame process and there might be significant changes in building fabric features, occupancy behavior, climate changes, and etc. Zhang et al. [40], in a comparative case study, investigated the uncertainty in the LCA of a building case study by adopting deterministic and stochastic approaches. The first term is basically defined as the emissions, which are equal to the quantity product and the associated emission factor of the analyzed process [41]. The second approach could be applied by Monte Carlo simulations by considering the data samples generation as the main technique, which necessitates the dissemination of input data [42]. The results showed that the uncertainty in the input parameters could lead the ratio of standard deviation to the results sample mean, which was in accordance with the deterministic results, to be obtained around 0.51. Zhang et al. [43] also carried out a similar investigation to quantify the uncertainties in LCA of building CO₂-eq emissions when applying different parameter, methods, and modelling. The methods included process based method [44,45], input-output analysis [46,47], and hybrid method [48,49]. LCA results of two residential buildings showed

that selection of methods could significantly affect the CO₂-eq emissions. Furthermore, regarding parameter uncertainty, the input-output analysis could result in substantial errors, and hybrid techniques were suggested in the emission evaluation instead. Goulouti et al. [50] applied a systematic method to investigate the uncertainties of life service of building components through a stochastic approach. This method was applied for LCA calculation of a multi-family house. Moreover, a comprehensive sensitivity analysis was applied. The results showed that the main influential building elements on the uncertainty of LCA replacement stage were external insulation, windows, roofing, flooring, internal layout, and ceiling covering, respectively.

As the aforementioned studies showed, in the building retrofitting context, applying new materials introduces extra embodied emissions although the impacts associated with the energy use are reduced. Furthermore, LCA is a proper tool to analyze the resulting shifting between the increased embodied emissions and the reduced impacts associated with the energy use from an environmental standpoint. Therefore, in this paper, we conducted a feasibility study through adapting a cradle to grave method to assess the environmental impacts associated with GHGs generated due to applying extra/new materials and systems, and the resulting reduction of building energy use, by applying several retrofit measures for a typical and existing Norwegian office building. The main aim and novelty of this study was to identify the environmental impacts associated with the aforementioned retrofit measures applied in two different HVAC scenarios: (1) radiator space heating (RSH) system with constant air volume (CAV) and (2) all-air (AA) system equipped with a demand control ventilation (DCV) system. Due to complexity of the building simulation modeling, the building energy models corresponding to these scenarios were taken from our previous studies [8,51]. In addition, the aim was to find an optimal set of design solutions contributing to achieve a zero emission building level with regard to these HVAC scenarios.

The rest of the paper is organized as follows. Section 2 introduces the case building study and its characteristics, LCA specifications for analysis of embodied emissions connected to building materials and components, and emissions related to the operational energy use both for the reference building and the retrofitting scenarios. Furthermore, the building LCA tool and its properties are described in this section (see Fig. 1). Section 3 presents the results obtained from the LCA tool and discuss and interpret the CO₂-eq emissions produced in different scenarios and stages of the building life cycle. Finally, Section 4 summarizes the conclusions and findings of this study and suggests a framework for future work.

2. Method, building description, and tools

In this study, the LCA method was adopted to obtain science based information about the environmental impact of different retrofit measures of an office building built in the 1980s, in terms of GHG emissions (kgCO₂ - eq/m²_{floor area}), implemented according to the Norwegian standard NS 3720 [52]. This reference is based on the European LCA standard EN 15978 [53] and is used for calculation of GHGs in buildings. The functional unit was considered as one square meter of heated floor area (m²_{floor area}) over a service lifetime of 60 years [54]. The GHGs were based on the Kyoto basket gases weighted by their global warming potential (GWP) and aggregated to give total greenhouse gas emissions in terms of CO₂-eq [55]. In the first stage, we conducted energy simulations using the building model and the optimized scenarios applied in our previous work [8]. In this respect, we updated the building technical system and envelope characteristics in the building Indoor Climate and Energy (IDA-ICE) simulation software [56] to comply with the Norwegian building regulation TEK 87. Afterwards, we calculated the CO₂-eq, using OneClick LCA, for various retrofit scenarios in different phase of the building life cycle.

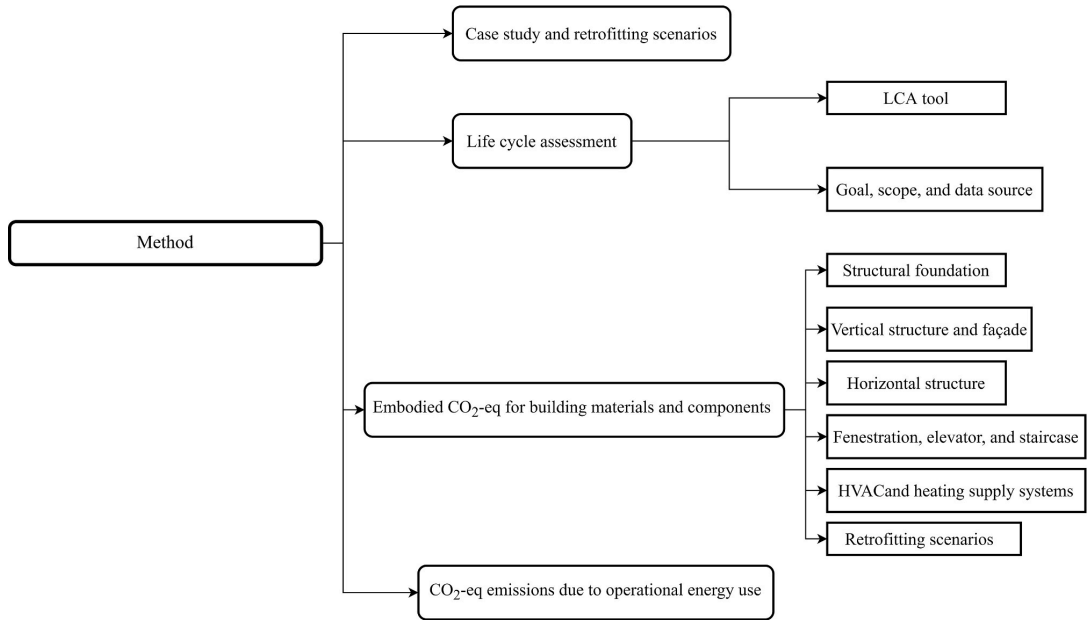


Fig. 1. Method and different stages of LCA process.

2.1. Case study and retrofitting scenarios

The case building that was simulated and analyzed in this study was a building model representing a typical and existing office building configuration located in Norway (Fig. 2). As shown in Fig. 2 (a) and (b), two office buildings, built on 1965 and 2015, have similar rectangular geometry and consist of combination of single and landscape offices. The considered building model in this study was an existing building from 1980 that was already applied in our previous studies [8,51]. The reference building properties were selected according to the Norwegian building regulation TEK 87 describing the characteristics of the typical existing Norwegian office buildings in the same time frame [57], as the majority of office buildings in Norway were built in the 1980s [7]. All data related to the building’s area, volume, and energy use were obtained from the IDA-ICE model in our previous study [8] and were used as a basis for the greenhouse gas calculations in the LCA tool.

The building had a compact square design with a total internal volume of 9062 m³ and a total floor area of 2940 m². Details about the building system and services can be found in the previous work [51] and the most important building properties are given in Table 1.

In addition, four retrofitting scenarios were considered based on the

Table 1

Properties of the building mass used in the energy simulation and LCA analyses.

Building component	Values
Gross volume (m ³)	10 200
Net volume (m ³)	9062
Gross area (m ²)	3000
Useable area (m ²)	2940
Heated area (m ²)	2290
Number of floors	3
Roof and Floor area (m ²)	1000
External wall gross area (m ²)	1326
External wall net area (m ²)	1025
Window area (m ²)	280
Exterior doors (m ²)	21

models in our previous work [8]:

- The first and second scenarios models were designed based on the Norwegian Passive House (PH) standard NS 3701 for non-residential buildings [58]. The difference between the two scenarios was the

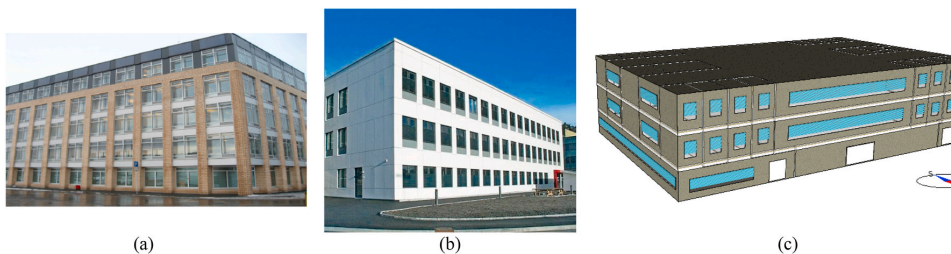


Fig. 2. (a) FN office building located in Arendal, which was built in 1965 and renovated in 2006 (b) An office building located in Bergen, which was completed in 2015 for the Norwegian Defence Estates Agency (NDEA) as a nearly zero energy building (nZEB) (c) Considered office building configuration modelled in the energy simulation software in our previous studies [8,51].

type of HVAC system in the zones. RSH and CAV ventilation system were used in the first scenario (the same HVAC system as the reference building) while the AA system was applied in the second scenario [8].

- The two other scenarios were the optimized models achieved in the previous work [8]. The optimized models were designed so that the minimum life cycle cost (LCC) of retrofit measures were reached while the building energy use for space heating and cooling did not exceed the requirements defined in the Norwegian PH standard NS 3701. Furthermore, a thermal comfort constraint was also considered in these cases. The difference between two scenarios was the type of space heating and cooling systems. The RSH system was adopted in the third scenario whereas AA system, was applied in the fourth scenario.

It should be noted that the space heating and cooling system in the reference building and first and second scenarios was the RSH system.

The minimum requirements for the building envelope and glazing properties for the reference building (TEK 87) and the PH cases, and the building envelope properties for two other retrofit scenarios were selected based on the previous work [8], are shown in Table 2.

2.2. Life cycle assessment

2.2.1. LCA tool

OneClick LCA was used for the LCA by taking into account the Norwegian standard NS 3720 [59]. It is a standardized web-based platform specifically designed for LCA of construction projects and contains EPDs [60], completed together with upstream data from well-established commercial LCA databases. It includes twelve third-party certifications and complies with more than 30 certifications and standards for the life cycle assessment, including NS 3720 [59]. Data points used in our life cycle analysis were mainly Norwegian EPDs for Norway or Nordic countries. In cases where none of the aforementioned standard were accessible in the database, data from other countries were used. It should be noted that this tool uses qualitative data input meaning that the user selects an option from a given list, i.e. the modules and indicators to be considered, the building substructure type, as well as pre-established scenarios for construction and end-of-life. It facilitates the data inputs, especially in the early stages of design, when exactly information is not yet available. However, one of the downsides of qualitative inputs is the “black box” approach that does not allow the user to modify or access the parameters considered. Moreover, the tool does not calculate the operational energy use, however, it allows the user to input this information, as well as the electricity and fuel grid.

2.2.2. Goal, scope, and data source

Fig. 3 illustrates all the life cycle stages for building constructions. In this study, we focused the LCA on the building GHG emissions, calculated in terms of CO₂-eq, from four main stages, i.e. production of materials, construction phase, operation stage, and the end-of-life (filled green and red boxes). The first stage included extraction of raw materials, transport of them to the production site, and production (A1-A3).

Table 2
Building envelope and glazing properties reported in the previous work.

Building component	TEK 87	PH	RSH_LCC	AA_LCC
External wall U-value (W/(m ² ·K))	≤0.3	≤0.1	0.12	0.12
Roof U-value (W/(m ² ·K))	≤0.2	≤0.08	0.18	0.08
Floor towards ground U-value (W/(m ² ·K))	≤0.3	≤0.08	0.18	0.18
Windows/doors U-values (W/(m ² ·K))	≤2.4 (doors, ≤ 2)	≤0.8	0.8	0.8
ψ (W/(m·K))	≤0.13	≤0.03	0.03	0.03
n ₅₀ (1/h)	≤4	≤0.6	0.6	0.6

The second stage encompassed transportation of materials/components to the construction site, construction, and installation work (A4-A5). The embodied emissions related to the operation of the building included renovation and replacement of building materials and components during the use of the building (B2-B5). The embodied emissions in the last phase covered the demolition, transportation, waste processing, and disposal (C1-C4). The life service period for the retrofitted building and the reference case study was assumed to be 60 years [54, 61]. In addition, the life service for various products in this study was selected based on the product information provided by the manufacturer and it available in the LCA tool. The emissions associated with the operational energy use (B6) were calculated based on the energy simulations performed by considering the details of retrofitting scenarios from our previous studies [8,51]. In fact, IDA ICE was used as a platform to compute the energy performance of the models, and that data was used in One Click LCA to compute the emission in the energy use. It should be pointed out that the reuse, recovery, and recycling potential of materials/components (phase D) were not taken into account due to considering a cut-off system modelling approach, implying that the avoided burdens of the recyclable materials were not modelled throughout the way to where they recycled to new production.

For the retrofitting process, we adopted the same framework as in Fig. 3, but considering a refurbished process instead of a new building construction. This infers that the inputs for materials and components of the LCA model were only associated with the retrofit measures and not to the entire building in the retrofitting scenarios. Furthermore, the database used for the greenhouse gas calculations at different life cycle stages in the LCA tool are shown in Table 3.

In the product stage (A1-A3), the quantity of materials and technical information of the building structural foundation, which mostly concerned the reference building, were obtained from the archive for the Norwegian Building Research Series for the office buildings constructed in the 1980s [57].

2.3. Embodied CO₂-eq for building materials and components at different scenarios

The material/component quantities, types, and their corresponding CO₂-eq emissions for the building structural foundation, vertical structures and facade, horizontal structures, and building HVAC and heating supply systems were described only for the reference building, according to the TEK87 code (see Fig. 2 c). For the retrofit scenarios, only the quantity and the emissions associated with the extra building materials and components were considered. Therefore, in the following sections, the quantity and CO₂-eq emissions of the materials used for the aforementioned building components are firstly described for the reference building and afterwards only the changes due to retrofitting are mentioned. It should be noted that the life service for building foundation, and vertical and horizontal structures was considered permanent if otherwise it was mentioned.

2.3.1. Structural foundation

The building materials used in the structural foundation are shown in Table 4. These materials were never replaced, considered with permanent lifetime in all scenarios, and their quantities were calculated per building gross area. The frost insulation was specified according to the Norwegian building instructions and was calculated for the externally insulated concrete with the maximum frost amount of 35 000 h°C [62].

2.3.2. Vertical structure and façade

Table 5 shows the list of all materials' quantity and their corresponding CO₂-eq emissions used in the vertical structures and façade. The insulation materials were mineral wool class 36, which were selected according to the archive for the Norwegian Building Research Series in 1987 [63]. For the material calculation of load-bearing vertical structures, the same calculation principles were used as proposed for the

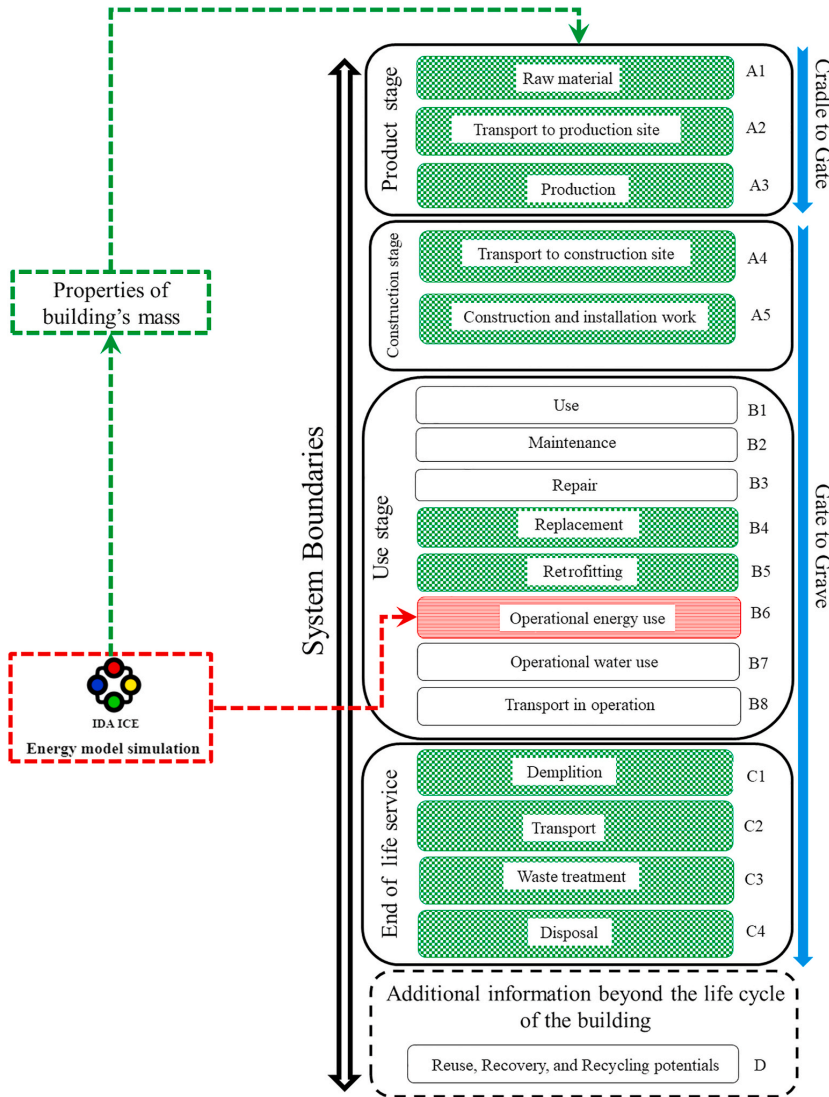


Fig. 3. Entire building life cycle stages according to NS 3720 [52]. In color: those considered in the boundaries of LCA in the present study. Stages assessed through the LCA tool database. Those evaluated using the optimized building energy models taken from our previous studies [8,51]. Those not considered in this study. (For interpretation of the references to color in this figure legend, the reader is referred to the Web version of this article.)

reference buildings in the Carbon Designer tool. Furthermore, the interior walls were assumed to be composed of 25% concrete walls and 75% timber frame. In addition, a layer of water-based interior paint was added to all interior walls in the calculation.

2.3.3. Horizontal structure

The quantities and corresponding CO₂-eq emissions of the materials used in the horizontal structure of the reference building are shown in Table 6. The components of the horizontal structure such as roof, floors and floor separators were set to be constructed of concrete.

2.3.4. Fenestration, elevator, and staircase

Table 7 shows an overview of the quantities and the corresponding CO₂-eq emissions of the materials used in the windows, stairs, elevators,

and doors. The considered material quantities corresponded to stairs with 11 m height and one elevator shaft. As there was no available window or door type with U-value of 2.4 W/(m².K) in the OnceClick LCA library, a generic two-layer windows with wooden/aluminum frame were used instead, because it had the same material impact on the CO₂-eq emissions as those had in 1987. The same assumptions were adopted in selecting the type of doors.

2.3.5. HVAC and heating supply systems

The HVAC system in the reference building consisted of a generic constant air volume system for cooling and heating of ventilation air and the RSH system. The materials used for the ventilation system were due to duct work and machinery. The materials used in the radiators or the RSH system were due to hydronic heating distribution system, as shown

Table 3
Data sources used for different LCA stages.

LCA stage	Source/assumption
Material quantities in production stage (A1-A3)	Quantities and material types were entered manually in the LCA tool based on the requirements for the reference building case and retrofit scenarios.
Transport of material to the production site (A4)	Automatic regional transport scenarios were used representing typical transport distances. If there was no data for the materials, the LCA's Norwegian default distance was used. The vehicles' type used for transportation was modelled using the available database, so that the maximum capacity of the vehicles nearly matches the transported mass.
Construction and installation work (A5)	Emission from waste materials associated with the construction and installation work was calculated based on the available standard values for each individual product.
Replacement and retrofitting (B4-B5)	Estimated lifetime was based on typical values for each material. Maintenance and repairs were omitted from the assessment as the materials were assumed to be replaced at the end of their technical life.
Operational energy use (B6)	Emissions from energy use were calculated based on the findings from building energy simulations and optimization in our previous study [8].
End-of-life service (C1-C4)	Emissions in connection with the end-of-life service were calculated according to the default scenarios in the tool representing the typical procedures for different types of material in accordance with the requirements in the Norwegian standard NS 3720.

Table 4
Materials' quantity and CO₂-eq emissions for the ground foundation.

Component	Source	Quantity	CO ₂ -eq (kg/m ²)
Foundation	Base plate, 0.3 m generic concrete	225 m ³	28
	Reinforced steel	18 750 kg	
Frost insulation	Gravel products	78 7500 kg	0.8
	EPS80	39 m ³	

in Table 8.

The systems were based on the generic available environmental products in the LCA tool and represented the average quantity of the materials for the performance criteria determined for the building gross area around 3000 m². The electric boiler was sized to cover the total building heating demands. However, there are still large uncertainties regarding the data sources used in the LCA tool since the available data may not be accurate or can be specific to the investigated system.

2.3.6. Retrofitting scenarios

In the retrofitting scenarios, only the additional materials, with corresponding CO₂-eq emissions, to the aforementioned building materials were taken into account. In the scenarios where the re-insulation of building envelope and façade was essential, a completely new construction component was replaced. This was performed to have a correct calculation of the life cycle assessment, so that the replacement of component was taken into consideration. In this respect, for example, the floor was replaced and the outer layer of asphalt in the roof was replaced in order to re-insulate these building components with additional insulation. All the building envelope components including floor, roof, and exterior walls were re-insulated with Glava Extrem 32 in the LCA tool.

Table 9 shows the quantity of extra materials and the associated emissions. In the PH scenarios (RSH_PH and AA_PH) the extra materials

Table 5
Materials' quantity and CO₂-eq emissions for vertical structure and facade.

Component	Source	Quantity	CO ₂ -eq (kg/m ²)
Exterior wall made of concrete	Wooden studwork	118.9 m ² × 148 mm	26
	Mineral wool insulation	906.1 m ² × 150 mm	
	wind barrier	1025 m ² × 9 mm	
	Generic concrete for external wall	1025 m ² × 200 mm	
Exterior cladding (external wall)	Reinforced steel	17 425 kg	1.5
	Fiber cement board cladding	1025 m ³	
	Concrete columns (support systems)	Generic mixed concrete	
Internal concrete wall with reinforcement and filler	Reinforced steel	4662 kg	9
	Mortar wall	960 m ² × 1 mm	
	Generic mixed concrete	480 m ² × 150 mm	
Timber framed wall and 100 mm steel stud with mineral wool insulation (internal walls)	Reinforced steel	6120 kg	7
	Plaster cast 13 mm	2 × 1440 m ²	
	Structural steel profiles	3984.5 kg	
Interior paint (internal walls)	Mineral wool insulation boards	1440 m ² × 100 mm	0.3
	Water-based interior paint (lifetime 15 years)	514.4 kg	

Table 6
Materials' quantity and CO₂-eq emissions for horizontal structure.

Component	Source	Quantity	CO ₂ -eq (kg/m ²)
Floor towards ground	EPS insulation	1000 m ² × 80 mm	39
	Generic concrete	1000 m ² × 300 mm	
	Vapor barrier in plastic	1000 m ² × 0.2 mm	
	Reinforced steel	27 000 kg	
Floor separator: hollow core slab with mineral wool insulation	Mineral wool insulation	1000 m ² × 3 mm	43
	Generic hollow core slab	1940 m ² × 265 mm	
	Generic concrete	1940 m ² × 50 mm	
	Reinforced steel	4306.8 kg	
Floor paint	Mineral wool insulation	1940 m ² × 20 mm	0.7
	Epoxy floor painting	2940 m ² × 0.1 mm	
Floor covering	Linoleum covering (lifetime 30 years)	2000 m ² × 2.25 mm	0.8
External roof: Compact concrete	EPS insulation and Mineral wool insulation boards	1000 m ² × 180 mm	33
	Vapor barrier plastic	1000 m ² × 0.2 mm	
	Generic concrete	1000 m ² × 200 mm	
	Reinforced steel	28 000 kg	
Roof membrane (external roof)	Double layer of asphalt roof membrane (lifetime 60 years)	1000 m ² × 3.5 mm	4

were chosen to meet the standard requirements. The RSH_LCC and AA_LCC scenarios were based on the previous work [8], where the requirements were obtained from the LCC optimized solutions. The HVAC

Table 7
Materials' quantity and CO₂-eq emissions for fenestration, elevator, and stairs.

Component	Source	Quantity	CO ₂ -eq (kg/m ²)
Stairs	Generic concrete	6.6 m ³	0.8
	Reinforced steel	658.4 kg	
Elevator shaft	Generic concrete	19 m ³	2
	Reinforced steel	1897.4 kg	
External doors	Steel door (lifetime 30 years)	12.6 m ²	0.7
	Steel garage door (lifetime 30 years)	8.4 m ²	
Internal doors	Wooden interior door (lifetime 30 years)	44 units	1.9
	Wooden double door (lifetime 30 years)	13.2 m ²	0.6
	Emergency door (lifetime 30 years)	6.15 m ²	0.1
Windows	Two-layer window with wooden/aluminum frame (lifetime 30 years)	280 m ²	12

Table 8
Materials' quantity and CO₂-eq emissions for HVAC system and central heating system.

Component	Source	Quantity (kg)	CO ₂ -eq (kg/m ²)
Ventilation system	Generic ventilation system (lifetime 50 years)	8250	55
Heating system	Radiator heating system (lifetime 30 years)	10 755	18
Electric boiler	Electric boiler, 280 kW (lifetime 22 years)	3558	8

system in the RSH_PH and RSH_LCC was the same as the reference building but with new waterborne radiators. In the AA_PH and AA_LCC the HVAC system was replaced by an AA system to cover space heating, space cooling, and ventilation air needs. In that case, the ventilation control method was changed to DCV.

To investigate the effect of different insulation materials, the same requirements for the building envelope characteristics should be considered. Therefore, we considered the U-value requirements for the

Table 9
Extra materials' quantity and CO₂-eq emissions for different retrofitting scenarios.

Component	Materials	RSH_PH		AA_PH		RSH_LCC		AA_LCC		
		Quantity	CO ₂ -eq (kg/m ²)	Quantity	CO ₂ -eq (kg/m ²)	Quantity	CO ₂ -eq (kg/m ²)	Quantity	CO ₂ -eq (kg/m ²)	
Extra insulation for external wall	Glava Extrem 32	1 025m ² ×	4.6	1 025m ² ×	4.6	1 025m ² ×	3.5	1 025m ² ×	3.5	
		215 mm		215 mm		160 mm		160 mm		
New exterior façade (external wall)	Fiber cement board cladding	1 025m ²	4.3	1 025m ²	4.3	1 025m ²	4.3	1 025m ²	4.3	
Extra insulation of the floor towards ground	Glava Extrem 32	1 000m ² ×	116	1 000m ² ×	116	1 000m ² ×	111	1 000m ² ×	111	
		240 mm		240 mm		20 mm		20 mm		
	Generic concrete	1 000m ² ×		1 000m ² ×		1 000m ² ×		1 000m ² ×		
		300 mm		300 mm		300 mm		300 mm		
	Plastic vapor barrier	1 000m ² ×		1 000m ² ×		1 000m ² ×		1 000m ² ×		
		0.2 mm		0.2 mm		0.2 mm		0.2 mm		
	Armouring	27 000 kg		27 000 kg		27 000 kg		27 000 kg		
		Mortar	1 000m ² ×		1 000m ² ×		1 000m ² ×		1 000m ² ×	
Epoxy floor paint	3 mm		3 mm		3 mm		3 mm			
	1 000m ² ×		1 000m ² ×		1 000m ² ×		1 000m ² ×			
Extra insulation of the roof	Glava Extrem 32	1 000m ² ×	17.5	1 000m ² ×	17.5	1 000m ² ×	12.9	1 000m ² ×	17.5	
		240 mm		240 mm		20 mm		240 mm		
	Double layer of asphalt roof membrane	1 000m ² ×		1 000m ² ×		1 000m ² ×		1 000m ² ×		
		3.5 mm		3.5 mm		3.5 mm		3.5 mm		
	Plastic vapor barrier	1 000m ² ×		1 000m ² ×		1 000m ² ×		1 000m ² ×		
		0.2 mm		0.2 mm		0.2 mm		0.2 mm		
	Window	Triple glazing, lifetime 30 years	280m ²	34	280m ²	34	280m ²	34	280m ²	34
		Existing doors were replaced by sliding door for use in exterior wall, lifetime 30 years	12.6m ²	4	12.6m ²	4	12.6m ²	4	12.6m ²	4
New hydronic system	For RSH_PH, and RSH_LCC, lifetime 30 years	10 755 kg	52	NA	NA	10 755 kg	52	NA	NA	

Norwegian PH standard NS 3701 [58]. The reason was that the PH standard required the thickest insulation layers associated with largest CO₂-eq emissions. Table 10 shows the overview of which products were assessed, and whether Norwegian EPDs were used. In the cases where the desired product and EPD were not found in the software, generic products were used instead, such as cellulose insulation.

Since a German product was used for the VIP insulation, the transportation distance to the construction site was set to 1160 km. Furthermore, the transportation distance to the construction site was considered 1000 km for Polyurethane foam due to use of a Finnish product. Otherwise, a standard Norwegian value was used for the transportation of other insulation materials to the construction site.

Furthermore, as the aim of the retrofitting was to reach a nZEB level, two types of PV were used, namely Monocrystalline and Polycrystalline. Similar to the comparison of CO₂-eq emissions for different insulation materials, the energy use for the PH standard was used as the criterion to balance the total delivered energy to the building and to calculate the necessary area of PV panels, which was calculated based on the method reported in Ref. [51]. The required area was obtained around 1500 m² and 1800 m² for Monocrystalline and Polycrystalline cells, respectively. The efficiency of these two types of PV cells was estimated based on typical figures for commercial PV panels. To allow these types of panels to be comparable in terms of CO₂-eq emission, a manufacturer that produced both types of panels were chosen, which is a Dutch manufacturer. Furthermore, the lifetime of PV cells was considered 30 years and their degradation rate neglected in this study.

2.4. CO₂-eq emissions due to operational energy use

GHG emissions due to operational energy use were calculated based on the delivered energy to the building and emission factors for electricity and district heating in accordance with NS 3720 [52]. Regarding the CO₂-eq factor related to the electricity production and transportation, 0.13 kg CO₂-eq/kWh was assumed based on production mix approach in the electricity supply (EU28 + Norge) with an expected average over 60 years and starting point based on the average for the last

Table 10
Required quantity of various insulation materials and their corresponding CO₂-eq emission to satisfy Norwegian PH standard.

Insulation product	Norwegian EPD	Quantity	CO ₂ -eq (kg/m ²)
Glass wool: Glava Extreme 32	Available	Roof and floor: 2 × 1000m ² × 240 mm External wall: 1025m ² × 215 mm	5
Rock wool: Rockwool-REDair Plate	Available	Roof and floor: 2 × 1000m ² × 248 mm External wall: 1025m ² × 221 mm	24
EPS80: EPS-group, EPS80	Available	Roof and floor: 2 × 1000m ² × 285 mm External wall: 1025m ² × 255 mm	17
VIP insulation, Vacuum VIP	Not available	Roof and floor: 2 × 1000m ² × 53 mm External wall: 1025m ² × 47 mm	121
Cellulose insulation	No EPD ^a	Roof and floor: 2 × 1000m ² × 278 mm External wall: 1025m ² × 248 mm	2.6
Polyurethane foam	No EPD ^b	Roof and floor: 2 × 1000m ² × 173 mm External wall: 1025m ² × 155 mm	12.2
XPS, Sundolit XPS	Available	Roof and floor: 2 × 1000m ² × 255 mm External wall: 1025m ² × 230 mm	30

^a A Norwegian generic model was selected.

^b A Finnish generic was used.

3 years [52,64]. The EU28 mix is a global power producer and the result of cooperation between the countries of the EU, where the goal is to reduce greenhouse gas emissions related to the production of electricity [64].

The CO₂-eq factor for district heating was selected 0.0138 kg CO₂-eq/kWh, which was based on the public data from Norwegian District Heating Fellowship [65]. Additionally, we compared the CO₂-eq for various types of energy supply system for heating. Four scenarios including district heating, a ground source heat pump (GSHP), electric boiler, and a combination of GSHP and electric boiler were considered. In order to find the necessary electricity required by the GSHP, a COP of 2.5 was considered for the GSHP [66]. In the hybrid scenario, the GSHP covered 60% of the heating demand and the rest was covered by the electric boiler. It should be mentioned that the embodied emissions related to the district heat distribution and the GSHP were selected based on the available data source for Norway in 2019, which were equal to 9.23 kg CO₂-eq/kW and 59.0 kg CO₂-eq/kW, respectively.

3. Results and discussions

In this section, the obtained results from the LCA tool are presented for both the reference case and the retrofitting scenarios. In this regard, the CO₂-eq emissions from different stages of building life cycle for the reference building are elaborated. Afterwards, the retrofitting scenarios are compared with the reference cases in terms of CO₂-eq during the whole building life span and the CO₂-eq payback period is discussed. In the third section, the CO₂-eq emissions for different insulation materials and various heating supply systems are described. In the fourth section, the CO₂-eq emissions for nZEB cases are presented.

3.1. CO₂-eq emissions for reference building

The amount of CO₂-eq emissions related to various stages of the building life cycle for the reference building is presented in Fig. 4. The

overview of the building life cycle shows that most of emissions, around 77%, was due to building operational energy use (B6), calculated based on the building energy simulation model in our previous study [51]. Furthermore, the product stage (A1-A3) stood for 16% of the total emissions, and the lowest emissions, around 1%, were related to transport to construction site (A4) and the end-of-life service (C1-C4). This implies the importance of improving the energy performance of the existing buildings as it leads to significant reductions in the building energy use and the corresponding CO₂-eq emissions.

Analyzing the embodied CO₂-eq emissions of materials shows that decks stood for the largest amount of the embodied CO₂-eq emissions, around 83 kg/m², and the stairs generated the lowest amount, approximately 3 kg/m² see Fig. 5. A Large part of CO₂-eq emissions for HVAC installations was related to the replacement and retrofitting stage, because the service life of the ventilation system, the eating system, and the electric boiler was estimated at 50, 30 and 22 years respectively and must be, therefore, replaced during the life of the building (60 years). It was also pointed out in Ref. [25] that the embodied emissions corresponding to the periodical maintenance of the HVAC system could be larger than the initial embodied emissions. However, the total production of materials (A1-A3) formed the largest source of emissions from the life cycle stages, with 73% of the total embodied emissions.

Fig. 6 shows the CO₂-eq emissions associated with 10 resources in the building that have the largest environmental impact in the reference building. The finished concrete was the largest driving source of the CO₂-eq emissions in all stages of building life cycle except the replacement and retrofitting, where the ventilation system was the most CO₂-eq emitted component. Overall, the finished concrete and ventilation system produced around 44% and 21% of the total embodied emissions in the entire life cycle stages. However, the minimum embodied CO₂-eq emissions were generated by the EPS insulation materials due to poor insulation quality of the reference building.

3.2. Environmental impacts of retrofitting scenarios

Fig. 7 shows the total CO₂-eq emissions for the reference building and retrofitting scenarios for the lifetime of 60 years. An obvious decrease of CO₂-eq emissions was obtained in the retrofitting scenarios, around 68% and 73% for the RSH and the AA scenarios respectively, mostly due to significant energy savings achieved by applying retrofitting measures. It should be noted that the emissions associated with the building operational energy use were calculated based on the reference and the optimized building energy models in our previous studies [8, 51]. Less CO₂-eq reduction in the cases with the RSH system was, firstly, due to the heating distribution network for radiators, which did not exist in the cases with the AA system, and secondly, because of the DCV in the AA system assisted in higher reduction of the building energy use than CAV ventilation in the RSH system. Although, due to the utilization of extra materials, the embodied CO₂-eq emissions increased in the retrofitting scenarios compared to the reference case, around 12–19%, the reduction of CO₂-eq emissions was much bigger in the operational stage. Accordingly, the share of operational energy use (B6) in the total CO₂-eq emissions was around 77% for the reference case whereas it was obtained around 43–46% for the retrofitting scenarios, and 54–57% of total emissions were due to embodied emissions of extra materials. In Ref. [38] it was also shown that applying the building retrofit measures could reduce the corresponding environmental impacts by 56–96% for a residential building in Norway, where the largest reduction was due to renovation of energy supply in addition to building envelope retrofitting. Overall, the AA_LCC produced the least CO₂-eq emissions, around 354 kg CO₂-eq/m², among all studied scenarios, owing to less materials used in the product stage together with less emissions generated in the operational energy use stage. It should be emphasized that the share of embodied CO₂-eq emissions related to material usage in the RSH and AA scenarios may vary depending on how these systems are implemented and installed.

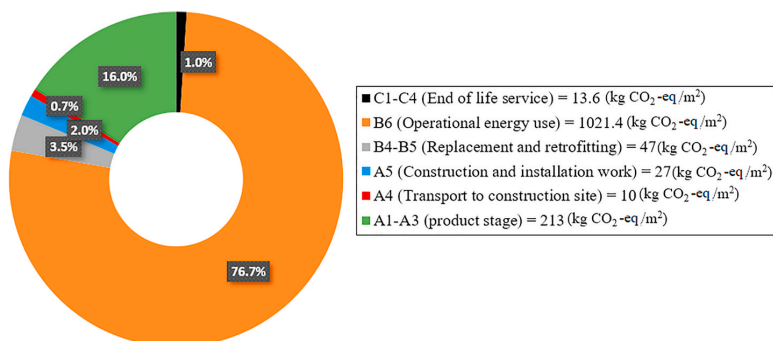


Fig. 4. Total CO₂-eq emissions related to various stages of the building life cycle.

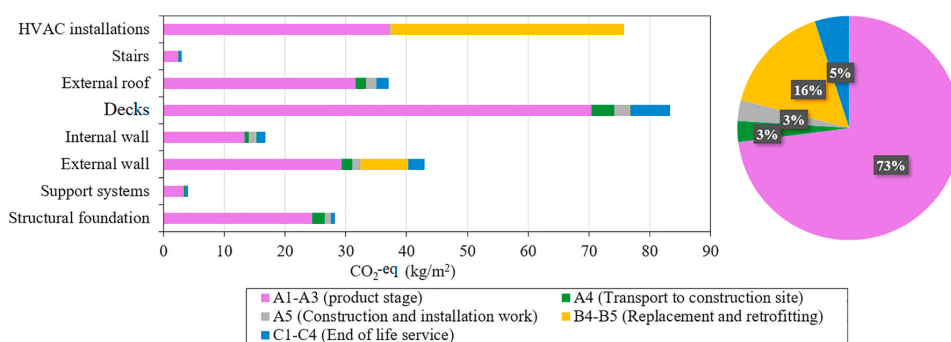


Fig. 5. Embodied CO₂-eq emissions of the materials in the reference building.

To further compare the embodied emissions for the reference building and retrofitting scenarios, the CO₂-eq emissions associated with different building component and materials are shown in Fig. 8. The change in the insulation thickness of the building envelope, together with replacement of various types of windows were the differences between the retrofitting scenarios. The cases equipped with AA system generated less emission related to HVAC installations. In this regard, the minimum embodied CO₂-eq emissions from materials were produced for the AA_LCC case.

Although HVAC installation generated almost the largest embodied CO₂-eq emissions among all building components and materials for all the five cases, which was mainly due to replacement (B4–B5), the largest increase in the embodied emissions, due to retrofitting, was associated with the re-insulation of the ground floor. Furthermore, to maintain the ceiling height the same as that in the reference building, due to re-insulation of floors, the ground floor had to be replaced. This retrofit measure is not only costly and time consuming, but also turned out to have a considerable impact on the total CO₂-eq emissions in the LCA analysis as it involves new pouring of concrete. It should be noted that the share of produced emissions in the operational energy use which was only corresponding to re-insulation of the ground floor should also be considered to find out if this retrofit measure could compensate for the large associated embodied emissions. However, it could have been more appropriate, from an environment perspective, to further re-insulate the other parts of the building envelope instead of ground floor. It can be also observed in Fig. 8 that the emissions associated with retrofitting of the exterior walls and the roof were considerably lower compared to the ground floor.

To obtain a comprehensive LCA of retrofit scenarios, the CO₂-eq payback time was used for the studied cases, as shown in Fig. 9. It is an

important indicator for finding the retrofit scenarios which have the best environmental performance in the building lifetime and determines how long it would take before the lower emissions from energy use will offset greenhouse gas emissions in connection with retrofitting. In this respect, the retrofitting scenarios were compared to the reference building, spread over a 60-year period.

In Fig. 9, the embodied emissions related to all building's life cycle stages, except the replacement, have been considered at the beginning of the lifetime period, while the emissions related to the operational energy use were successively added over the building lifetime. As the results demonstrated, the CO₂-eq payback times for the AA_LCC and RSH_LCC scenarios were almost the same and equal to 3.9 years, followed by the AA_PH and RSH_PH scenarios with CO₂-eq payback times equal to 4.6 and 5.1 years, respectively. These payback periods were obtained without considering the retrofitting of the building energy supply system and changing the energy supply could shorten the CO₂-eq payback period. A case in this point was stated in Ref. [38], where retrofitting of building envelope along with changing the energy supply system resulted in a CO₂-eq payback period 1.09 years for a residential building in Norway. Overall, considering both the carbon payback times and the total CO₂-eq emissions generated at various stages of the building life cycle, the AA_LCC had the best environmental performance among all retrofitting scenarios. It should be noted that these retrofitting scenarios are not the most environmentally friendly solutions and are already based on our previous LCC optimization study [8]. Nevertheless, they can provide worthwhile information about the environmental impacts associated with the cost-efficient solutions for the buildings in cold climate.

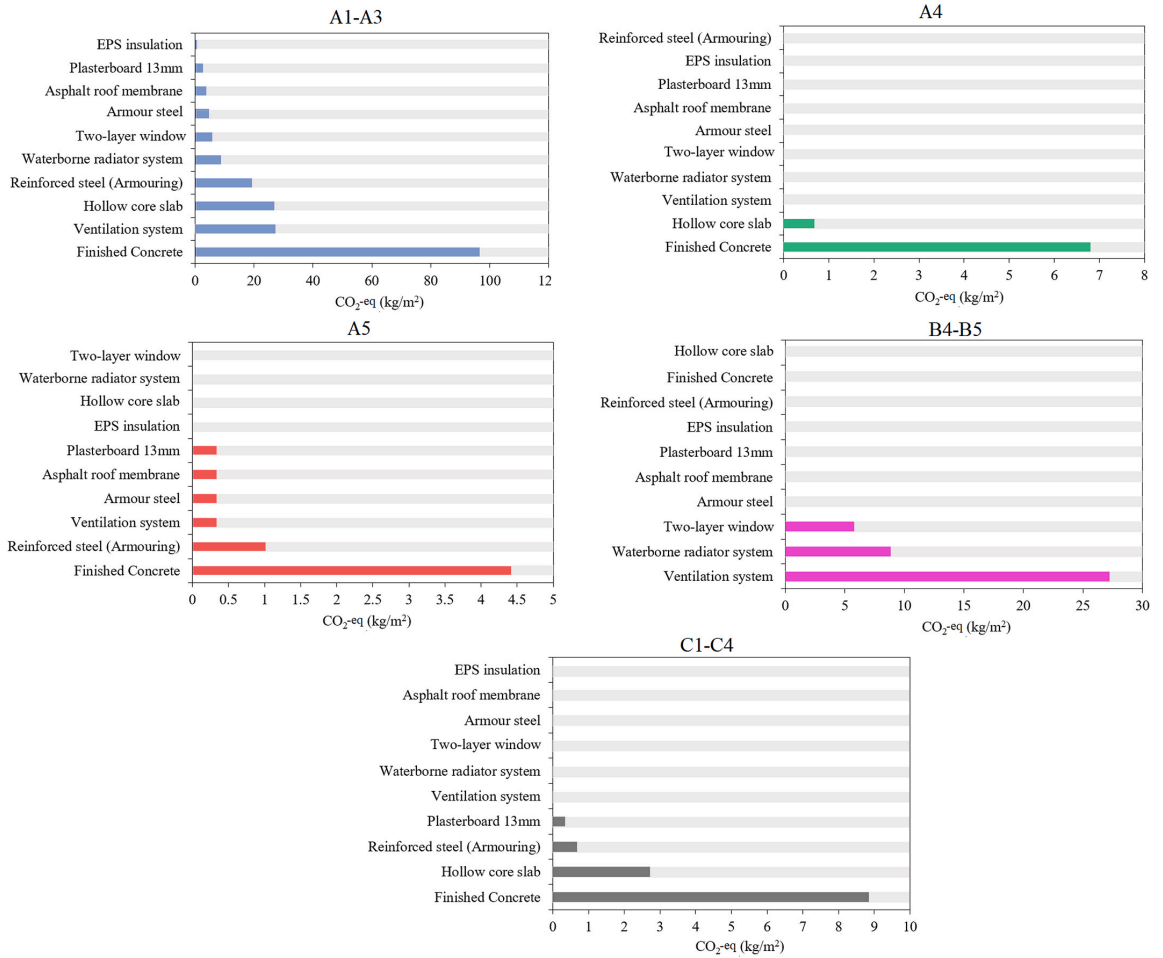


Fig. 6. Ranking of embodied CO₂-eq emissions of different building materials in various life cycle stages for the reference building.

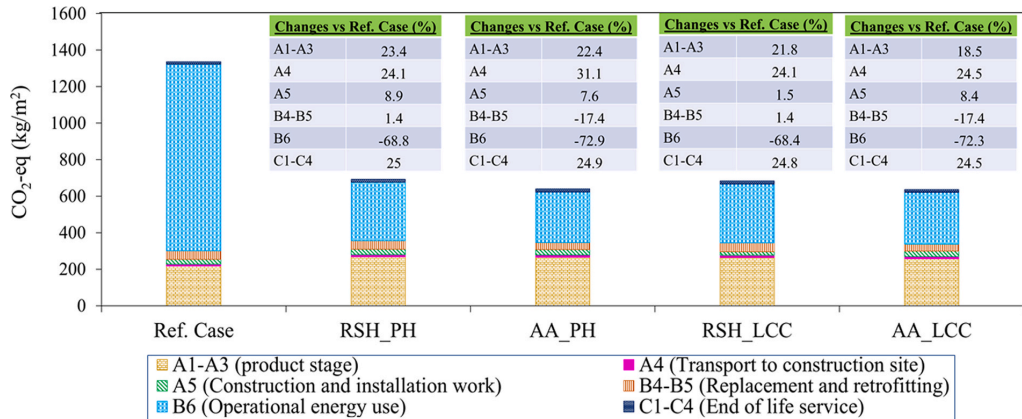


Fig. 7. Total CO₂-eq emissions related to various stages of the building life cycle for the reference building and retrofitting scenarios.

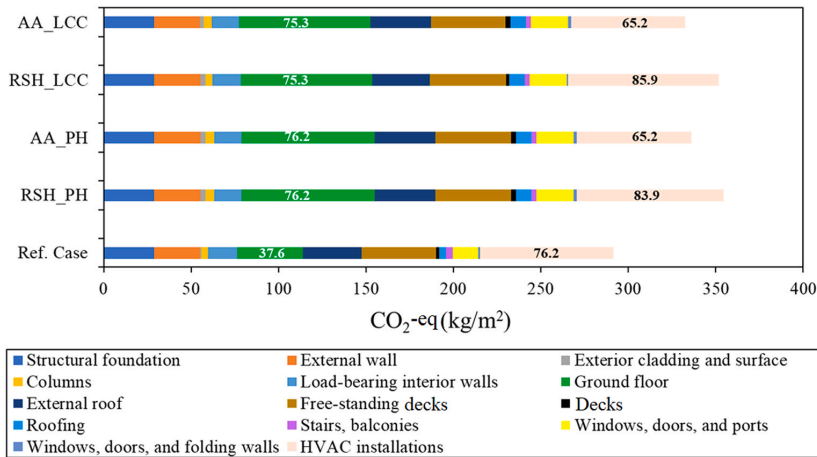


Fig. 8. Embodied CO₂-eq emissions from materials for the reference building and the retrofitting scenarios.

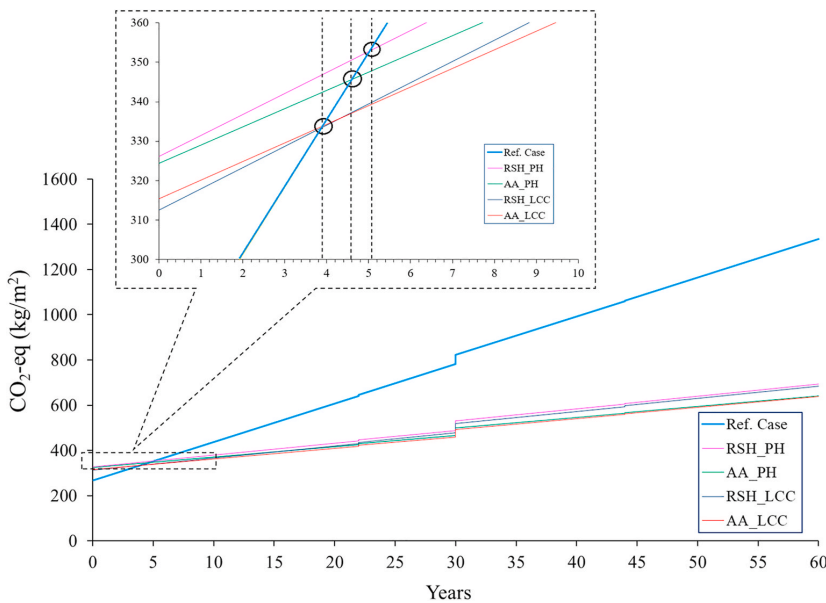


Fig. 9. Time plot of CO₂-eq for the reference case and different retrofit scenarios.

3.3. Environmental impacts of various insulation materials and heating supply systems

To investigate the carbon life cycle impact of various heating supply systems and insulation materials, the RSH_PH case was considered as a case study, since the environmental impact of the type of insulation and heating supply system would be the same for all the scenarios.

Fig. 10 shows the CO₂-eq emissions related to the four supply heating systems described in section 3.4. The emissions include only the environmental impacts related to the operational energy use and the embodied emissions for installation of heating supply systems.

As Fig. 10 shows, the district heating systems resulted in the minimum CO₂-eq emissions among all the considered systems, in terms of embodied CO₂-eq emissions corresponding to the materials and those

associated with the operational energy use. The reason was that the electricity was supplied to the heating systems by considering the EU28 mix supply scenario in which 49% of the power production sources is from fossil fuels, having a large effect on greenhouse gas emissions. It was also pointed out in Ref. [67] that the district heating may reduce the CO₂-eq more than other supply systems. The reduction amount still depends on the source of the district heating system, as reported in Ref. [68] that the district heating provided by CHP plants competes with other forms of heat generation such as heat pumps. Furthermore, the hybrid system did not show better environmental performance than the GSHP because the electricity source was the EU28 mix. However, it could be an interesting alternative if the boiler was supplied by renewable sources and if the Norwegian electricity mix, which has much lower CO₂-eq impact than the EU28 mix, was used to drive the GSHP.

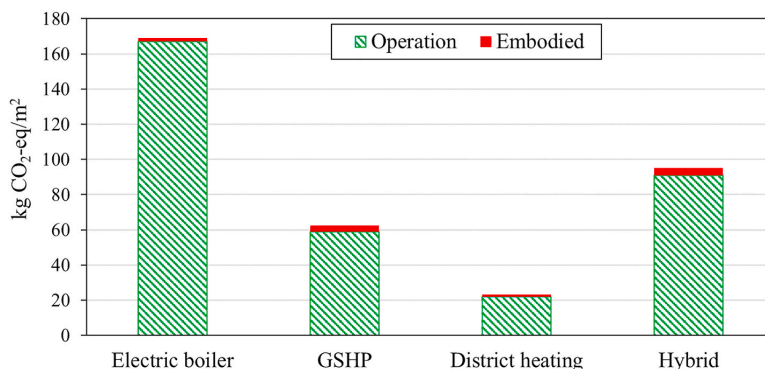


Fig. 10. CO₂-eq emissions associated with various types of heating systems for the RSH_PH case.

This analysis could be a further research in this area.

The total embodied CO₂-eq emissions of the entire building corresponding to various insulation materials are shown in Fig. 11. Using VIP and Glass wool insulation materials led to maximum and minimum CO₂-eq emissions among all types of insulation materials, respectively. The high CO₂-eq emissions were mostly associated with the product stage (A1-A3) and end-of-life service (C1-C4). However, Cellulose insulation material resulted in the minimum CO₂-eq emissions in the product stage. Although VIP is not an Eco-friendly product, it is still a desirable insulation material in rehabilitation projects with little space for extra insulation materials.

It should be noted that the choice of insulation material will always depend on the type of building, type of building components, climate conditions at the location, and the thickness and positioning of the insulating material. Environmental impact, heat resistance, and area to be insulated will be factors that come into play. For example, it was found in Ref. [30] that by using a strip foundation of low carbon concrete with glass wool insulation and a timber construction, a considerable reduction of embodied emissions in terms of CO₂-eq is achieved, around 40%, for a zero emission single family house located in Norway. However, it was reported that retrofitting a Swedish residential building with glass wool insulation along with other materials such as aluminum-framed windows and aluminum cladding results in trivial saving in CO₂-eq [27]. The cost of insulations also plays an important role in the assessment of various insulation materials. For instance, it was reported in Ref. [69] that Cellulose insulation shows the best overall

performance for the considered areas of applications (energy, environmental, economic) in a residential building in Ireland. Nevertheless, each investigation regarding the environmental impacts of insulation materials may provide worthwhile information about the environmental and economic aspects of them in various conditions.

3.4. CO₂-eq emissions for nZEB scenario

As mentioned in Section 3.3.5, the nZEB scenario was achieved by installing PV panels to balance the total delivered energy to the building. The environmental impacts of two types of PV panels were studied for the RSH_PH scenario, as shown in Fig. 12.

Although Monocrystalline resulted in less material usage (smaller PV panel areas) to reach nZEB level, due to its higher efficiency than Polycrystalline, it generated more CO₂-eq emissions than Polycrystalline, especially in the product stage and replacement and retrofitting see Fig. 12(a). This was due to extra Czochralski process in the production of the Monocrystalline PV panels. In addition, in both cases, the replacement and retrofitting stood for more than 49% of CO₂-eq emissions production. Fig. 12(b) shows that installing the PV panels to balance the delivered energy use for RSH_PH led to increase of embodied emissions around 11% and 6% when applying the Monocrystalline and the Polycrystalline, respectively. However, the emissions related to the operational energy use, accounting for 50% of total emissions in RSH_PH, were decreased resulting in approximately 39% and 44% net reduction of CO₂-eq emissions in the nZEB 2 and nZEB 1 scenarios,

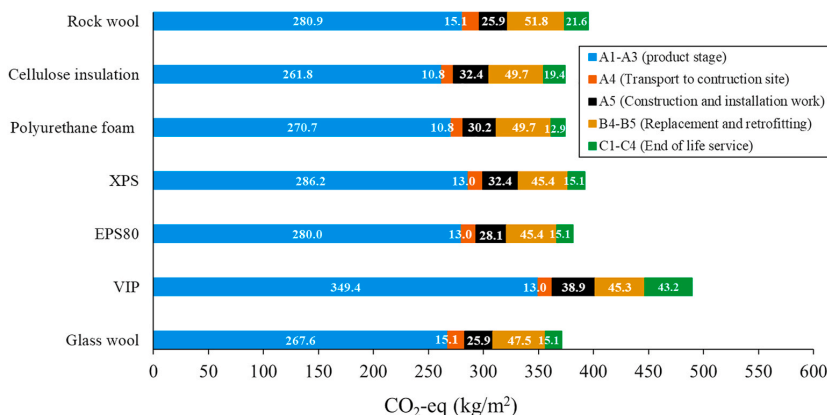


Fig. 11. Total building embodied CO₂-eq emissions associated with using various types of insulation materials for the RSH_PH case.

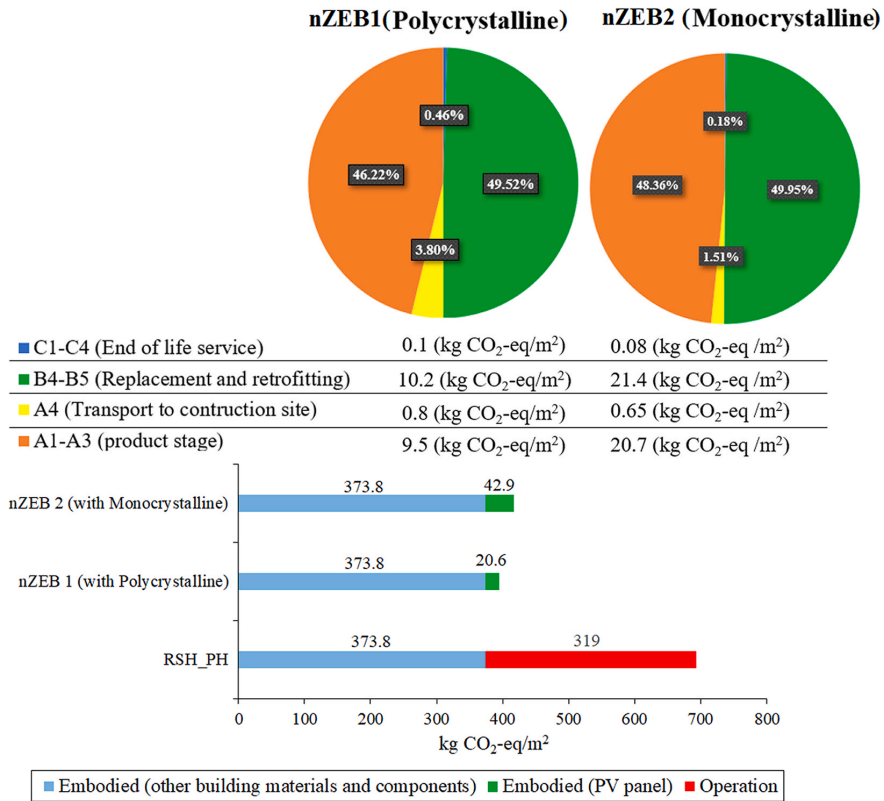


Fig. 12. (a) CO₂-eq emissions for two types of PV panels to reach nZEB level and (b) total CO₂-eq emissions for the RSH_PH and two nZEB cases.

reactively.

Fig. 13 shows the time profile of CO₂-eq emissions for the RSH_PH case and the two nZEB scenarios over the lifetime period 60 years. As it can be observed, the nZEB 1 had carbon payback time around six years while, the payback time was obtained around 12 years for the nZEB 2 scenario.

Comparing the results obtained in Figs. 12 and 13 shows that the case with the Polycrystalline PV panels had better performance than the Monocrystalline ones in terms of environmental impact even though

with a larger PV area, around 20%, was needed for the Polycrystalline PV panels to reach nZEB level. However, the high efficiency and space saving make Monocrystalline PV panels attractive on the market, as there is often limited installation space.

4. Conclusions

This paper investigated a detailed LCA of various retrofit scenarios, in terms of CO₂-eq, for a typical existing office building built in Norway

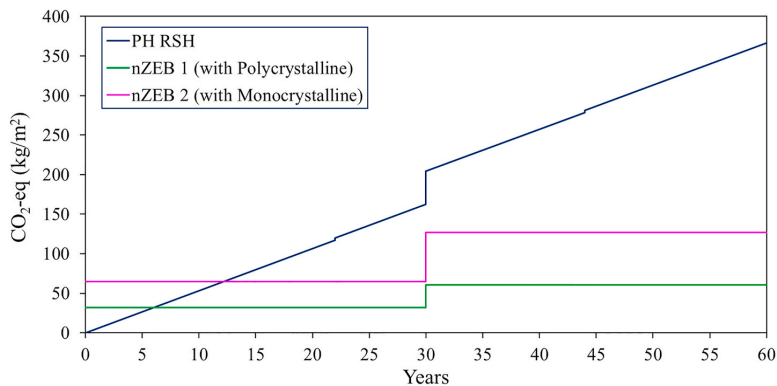


Fig. 13. Time plot of CO₂-eq for the RSH_PH and two nZEB cases.

in 1987, by assuming a 60-years lifetime for both the existing and the retrofitted buildings. The alternative design solutions for different scenarios were based on the optimized building energy models obtained in our previous studies. These alternatives were accordingly based on the Norwegian passive house standard and a LCC optimization study. Furthermore, in the retrofitting scenarios, two different HVAC systems including the AA with a DCV system and the RSH system equipped with a CAV ventilation system were taken into consideration. The LCA was conducted using OneClick LCA tool by considering the national Norwegian standard NS 3720. Analysis of the reference building showed that around 77%, 1021.4 kg CO₂-eq/m², of the total GHG emissions were due to building energy use and the 23% were attributed to the embodied emissions of building materials and components, of which 16%, 213 kg CO₂-eq/m², of embodied emissions were related to product stage in the building life cycle. The most carbon emitted materials in this respect were finished concrete and the ventilation system components. Applying the retrofit measures increased the embodied emissions for different retrofit scenarios owing to use of extra materials, their transport to construction site, and the end-of-life service, and they were accounted for around 18–23%, 25–31%, and around 25%, respectively. However, the reduction of CO₂-eq emissions associated with the operational energy use, which were calculated around 69–73%, over-weighted the embodied CO₂ emissions of the extra materials. Among all the retrofitting scenarios, the LCC optimized case with the AA system (AA_LCC) showed the best performance in terms of environmental impact, so that the total CO₂-eq emissions were decrease from 1336 kg CO₂-eq/m², in the reference case, to 637 kg CO₂-eq/m² in the AA_LCC scenario. The reason was that this scenario showed better energy performance with less material use, due to omitting radiators for heating, which resulted in less embodied and operational CO₂-eq emissions compared to other retrofitting scenarios. Looking at the CO₂-eq payback times of retrofitting scenarios, the LCC scenarios had shorter return period, around 3.9 years, than the PH scenarios. In addition, we assessed the GHG emissions associated with adopting various heating supply system and insulation materials. The results confirmed that the district heating system generated the minimum emissions related to operational energy use and the embodied emissions for the heating supply systems, while the Glass wool and cellulose insulation led to minimum embodied emissions related to building materials. Eventually, the GHG missions associated with the two nearly zero energy (nZEB scenarios) corresponding to use of the Polycrystalline and the Monocrystalline PV panels showed a considerable reduction, around 39–44%, of the total CO₂-eq emissions compared to the PH case with the RSH system. Although the material usage for the Monocrystalline PV panels was less than the Polycrystalline ones, due to higher efficiency, the extra Czochralski process in the production of Monocrystalline resulted in higher embodied emissions for nZEB case for the Monocrystalline PV panels. Therefore, based on the LCA for the retrofitting scenarios in terms of CO₂-eq emissions, the AA_LCC scenario taking advantage of the Glass wool insulation material, the district heating supply system, and the Polycrystalline PV panels could be considered as a potential retrofitting solution greatly contributing to achieve a ZEB level. Nevertheless, they can provide worthwhile information about the environmental impacts associated with the cost-efficient solutions for the buildings in cold climate. Furthermore, the data sources used in this LCA work may include some uncertainties arising from inaccuracy of available data or their dependency on the specific analyzed systems and inaccuracy of parameters modelled in this study.

To finish, let us recall that the scenarios investigated in our study was limited to the Norwegian passive house standard and a LCC optimization model obtained in our previous work. As a cost-effective model may not fully represent the most environmentally friendly solutions for building retrofitting, it would be very interesting to focus on ZEB level by broad use of low CO₂-eq emission materials and those having negative embodied carbon in the construction phase such trees and short-term crops. Alternatively, an extensive use of renewable energy sources

such as PV panels, biomass combined heat and power (CHP), etc. Can also be considered to compensate both the embodied and operational emissions during entire building life cycle. It would be worth finding out which approach is more efficient because if, for example, a scenario of low carbon electricity grid is considered, it would be more difficult to achieve a zero emission level through extensive use of PV panels. However, a combination of LCC and LCA would give a more practical perspective in achieving a zero emission level.

Declaration of competing interest

The authors declare that they have no known competing financial interests or personal relationships that could have appeared to influence the work reported in this paper.

References

- [1] F. Aragón-Durand, W. Cramer, S. Humphreys, M. Kainuma, J. Kala, N. Mahowald, Y. Mulugetta, R. Perez, M. Wairuri, K. Zickfeld, Special Report on Global Warming of 1.5° C (SR15)-Chapter 1: Framing and Context, 2018.
- [2] M. Company, Pathways to a Low-Carbon Economy, Version 2 of the Global Greenhouse Gas Abatement Cost Curve, 2009.
- [3] T. Johansson, T. Olofsson, M. Mangold, Development of an energy atlas for renovation of the multifamily building stock in Sweden, *Appl. Energy* 203 (2017) 723–736.
- [4] L. Bakken, S. Bjørberg, K. Kalhagen, N. Lassen, L. Palm, E. Weydahl, Konsekvensanalyse av å innføre nye forskriftskrav til energieffektivisering av bygg (in Norwegian), *Regjeringens Analyse & Strategi, Multiconsult* (2011) 5–96.
- [5] C. Skaar, K. Elvebak, K. Skeie, Klimafotspor fra byggematerialer ved ambisiøs oppgradering av boligblokker, 2018.
- [6] N.H. Sandberg, I. Sartori, O. Heidrich, R. Dawson, E. Dascalaki, S. Dimitriou, T. Vimm-r, F. Filippidou, G. Stegnar, M. Sijaneč Zavrli, H. Brattebo, Dynamic building stock modelling: application to 11 European countries to support the energy efficiency and retrofit ambitions of the EU, *Energy Build.* 132 (2016) 26–38.
- [7] S.S.B. Statistics Norway, Energy use in municipal property management, by function and energy type (M) 2015, 2020. 2020, <https://www.ssb.no/en/statab/ank/table/12150/>, 2019.
- [8] M. Rabani, H. Bayera Madessa, O. Mohseni, N. Nord, Minimizing delivered energy and life cycle cost using Graphical script: an office building retrofitting case, *Appl. Energy* 268 (2020).
- [9] F. Rosso, V. Ciancio, J. Dell’Olmo, F. Salata, Multi-objective optimization of building retrofit in the Mediterranean climate by means of genetic algorithm application, *Energy Build.* 216 (2020).
- [10] C. Waibel, R. Evins, J. Carmeliet, Co-simulation and optimization of building geometry and multi-energy systems: interdependencies in energy supply, energy demand and solar potentials, *Appl. Energy* 242 (2019) 1661–1682.
- [11] A.J. Marszal, P. Heiselberg, J.S. Bourrelle, E. Musall, K. Voss, I. Sartori, A. Napolitano, Zero Energy Building – a review of definitions and calculation methodologies, *Energy Build.* 43 (4) (2011) 971–979.
- [12] P. Hernandez, P. Kenny, From net energy to zero energy buildings: defining life cycle zero energy buildings (LC-ZEB), *Energy Build.* 42 (6) (2010) 815–821.
- [13] L. Georges, M. Haase, A. Houlihan Wiberg, T. Kristjansdottir, B. Risholt, Life cycle emissions analysis of two nZEB concepts, *Build. Res. Inf.* 43 (1) (2015) 82–93.
- [14] A. Stephan, L. Stephan, Achieving net zero life cycle primary energy and greenhouse gas emissions apartment buildings in a Mediterranean climate, *Appl. Energy* 280 (2020), 115932.
- [15] T.F. Kristjansdottir, C.S. Good, M.R. Inman, R.D. Schlanbusch, I. Andresen, Embodied greenhouse gas emissions from PV systems in Norwegian residential Zero Emission Pilot Buildings, *Sol. Energy* 133 (2016) 155–171.
- [16] C. De Wolf, F. Yang, D. Cox, A. Charlson, A.S. Hattan, J. Ochsendorf, Material quantities and embodied carbon dioxide in structures, *Proceedings of the Institution of Civil Engineers - Engineering Sustainability* 169 (4) (2016) 150–161.
- [17] K. Simonen, B.X. Rodriguez, C. De Wolf, Benchmarking the embodied carbon of buildings, *Technology|Architecture + Design* 1 (2) (2017) 208–218.
- [18] F. Asdrubali, I. Ballarini, V. Corrado, L. Evangelisti, G. Grazieschi, C. Guattari, Energy and environmental payback times for an NZEB retrofit, *Build. Environ.* 147 (2019) 461–472.
- [19] T. Opher, M. Duhamel, I.D. Posen, D.K. Panesar, R. Brugmann, A. Roy, R. Zizzo, L. Sequeira, A. Anvari, H.L. MacLean, Life cycle GHG assessment of a building restoration: case study of a heritage industrial building in Toronto, Canada, *J. Clean. Prod.* 279 (2021).
- [20] B.X. Rodriguez, M. Huang, H.W. Lee, K. Simonen, J. Ditto, Mechanical, electrical, plumbing and tenant improvements over the building lifetime: estimating material quantities and embodied carbon for climate change mitigation, *Energy Build.* 226 (2020), 110324.
- [21] J. García-Sanz-Calcedo, N. de Sousa Neves, J.P. Almeida Fernandes, Measurement of embodied carbon and energy of HVAC facilities in healthcare centers, *J. Clean. Prod.* 289 (2021), 125151.
- [22] P. Ylmén, D. Peñaloza, K. Mjörnell, Life cycle assessment of an office building based on site-specific data, *Energies* 12 (13) (2019) 2588.

- [23] S. Chen, System Dynamics Based Models for Selecting HVAC Systems for Office Buildings: A Life Cycle Assessment from Carbon Emissions Perspective, Master Thesis, RMIT University, 2011.
- [24] C. Kiamili, A. Hollberg, G. Habert, Detailed assessment of embodied carbon of HVAC systems for a new office building based on BIM, *Sustainability* 12 (8) (2020) 3372.
- [25] M. Medas, D. Cheshire, A. Cripps, J. Connaughton, M. Peters, Towards BIM-Integrated, Resource-Efficient Building Services, Product Lifetimes And The Environment, 2015.
- [26] R. Moschetti, H. Brattebø, M. Sparrevik, Exploring the pathway from zero-energy to zero-emission building solutions: a case study of a Norwegian office building, *Energy Build.* 188–189 (2019) 84–97.
- [27] C. Piccardo, A. Dodoo, L. Gustavsson, Retrofitting a building to passive house level: a life cycle carbon balance, *Energy Build.* 223 (2020).
- [28] X. Chen, K. Qu, J. Calautit, A. Ekambaram, W. Lu, C. Fox, G. Gan, S. Riffat, Multi-criteria assessment approach for a residential building retrofit in Norway, *Energy Build.* 215 (2020).
- [29] S.K. Pal, A. Takano, K. Alanne, K. Siren, A life cycle approach to optimizing carbon footprint and costs of a residential building, *Build. Environ.* 123 (2017) 146–162.
- [30] T.F. Kristjansdottir, A. Houlihan-Wiberg, I. Andresen, L. Georges, N. Heeren, C. S. Good, H. Brattebø, Is a net life cycle balance for energy and materials achievable for a zero emission single-family building in Norway? *Energy Build.* 168 (2018) 457–469.
- [31] A. Houlihan Wiberg, L. Georges, T.H. Dokka, M. Haase, B. Time, A.G. Lien, S. Mellegård, M. Maltha, A net zero emission concept analysis of a single-family house, *Energy Build.* 74 (2014) 101–110.
- [32] T.H. Dokka, A.A.M. Houlihan Wiberg, L. Georges, S.E. Mellegård, B. Time, M. Haase, M.M. Maltha, A.G. Lien, A Zero Emission Concept Analysis of a Single Family House, 2013.
- [33] N. Llantoy, M. Cháfer, L.F. Cabeza, A comparative life cycle assessment (LCA) of different insulation materials for buildings in the continental Mediterranean climate, *Energy Build.* 225 (2020).
- [34] V. Echarri-Iribarren, F. Echarri-Iribarren, C. Rizo-Maestre, Ceramic panels versus aluminium in buildings: energy consumption and environmental impact assessment with a new methodology, *Appl. Energy* 233–234 (2019) 959–974.
- [35] C.C. Chang, W. Shi, P. Mehta, J. Dauwels, Life cycle energy assessment of university buildings in tropical climate, *J. Clean. Prod.* 239 (2019), 117930.
- [36] J. Sierra-Pérez, B. Rodríguez-Soria, J. Boschmonart-Rives, X. Gabarrell, Integrated life cycle assessment and thermodynamic simulation of a public building's envelope renovation: conventional vs. Passivhaus proposal, *Appl. Energy* 212 (2018) 1510–1521.
- [37] L. Luo, Y. Chen, Carbon emission energy management analysis of LCA-Based fabricated building construction, *Sustainable Computing: Informatics and Systems* 27 (2020).
- [38] B. Wrånsen, R. O'Born, C. Skaar, Life cycle assessment of an ambitious renovation of a Norwegian apartment building to nZEB standard, *Energy Build.* 177 (2018) 197–206.
- [39] A. Shirazi, B. Ashuri, Embodied Life Cycle Assessment (LCA) Comparison of Residential Building Retrofit Measures in Atlanta vol. 171, *Building and Environment*, 2020.
- [40] X. Zhang, R. Zheng, F. Wang, Uncertainty in the life cycle assessment of building emissions: a comparative case study of stochastic approaches, *Build. Environ.* 147 (2019) 121–131.
- [41] X. Zhang, F. Wang, Life-cycle assessment and control measures for carbon emissions of typical buildings in China, *Build. Environ.* 86 (2015) 89–97.
- [42] J. Hong, G.Q. Shen, Y. Peng, Y. Feng, C. Mao, Uncertainty analysis for measuring greenhouse gas emissions in the building construction phase: a case study in China, *J. Clean. Prod.* 129 (2016) 183–195.
- [43] X. Zhang, K. Liu, Z. Zhang, Life cycle carbon emissions of two residential buildings in China: comparison and uncertainty analysis of different assessment methods, *J. Clean. Prod.* 266 (2020).
- [44] A. Dodoo, L. Gustavsson, R. Sathre, Lifecycle carbon implications of conventional and low-energy multi-storey timber building systems, *Energy Build.* 82 (2014) 194–210.
- [45] J. Hong, G.Q. Shen, Y. Peng, W.S.-t. Lau, C. Mao, Greenhouse gas emissions during the construction phase of a building: a case study in China, *J. Clean. Prod.* 103 (2015) 249–259.
- [46] L. Shao, G.Q. Chen, Z.M. Chen, S. Guo, M.Y. Han, B. Zhang, T. Hayat, A. Alsaedi, B. Ahmad, Systems accounting for energy consumption and carbon emission by building, *Commun. Nonlinear Sci. Numer. Simulat.* 19 (6) (2014) 1859–1873.
- [47] J.-J. Ma, G. Du, Z.-K. Zhang, P.-X. Wang, B.-C. Xie, Life cycle analysis of energy consumption and CO2 emissions from a typical large office building in Tianjin, China, *Building and Environment* 117 (2017) 36–48.
- [48] X. Zhang, F. Wang, Assessment of embodied carbon emissions for building construction in China: comparative case studies using alternative methods, *Energy Build.* 130 (2016) 330–340.
- [49] R.H. Crawford, Post-occupancy life cycle energy assessment of a residential building in Australia, *Architect. Sci. Rev.* 57 (2) (2014) 114–124.
- [50] K. Goulouti, P. Padey, A. Galimshina, G. Habert, S. Lasvaux, Uncertainty of building elements' service lives in building LCA & LCC: what matters? *Build. Environ.* 183 (2020).
- [51] M. Rabani, H. Bayera Madessa, N. Nord, Achieving zero-energy building performance with thermal and visual comfort enhancement through optimization of fenestration, envelope, shading device, and energy supply system, *Sustainable Energy Technologies and Assessments* 44 (2021), 101020.
- [52] NS 3720- Method for Greenhouse Gas Calculations for Buildings (In Norwegian), Norsk standard, 2018.
- [53] EN 15978- Sustainability of Construction Works- Assessment of Environmental Performance of Buildings- Calculation Method, Standard Norge, Norway, 2011.
- [54] A.G. Hestnes, N.L. Eik-Nes, *Zero Emission Buildings*, Fagbokforlaget Bergen 2017.
- [55] L.A. Wright, S. Kemp, I. Williams, 'Carbon footprinting': towards a universally accepted definition, *Carbon Manag.* 2 (1) (2011) 61–72.
- [56] N. Bjørsell, A. Bring, L. Eriksson, P. Grozman, M. Lindgren, P. Sahlin, A. Shapovalov, M. Vuolle, IDA indoor climate and energy, in: *Proc. Of the 6-th IBPSA Conference*, 1999, pp. 1035–1042.
- [57] Byggeforskrift- TEK 87 (1987).
- [58] NS-3701-Criteria for Passive Houses and Low Energy Buildings, Non-residential buildings, Standard Norge, Norway, 2012.
- [59] Bionova, Calculate your environmental impacts in minutes [Online]. <https://www.oneclicklca.com/>, 2020. (Accessed 5 March 2020).
- [60] ISO 14020: Environmental Labels and Declarations, General Principles, Standard Norge, 2002.
- [61] Calculation of Areas and Volumes of Buildings, NS 3940:2012. Standard, Standards Norway, Oslo, Norway, 2012.
- [62] Byggeforsk, 521.111 golv på grunnen med ringmur. Oppvarmede bygninger. Arkivsemlar (in Norwegian) 1986-1998.
- [63] Byggeforsk, 471.010 varmegjennomgang. U-verdier for bygningskonstruksjoner (in Norwegian). Arkivsemlar (tabell 381), 1987-1995.
- [64] R. Turconi, A. Boldrin, T. Astrup, Life cycle assessment (LCA) of electricity generation technologies: overview, comparability and limitations, *Renew. Sustain. Energy Rev.* 28 (2013) 555–565.
- [65] Norsk fjernvarme, Energikilder, Retrieved April, 2020, <https://www.fjernvarme.no/fakta/energikilder>, 2020.
- [66] NS 3031, Calculation of Energy Performance of Buildings - Method and Data, Standard Norge, 2014, p. 100.
- [67] T. Lidberg, M. Gustafsson, J.A. Myhren, T. Olofsson, L. Ödlund, Environmental impact of energy refurbishment of buildings within different district heating systems, *Appl. Energy* 227 (2018) 231–238.
- [68] J. Karlsson, L. Brunzell, G. Venkatesh, Material-flow analysis, energy analysis, and partial environmental-LCA of a district-heating combined heat and power plant in Sweden, *Energy* 144 (2018) 31–40.
- [69] T. Dickson, S. Pavia, Energy performance, environmental impact and cost of a range of insulation materials, *Renew. Sustain. Energy Rev.* 140 (2021), 110752.

